

**"AN INVESTIGATION OF THE DAMPING INFLUENCES IN ENGINE
TORSIONAL OSCILLATION"**

BY

JAMES FORREST SHANNON, A.R.T.C.

**THESIS PRESENTED FOR THE DEGREE OF DOCTOR OF PHILOSOPHY
(PH.D.) IN THE FACULTY OF ENGINEERING, UNIVERSITY OF
GLASGOW.**

**The Royal Technical College,
Glasgow, June, 1933.**

ProQuest Number: 13905476

All rights reserved

INFORMATION TO ALL USERS

The quality of this reproduction is dependent upon the quality of the copy submitted.

In the unlikely event that the author did not send a complete manuscript and there are missing pages, these will be noted. Also, if material had to be removed, a note will indicate the deletion.



ProQuest 13905476

Published by ProQuest LLC (2019). Copyright of the Dissertation is held by the Author.

All rights reserved.

This work is protected against unauthorized copying under Title 17, United States Code
Microform Edition © ProQuest LLC.

ProQuest LLC.
789 East Eisenhower Parkway
P.O. Box 1346
Ann Arbor, MI 48106 – 1346

ABSTRACT.

This paper describes an investigation of the damping influences occurring in multi-crank engines when in a state of torsional oscillation. The major part of the experimental work is carried out on a four-cylinder petrol engine. The crankshaft is of the four-throw-two-bearing type and its torsional flexibility is examined analytically for the condition of no constraint and complete constraint at the bearings. Torsion experiments are carried out with the crankshaft in place, and the results are in close agreement with analysis.

In the vibration experiments a Geiger torsigraph is used and resonance conditions are examined. Extreme methods of lubrication are adopted and the outstanding influence of lubrication in the control of amplitude at resonance is demonstrated. For the engine dealt with the principal source of damping is traced to the main bearing.

The dissipation of energy in an oil film, due to journal vibration is examined analytically and expressed in terms of journal displacement. From an investigation of the journal displacements caused by crankshaft oscillation, it is found that practically all the input energy of vibration could be accounted for in this manner, thus confirming the experimental observations.

The results are finally reduced to an overall non-dimensional factor which is practically constant for the range of frequencies investigated.

Results from a number of multi-crank engines on which further experiments had been carried out were available and these, together with other published data, are also reduced to this simple non-dimensional form. The value of the factor is not constant for the different engine systems, but appears to be correlated to the elastic curve form at the engine, and an average curve taken on this basis is presented as a guide in design.

	Page.
Damping at Main Journal Bearing, due to simple shear resistance of oil film,	52.
Elastic deformation at journal due to inertia torques of oscillation,	56.
The dissipation of energy due to journal vibration in a flooded bearing,	57.
Comparison with dissipation due to whirling of a journal in its bearing,	60.
Form of damping expression,	62.
Overall velocity damping and non-dimensional factor,	63.

Part. III.

Application of the non-dimensional factor to results obtained from further experiments carried out on multi multi- crank engines,	65.
Method of analysis,	65.
Variation of factor for different engine systems and correlation with the elastic curve form at the engine,	67.
Proposed design curve,	76.
Bibliography,	79.

INTRODUCTORY REVIEW.

In modern machinery where periodic torsional forces occur it is generally necessary to include in the design procedure an investigation of the torsional characteristics of the dynamical system. This phase of design is essential in marine installations, and it is compulsory in high speed reciprocating engines including the automobile and aircraft types. In all these spheres many examples of severe torsional vibration are on record showing the penalty of resonance ultimately taking the sinister form of shafting failure. Milder cases of resonance usually result in some form of disturbance, coarse and uneconomical running or irregularity of operation.

The problem of determining the torsional vibration characteristics becomes one of first estimating the natural frequencies of torsional vibration of the shaft arrangement. There are various methods available for this calculation, but for multi-elastic systems, the most common is the modified Gumbel - Holzer¹ method. This involves the determination of inertia quantities and shaft rigidities and their reduction to an equivalent dynamical system having torsional characteristics equivalent to the entire running gear.

The accuracy of the natural frequency calculations chiefly depends upon the estimation of shaft flexibilities, the main difficulty occurring in vibration forms where crankshaft rigidity is important. However, with further data continuing to support recent empirical formulae for crankshaft stiffness², calculated frequencies can be relied upon to within 3 per cent. Thus the primary problem of determining natural

1. Holzer, Die Berechnung der Drehschwingungen. Berlin, 1921.

2. Carter, Engineering, July 13th, 1928.

frequencies and vibration form may be regarded as being sufficiently clear from an engineering point of view.

With the natural frequencies determined, there follows the possible critical speeds since theoretically these occur when the periodic forces synchronise with the natural frequencies. Fortunately only comparatively few are violent enough to cause damage. Some of these, however, are so severe that their synchronism must be avoided entirely since even a passage through the region would be serious. Hence the further problem of assessing the magnitude of the several criticals becomes important.

The simplest basis for this examination is the energy method developed by Wydler³ and Lewis⁴. This method depends upon the fact that at resonance the vibrational energy given to the shaft by the periodic forces is absorbed by the damping forces alone. For reciprocating engines the periodic inertia torques are definite and the disturbing torques due to the fluid pressure can be calculated with reasonable accuracy from the indicator cards. Hence, since the free vibration form is assumed at resonance and the input energy is proportional to the vector sum of the products of harmonic torque and amplitude of vibration at which it acts, the relative value of this energy for a particular vibration form can be estimated closely for each critical.

At this stage it will be possible to predict whether the operating speeds are clear of criticals which are expected to be severe. In many slow speed engines this can be attained, but with heavier engine masses, greater number of cylinders and higher running speeds, the avoidance is not altogether a practicable possibility. In such cases, methods of evading severe resonance conditions must be employed, such as

3. Wydler, "Drehschwingungen in Kolbenmaschinenanlagen"
Berlin, 1922.

4. Lewis, Trans. New York Soc. of Naval Architects and Marine
Engs. Nov. 1925.

readjustment of mass and elasticity for frequency change or rearrangement of firing order, crank angles etc., in conjunction with vibration form for cancellation of certain impulses. Even correct phasing of the load if it has suitable periodic variations can be employed to attain minimum vibrational energy at resonance.

In all such methods, success is possible to a varied degree since the avoidance of extreme criticals very often introduces those of minor order which still might be dangerous. In many oil engines running at present the operating range lies between severe criticals, while the high speeds and wide speed range of automobile and aircraft engines makes it impossible to avoid altogether the occurrence of criticals in the operating range. These cases are quite common and it becomes necessary to estimate the actual values of these criticals at and near resonance in order to decide whether it is safe deliberately to run at these speeds. This involves a knowledge of the damping influences and factors controlling amplitude at resonance.

The damping property of any particular source is usually known when the energy absorption is expressed as a function of amplitude and frequency. Where torque characteristics permit, as in the case of propellers⁵, it is possible to derive damping factors, such that the amplitude of vibration when damped mainly by this source can be calculated with sufficient accuracy to be of practical value.

However, it is quite common to have other modes of vibration with a node practically at the propeller so that damping from this source is ineffective. This class of vibration is similar to that which occurs in air-craft drives, engine-generator sets, and many other spheres. The damping occurs at the engine and shaft but its nature and distribution is indeterminate.

5. Porter, Trans. Amer. Soc. Mech. Eng. A.P.M., 51 - 22, 1929.

It appears that there have been no detailed investigations carried out from which the nature of engine damping could be elucidated. Information from actual engines is usually limited to an overall value from one important critical and it appears impossible and unreliable to consider the damping from the engine frictional torque characteristics. There is also a diversity of opinion as to the most rational way of considering the results. Wydler³, Holzer¹, Carter⁶, &c., take the nature of engine damping to be unknown, and reduce observations to an equivalent overall viscous damping occurring within the engine. Each modifies the factor slightly, expressing it in terms of cylinder area, mass or equivalent amplification factor.

On the other hand, Lewis⁴ considers that there is no damping within the engine since there appears to be no frictional torque variation with speed change. He therefore assumes that all the vibrational energy is absorbed by hysteresis in the shafting, the overall damping taking a form based on the hysteresis results of Rowett⁷. However, from a list of overall results given by Porter⁸, it is seen that hysteresis energy is but a fraction of the energy absorbed.

Object.

In view of these opinions it was thought that an attempt should be made to investigate the nature and distribution of damping influences in engine torsional oscillation and factors controlling amplitude at resonance on a small scale plant suitably arranged so that effects of mass, frequency and amplitude could be examined, together with lubrication and piston ring effects.

3. 1. 4. Loc. cit.

6. Carter, Aero. Research Comm. R. and M. No. 1053. (E.22) 1926.

7. Rowett, Proc. Roy. Soc. London. Series A. Vol. 89. 1914.

See Lewis loc. cit.

8. Porter, see discussion in paper by Hartog. Trans. Amer. Soc. Mech. Eng. A.P.M. 52-13, 1930.

PART I. EXPERIMENTAL PLANT AND ITS CHARACTERISTICS.

Description of Plant.

Since the investigation consisted mainly of studying damping within the engine, a plant was required such that large oscillation took place only at the engine, and that amplitude and frequency could be varied.

A four-cylinder Dorman petrol engine, $2\frac{1}{2}$ in. x $4\frac{3}{4}$ in. stroke was driven by a D.C. shunt motor, through a long flexible shaft, the speed of the motor being controlled by a number of resistances in series with the armature circuit. Two relatively heavy fly-wheels fixed close to the armature gave a combined inertia much greater than the engine running gear which consisted only of the crankshaft, connecting rods and pistons. In order to vary the natural frequencies a number of split pulleys could be fitted close to the engine masses.

The cylinder head was removed to eliminate the uncertain periodic torques introduced by the pumping effect, particularly in the case when the piston rings were removed. When running, inertia torques arise in the engine and incite torsional vibration in the engine and motor masses. The source of vibration occurring at the position of maximum amplitude on the dynamical system gives the best position for developing the greatest vibrational energy.

The masses and shaft flexibilities were such that one mode vibration, stimulated by the large 2nd and small 3rd order torques could be studied. Fig. 1 shows a general view of the plant.

The engine and motor flywheel units were fitted to heavy baseplates as shown in Figs. 2 and 3, these being secured by fitted bolts to two rolled steel joists 8 in. x 6 in. x 20 ft. long. The girders were further secured by placing at suitable distances apart, two stools which also served to support plummer blocks carrying the long shaft. Thus the whole plant was

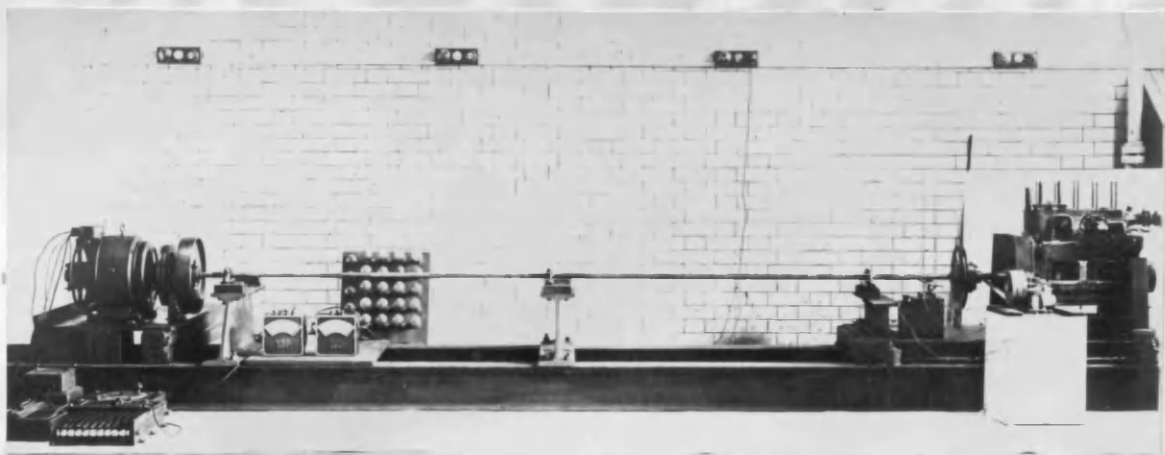


Fig. 1. General view of Experimental Plant.

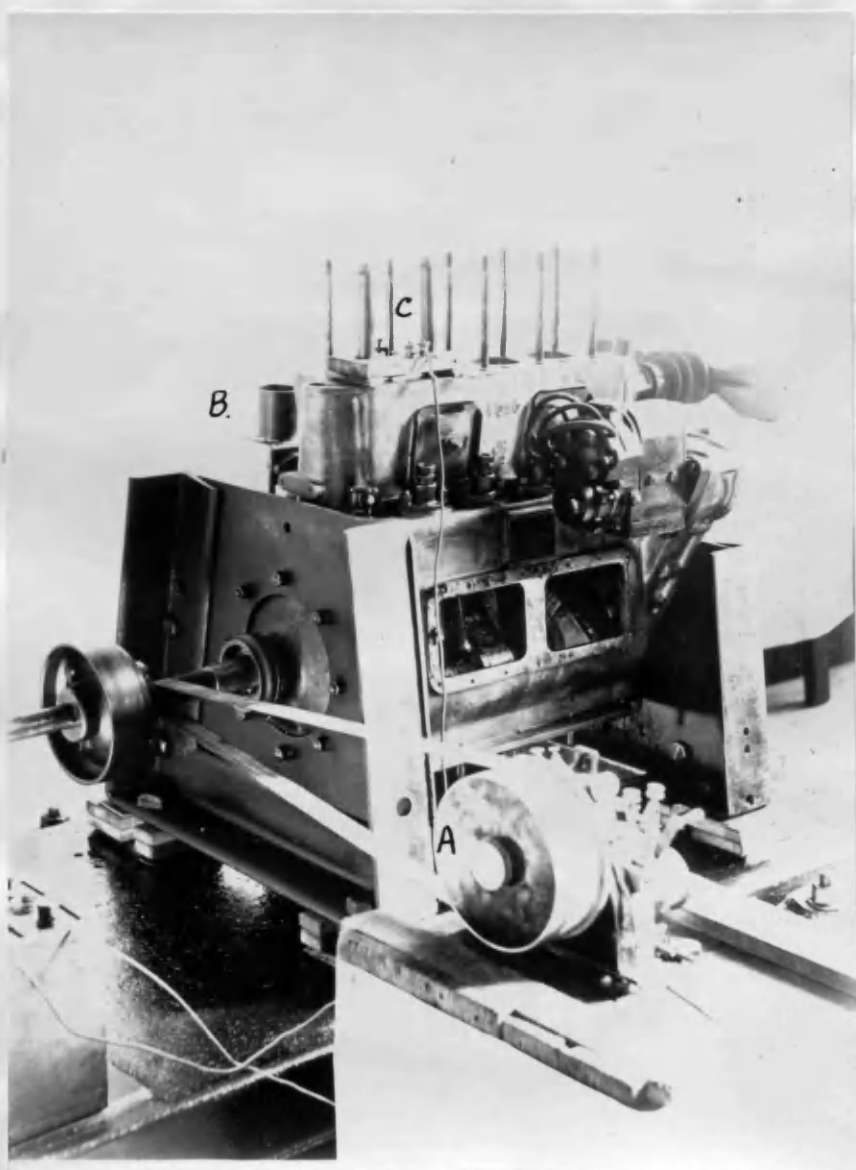


Fig 2. View at Engine . A. - Torsiograph.
B. - Oil-well for Gravity supply to main-bearing,
C. - Dead-centre timing.

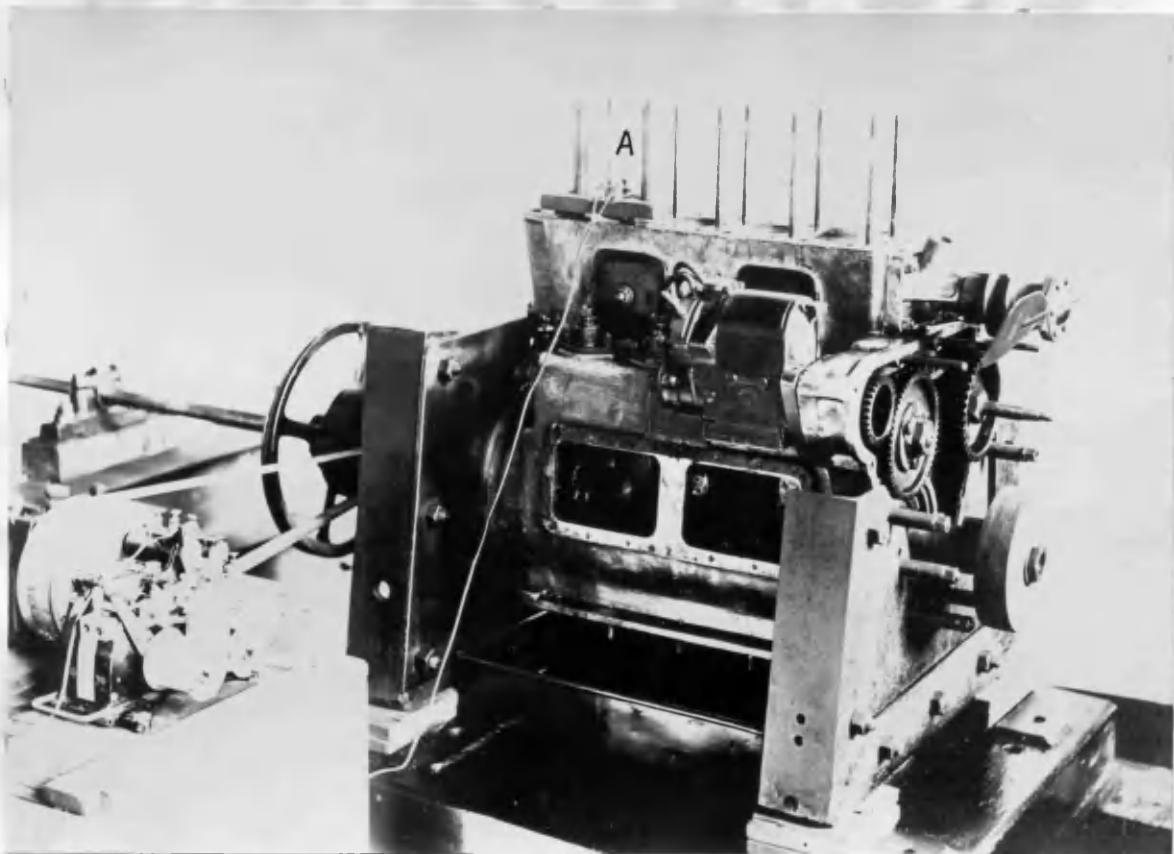


Fig. 2a. View at Engine.

A - Dead-centre timing.

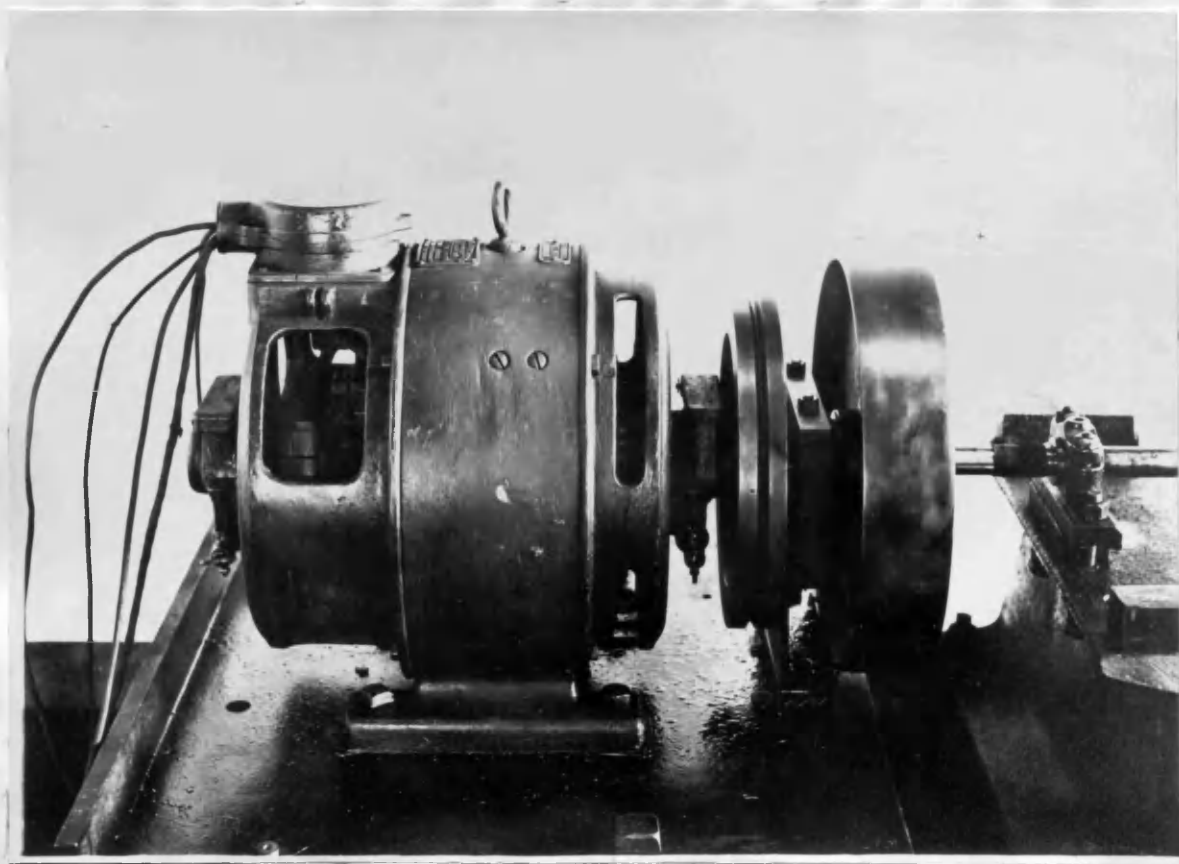


Fig. 3. View at Motor.

rigidly connected to a solid foundation.

A flywheel and extension sleeve were heavily keyed and pinned to the armature shaft, the extension sleeve carrying the weight of the flywheel on a ball bearing, fitted to the motor base plate.

The shafting was supported by three plummer blocks and was connected to the crankshaft by a solid flanged coupling. A heavy belt pulley, keyed and pinned to the other end of the shafting was bolted to the extension sleeve on the armature shaft by three fitted bolts. Figs. 4a,b,c. show in detail the arrangement at both ends of the system.

From preliminary runs it was found that all fittings had to be heavily keyed and pins countersunk and fitted into the shaft. This was important as small slips would absorb considerable energy. The vibrations were more severe than anticipated and saddle keys and ordinary pinching pins failed to hold and proved useless. With the most severe oscillation, the revised fittings proved successful, as there was no evidence of slip having taken place.

At speeds removed from resonance, smooth and satisfactory running was obtained.

Bearings and Lubrication. The motor was a 2 pole D.C. shunt type rated 3 H.P. at 1500 r.p.m. The armature was carried on two ring oil bearings and the extension sleeve on a ball bearing. The plummer blocks supporting the shafting were of gunmetal, one being placed adjacent to the pulley flywheel and the other two conveniently spaced along the shaft. The engine crankshaft was of the two bearing type, having a long white metal bearing at the aft end and a roller bearing at the forward end of the frame. Normally these bearings were forced lubricated by a pump, gear driven from the crankshaft, but this was dismantled for simplicity in engine running gear and gravity feed substituted to the white metal

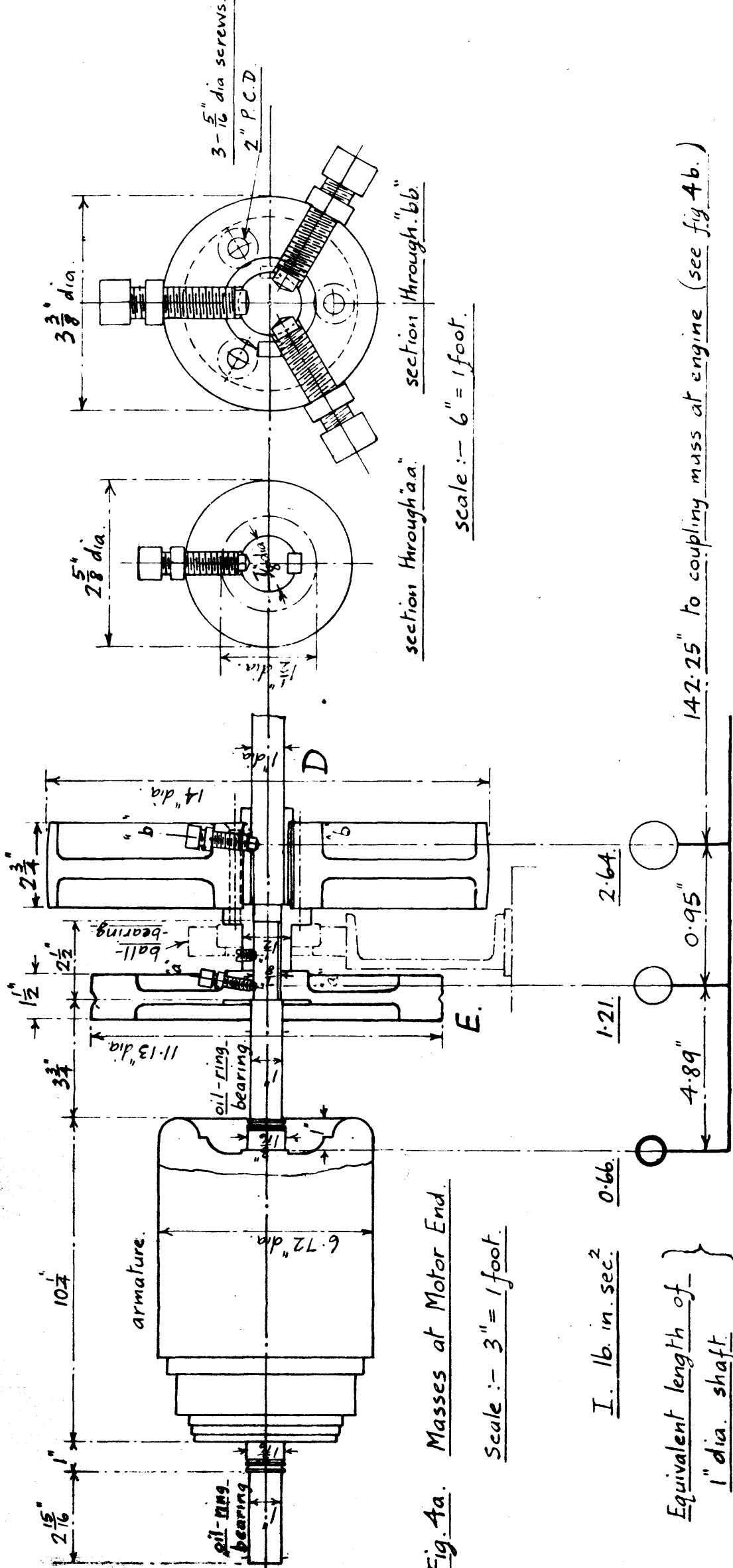


Fig. 4a. Masses at Motor End.

Scale :- 3" = 1 foot.

I. lb. in. sec.² 0.66.

Equivalent length of
1" dia. shaft

142.25" to coupling mass at engine (see fig 4b.)

Equivalent Dynamical System at Motor.

Torsiograph positions D. 1.03"

Effective diameters. E. 11.2"

D 1.03" { distance along shaft measured from pins at section 'bb' }

E 11.2"

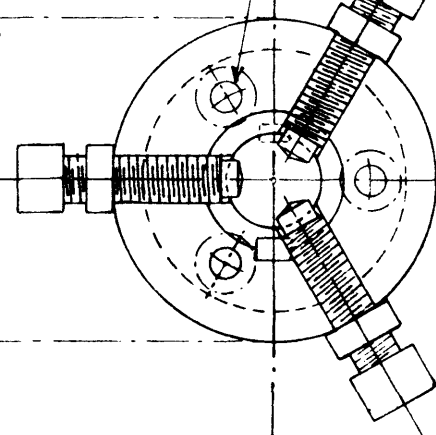
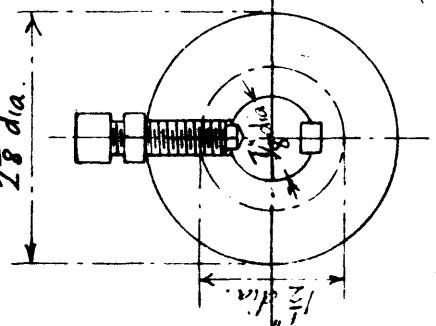
section through 'aa' section through 'bb'

scale :- 6" = 1 foot.

3 3/8" dia.

3-5/16" dia screws.
2" P.C.D.

5" dia.



bearing. Fig. 2 shows the gravity feed supply. The connecting rods had been designed for splash lubrication, but with constant dismantling this was not considered consistent, so the oil sump was removed and the lubrication of the rods left to deteriorate to the boundary film type.

INERTIA MEASUREMENT.

(a) Rotating Parts. The Polar moment of inertia of all rotating masses was determined by the Bifular Suspension method and checked by calculation where possible. Strong cord suspended from a cross-girder was used to support a carrier into which the object could be centered with its longitudinal axis vertical. The length l of the suspension was approximately 10 ft., but this varied with the weight on the carrier. The distance r from the axis to the points of attachment of the cords was $11\frac{15}{16}$ in.. By vibrating through a small angle the time to complete 100 vibrations could be found to within a fraction of a second for three trials.

The polar moment of inertia I was then obtained from usual equation :-

$$T = 2\pi \sqrt{\frac{I_2 l}{(W+w) r^2}}$$

where T = time of one oscillation.

I_2 = M of I of carrier + M or I of object.
 = $i + I$

w = weight of carrier.

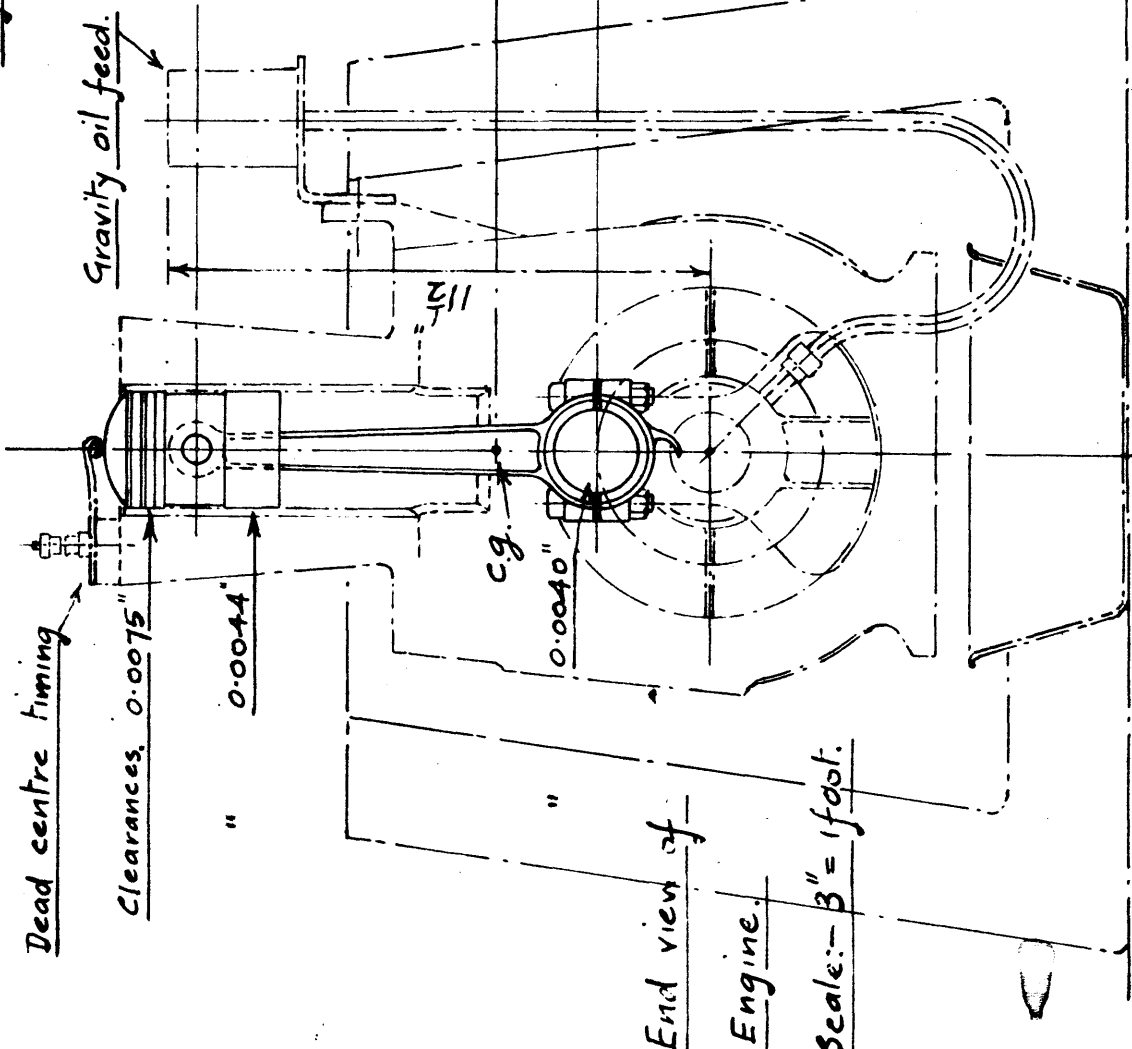
W = " " object.

The results of all rotating masses are given in the following table:

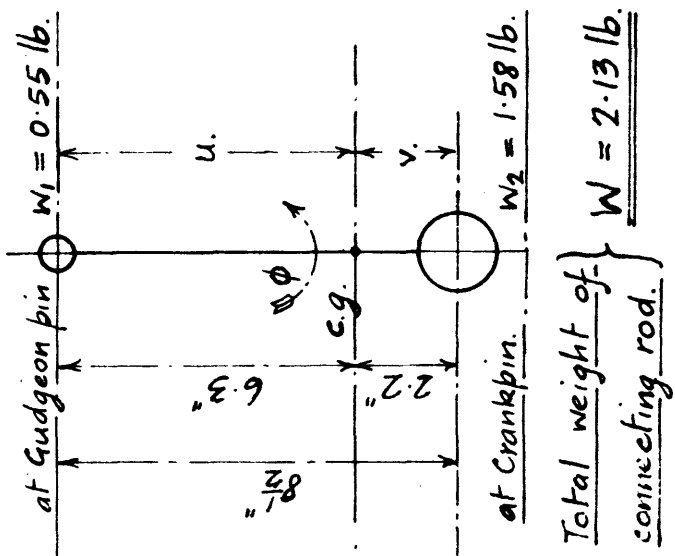
Inertia of Rotating Masses.

Part.	Weight lbs.	Polar Moment of Inertia lb. in. sec ² .
Armature.	47.01	0.660
Armature Flywheel.	25.00	1.21
Pulley flywheel.	36.75	2.64
Flanged Coupling.	6.98	0.09
17" split pulley	8.13	0.880
12" " "	5.40	0.241
11" " "	4.70	0.165
Crankshaft	39.00	0.422
Wooden pulley	3.05	0.007

Fig. 4c



Equivalent Dynamical System for Connecting Rod.



$$\left(\frac{\text{radius of gyration}}{\text{about c.g.}} \right)^2 = k^2 = 10.85 \text{ in}^2$$

$$I. \text{ about c.g.} = \frac{W}{g} k^2 = 0.0599 \text{ in.lb.sec}^2$$

$$\left. \begin{aligned} \text{Apparent } I \text{ about c.g.} \\ \text{with simple two-mass} \\ \text{substitution.} \end{aligned} \right\} = \frac{W}{g} u.v. = 0.0765 \text{ in.lb.sec}^2$$

$$\text{Correction couple. } T = -\frac{W}{g} (k^2 - uv) \ddot{\phi}$$

Piston mass and gudgeon pin = 1.16 lb \therefore Equivalent reciprocating mass = 1.71 lb.

$$\left. \begin{aligned} \text{Equivalent } I_p \text{ of piston and} \\ \text{conn. rod about crank-} \\ \text{-shaft. in.lb.sec}^2 \end{aligned} \right\} = \left\{ \begin{aligned} 0.0352 + 0.0036 \cos \theta - 0.0132 \cos 2\theta \\ - 0.0036 \cos 3\theta \end{aligned} \right.$$

Connecting Rods. The c.g. of each rod was obtained by the knife edge test. For the radius of gyration about the c.g. the rods were treated as compound pendulums and the oscillation method employed.

Suspending the rod by the knife edge in the small end bush, the periodic time for 100 vibrations was found, and the radius of gyration k determined from

$$t = 2\pi \sqrt{\frac{k^2 + x^2}{gx}}$$
 where x is the distance from the point of suspension to the c.g., and g the

gravitational constant. Repeating the process by suspending the rod on the knife edge at the big end bush, a similar value for k was found. All four rods were treated thus and the average of the eight values of k^2 was found to be 10.85 in².

Reduction of Connecting Rod. Before reducing the piston and connecting rod to an equivalent polar moment of inertia, it is convenient to substitute an equivalent dynamical system for the connecting rod. The usual two mass substitution, together with a correction couple is adopted in the reduction as explained by Kerr⁹. The rod is thus equivalent to a mass w_1 reciprocating with the piston and a mass w_2 rotating with the crankpin such that $w_1 u = w_2 v$ where u and v are the distance of the masses from the c.g. of the rod.

This, however, gives an apparent moment of inertia for the rod about the c.g. of $\frac{W}{g} uv$, in place of the correct value $\frac{W}{g} k^2$, W being the weight of the rod. It is therefore necessary to introduce a correction couple $T = -\frac{W}{g}(k^2 - uv)\ddot{\phi}$ acting on the rod, where $\ddot{\phi}$ is the angular acceleration of the rod.

Fig. 4c gives particulars of this reduction.

On the basis of kinetic energy the complete piston line can now be reduced to an equivalent polar moment of inertia using the expressions given by Cormac¹⁰.

9. Kerr, Trans. Inst. Eng. Ship. Scotland. 1927 - 28.
 10. Cormac, "A Treatise on Engine Balance using Exponentials".

RECIPROCATING MASSES.

The Kinetic energy of the reciprocating masses is :-

$$\frac{1}{2} mv^2 = \frac{1}{2} m\omega^2 r^2 (e_0 + e_1 \cos \theta + e_2 \cos 2\theta + e_3 \cos 3\theta + \dots)$$

$$= \frac{1}{2} I_r \omega^2$$

where I_r is the equivalent polar moment of inertia;

hence $I_r = mr^2 (e_0 + e_1 \cos \theta + e_2 \cos 2\theta + e_3 \cos 3\theta + \dots)$

For crank/conn. rod ratio $\lambda = 0.2795$ the values of e_0, e_1, e_2 etc., are :-

e_0	e_1	e_2	e_3	e_4	e_5	e_6	e_7
0.51016	0.14251	-0.50021	-0.14395	-0.01015	0.00147	0.00021	-0.00002

From Fig. 4c the equivalent reciprocating masses are

1.71 lb. hence the equivalent polar moment is :-

$$I_r \left. \begin{matrix} \text{lb. in. sec}^2 \end{matrix} \right\} = 0.01275 + 0.00356 \cos \theta - 0.0125 \cos 2\theta - 0.0036 \cos 3\theta - 0.00025 \cos 4\theta + \dots$$

CORRECTION COUPLE.

$$\left. \begin{matrix} \text{Kinetic energy} \end{matrix} \right\} = \frac{1}{2} \frac{W}{g} (uv - k^2) \dot{\phi}^2 = \frac{1}{2} \frac{W}{g} (uv - k^2) \omega^2 (s_0 + s_2 \cos 2\theta + s_4 \cos 4\theta + \dots)$$

$$= \frac{1}{2} \frac{W}{g} (uv - k^2) \omega^2 (-0.03982 - 0.03901 \cos 2\theta + 0.00079 \cos 4\theta - 0.00002 \cos 6\theta - \dots)$$

$$= \frac{1}{2} I_c \omega^2$$

where I_c is the equivalent polar moment of inertia due to the correction couple. From particulars on Fig. 4c

this becomes :-

$$\left. \begin{matrix} I_c \\ \text{lb. in. sec}^2 \end{matrix} \right\} = -0.00066 - 0.000647 \cos 2\theta + 0.00001 \cos 4\theta - \dots$$

$$\therefore \left. \begin{matrix} I_r + I_c \\ \text{lb. in. sec}^2 \end{matrix} \right\} = 0.01209 + 0.00356 \cos \theta - 0.01315 \cos 2\theta - 0.00360 \cos 3\theta - 0.00024 \cos 4\theta - \dots$$

Big End Rotating Mass.

$$I = \frac{W_2 r^2}{g} = \frac{1.58 \times 5.64}{386} = 0.0231 \text{ lb. in. sec}^2$$

Hence the polar moment of inertia for the piston and connecting rod is :-

$$I_p \text{ lb. in. sec}^2 = 0.0352 + 0.0036 \cos \theta - 0.0132 \cos 2\theta - 0.0036 \cos 3\theta - 0.0002 \cos 4\theta - \dots$$

TORSIONAL RIGIDITIES.

(a) Extension Shafting. It is seen from the general view of the plant in Fig. 1 and from the details in Fig. 4 that as arranged, the main torsional flexibility is provided by the long 1 inch diameter shafting.

Reversed torsion tests were carried out on a 15,000 in. lb. Avery machine with the object of detecting hysteresis on a length of 1 in. diameter bar from the same material. From these tests, which are reported later in page 46, the elastic properties are :-

Modulus of Rigidity 12.0×10^6 lb. per in².

Shear stress at limit of proportionality 13.2 ton per in².

The reduction of the flexible parts beyond the pulley flywheel, Fig. 4, to equivalent lengths of 1 in. diameter, can be calculated with little difficulty since it comprises circular sections. As these parts are short and rigid, any errors made in the assumptions will have negligible effect on the final result.

Beginning at the countersunk pins, where the shafting flexibility is assumed to finish, the flexibility comprises that of the pulley boss, flange of the sleeve, and sleeve up to the pins. From there on to the armature flywheel the rigidity is the composite effect of the heavily keyed shaft and flywheel boss, after which the armature shaft is simple and straightforward.

Reducing to an equivalent 1 in. diameter shaft this is approximately 4.89 in. from armature mass to the flywheel and 0.95 in. from the flywheel to the belt pulley. Thus the two flywheels may be combined as one mass, connected to the armature by a length equivalent to 5.4 in.

At the engine end, the shaft elasticity in the flanged coupling which has double keys, can be reasonably assumed to be effective in the boss for a length equal to the shaft diameter. The flexibility of the coupling is taken as that of the boss slightly stiffened by the flange.

(b) Crankshaft. The crankshaft is of the four-throw-two-bearing type, and is relatively stiff compared to the long extension shaft. Nevertheless, since the vibrations at resonance would be most severe at the crankshaft, and important damping forces would also

appear at the bearings, several problems arise which must be investigated. It was therefore considered essential at this stage to examine the flexibility of the crankshaft in detail.

As shown in Figs. 4 and 5 the forward journal is fitted in a roller bearing 1 in. long, having a push-fit clearance of 0.0004 in. and the aft journal is supported in a plain white metal lined bearing $4\frac{1}{2}$ in. long with a running clearance of 0.0025 in. Thus the aft journal will have a maximum lateral displacement in its bearing of the order of 0.0013 in. which value will be reduced by oil film thickness. It was decided therefore to measure the twist with the shaft in its own bearings.

- Experimental -

Method of applying Torque. With the engine casing bolted to the heavy baseplate, a secure foundation was provided. Facilities were also available for securing the forward end of the shaft to the engine casing by means of a flange, keyed to the shaft and bolted to the casing, as shown in Fig. 5. At the aft end the torque is applied at the original flywheel which is keyed to the tapered portion of the shaft. Since the keys are of the Woodruff type and a sliding fit is employed in each case, the length of the shaft under torque is equal to the length between the centres of the keys.

In order to apply a pure torque to the shaft in place a special gear had to be arranged. This ultimately took the simple form shown in Fig. 6. Two ropes carried by a wooden beam are attached to the circumference of the flywheel, one directly and the other after passing round a ball-bearing pulley secured to the baseplate. The beam is carried by a rope passing over a support pulley and is balanced by a similar beam which acts as a weight carrier. Both beams are supported by pulleys with hook-attachments

to ensure further the application of pure torque.

The support pulley was secured to a roof girder.

Method of Measuring Angle of Twist. The method adopted for observing the angle of twist is that of measuring the travel of a spot of light on a scale reflected by a mirror attached to the shaft. Although the forward end of the crankshaft is bolted to the engine frame, it is necessary to fit mirrors at both ends in order to eliminate the deflection of the frame itself.

Two pieces of $\frac{5}{8}$ in. outside diameter tubing were employed, one fastened to the flywheel and the other forward of the fixed end, as shown in Fig. 6. The tubing was set to hold adjustable mirrors of a Martens mirror extensometer at a suitable distance apart for the telescopes, and was stiff enough not to be affected by vibration. The mirrors were carefully set in the vertical plane passing through the axis of the shaft. Two telescopes and scales were arranged as in the Martens extensometer arrangement. The difference between the readings from each mirror at each small increment of torque gives the angle of twist for that increment on a length equal to the distance between the centres of the keys, when multiplied by the constant depending on the scale distance.

Frictional Effort. Since the method of applying the torque involves a fair amount of friction both in the pulley gear and in the shafting, a preliminary experiment is necessary to determine the law of frictional effort. The only changes made to the apparatus to accomplish this were the freeing of the shaft at the forward end and the introduction of a spring balance as shown in Fig. 7. Observations were made of loads and corresponding balance readings for progressive steps of 20 lb. load. Similar readings were taken during unloading. On unloading the relation between the loads and the spring balance reading is, of course, valid only when the energy stored in the

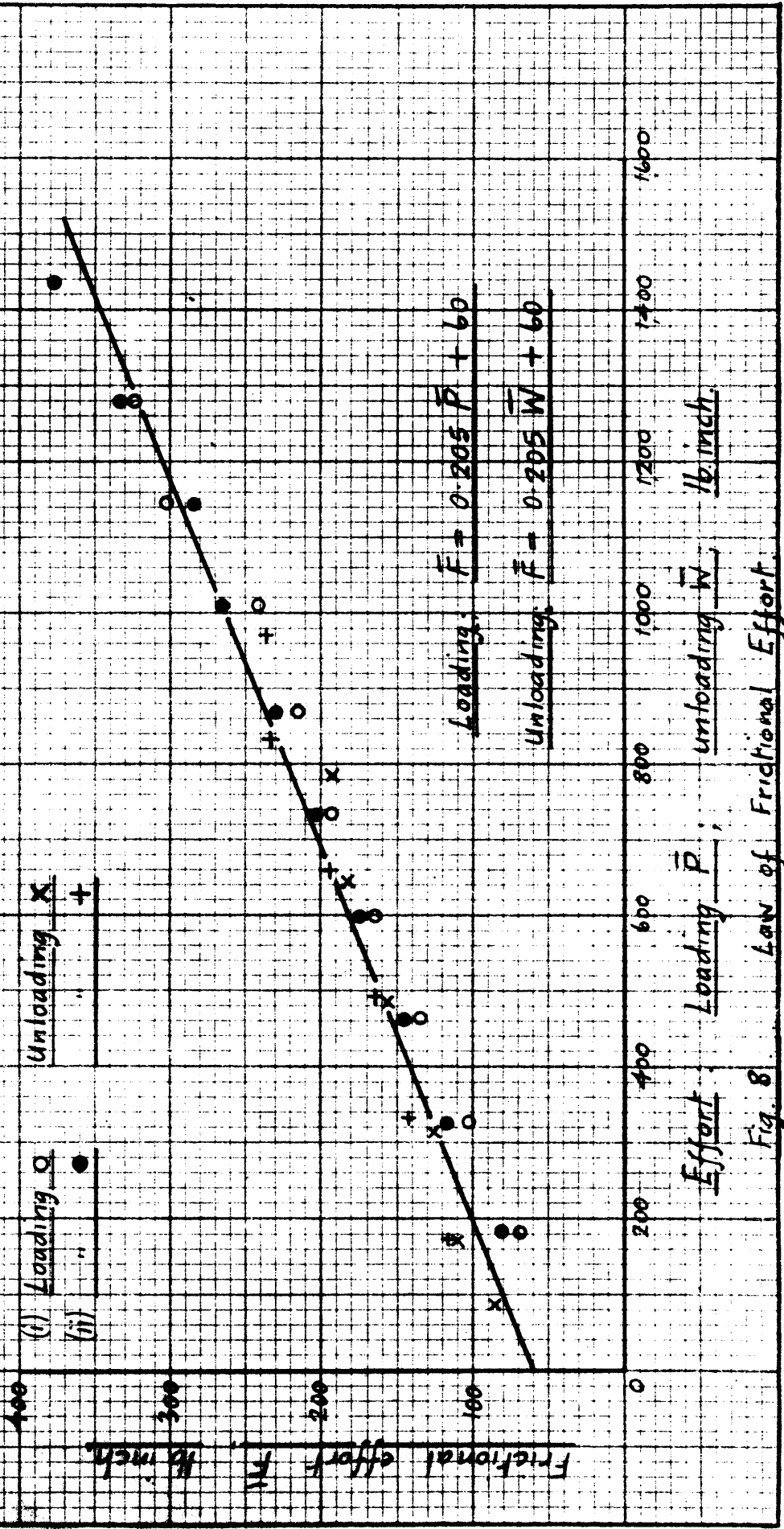


Fig. 8 Law of Frictional Effort

spring overcomes the frictional effort. The spring balance had an open scale reading from 0 to 300 lb., and a calibration showed an error of only ± 0.25 lb.

Two trials were made and the plotting of the results as in Fig. 8 gives the law of frictional effort as :-

$$\text{Loading :- } \bar{F} = 0.205 \bar{P} + 60.$$

$$\text{Unloading :- } \bar{F} = 0.205 \bar{W} + 60$$

where \bar{F} is the frictional effort, lb. in. and \bar{P} and \bar{W} are the efforts for loading and unloading respectively.

Torsion Experiments. Two tests were made with the scale distance changed in each case. In each test the load was gently applied in steps of 20 lb., and the corresponding mirror readings noted until a torque was obtained which was considered to give the limiting safe stress on the shaft. The load was taken off in steps of 20 lb.

The readings were reduced to the effective torque applied to the shaft from the frictional effort equation. The final result of the effective torque is plotted on a base of angle of twist in Fig. 9, where it is seen that two experimental curves are obtained, one for loading and the other for unloading, both having practically the same gradient.

The two curves also show an apparent initial twist but this, however, does not exist. Since only the gradient of these curves is required, a corrected line can be drawn through zero to represent the gradient for both curves. Thus the experimental relation between the effective torque and the angle of twist for the gauge length between the centres of the keys may be expressed by $\theta = 0.1530$ degrees per 1,000 lb. in. torque.

CRANKSHAFT BY ANALYSIS. In order to determine the effects of constrained lateral displacement of the journals for the extreme conditions of no constraint and

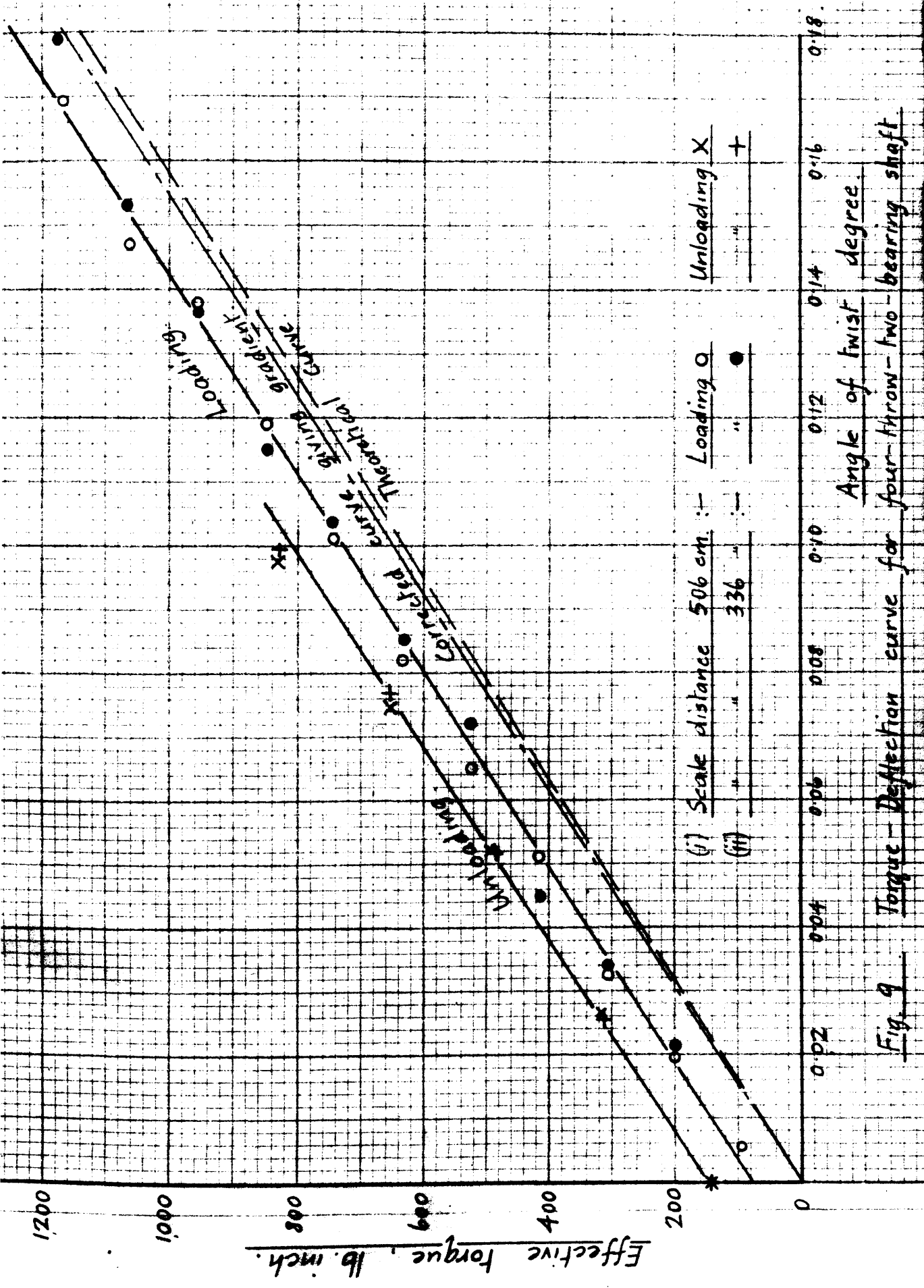


Fig. 9 Torque-Deflection curve for four-throw-two-bearing shaft

of complete constraint at the bearings, an analysis, which is a development of that used by Timoshenko¹¹ for the simple crank, is given.

Before the analysis can be accomplished, it will be assumed that the actual crankshaft has been reduced to a simplified form consisting of plain webs, journals and pins as shown in Fig. 10. These reductions will be discussed later. For the simplified form the following terms are used :-

$$\theta = \frac{M\ell}{C}, \text{ where } C = GJ.$$

$$C_0 = GJ_0 = \frac{\pi}{32} d_0^4 G = \text{torsional rigidity of equivalent shaft of diameter } d_0 \text{ and length } \ell_0.$$

$$C_1 = GJ_1 = \frac{\pi}{32} d_1^4 G = \text{torsional rigidity of journal.}$$

$$C_2 = GJ_2 = \frac{\pi}{32} d_2^4 G = \text{torsional rigidity of outer crankpin.}$$

$$C_3 = GJ_3 = \quad \quad \quad = \text{torsional rigidity of centre crankpin.}$$

$$C_4 = GJ_4 = \text{torsional rigidity of the outer web twisting about } O_1O_1. \text{ This rectangular cross-section is arbitrarily chosen with sides } r \text{ and } c \text{ to take approximate account of the local yielding of the webs at the juncture of the pins and webs.}$$

$$\therefore J_4 = \frac{c_1^3 r^3}{3.6[c_1^2 + r^2]}$$

$$C_5 = GJ_5 = \text{torsional rigidity of the inside webs about } O_2O_2, \text{ where}$$

$$J_5 = \frac{c_2^3 (2r)^3}{3.6[c_2^2 + (2r)^2]}$$

$$C'_4 = GJ'_4 = \text{torsional rigidity of web, twisting about } p_1p_1. \text{ Again the cross-section is rectangular having sides } h_1 \text{ and } c_1, \text{ hence :-}$$

$$J'_4 = \frac{c_1^3 h_1^3}{3.6[c_1^2 + h_1^2]}$$

$$C'_5 = GJ'_5 = \text{torsional rigidity of web twisting about } p_2p_2.$$

$$J'_5 = \frac{c_2^3 h_2^3}{3.6[c_2^2 + h_2^2]}$$

$$B_2 = EI_2 = \frac{\pi}{64} d_2^4 E = \text{flexural rigidity of the outer crankpin.}$$

11. Timoshenko, Trans. Amer. Soc. Mech. Eng. 1922.

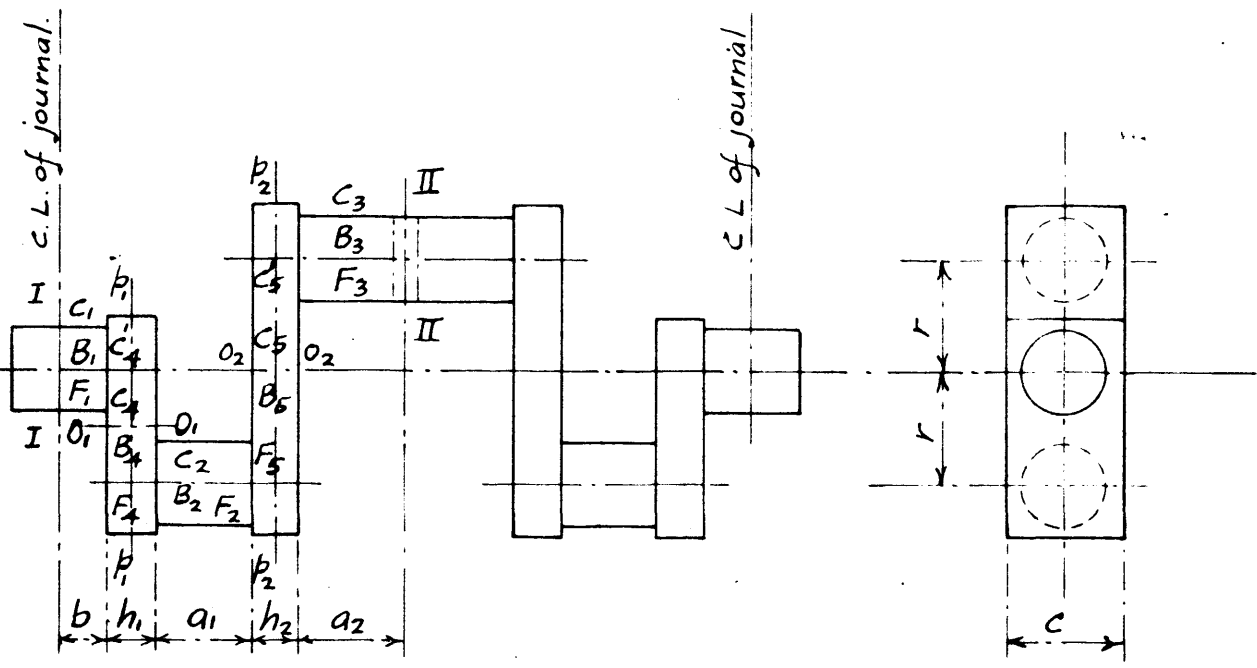


Fig. 10. Simplified form of shaft showing constants.

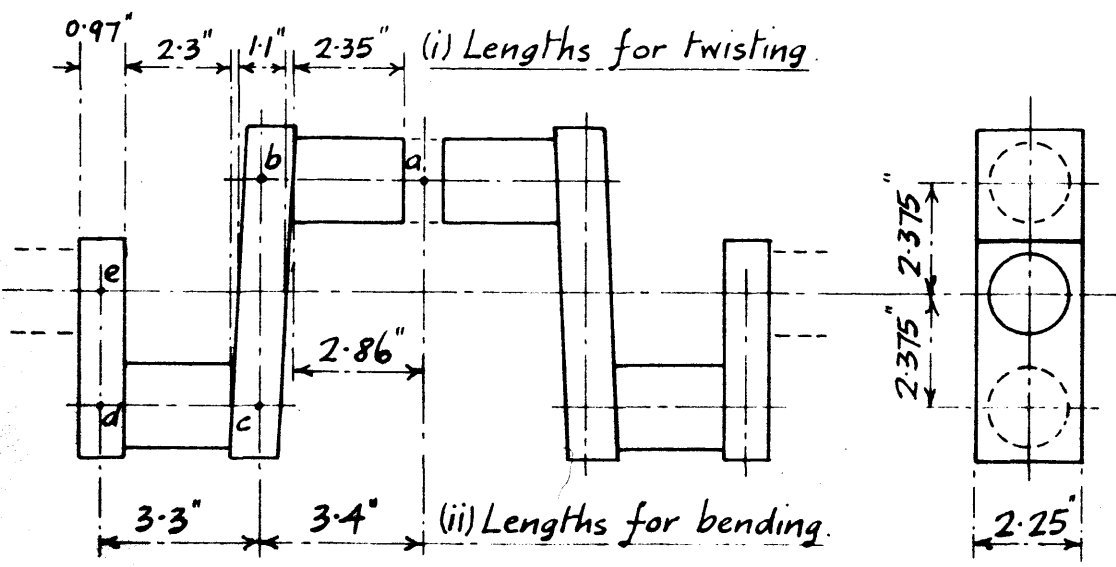


Fig. 13. Simplified shaft showing lengths for (i) twisting of pins and bending of webs and (ii) bending of pins and twisting of webs.

$$B_3 = EI_3 \left. \begin{array}{l} \\ = \frac{\pi}{64} d_2^4 E \end{array} \right\} = \text{flexural rigidity of the inner crankpin.}$$

$$B_4 = EI_4 \left. \begin{array}{l} \\ = \frac{h_1 c_1^3}{12} E \end{array} \right\} = \text{flexural rigidity of outer webs with respect to bending in plane } p_1 p_1 \text{ perpendicular to plane of figure.}$$

$$B_5 = EI_5 = \frac{h_2 c_2^3}{12} E = \text{ " " " " plane } p_2 p_2 .$$

$$F_2 = \frac{\pi}{4} d_2^2 = \text{cross-sectional area of outer pin.}$$

$$F_3 = \text{ " " " " " " " " centre pin.}$$

$$F_4' = h_1 \times c_1 = \text{cross-sectional area of outer web taken on } O_1 O_1 .$$

$$F_5' = h_2 \times c_2 = \text{cross-sectional area of inner web taken on } O_2 O_2 .$$

$$F_4 = r \times c_1 = \text{assumed cross-section of outer web taken on } p_1 p_1 .$$

$$F_5 = (2r) \times c_2 = \text{assumed cross-section of inner web taken on } p_2 p_2 .$$

Twist of Free Shaft. - No Bearing Restraint - Fig. 11

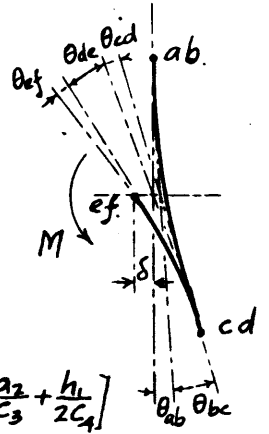
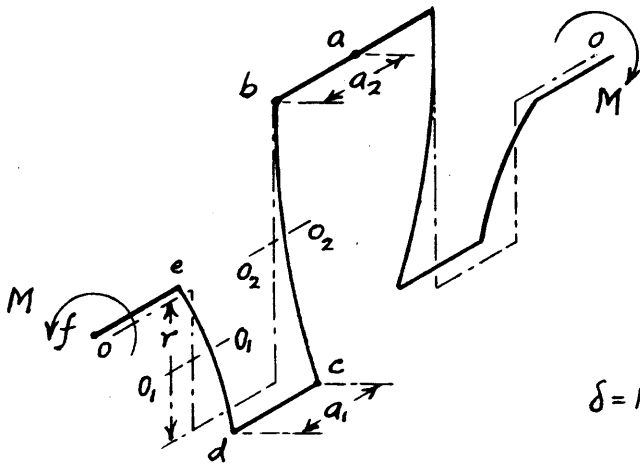
shows a diagrammatic sketch of the crankshaft with twisting moments M applied at the centre line of the journals, and Fig. 11a, gives a side view of the deformed shaft. The total twist of the half shaft a to f consists of the sum of the angular deformations of the portions ab , bc , cd and ef . The journal and pins are subjected to pure torsion while the webs are merely under the influence of bending.

The angle of twist for each portion is then :-

$$\theta_{ab} = Ma_2/c_3 ; \quad \theta'_{bc} = Mh_2/c_5 ; \quad \theta_{cd} = Ma_1/c_2 ;$$

$$\theta'_{de} = Mh_1/c_4 ; \quad \theta_{ef} = Mb = C_1$$

while the angular deflection due to the bending of each web is equal to the angle between the tangents to the curve of flexure at its ends. Since the bending moment



$$\delta = Mr \left[\frac{r}{2B_1} + \frac{a_1}{C_2} - \frac{a_2}{C_3} + \frac{h_1}{2C_4} \right]$$

Side View of half shaft.

Fig. 11. Free shaft under pure torque.

is equal to the twisting moment M and is constant at each cross-section, the curve of flexure of the web is a circle. The torsional displacement, when the web is considered as a beam of length (i) $2r$ and (ii) r , is then :-

$$\theta''_{bc} = \frac{2Mr}{B_5} ; \quad \theta''_{de} = \frac{Mr}{B_4}$$

Reducing this to an equivalent shaft of uniform diameter having the same torsional rigidity where $\theta_o = \frac{M\ell_o}{C_o}$, we get :-

$$\ell_o \text{ for half shaft, a to f} = C_o \left\{ \frac{a_2}{C_3} + \frac{h_2}{C_5} + \frac{a_1}{C_2} + \frac{h_1}{C_4} + \frac{b}{C_1} + \frac{2r}{B_5} + \frac{r}{B_4} \right\} \dots (1)$$

Lateral Deflection of Journals for Free Shaft.

The lateral deflection of the journals due to torque on the free shaft is easily obtained by considering the effect on the journals due to each component part.

Thus for the half shaft :-

- (1) the twist $\frac{Ma_2}{C_3}$ of the centre pin ab causes a lateral displacement at the journal of :- $-\frac{Ma_2r}{C_3}$;
- (2) the twist Ma_1/C_2 of the outer pin cd causes a lateral displacement at the journal of :- $+\frac{Ma_1r}{C_2}$;
- (3) the bending of the centre web bc and the twisting about O_2O_2 causes no lateral displacement at the journal ;
- (4) the bending of the outer web de and the twisting about O_1O_1 causes a lateral displacement at the journal of $+\frac{Mr^2}{2B_4}$ and $+\frac{Mh_1r}{2C_4}$ respectively.

The net lateral deflection of the journals for the complete shaft is then :-

$$2\delta = \frac{Mr^2}{B_4} + 2Mr \left\{ \frac{a_1}{C_2} - \frac{a_2}{C_3} + \frac{h_1}{2C_4} \right\} \dots (2)$$

occurring in a plane perpendicular to the plane of the throw.

Effect of Complete Bearing Restraint. If this lateral displacement is restrained by the bearings, additional forces and couples are introduced, involving a force A and a moment M_1 at each journal, acting in the plane

Fig. 12. Shaft under pure torque with complete bearing constraint.

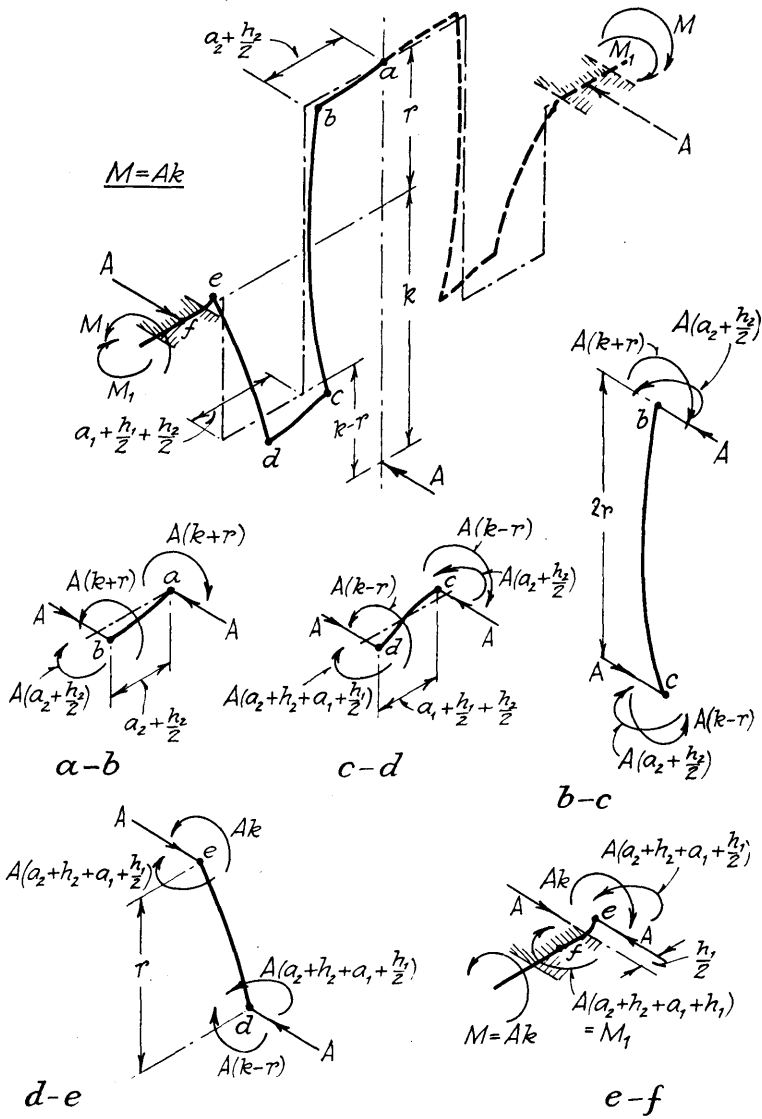


Fig. 12a. Forces and Couples on each component.

(3) Pin c-d.

$$(i) \text{ Torsion of pin} = \frac{(M - Ar)^2 a_1}{2C_2} \quad \text{--- (10)}$$

$$(ii) \text{ Bending of pin} = \int_0^{a_1} \frac{\{A(a_2 + h_2) + Ax\}^2 dx}{2B_2}$$

$$= \frac{A^2}{2B_2} \left\{ \frac{1}{3} a_1^3 + a_1^2 (a_2 + h_2) + a_1 (a_2 + h_2)^2 \right\} \quad \text{--- (11)}$$

$$(iii) \text{ Shear of pin} = \frac{\gamma A^2 a_1}{2GF_2} \quad \text{--- (12)}$$

(4) Web d-e

$$(i) \text{ Twist of web} = \frac{\{A(a_2 + h_2 + a_1 + \frac{1}{2}h_1)\}^2 r}{2C_4} \quad \text{--- (13)}$$

$$(ii) \text{ Bending of web} = \int_0^r \frac{(M - Ay)^2 dy}{2B_4}$$

$$= \frac{M^2 r - MAr^2 + \frac{1}{3}(A^2 r^3)}{2B_4} \quad \text{--- (14)}$$

$$(iii) \text{ Torsion of web about } O, O = \frac{(M - \frac{1}{2}Ar)^2 h_1}{2C_4} \quad \text{--- (15)}$$

$$(iv) \text{ Shear of web} = \frac{\gamma A^2 r}{2GF_4} + \frac{\gamma A^2 h_1}{2GF_4} \quad \text{--- (16)}$$

The strain energy of the half shaft a to e is then the sum of the terms (3) to (16).

Considering complete constraint at the bearings, the displacement due to A is zero, and therefore $\frac{\delta\phi}{\delta A} = 0$. Differentiating the strain energy and substituting $M = Ak$,

we obtain:-

$$k = \frac{\left\{ \frac{a_2 r}{C_3} + \frac{a_2^3}{3rB_3} + \frac{2(a_2 + \frac{1}{2}h_2)^2}{C_5} + \frac{2r^2}{3B_5} + \frac{a_1 r}{C_2} + \frac{1}{rB_2} \left[\frac{1}{3} a_1^3 + a_1^2 (a_2 + h_2) + a_1 (a_2 + h_2)^2 \right] \right.}{\left. + \frac{(a_2 + h_2 + a_1 + \frac{1}{2}h_1)^2}{C_4} + \frac{r^2}{3B_4} + \frac{rh_1}{4C_4} + \frac{\gamma a_2}{rGF_3} + \frac{2\gamma}{GF_5} + \frac{\gamma h_2}{rF_5 G} + \frac{\gamma a_1}{GF_2 r} + \frac{\gamma}{GF_4} + \frac{\gamma h_1}{rGF_4} \right\}}$$

$$\div \left(\frac{a_1}{C_2} + \frac{r}{2B_4} + \frac{h_1}{2C_4} - \frac{a_2}{C_3} \right) \quad \text{--- (17)}$$

Also, since $\frac{\delta\phi}{\delta A} = 0$, the angle of twist $\theta = \frac{\delta\phi}{\delta M}$. Differentiating and expressing A in terms of k, we obtain:-

$$\theta = M \left\{ \frac{\left(1 + \frac{r}{k}\right) a_2}{C_3} + \frac{2r}{B_5} + \frac{h_2}{C_5} + \frac{\left(1 - \frac{r}{k}\right) a_1}{C_2} + \frac{r}{B_4} \left(1 - \frac{r}{2k}\right) + \frac{\left(1 - \frac{r}{2k}\right) h_1}{C_4} \right\} \quad (18)$$

or from $\theta = M_o l_o / C_o$ the equivalent length is :-

$$l_o = C_o \left\{ \frac{\left(1 + \frac{r}{k}\right) a_2}{C_3} + \frac{2r}{B_5} + \frac{h_2}{C_5} + \frac{\left(1 - \frac{r}{k}\right) a_1}{C_2} + \frac{r}{B_4} \left(1 - \frac{r}{2k}\right) + \frac{\left(1 - \frac{r}{2k}\right) h_1}{C_4} \right\} \quad \text{--- (18a)}$$

These results were checked by applying the slope deflection method to each component. Complete agreement was obtained. For the condition of no bearing constraint $k = \infty$ or $A = 0$. Hence, the substitution of $k = \infty$ in (18a) reduces that equation to the expression (1) for the free shaft.

Similarly the factor k for the single-throw-two-bearing shaft, if completely restrained, can be determined from equation (17) by substituting a_2 and $h_2 = 0$ and applying the force A at the plane passing through the centre of pin a_1 . This reduces exactly to Timoshenko's¹¹ formula.

Reduction of shaft to simplified form. Reductions to a simplified form must be made before the equations are applied. Some of the simplifications used are arbitrary—such as dispensing with facings and slightly increasing the journals and pins to account for the local yielding in the webs at their point of juncture. Such effects cannot be determined exactly owing to the changes in section and direction, but certain points which act as a guidance may be noted.

For instance, in order to determine the value of the bearing restraint correctly, it will be necessary to retain the same longitudinal spacing, i.e., the distance from the point "a", Fig. 11. to the centre line of webs must be the same as in the actual case so as to cover exactly the bending of pins and the torsion of webs. In this case, therefore, there will be two sets of dimensions to be applied simultaneously in the equations, one for the twisting of the pins and the bending of the webs, and the other for the bending of the pins and the twisting of the webs. The two sets are shown in Fig. 13. The slight stiffening effect due to the enlargement of the

11. loc. cit.

centre pin at "a" has also been reduced to an equivalent length of uniform diameter.

Calculations - Shaft Values.

$$C_o = \frac{\pi}{32} d_o^4 G = 0.9208 \times 11.8 \times 10^6 = 10.87 \times 10^6 \text{ lb. in}^2 ;$$

$$d_o = 1.75 \text{ in.}$$

$C_1 = 10.87 \times 10^6 \text{ lb. in}^2$	$B_2 = 13.8 \times 10^6 \text{ lb. in}^2$
$C_2 = \text{ " x " " " }$	$B_3 = \text{ " x " " " }$
$C_3 = \text{ " x " " " }$	$B_4 = 27.6 \times \text{ " " " }$
$C_4 = 47.0 \times \text{ " " " }$	$B_5 = 31.3 \times \text{ " " " }$
$C_5 = 145.0 \times \text{ " " " }$	
$C'_4 = 5.68 \times \text{ " " " }$	$F_2 = 2.41 \text{ in.}^2$
$C'_5 = 7.95 \times \text{ " " " }$	$F_3 = \text{ " " }$
	$F'_4 = 2.18 \text{ "}$
	$F'_5 = 2.48 \text{ "}$
	$F_4 = 5.35 \text{ "}$
	$F_5 = 10.70 \text{ "}$

The coefficient $\gamma = 1.2$

From equation (17) the value of k becomes 285.0 in., hence for complete constraint the equivalent length between the bearings becomes $2\ell_o = 15.072 \text{ in.}$ of 1.75 in. diameter shaft. Also for unconstrained condition,

$$2\ell_o = 15.090 \text{ in.}$$

Gauge Length of Shaft.

Equivalent length between bearings = $\frac{15.08}{\text{diameter shaft}}$ in. of $1\frac{3}{4}$ in.

Forward journal = $1.25 + 0.15 \text{ in.} = \frac{1.40}{\text{diameter shaft}}$ in. of $1\frac{3}{4}$ in.

Extension to centre line of key = 1.25 in. of $\frac{1}{8}$ in. diameter shaft.

$$= \frac{7.32}{\text{diameter shaft}} \text{ in. of } 1\frac{3}{4} \text{ in. diameter shaft.}$$

Aft journal = $5 + 0.15 \text{ in.} = \frac{5.15}{\text{shaft}}$ in. of $1\frac{3}{4}$ in. diameter

Aft journal to centre line of key = 0.93 in. of shaft having taper 1.75 to 1.6 in.
 $= \frac{1.13}{\text{diameter shaft}}$ in. of $1\frac{3}{4}$ in. diameter shaft.

\therefore Gauge length of equivalent shaft = $\frac{30.08}{\text{diameter shaft}}$ in. of $1\frac{3}{4}$ in.

$$\text{Hence } \theta = \frac{M\ell_o}{C_o} = \frac{M \times 30.08}{10.87 \times 10^6}$$

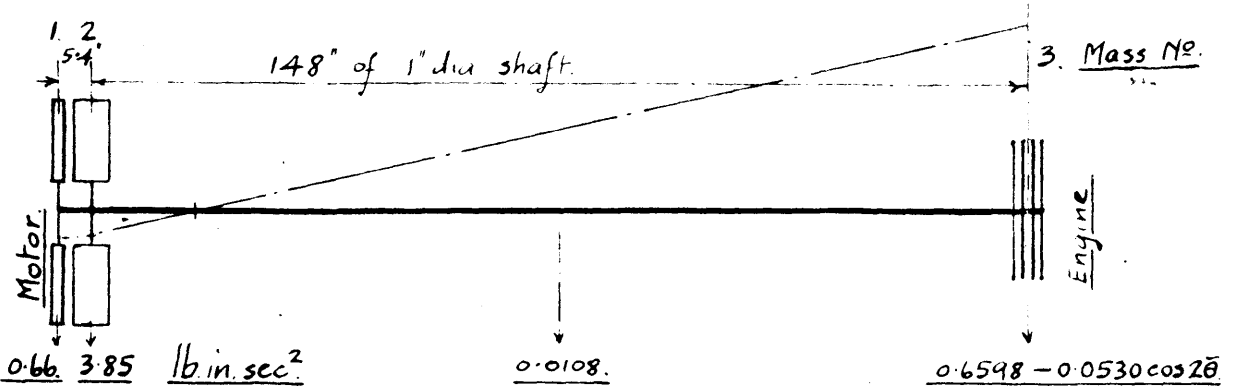
or $\theta = 0.1585$ degrees per 1,000 lb. in. torque. ---(19)

A plot of this result on the graph of experimental values Fig. 9 shows that the curves practically coincide.

Lateral Deflection. Substituting the shaft values in equation (2) the net lateral displacement of the journals for the complete shaft is 0.000232 in. per 1,000 lb. in. torque. The effect of this displacement will be referred to later.

Equivalent Shaft. It will be noticed that with complete constraint the consequent induced web torque is merely 2.35 per cent. of the torque applied at the journals. This small effect, as indicated by the complete analysis, has little or no influence on the torsional rigidity. On further reduction the length of the crankshaft between the bearings is found to be equivalent to 1.607 in. of 1 in. diameter shaft so that all piston lines will vibrate in phase and the engine mass can be considered concentrated at the engine centre line. The remaining portion of shaft from the journal to the coupling is easily reducible and the final reduction of the complete elastic system is shown in Figs. 4a and b.

Fig. 14.



Mass No.	Relative Amplitude
Motor. 1	$\theta_1 = -0.1520$
Flywheels 2	$\theta_2 = -0.1458$
Engine. 3	$\theta_3 = +1.0000$

Mass System M.1.4p.

as three mass system

Natural Frequency 1. node 1123 v.p.m.

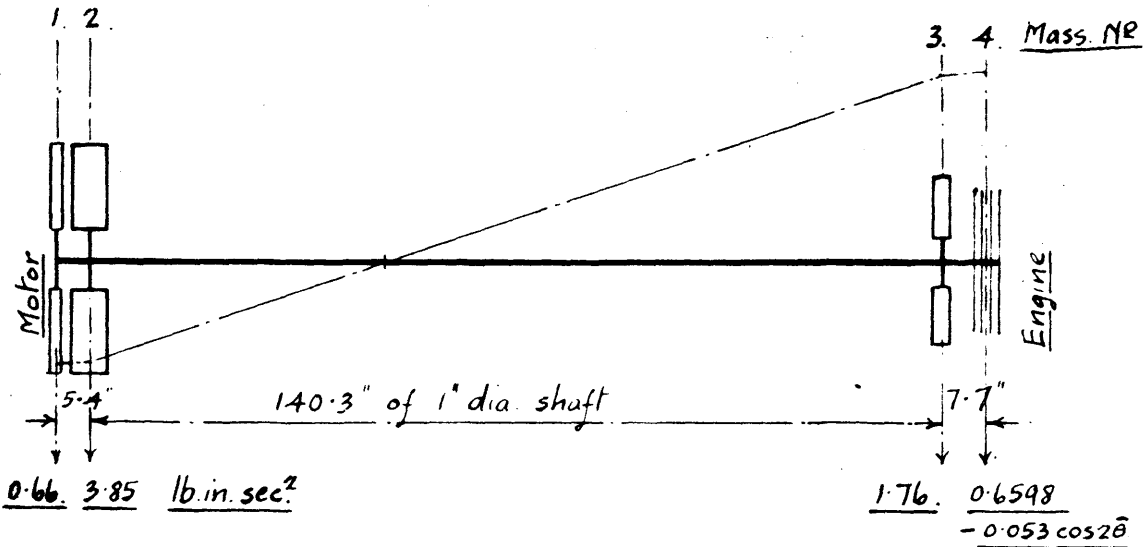


Fig. 15

Mass System M.5.4p.

as a four mass system.

Frequency. 1 node $f = 695.5$ v.p.m

$n = 72.8$ rad/sec.

Mass No.	I lb.in.sec ²	In^2	Relative amplitude θ radian	$In^2\theta$ lb.in.	$\Sigma In^2\theta$ lb.in.	$\frac{GJ}{l} = F$ lb.in/rad	$\frac{\Sigma In^2\theta}{F} = d\theta$
Motor. 1.	0.66	3500	1.0000	3500	3500	218.1×10^3	0.01602
Flywheels 2.	3.85	20,410	0.9840	20,100	23,600	8.4×10^3	2.81
Pulley. 3.	1.76	9,330	-1.8260	-17,050	6,550	153.0×10^3	0.0428
Engine 4	0.66	3500	-1.8688	-6,540	+10.		

Mass Arrangements and Frequency Calculations.

Throughout the experiments the mass at the motor was kept constant, but in order to vary the shaft frequencies, split pulleys were fitted at the engine end. The following notation is adopted for the various mass systems :-

Mass Arrangement.

					Notation.
	No pulleys fitted at engine end.				M1.
12 in. diam. pulley	"	"	"	"	M2.
11 and 12 in. diam.	"	"	"	"	M3.
17 in. diam pulley	"	"	"	"	M4.
2 - 17 in."	"	"	"	"	M5.

To include the number of pistons in each scheme, the corresponding suffix is added. e.g.

M1.1p. ; M1.2p. etc..

With very close reduction it is possible to reduce the M1 group to equivalent three-mass systems. The extreme case M1.4p. is shown in Fig. 14. The frequencies as a three-mass system are :-

One node vibration :- 1123 v.p.m. and two node vibration :- 5950 v.p.m.

In the one node vibration the ratio of amplitudes are :

$$\frac{\theta_1}{\theta_2} = 1.042 \quad \text{and} \quad \frac{\theta_3}{\theta_2} = 6.86$$

Treating as a two-mass system, with masses (1) and (2) combined,

$$f = \frac{60}{2\pi} \sqrt{\frac{7950 \times 5.17}{4.51 \times 0.6598}} = 1123 \text{ v.p.m. as above.}$$

$$\text{Ratio of amplitudes :- } \frac{\theta_3}{\theta_2} = \frac{4.51}{0.6598} = 6.84$$

It is obvious therefore that the assumption of a two-mass system is justified.

In the remaining groups, it was most convenient to fit the pulley masses close to the coupling on the side furthest away from the engine, as shown in Fig. 4b. This slightly modifies the conditions at the engine end and with close reduction a four-mass system is possible.

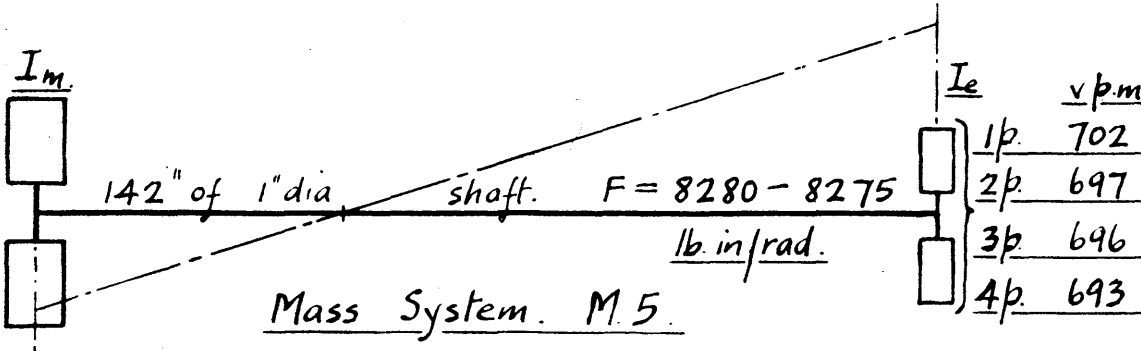
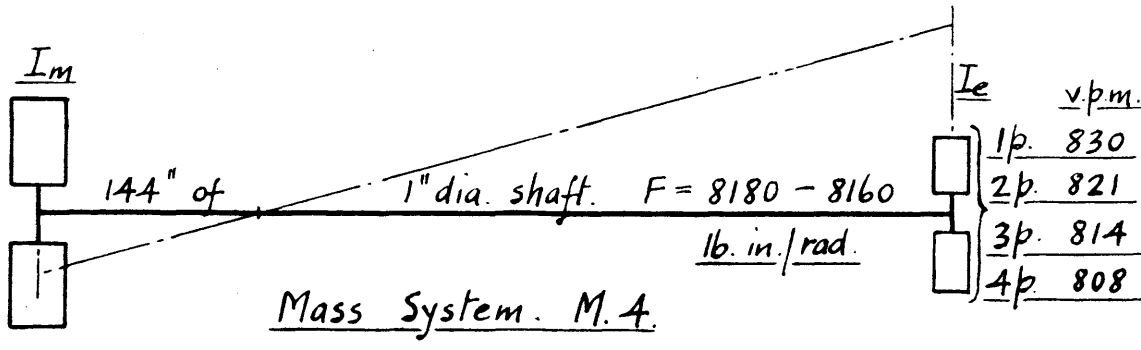
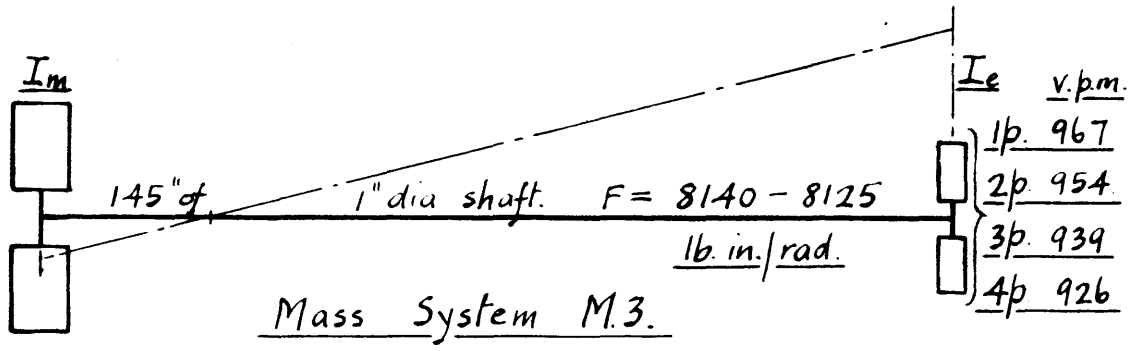
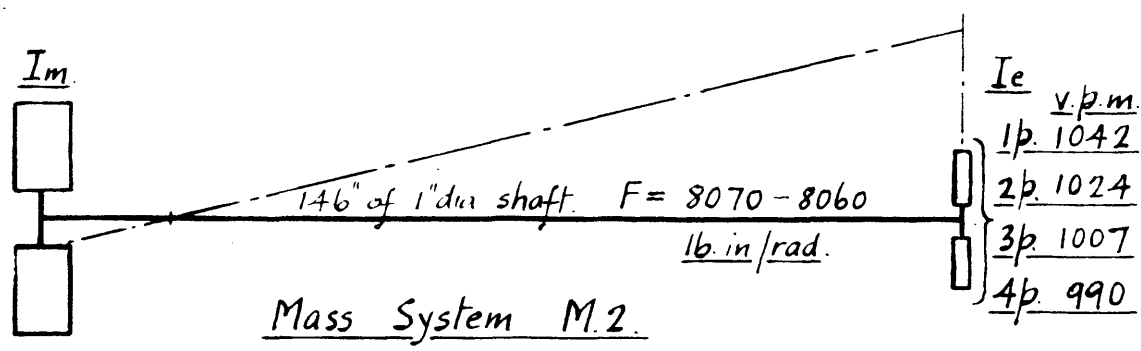
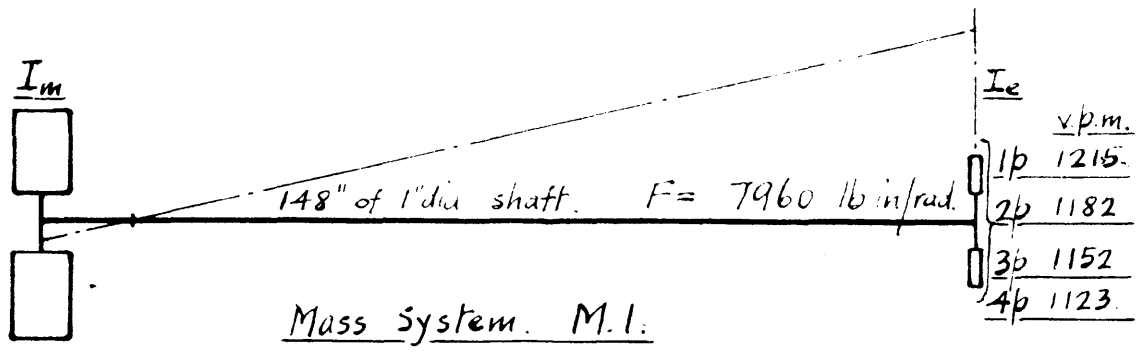


Fig. 16 Equivalent Two-Mass Systems.
Torsional Vibration Forms.

Mass Arrangements as Equivalent Two-Mass Systems.

Frequencies, mass ratios and relative amplitudes.

Table. 1. 1. Piston Series.

Mass at Motor End. $I_m = 4.51 \text{ lb. in. sec}^2$

Mass Arrangement	Mass at Engine. I_e lb. in. sec ²	Mass Ratio:— $\frac{I_m}{I_e} = r$	Equivalent length between masses $\frac{l}{\text{inches}}$	Torsional Flexibility F lb.in/radian	Natural Frequency f v. p. m.	Relative Amplitude $y_e + x_m$.
M.1. 1p.	0.5542	8.14	148	7960	1215	1.123
M.2. 1p.	0.7952	5.66	146	8070	1042	1.177
M.3. 1p.	0.9602	4.7	144.7	8140	967	1.213
M.4. 1p.	1.4342	3.14	143.9	8180	830	1.319
M.5. 1p.	2.3142	1.95	142.1	8280	702	1.513.

Table. 2 2 Piston Series.

Mass at Motor End. $I_m = 4.51 \text{ lb. in. sec}^2$.

M.1. 2p.	0.5894	7.65	148	7960	1182	1.131
M.2. 2p.	0.8304	5.44	146.1	8070	1024	1.184
M.3. 2p.	0.9954	4.53	144.9	8140	954	1.221
M.4. 2p.	1.4694	3.07	144.0	8180	821	1.326
M.5. 2p.	2.3494	1.92	142.2	8280	697	1.521

Table 3 3 Piston Series.

Mass at Motor End. $I_m = 4.51 \text{ lb. in. sec}^2$

M.1. 3p.	0.6246	7.22	148	7960	1152	1.139
M.2. 3p.	0.8656	5.21	146.1	8060	1007	1.192
M.3. 3p.	1.0306	4.37	145.0	8130	939	1.228
M.4. 3p.	1.5046	3.0	144.1	8170	814	1.333
M.5. 3p.	2.3846	1.89	142.3	8275	696	1.529

Table 4 4 Piston Series.

Mass at Motor End $I_m = 4.51 \text{ lb. in. sec}^2$

M.1. 4p.	0.6598	6.84	148	7960	1123	1.146
M.2. 4p.	0.9008	5.01	146.2	8060	990	1.20
M.3. 4p.	1.0658	4.23	145.1	8125	926	1.236
M.4. 4p.	1.5398	2.93	144.2	8160	808	1.341
M.5. 4p.	2.4198	1.865	142.4	8275	693	1.536

Taking the extreme case *M5.4p.*, the final calculation of fundamental frequency is given in tabular form in Fig. 15. The frequency obtained is 695.5 v.p.m. and the ratio of the amplitudes $\frac{\theta_3}{\theta_2} = 1.86$.

As a two-mass system, taking the equivalent masses at the c.g. of the masses at either end, the frequency becomes :-

$$f = \frac{60}{2\pi} \sqrt{\frac{8275 \times 6.93}{4.51 \times 2.42}} = 692.5 \text{ v.p.m.}$$

The ratio of the amplitudes $\frac{\theta_3}{\theta_2} = \frac{4.51}{2.42} = 1.862$.

Hence the two-mass system is again quite approximate as regards frequencies and amplitude ratios.

The complete list of frequencies, mass ratios, rigidities etc., for the equivalent two-mass systems are given in tables 1 to 4, for all the mass arrangements, and the amplitude ratios are indicated in Fig. 16.

Torque Calculations.

In the motor driven system, the important periodic torques are stimulated at the engine by the inertia-resistance of the reciprocating masses and the connecting rods. Periodic variations due to gravity effects and engine frictional torque also arise, and although their effects are generally small it is necessary to examine their relative value. It is convenient to express all the torque effects as a Fourier series. The reduction of the inertia and gravitational torques to this form is given by Cormac¹⁰, Kerr⁹, etc., for a constant speed of rotation ω and may be stated briefly as follows:-

(a) Inertia torque due to Reciprocating Mass.

$T = -\frac{W}{g} \omega \cdot v \frac{dv}{dt}$ in which v is the piston velocity.

Expressed in series form this becomes :

$$T_1 = \frac{W}{g} \omega^2 r^2 \left(t_1 \sin \omega t + t_2 \sin 2\omega t + t_3 \sin 3\omega t + \dots \right) \dots (20)$$

The calculated values for t_1, t_2, t_3, \dots , for the crank/ conn. rod ratio $\lambda = 0.2795$ are :

t_1	t_2	t_3	t_4	t_5	t_6	t_7
0.07125	-0.50021	-0.21593	-0.02030	0.00366	0.00062	-0.00007

(b) Inertia Torque due to Connecting Rod.

By adopting the two-mass substitution and correction couple as explained in page 9, the inertia torque of the rod on the crankshaft can be obtained. Thus the torque due to the equivalent reciprocating mass is given by equ. (20) while the correction couple, expressed as a crankshaft torque becomes :

$$T_2 = -\frac{W}{g}(k^2 - uv) \frac{\ddot{\phi}}{\omega} \quad \text{--- (21)}$$

For $\frac{r}{l} = 0.2795$ equ.(21) becomes :

$$T_2 = \frac{W}{g}(uv - k^2)\omega^2(-0.03901 \sin 2\theta + 0.00159 \sin 4\theta - 0.000048 \sin 6\theta \text{---})$$

(c) Gravity Torques.

Since the crankshaft is dynamically balanced, gravitational torques are due only to the piston and connecting rod. For the reciprocating mass these become :

$$T_g = Wr(\sin \theta + 0.1425 \sin 2\theta - 0.0015 \sin 4\theta + \text{---})$$

and for the revolving mass W_2 of the connecting rod the gravitational torque is $W_2 r \sin \theta$.

Substituting the values of the equivalent reciprocating mass and correction couple as given in Fig. 4c. the resultant torque due to a single piston line is : Inertia + Gravity =

$$T = \omega^2 \left\{ 0.0018 \sin \theta - 0.0132 \sin 2\theta - 0.0054 \sin 3\theta - 0.0005 \sin 4\theta + \text{---} \right\} + \left\{ 7.81 \sin \theta + 0.578 \sin 2\theta - 0.0059 \sin 4\theta + \text{---} \right\} \text{ lb.in.}$$

The orders concerned in the investigation are the 2nd and 3rd, and for speeds ranging between 300 and 600 r.p.m. the gravitational effects are of no consequence.

(d). Engine Frictional Torque.

The frictional resistances at the engine affecting the torque are due to the piston rings, side thrust on the cylinder walls, gudgeon and crank pins and main bearings. When the engine was running, the lubrication of the piston, gudgeon and crank pins ultimately became imperfect and in a later investigation, referred to in page 50, the relative values of the sliding friction coefficients and periodic frictional torques were obtained.

For the 2nd and 3rd orders the frictional torques were found to be :-

$$\begin{aligned} & (-0.0003 \omega^2 \cos 2\theta - 0.0006 \omega^2 \cos 3\theta) \\ & + (6.72 \cos 2\theta + 1.16 \cos 3\theta) \text{ lb.in. per piston.} \end{aligned}$$

in which the latter bracketed term is that due to the piston rings. There is therefore a slight modification to the main inertia terms at speeds in the region of 300 r.p.m. due to the piston rings but at 600 r.p.m. the effect is quite negligible. It is thus seen that the main periodic effects to be considered are those of inertia.

Equations of Motion.

Two-mass System

The motor is called upon to drive against frictional resistances and engine inertia. Let the mean resistance be called K and let I_m and I_e be the moment of inertia of the motor and engine masses respectively and I_p be the equivalent moment of inertia of the piston line. From page 10.

$$I_p = (0.0352 + 0.0036 \cos \theta - 0.0132 \cos 2\theta - 0.0036 \cos 3\theta - \dots)$$

lb. in. sec².

Also let θ_m and θ_e be the angular displacements at the motor and engine ends of the shaft and let F be its

torsional rigidity. Then if T and V be the kinetic and potential energies of the vibrating system, substitution in the Lagrange¹² equation

$$\frac{d}{dt} \left(\frac{\partial T}{\partial \dot{\theta}} \right) - \frac{\partial T}{\partial \theta} + \frac{\partial V}{\partial \theta} = \text{Impressed Forces} \quad \dots (22)$$

gives the equation of motion which on further reduction may be written as follows :-

$$\begin{aligned} I_m \ddot{\theta}_m &= K - F(\theta_m - \theta_e) \\ I_e \ddot{\theta}_e + [0.0352 + 0.0036 \cos \theta - 0.0132 \cos 2\theta - 0.0036 \cos 3\theta \dots] \ddot{\theta}_e \\ &= -K - F(\theta_e - \theta_m) + \dot{\theta}_e^2 [0.0018 \sin \theta - 0.0132 \sin 2\theta - 0.0054 \sin 3\theta \dots] \end{aligned} \quad \dots (23)$$

These equations completely express the motion of the motor and engine. On the right hand side of the second equation it will be noticed that the coefficients deduced in this manner agree with those obtained for the resultant inertia torque given on page 25.

Also, since mean applied torque K = mean resisting torque K , $F(\theta_m - \theta_e)$ must contain a corresponding part equal to K , which represents the mean twist of the shaft due to the mean driving torque. Let the motions be represented by fluctuations about a constant angular velocity ω , then

$$\left. \begin{aligned} \theta_m &= \omega t + \alpha + x \\ \theta_e &= \omega t + y \end{aligned} \right\} \dots (24)$$

where α is the constant angular twist between θ_m and θ_e and is such that $F\alpha = K$. x and y represent the torsional oscillations.

Substituting equ.(24) in equ.(23) the equations of motion become

$$\begin{aligned} I_m \ddot{x} + F(x - y) &= 0 \\ (I_e + 0.0352 + 0.0036 \cos \theta - 0.0132 \cos 2\theta - 0.0036 \cos 3\theta \dots) \ddot{y} \\ + F(y - x) &= (\omega + \dot{y})^2 (0.0018 \sin \theta - 0.0132 \sin 2\theta - 0.0054 \sin 3\theta \dots) \end{aligned} \quad \dots (25)$$

Discussion of the Equations.

No general solution has been established for this type of equation even considering the inertia of the motor masses to be infinite and methods of approximation must be adopted. By substituting a new independent variable, determined by $\theta = \omega t$ the equation of motion can be reduced to the approximate form :-

$$(a + b \cos 2\theta) \omega^2 \frac{d^2 y}{d\theta^2} + Fy = (\omega + \dot{y})^2 b \sin 2\theta \dots \dots (26)$$

in which y represents the angular oscillation and θ the crank position. By considering small oscillations, an approximate solution of this equation has been developed by Goldsbrough¹³. He concluded that, due to the periodic variation in the inertia term, there is a range of instability in the vicinity of the first order resonance condition, but for all other criticals there is practically no range of instability but only a definite critical speed. This appears to hold even for very large reciprocating masses as represented by the ratio $\frac{b}{a} = 0.42$.

In the systems adopted for the present experiments the extreme value of $\frac{b}{a}$ is only 0.08, hence for the second and third order criticals it is reasonable to suppose that there will be no distortion of the motion due to inertia variation and for these criticals it is sufficient to apply the simple mean inertia.

In the vicinity of resonance the oscillations are large and the consequent change in the inertia forces cannot be ignored. As a first approximation, however, it is necessary to consider the vibrations small. Thus, the free vibration equations may be taken as :-

$$\left. \begin{aligned} I_m \ddot{x} + F(x - y) &= 0 \\ I_e \ddot{y} - F(x - y) &= P\omega^2 \sin n\omega t. \end{aligned} \right\} \dots \dots \dots (27)$$

Since the oscillations are measured at the engine end, it is necessary to obtain the value of y .

Eliminating x from these equations gives :-

13. Goldsbrough, Proc. Roy. Soc. Vol. CXIII. Series A. 1926-27

$$\frac{I_m I_e \ddot{y}}{F} + (I_m + I_e) \ddot{y} = P \omega^2 \sin n \omega t \left\{ 1 - \frac{I_m n^2 \omega^2}{F} \right\}$$

Solving for y the amplitude of oscillation at the engine becomes :-

$$|Y| = \frac{P \omega^2 \left\{ 1 - \frac{n^2 \omega^2 I_m}{F} \right\}}{n^2 \omega^2 \left\{ \frac{I_m I_e n^2 \omega^2}{F} - (I_m + I_e) \right\}} \quad \text{--- (28)}$$

If the natural frequency is $\frac{k}{2\pi}$, then $k^2 = \frac{F(I_m + I_e)}{I_m I_e}$

Substituting and reducing equ. (28) finally gives :-

$$\text{Amplitude at engine} = |Y| = \frac{\frac{PF}{n^2 I_m I_e} - \frac{P \omega^2}{I_e}}{n^2 \omega^2 - k^2} \quad \text{--- (29)}$$

If I_m is infinite equ. (29) reduces to standard form.

Modified Inertia Torque.

Using the value obtained from equ. (29) in the vicinity of resonance, the inertia torque may be corrected for the effect of large amplitudes of vibration, and a further approximation obtained for the resulting motion. The value of the modified inertia torque at resonance condition may be calculated as follows :-

The motion at the second order critical speed will be $\theta_e = \omega t + y \cos 2 \omega t$, hence substituting for $(\dot{\theta})_e^2$ in the expression :-

$$(\dot{\theta})_e^2 (0.0018 \sin \theta - 0.0132 \sin 2\theta - 0.0054 \sin 3\theta - 0.0005 \sin 4\theta \dots)$$

- from equ. (23)-, the corrected second order inertia torque becomes :-

$$-0.0132 \omega^2 \sin 2 \omega t - 0.0395 \omega^2 y^2 \sin 2 \omega t. \quad \text{lb. in. per piston.}$$

Similarly the corrected third order is :-

$$-0.0054 \omega^2 \sin 3 \omega t - 0.0364 \omega^2 y^2 \sin 3 \omega t. \quad \text{lb. in. per piston.}$$

The Measurement of the Torsional Oscillation.

The torsional oscillations were recorded by a standard Geiger torsigraph. This instrument consists of a light pulley and a heavy flywheel, mounted concentrically on the same axis, and connected to each other by means of a flexible spiral spring. The light pulley is driven by a short stiff belt from the shaft and follows the shaft vibratory motion exactly, but the heavy flywheel, being driven by the flexible spring, rotates at practically uniform velocity, provided the frequency of the torsional oscillations is well above the natural frequency of the instrument.

The relative motion between the pulley and the flywheel is transmitted through a lever system to a pen, which traces a record of it on a strip of paper driven by clockwork. A range of magnification of the oscillatory motion of the shaft is available. The clockwork can be set at various speeds and from a timing vibrator in conjunction with a revolution marking device, the average speed for any particular revolution can be calculated.

In the present experiments, the revolution marking device was operated from a simple electric contact, situated at the top of No. 4 cylinder, as shown in Fig. 4b. making contact only at the top dead centre of this cylinder. Thus a complete cycle was indicated on the torsigraph record. At speeds above 450 r.p.m. this dead centre timing failed to operate regularly with this simple contact and an attempt was made to fit an insulated ring to the shaft having one half of the circumference copper and the other mica. This, however, was only moderately successful and was finally discarded, particularly as a complete cycle was clearly indicated on the vibration record itself, and a speed calculation therefore could be accurately determined. As a precautionary measure, speeds were also observed from a tachometer.

The timing vibrator, having a frequency of 1,500 per minute was operated electrically.

Geiger torsigraph belting was employed and with the instrument secured to a wooden base suitably placed at the recording position as shown in Fig. 2, the belt centres were approximately $21\frac{1}{2}$ in. A wooden pulley of about 6 inch diameter had been fitted at the forward end of the crankshaft to drive the torsigraph, but the oscillations were so large that they could not be recorded from this pulley. To keep the vibrations within the limits of the instrument, the belt drive had to be taken from such positions as the steel centre of the pulley and the 1 inch diameter shaft, aft of the engine.

Method of recording the Torsional Oscillations.

The recording of the oscillations for any particular experiment was carried out by taking continuous diagrams and slowly increasing the speed of the motor in uniform steps throughout the complete speed range available. An examination of the diagrams showed that it was only necessary to investigate the 2nd and 3rd order critical speeds, so particular attention was given to these conditions.

On repeating the records in the vicinity of resonance, the speed of the motor was again increased very slowly by steps, and when the instrument was recording the maximum amplitude, an attempt was made to sustain the motor at that mean speed. With reasonable care, the fine resistances controlling speed enabled this to be achieved and thereby allowed the amplitude to build up $\overset{t_0}{\underset{\wedge}{}}$ a maximum value, which may be taken to represent the ultimate conditions at resonance.

In all experiments, the critical speeds were approached both from a lower and a higher speed.

In cases where the recorded amplitude was small, another record was taken, the pen of the instrument being reset for a higher magnification.

Experiences with plant.

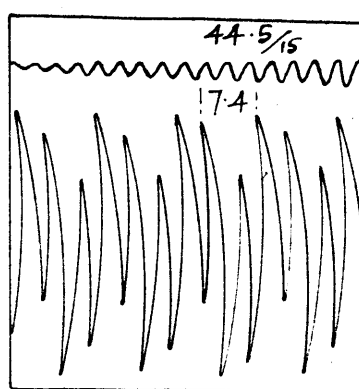
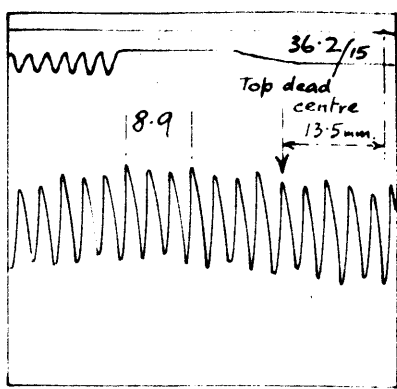
Preliminary Experimental Work.

The vibrations were more severe than anticipated and breakdown of the ordinary pinching pins and saddle keys at the couplings resulted. This was overcome by making all keyways and pins countersunk and of a more robust design. The revised fittings proved successful in withstanding the most severe oscillations, and there was no evidence of slip having taken place.

On recording the vibrations at various positions along the shaft, it was found, by comparing the maximum amplitude ratio with the mass ratio of the engine and motor masses, that false records were obtained at the engine due to belt slip on the glossy surface of the small diameters when transmitting large oscillations. To surmount this, adhesive tape was carefully wound round the Geiger drive positions and an examination of the resonance vibration form carried out with the object of verifying the records obtained.

The mass arrangement used in this investigation was M1.1p, and the particular piston employed was No. 4 with rings. Torsiograph records were taken at the forward and aft ends of the engine and also at the motor flywheel as shown by positions A, B and E on Fig. 4. As only one instrument was available, repeat runs had to be made at the different positions. Before records were taken the apparatus was run for some time to enable the lubricating conditions to become stable.

Strips of the records showing maximum amplitudes at resonance are given in Fig. 17, from which the following results are obtained :-



Torsion graph position:-

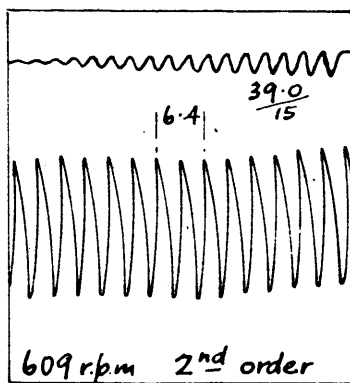
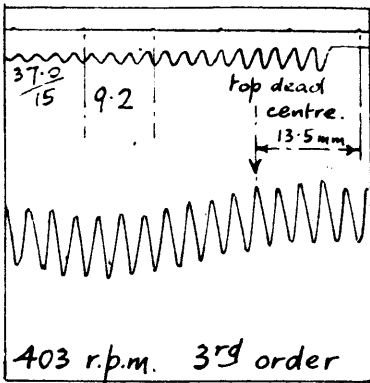
A. Forward of engine.

dia. 1.92". Magnification $\frac{3}{1}$.

407 r.p.m. 3rd order

604 r.p.m. 2nd order

double amp. 12.8mm = $\pm 5.02^\circ$ double amp 29.5mm = $\pm 11.5^\circ$



Torsion graph position:-

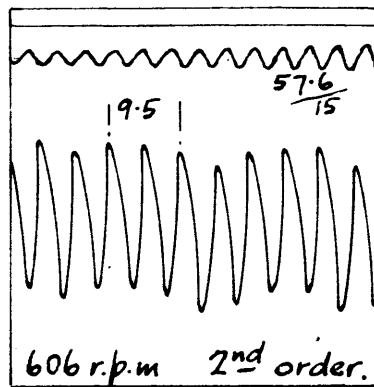
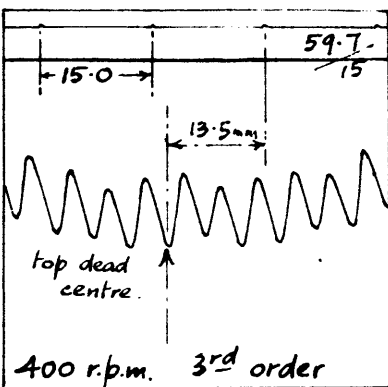
B. Aft of engine.

dia. 1.25". Magnification $\frac{3}{1}$.

403 r.p.m. 3rd order

609 r.p.m. 2nd order

double amp. 8.20mm = $\pm 4.93^\circ$ double amp 19.0mm = $\pm 11.4^\circ$



Torsion graph position:-

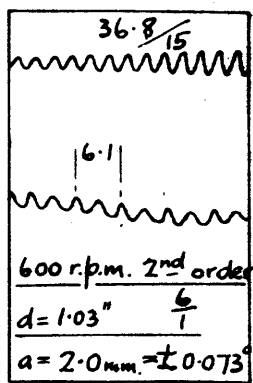
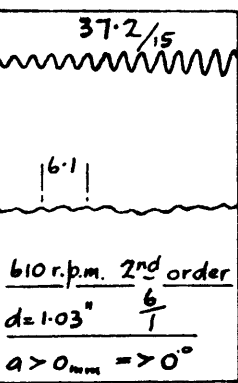
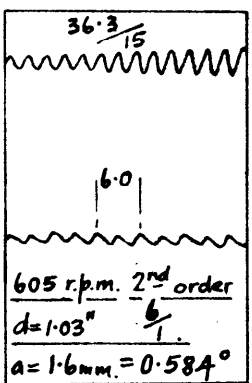
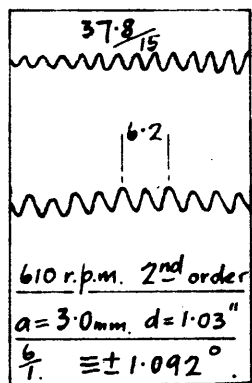
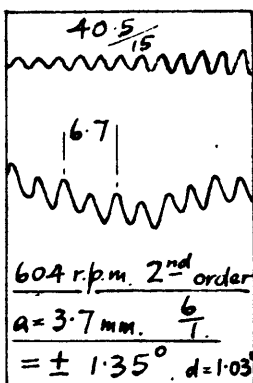
E Motor Flywheel.

dia. 11.2". Magnification $\frac{3}{1}$.

400 r.p.m. 3rd order

606 r.p.m. 2nd order.

double amp. 8.8mm = $\pm 0.59^\circ$ double amplitude 20.5mm. = $\pm 1.38^\circ$



$1\frac{3}{4}"$ from pins.

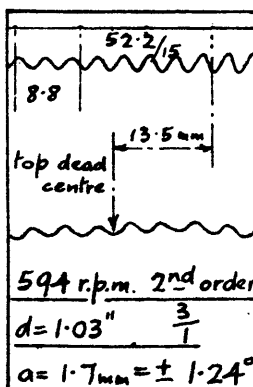
$4\frac{1}{2}"$ from pins.

8" from pins.

$14\frac{1}{2}"$ from pins.

22" from pins.

Distance along shaft measured from pins at section "bb". see fig. 4a.



$1\frac{3}{4}"$ from pins.

Fig. 17. Examination of resonance

vibration form. Mass System M.I. I.p. No 4

piston with rings. Imperfect Lubrication.

Position.	Maximum resonance amplitudes.			
	2 nd order.		3 rd order.	
	± degree	r.p.m.	± degree	r.p.m.
Forward of Engine A.	11.5	604	5.02	407
Aft of Engine B.	11.4	609	4.93	403
Motor Flywheel D.	1.38	606	0.59	400

The records taken at the engine show very good agreement and the amplitude ratios indicating resonance vibration form are :-

$$\frac{\text{Engine amplitude.}}{\text{Motor amplitude.}} = \frac{11.45}{1.38} = 8.30 \quad \text{and} \quad \frac{4.97}{0.59} = 8.40$$

The corresponding mass ratio is :- $\frac{\text{Motor masses}}{\text{Engine masses}} = \frac{8.14}{1}$

Further records were taken at various positions on the shaft about the node, and these are also given in Fig. 17. Plotting the maximum amplitudes on a base of distance along the shaft, Fig. 18, the position of the node from the c.g. of the motor masses is found to be 15.3 in., against 16.1 in., by calculation.

The average natural frequency from the records is 1208 v.p.m. while the calculated value is 1215 v.p.m. Similarly mass system M3.1p., was examined, the torsigraph records being given later in Fig. 19. The results obtained were :- (see fig. 62).

Position.	Maximum resonance amplitudes. 2 nd order.	
Forward of Engine A.	± 6.32°	480
At motor flywheel D.	± 1.49°	472.

The amplitude ratio is $\frac{4.24}{1}$, and the mass ratio $\frac{4.7}{1}$. The average natural frequency from the records is 952 v.p.m. and by calculation 957 v.p.m.

From these preliminary results at resonance, it is concluded that the theoretical two-mass vibration form is followed quite closely, and that with the precautions taken for the belt drive, the torsional oscillations can be accurately recorded.

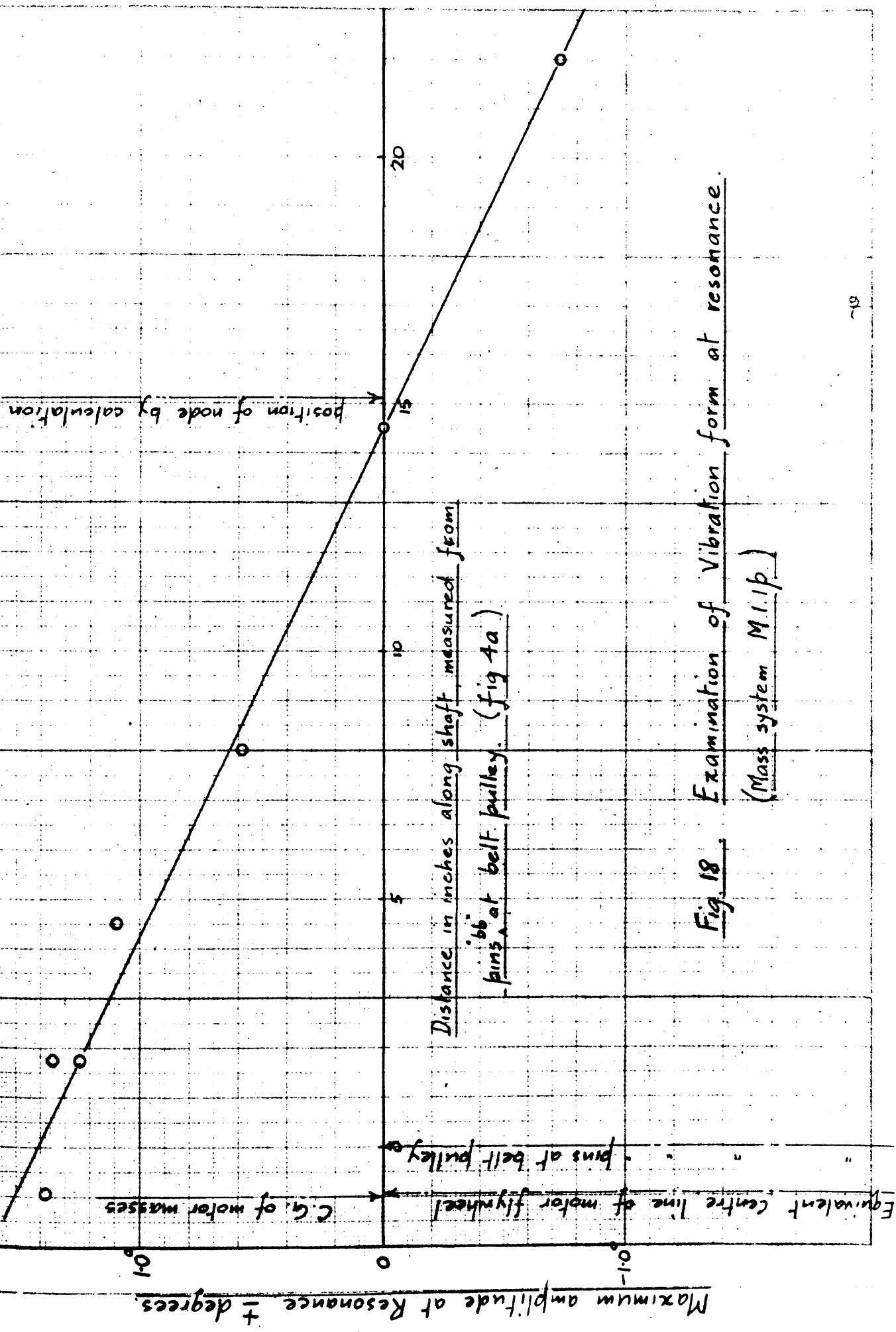


Fig 18. Examination of Vibration form at resonance.
(Mass system M.I.P.)

Part II.

INVESTIGATION OF OSCILLATION ABOUT STEADY MOTION.

(1) Importance of Lubrication.

Early experiments during the exploration of the apparatus showed that lubrication of the white metal main bearing of the engine was important in the control of amplitude at resonance. Normally this bearing was forced lubricated by a pump, gear-driven from the crankshaft, but this was dismantled for simplicity in engine running gear and gravity oil feed substituted.

Before applying the gravity feed, trial runs were carried out, mainly for the purpose of estimating the range of the apparatus. At the commencement of these runs, the bearings, big ends, and pistons were given a copious supply of oil. It was observed on continuous running that when operating at resonance the maximum amplitudes for the same critical speed were at first moderate then increased in value until after some time a final maximum value was reached which could be repeated thereafter.

This behaviour seemed to suggest that due to the limited supply of oil to all sources at the engine, and general decrease in viscosity due to warming up, the film conditions had degenerated to a constant state of greasy friction resulting in a reduced damping effect. With the light loads it was quite safe to run for long periods as there was no sign of overheating.

Crankshaft Main Bearing.

With gravity feed to the main bearing, however, and the same general oiling of the pistons and big-ends the resonance amplitudes remained quite moderate and there was no appreciable increase after continuous running.

Big-End Bearing.

The effect of lubrication of the big-end bearing at the crankpin was investigated and in order to intensify the effects, the gravity feed to the engine main bearing was removed, and the same initial oiling was given to the pistons. Splash lubrication of the big-ends was arranged by fitting the original oil trough into which the big-end ^{cover} dipped. In the normal design, the oil trough was supplied continuously from the forced feed system, and as this had been removed the supply to the crankpin bearing and trough was maintained intermittently by a syringe.

After continuous running there appeared to be no definite change in the maximum resonance amplitude from the previous trials with imperfect lubrication all over. It was thought, however, that the splash lubrication as arranged was ineffective and with continual dismantling was not always consistent.

The gudgeon pins were inaccessible while running so that greasy friction will exist at all times, both on account of inadequate oil supply and the type of motion taking place.

Pistons.

With the cylinder head removed, oil could be poured into the cylinders while the machine was running. The pistons protrude beyond the cylinder body and push the excess oil out of the cylinder. Thus the oil supply to the cylinder walls is really maintained by the trace picked up again by the piston at top dead centre.

After continuous operation and renewal of oil supply to the pistons while running, it was observed that although slight variations in resonance amplitude took place there was no decided change in maximum amplitude from the previous trials.

This was taken to mean that if a film did form at mid-stroke, its effectiveness as a source of viscous damping was diminished by the frictional work done upon it, in conjunction with the heat received from the cylinder walls.

Conclusion.

For the apparatus, as arranged, only slight variations resulted from changes in the piston and the big-end conditions, but marked changes in amplitude occurred with changes in the main bearing lubrication. Hence in the subsequent experiments, attention was given to the lubrication conditions particularly at the main bearing.

Experimental Procedure and Range of Tests.

I. Imperfect Lubrication Series.

(a) The effect of different pistons was investigated on mass-system M1.1p. Each piston was tried singly, and in order to obtain large amplitudes, thus emphasizing the effects, gravity feed was removed from the main bearing. The piston and big-end were given an initial supply of oil but before taking records the apparatus was run for a considerable time to allow the lubrication to degenerate to the greasy film type and to ensure similarity in conditions. In all cases the pistons were fitted with their rings.

Torsiograph records were taken at position B, Fig. 4, aft of the engine, several records being taken at resonance. Tracings of representative strips of the records are given in Figs. 20 to 24, for the speed range. The records chosen, represent the maximum amplitudes attained at resonance.

(b) Similarly the two, three and four piston arrangements on the M1., mass-system were examined. For the two piston series, piston Nos. 1 and 4, and Nos. 3 and 4 were employed giving the effect of in-line and

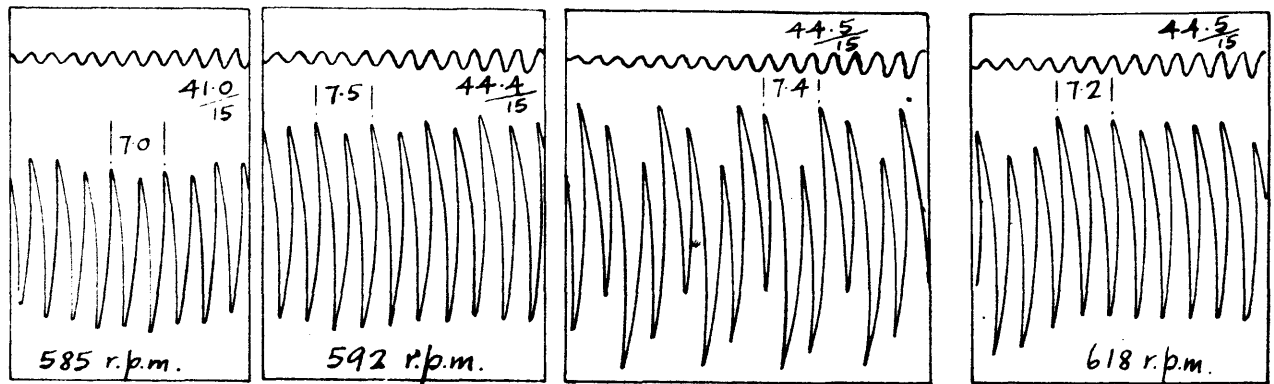
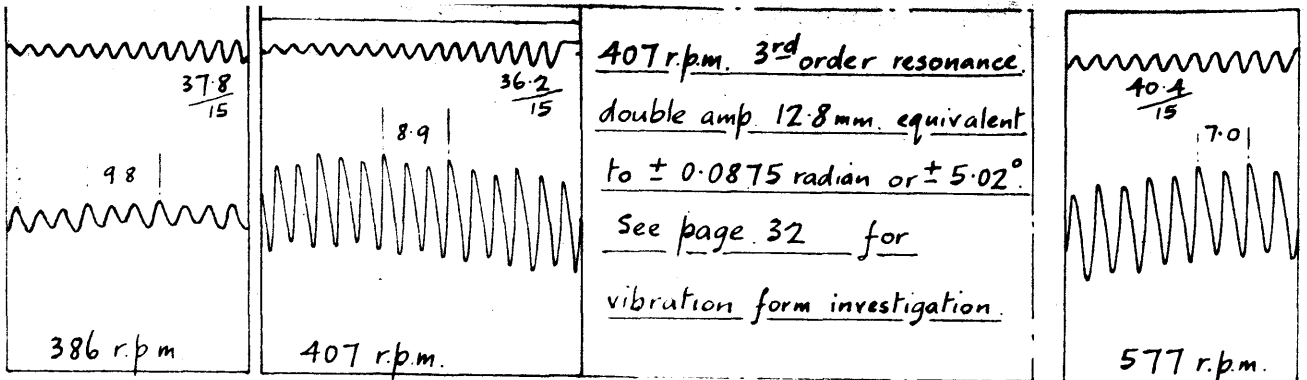


Fig. 20. Series No. 1. Piston No. 4. 604 r.p.m. 2nd order. double amp. 29.5 mm.
 Imperfect Lubrication equivalent to ± 0.202 radian or $\pm 11.5^\circ$.
 Mass system M.I. 1p. with rings. See page 32 for vibration form investigation
 Torsigraph posⁿ A. dia. 1.92" Magnification $\frac{3}{1}$.

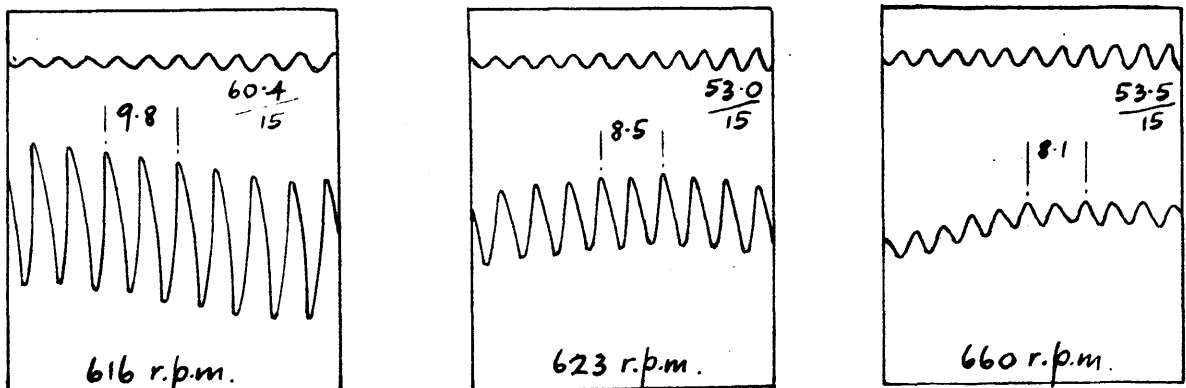
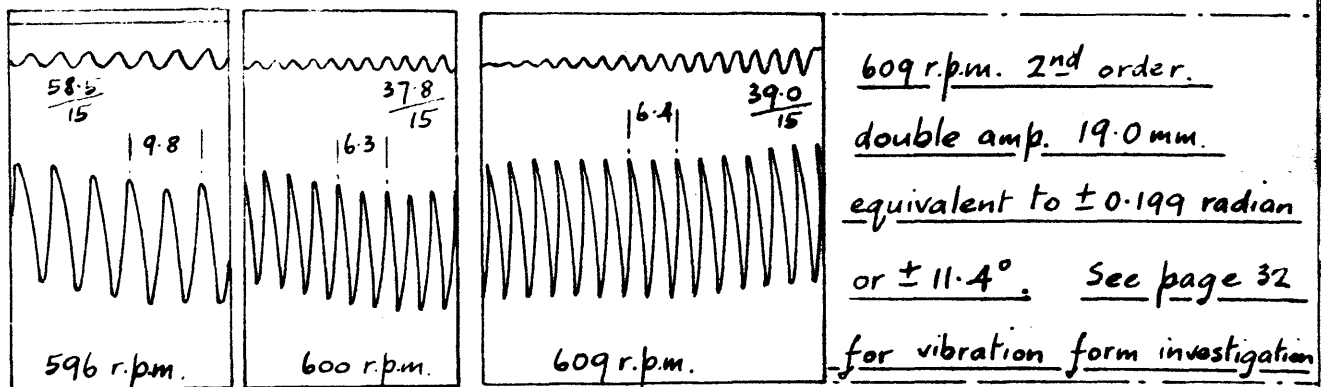
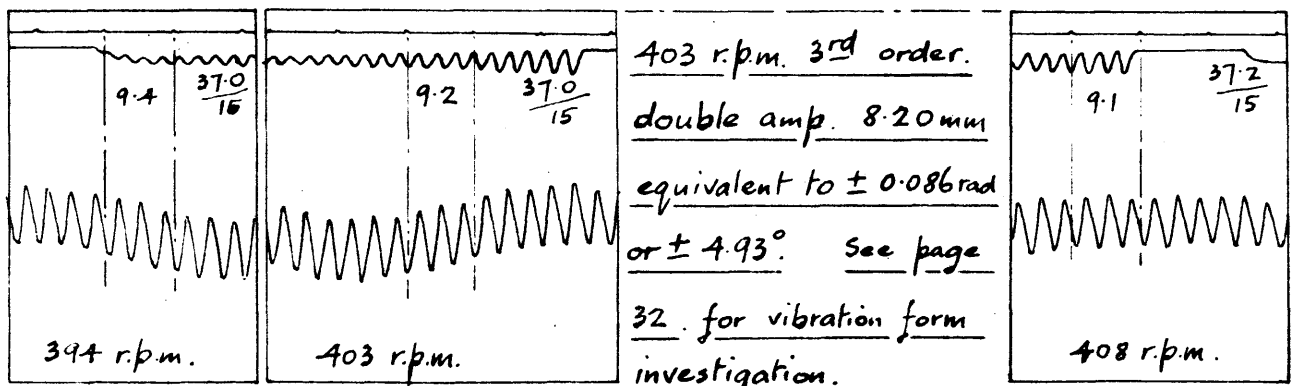
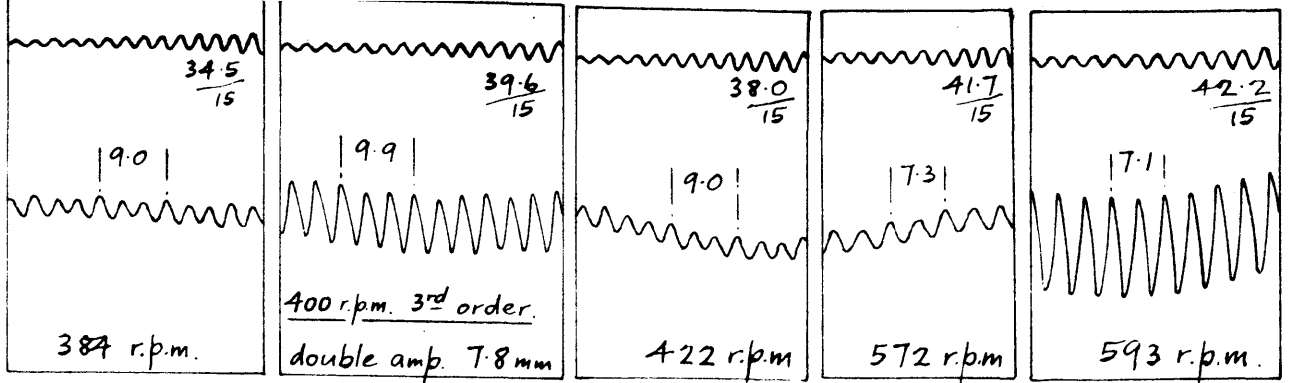
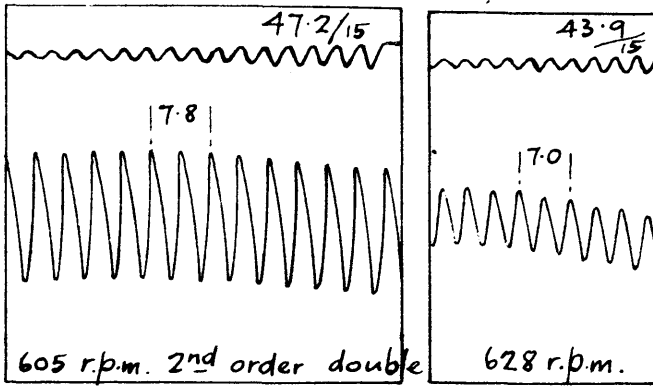


Fig. 21. Series No. 1. Imperfect Lubrication. Mass System M.I. 1p.
 Piston No. 4. with rings.
 Torsigraph position. B. dia. 1.25" Magnification $\frac{3}{1}$.



equivalent to ± 0.082 rad.



amp 17.3 mm. equivalent to ± 0.182 radian.

Fig. 22. Series No 1. Imperfect Lubⁿ.

Mass system M.I. 1p. No 1. piston

with rings. Torsiograph posⁿ B.

dia. 1.25" Magnification $\frac{3}{1}$.

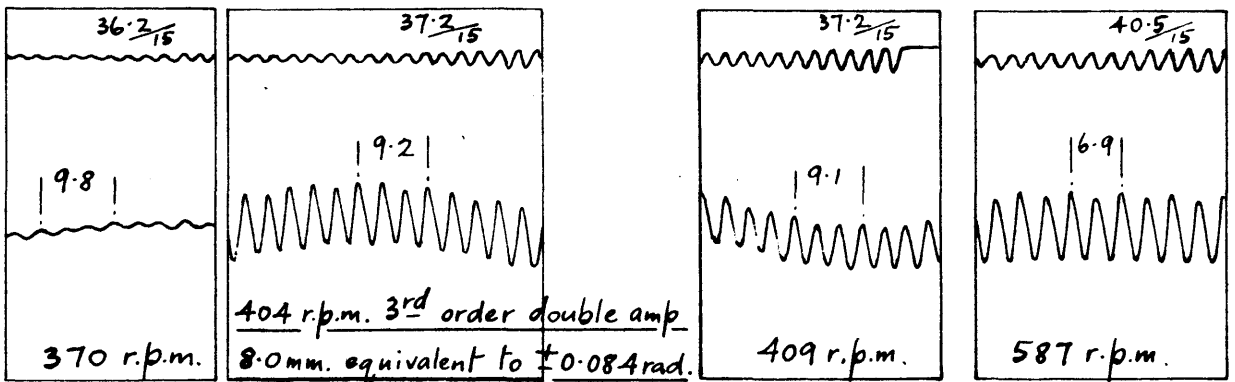


Fig. 23. Series No 1.

Imperfect Lubrication. Mass-

system M.I. 1p. No 2 piston with

rings. Torsiograph posⁿ B.

dia. 1.25" Magnification $\frac{3}{1}$.

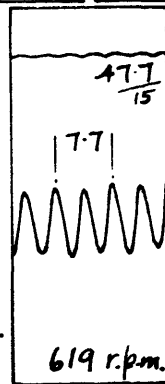
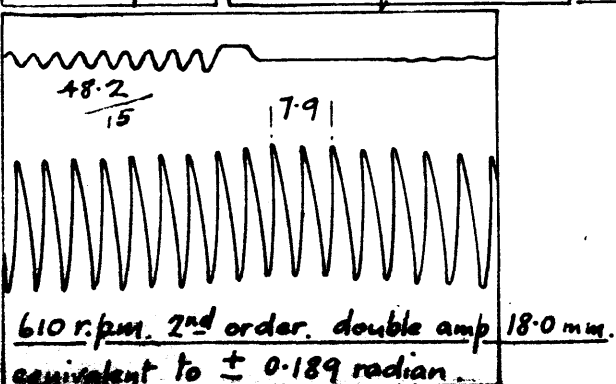
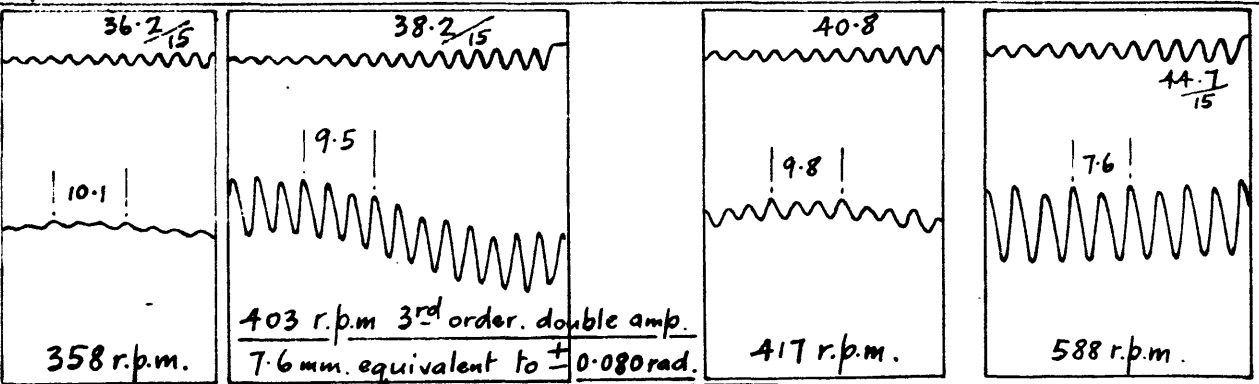
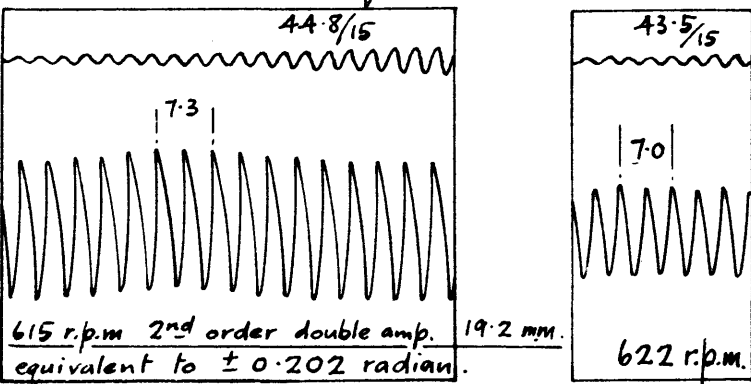


Fig. 24. Series No 1.

Imperfect Lubrication. Mass-

system M.I. 1p. No 3 piston

with rings. Torsiograph posⁿ B.

dia 1.25" Magnification $\frac{3}{1}$.

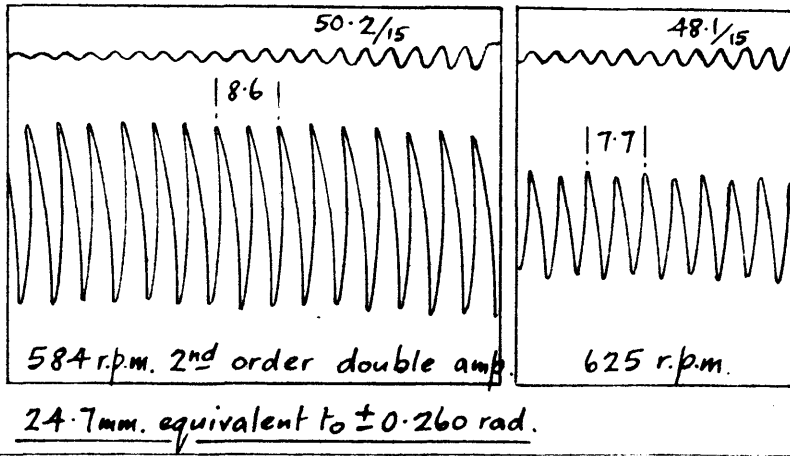
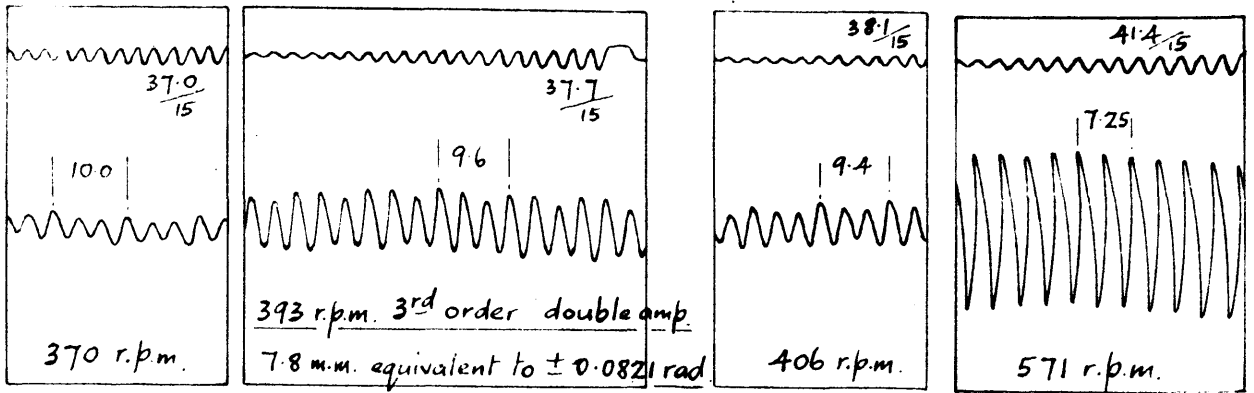
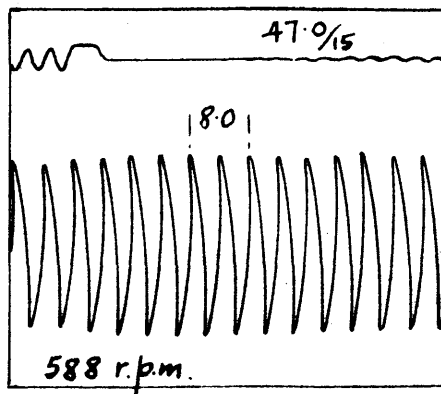
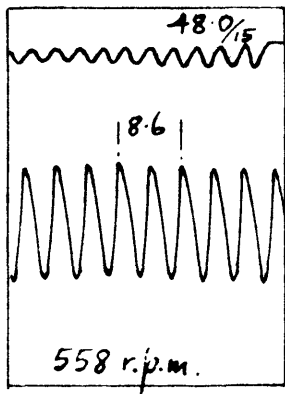


Fig. 25. Series No. 1.
Imperfect Lubrication.
Mass system M.1.2.p.
Piston Nos 1 and 4. with rings.
Torsiograph posⁿ B. dia 1.25"
Magnification $\frac{3}{1}$.



588 r.p.m. 2nd order
 double amp. 24.9 mm.
 equivalent to ± 0.262 rad.

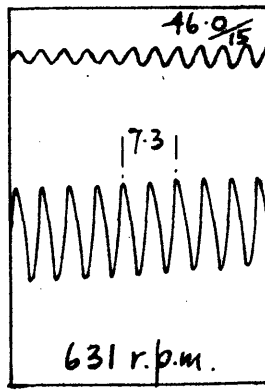
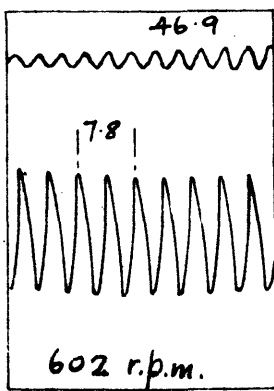


Fig. 26. Series No. 1. Imperfect Lubrication.
Mass System. M.1.2.p. Piston Nos 3 and 4 with rings.
Torsiograph position B. dia 1.25". Magnification $\frac{3}{1}$.

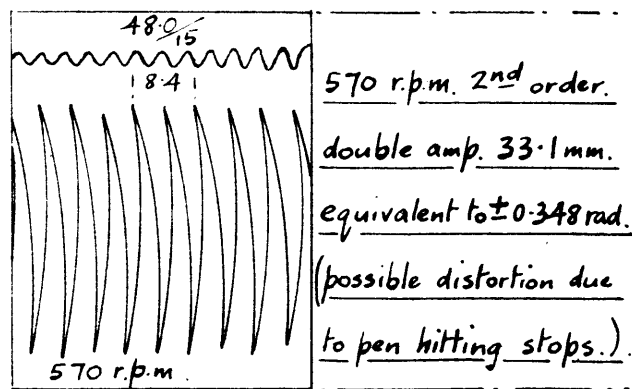
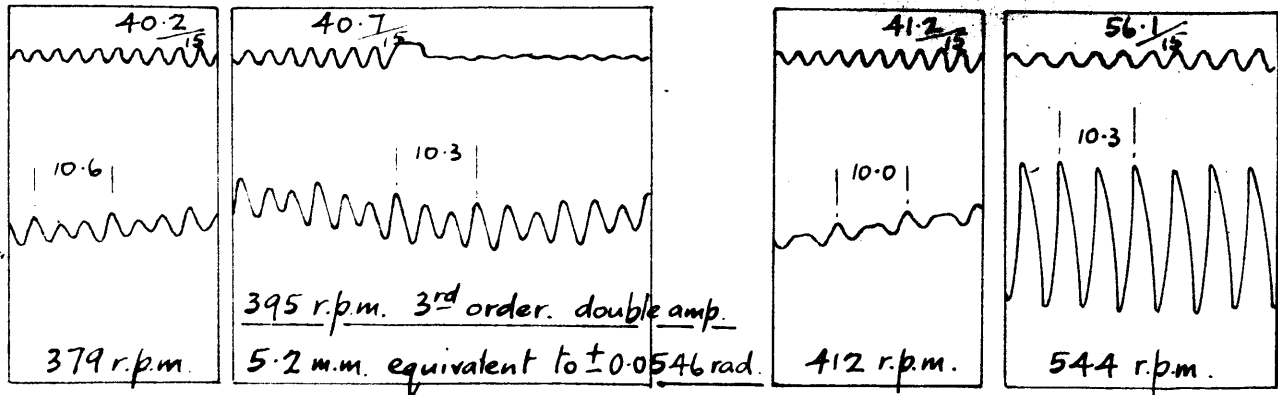


Fig. 27. Series No. 1.
Imperfect Lubrication.
 Mass System M.1.3p.
 with piston rings. Torsio-
 graph posⁿ B. dia 1.25. Magⁿ 3/1.

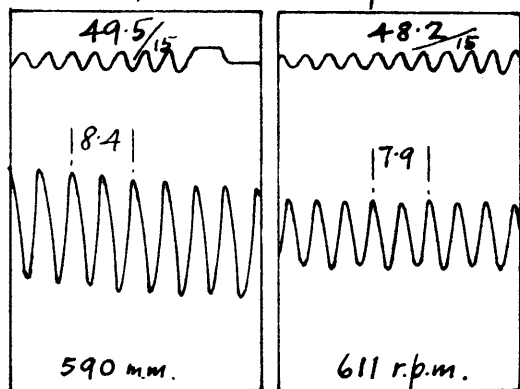
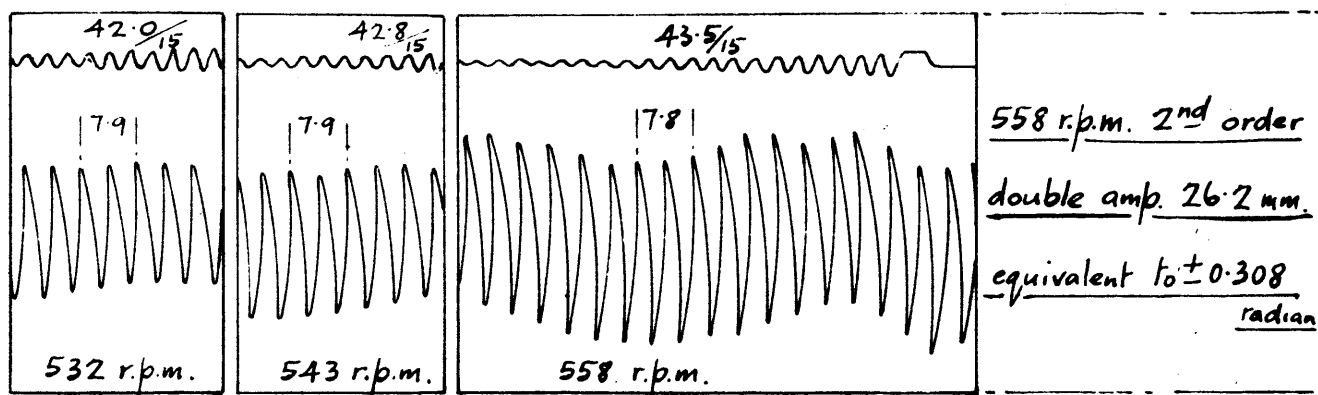


Fig. 28. Series No. 1. Imperfect Lubrication
 Mass System M.1.3p. with piston rings.
 Torsigraph posⁿ C. dia 1.115".
 Magnification $\frac{3}{1}$.

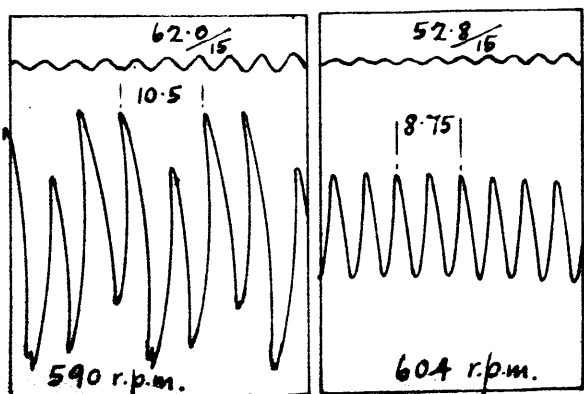
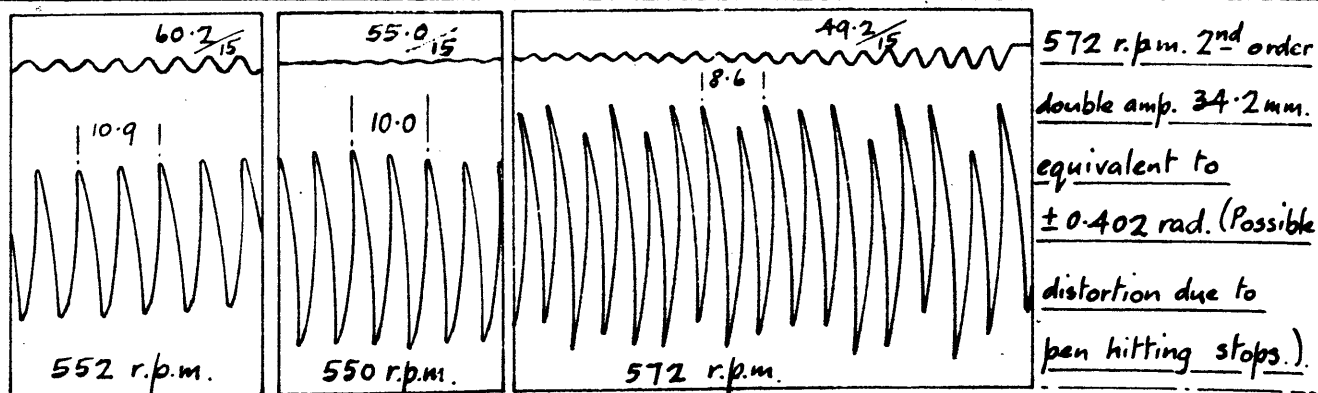


Fig. 29. Series No. 1. Imperfect Lubrication.
 Mass System M.1.4p. with piston rings.
 Torsigraph posⁿ C. dia. 1.115"
 Magnification $\frac{3}{1}$.

opposed pistons respectively.

The records for the speed range are given in Figs. 25 to 29 where again the records at resonance represent the ultimate amplitude when no lubrication is supplied to the main bearing and greasy friction prevails throughout the engine.

II. Series with Gravity Oil Feed to Main Bearing.

(a) Pistons with Rings.

With gravity feed to the main bearing and initial oiling of the piston and big-end, torsigraph records were taken after continuous running from mass-systems *M1.1p.*; *M1.2p.* and *M1.4p.*. Records are given in Figs. 30 to 32, and again they represent the ultimate amplitudes.

(b) Pistons without Rings.

With similar lubrication conditions, but with the piston rings removed, a torsigraph examination was made of mass systems *M1.1p.*; *M1.2p.*; *M1.3p.*; and *M1.4p.*.

Further examination was made at resonance when oil was supplied to the piston while running, but little or no difference in maximum amplitude could be detected, and the records shown on Figs. 33 to 37 may be taken to represent the final results of the two sets of experiments.

III. The Effect of Frequency on Resonance Amplitude.

(a) Gravity Oil Feed to Main Bearings.

The additional mass-systems *M2*, *M3*, *M4*, and *M5*, giving a range of natural frequencies were each examined under the following conditions :-

(i) one and two piston series with piston rings.

(ii) one, two, three and four piston series, without piston rings.

Torsigraph records are given in Figs. 38 to 61.

(b) Mass-system *M3.1p.* with rings but with the

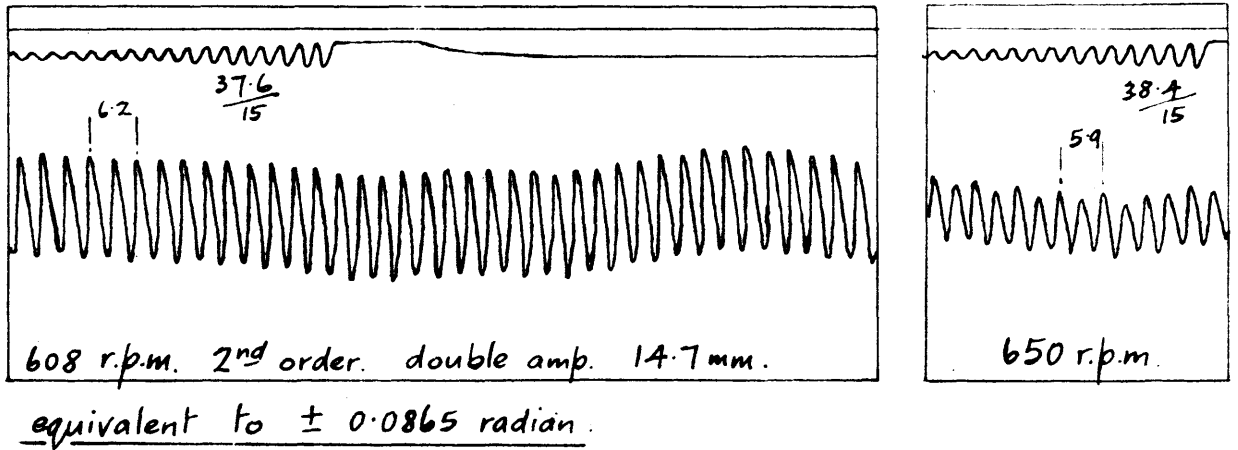
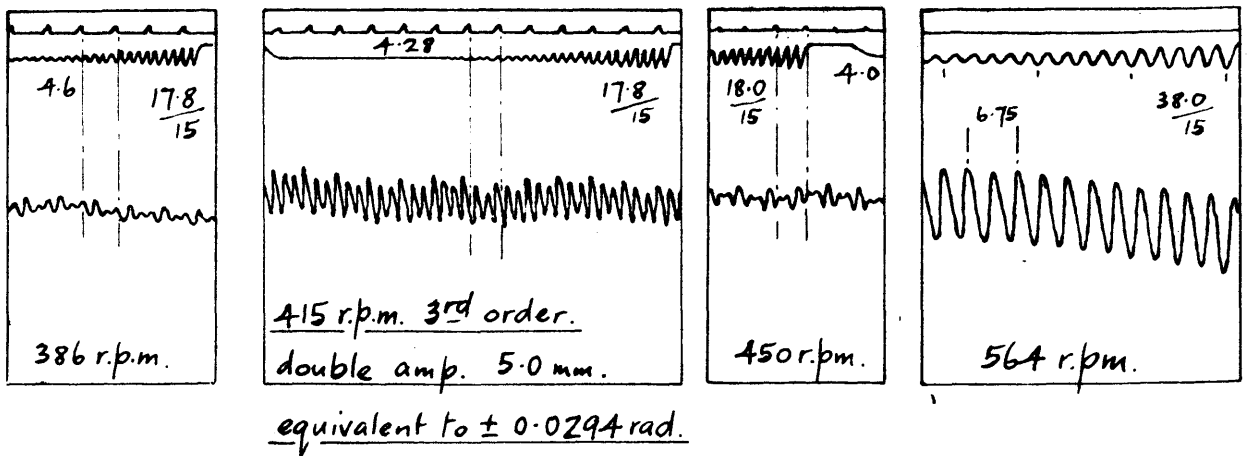


Fig. 30. Series II. Gravity oil feed to main bearing.
Mass System. M.I. I.p. with piston rings.
Torsiograph posⁿ C. dia. 1.115" Magnification. $\frac{6}{1}$.

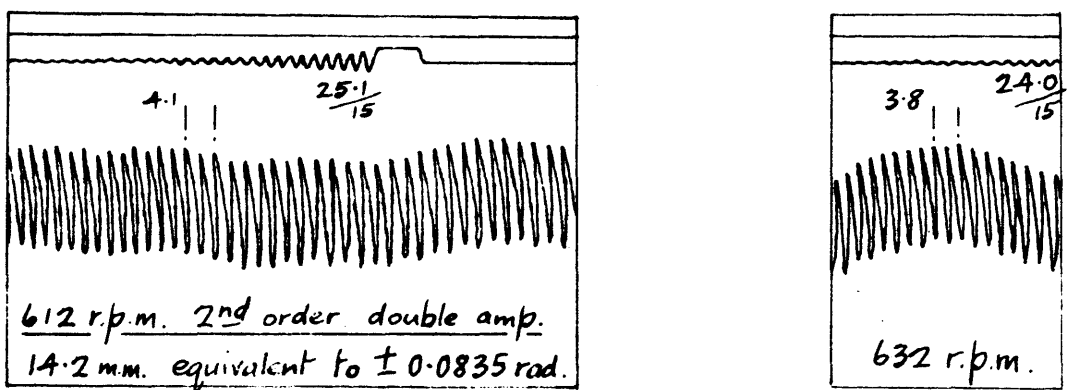
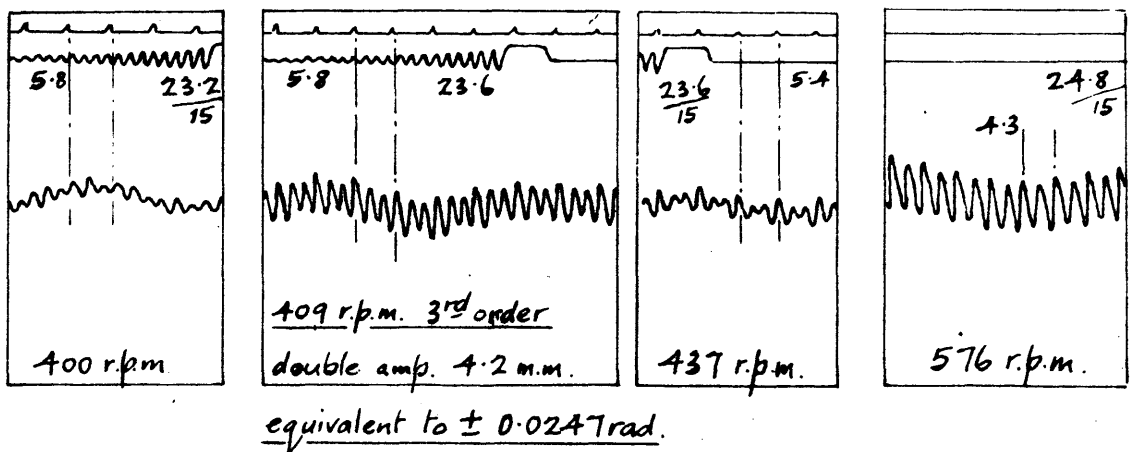


Fig. 33. Series II. Gravity oil feed to main bearing.
Mass System M.I. I.p. without piston rings.
Torsiograph posⁿ C. dia 1.115" Magnification $\frac{6}{1}$.

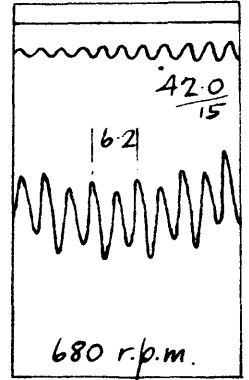
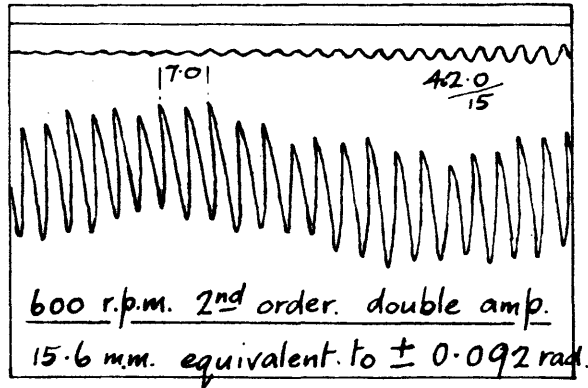
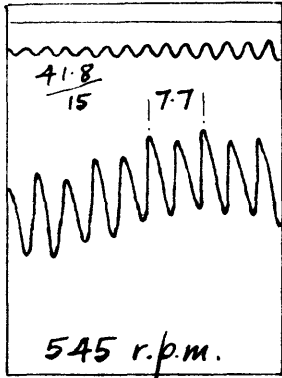
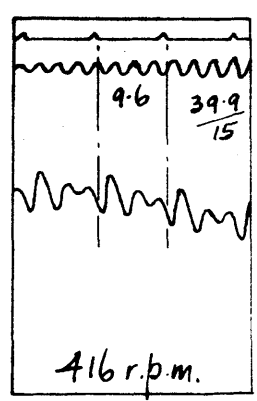
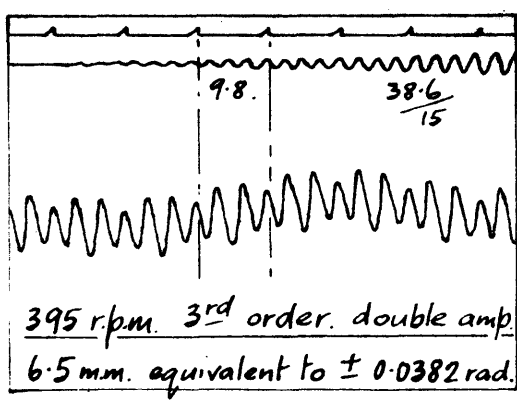
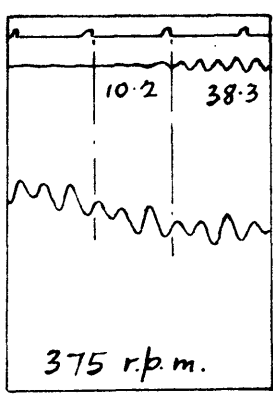


Fig. 31. Series II. Gravity oil feed to main bearing.
Mass System M.I. 2p. with piston rings.
Torsiograph posⁿ C. dia 1.115". Magnification $\frac{6}{1}$

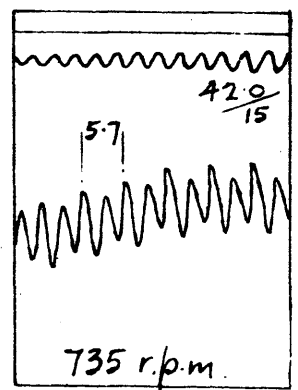
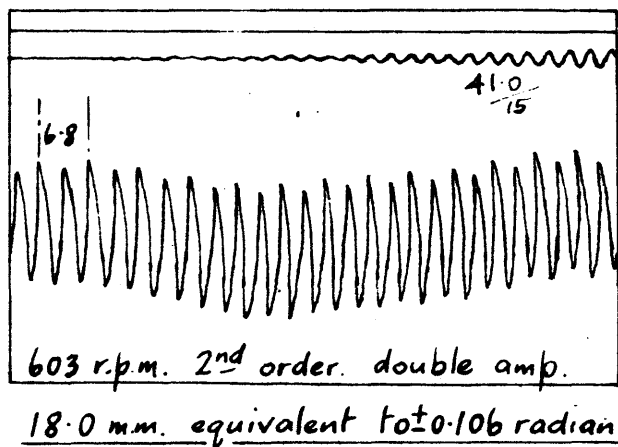
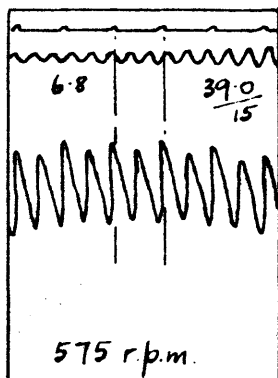
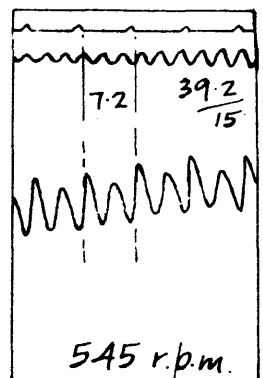
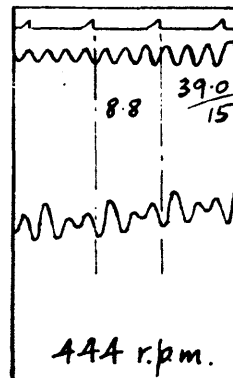
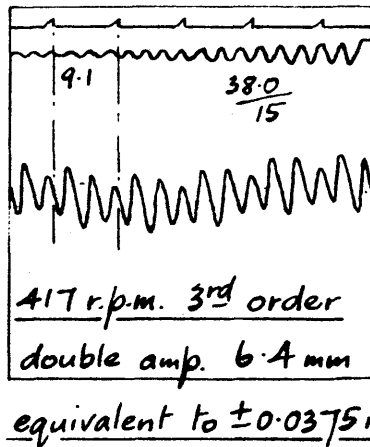
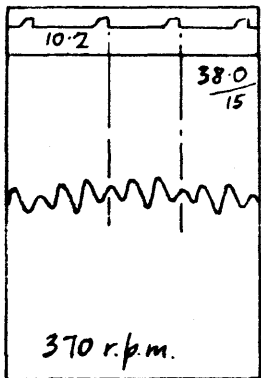
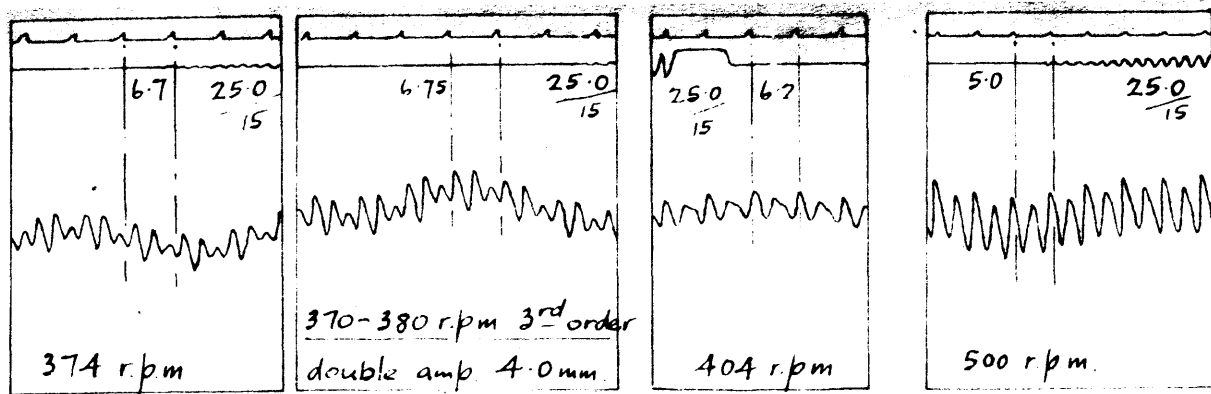
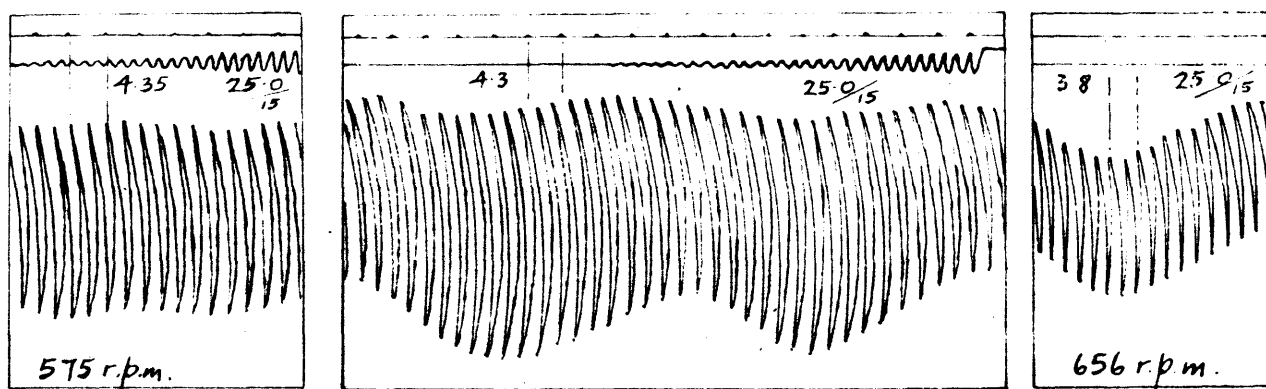


Fig. 34. Series II. Gravity oil feed to main bearing.
Mass System M.I. 2p. without piston rings.
Torsiograph posⁿ C. dia 1.115" Magnification $\frac{6}{1}$



equivalent to ± 0.0235 rad



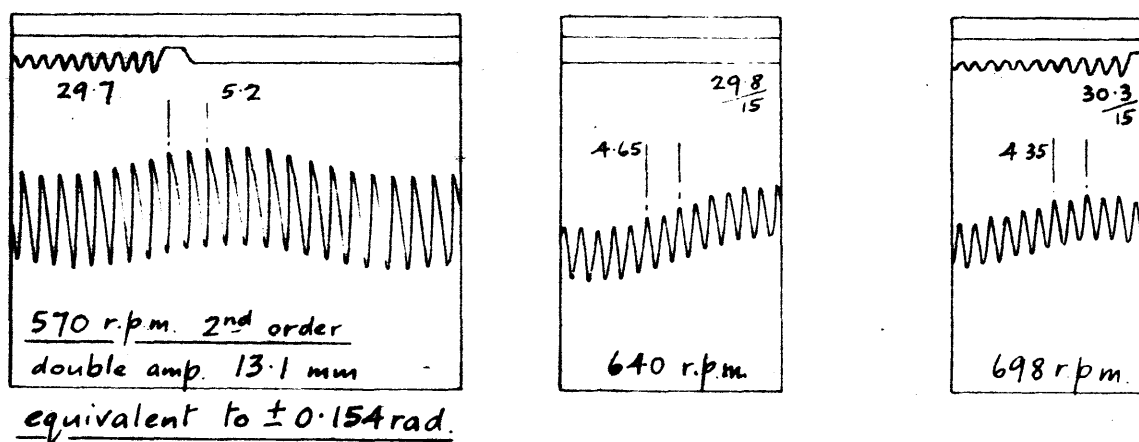
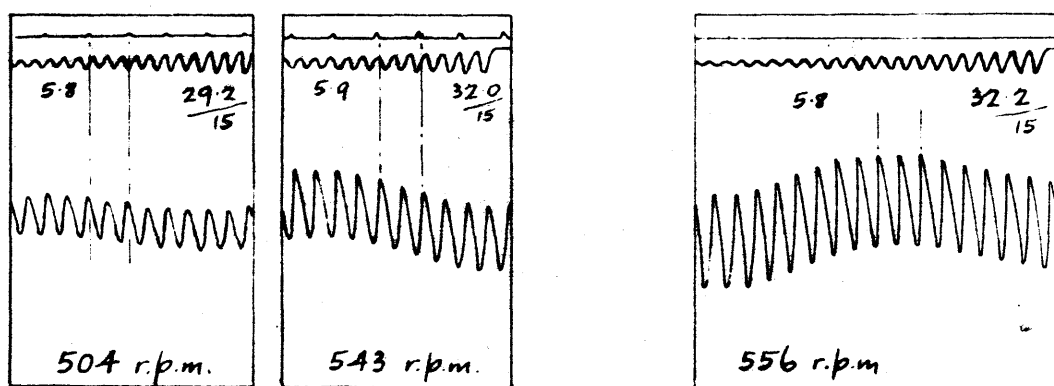
582 r.p.m. 2nd order. double amp. 32.2 mm.

equivalent to ± 0.190 radian.

Fig. 35. Series II. Gravity oil feed to main bearing.

Mass system M.1.3p without piston rings Torsiograph posⁿ C.

dia. 1.115" Magnification $\frac{6}{1}$ { possible distortion due to pen hitting stops. }

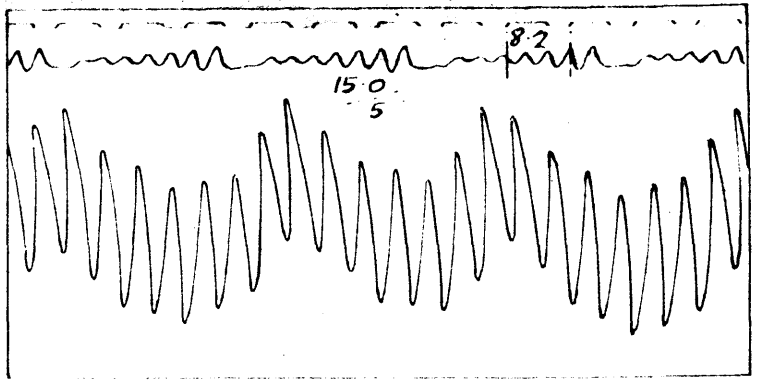
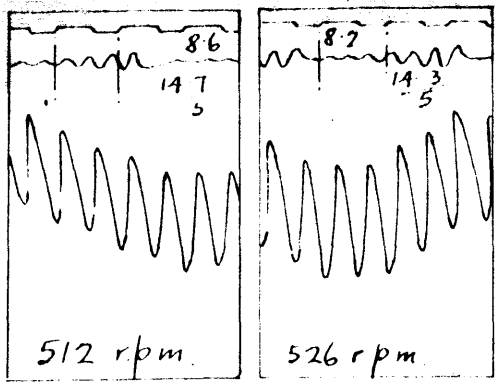


equivalent to ± 0.154 rad.

Fig. 36. Series II. Gravity oil feed to main bearing.

Mass System M.1.3p. without piston rings.

Torsiograph posⁿ C. dia 1.115" Magnification $\frac{3}{1}$



549 rpm 2nd order double amp. 200 mm.
equivalent to ± 0.210 radian.

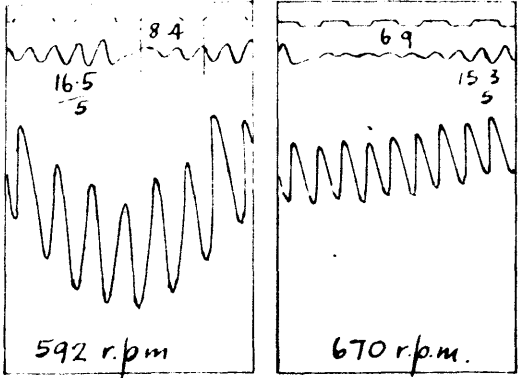
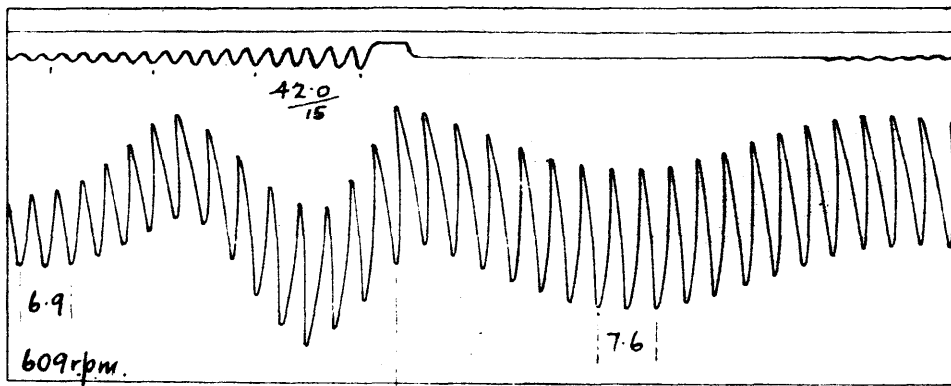
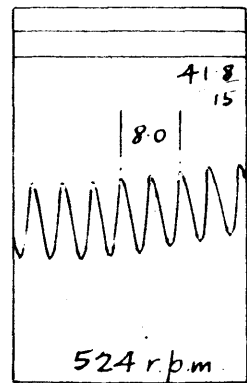
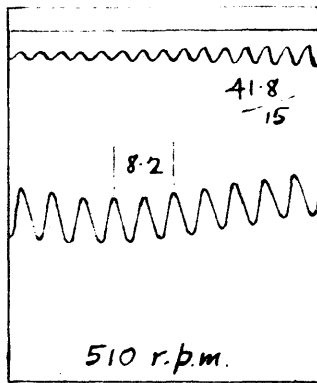
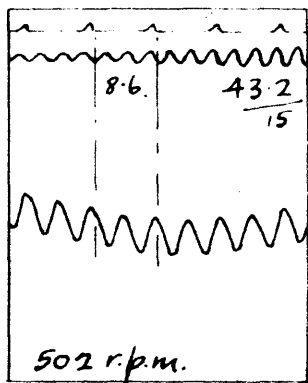
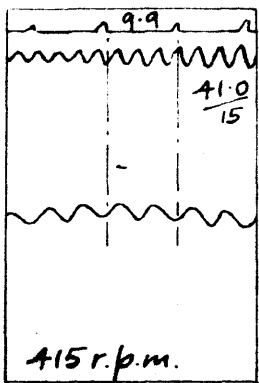


Fig 32. Series II. Gravity oil feed to main bearing

Mass system M.1.4p. with piston rings

Torsiograph posⁿ B. dia 1.25" Magⁿ $\frac{3}{1}$.

{ For this case only, the dead centre timing was
operated by the insulated ring on the shaft. }



Record showing general
acceleration, after
sustaining speed
at resonance.
See page 38.

553 r.p.m. 2nd order. double amp.
19.0 mm. equivalent to ± 0.223 radian.

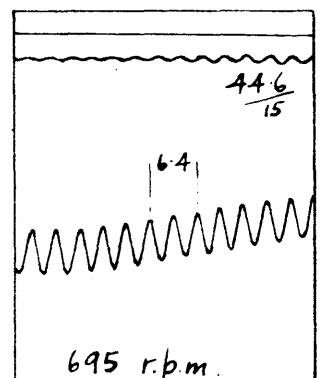
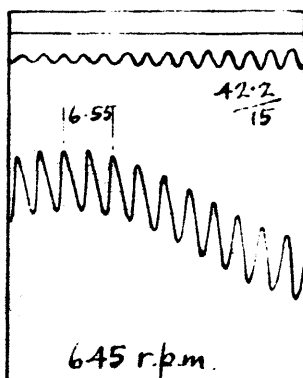
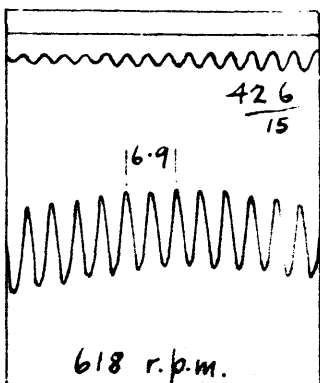


Fig. 37. Series II Gravity oil feed to main bearing.

Mass System M.1.4p. without piston rings.

Torsiograph position. C. dia. 1.115" Magnification $\frac{3}{1}$

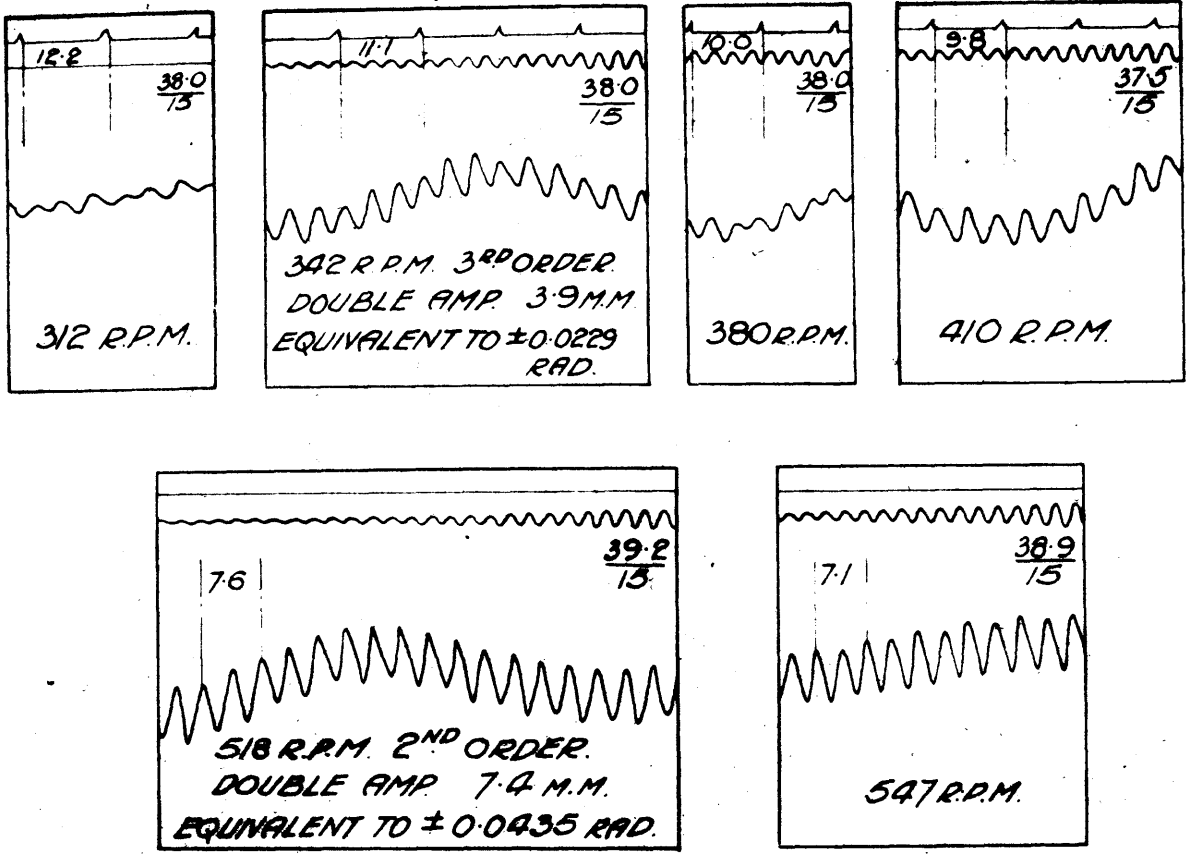


FIG. 38 SERIES III GRAVITY OIL FEED TO MAIN BEARING.

MASS SYSTEM M2 1P WITH RINGS.

TORSIOGRAPH POS^N C. DIA. 1.115" MAGNIFICATION $\frac{6}{7}$

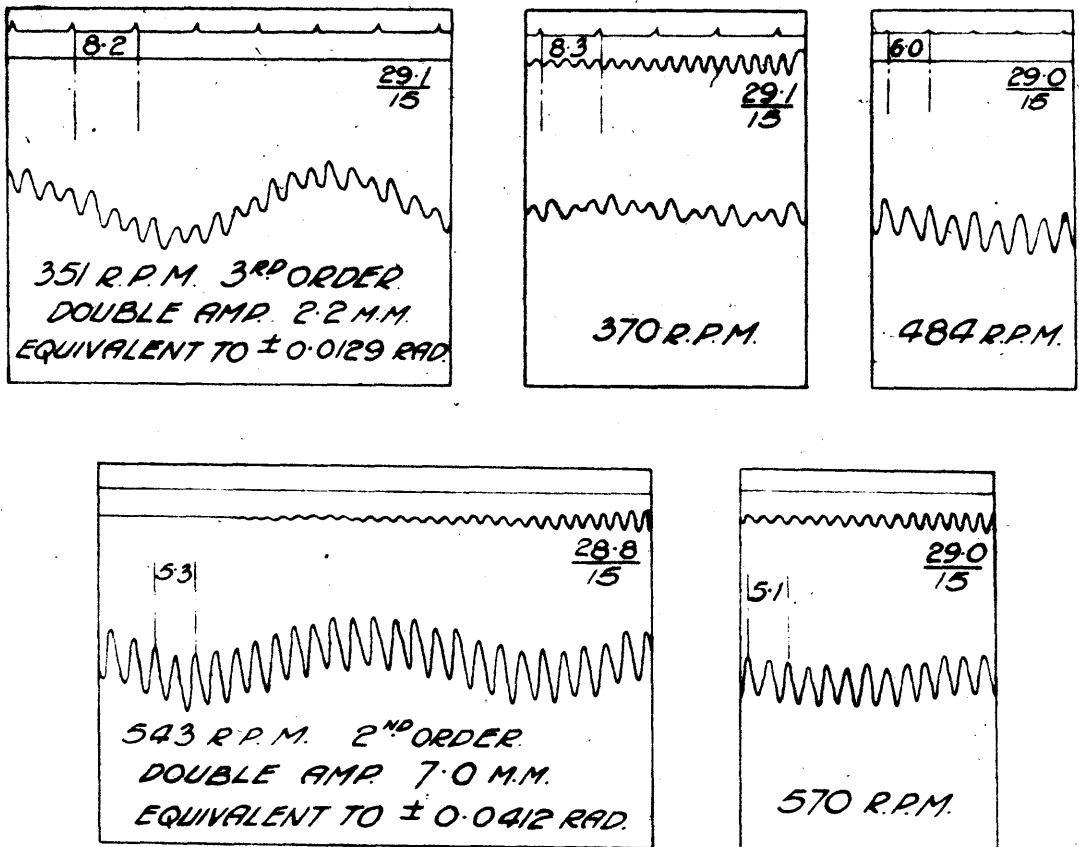


FIG. 39 SERIES III GRAVITY OIL FEED TO MAIN BEARING.

MASS SYSTEM M2. 1P. WITHOUT RINGS.

TORSIOGRAPH POS^N C. DIA. 1.115" MAGNIFICATION $\frac{8}{9}$

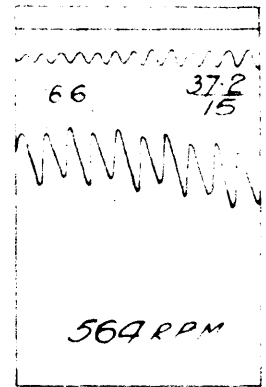
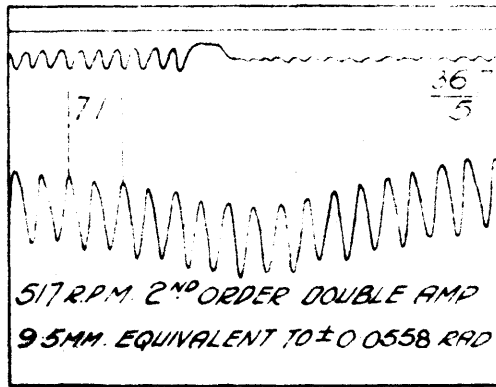
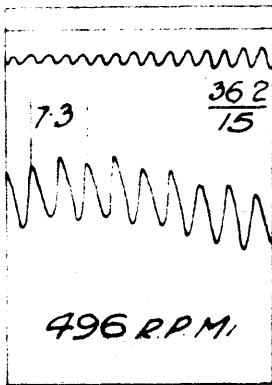
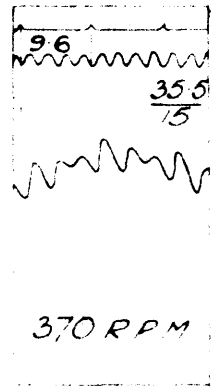
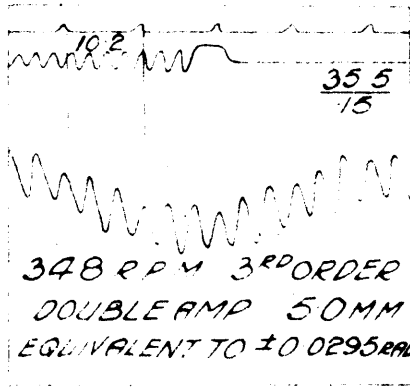
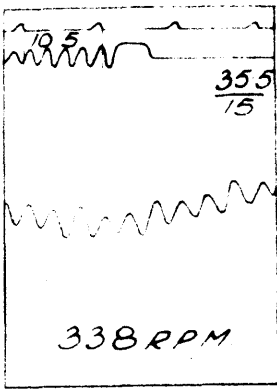


FIG 40 SERIES III GRAVITY OIL FEED TO MAIN BEARING

MASS SYSTEM M2. 2p WITH RINGS.

TORSIOGRAPH POS^N C. DIA 1.115" MAGNIFICATION $\frac{6}{1}$

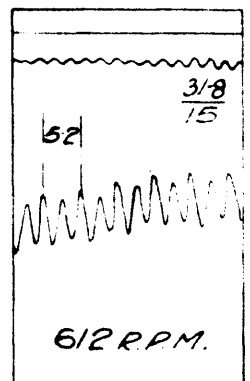
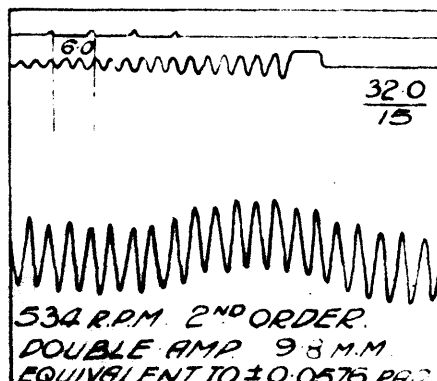
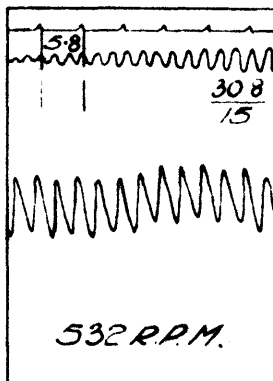
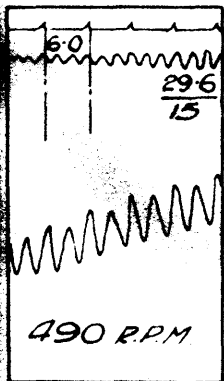
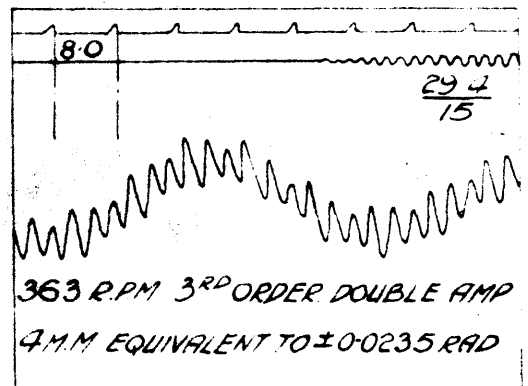
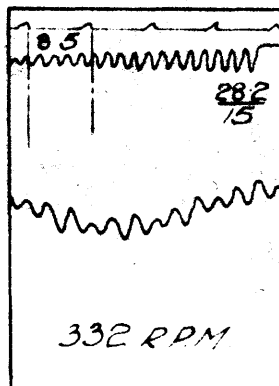
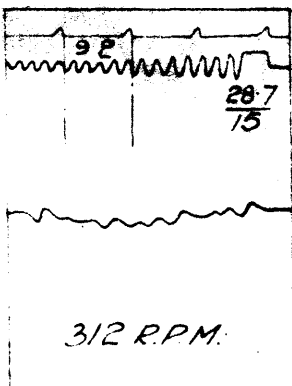


FIG 41. SERIES III GRAVITY OIL FEED TO MAIN BEARING

MASS SYSTEM M2. 2p. WITHOUT RINGS

TORSIOGRAPH POS^N C. DIA 1.115" MAGNIFICATION $\frac{6}{1}$

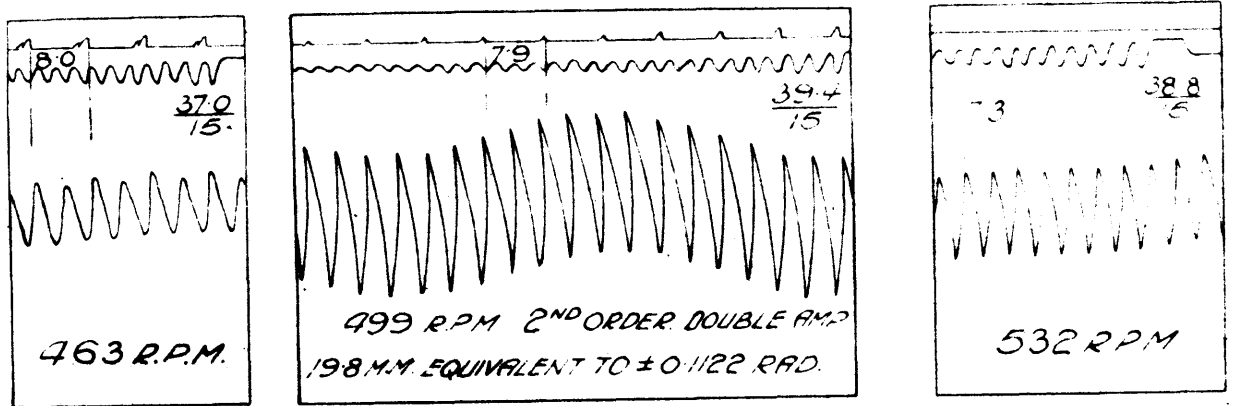
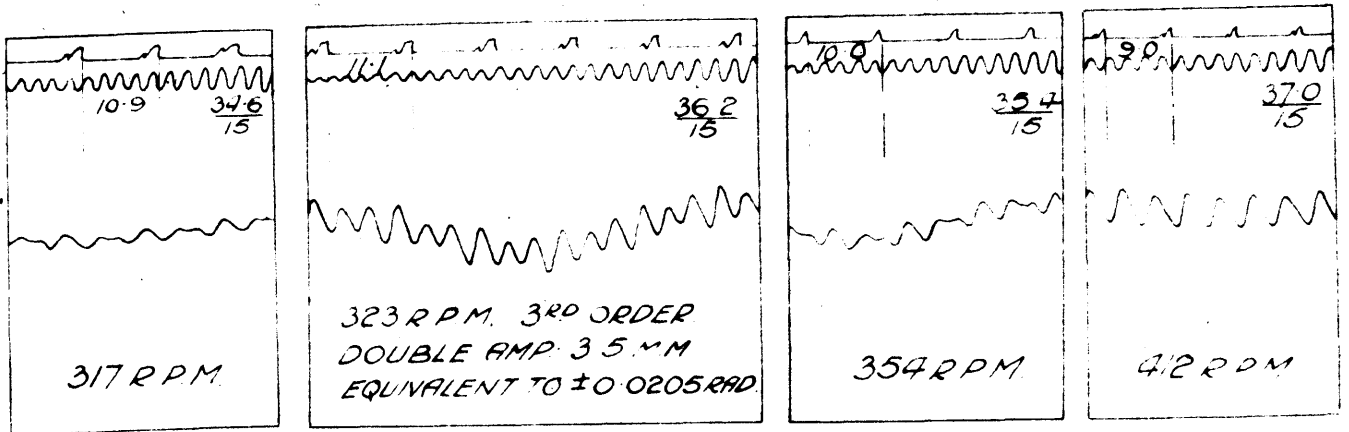


FIG. 42 SERIES III GRAVITY OIL FEED TO MAIN BEARING
MASS SYSTEM M.2. 3p. WITHOUT RINGS.
TORSIOGRAPH POS^N C. DIA. 1.115" MAGNIFICATION $\frac{6}{7}$

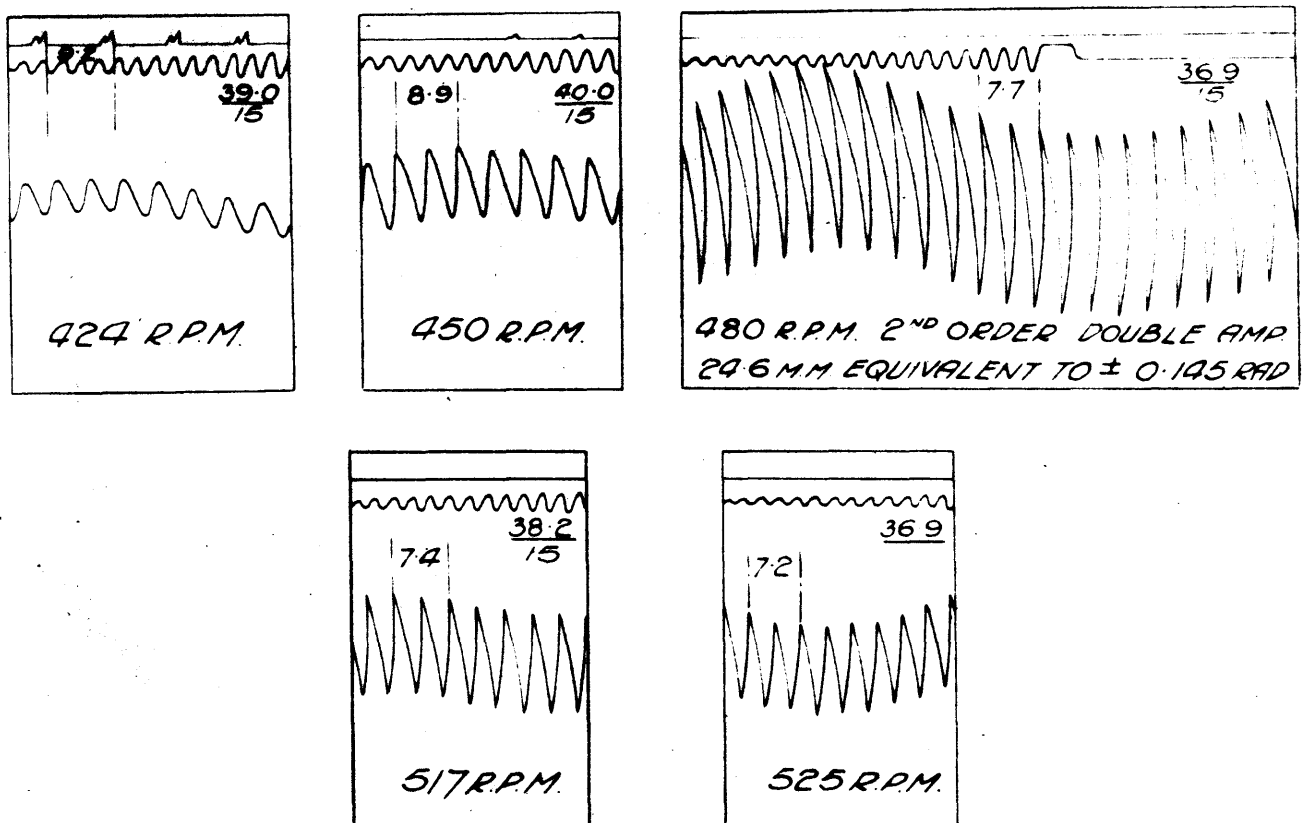


FIG. 43 SERIES III GRAVITY OIL FEED TO MAIN BEARING
MASS SYSTEM M.2. 4p. WITHOUT RINGS.
TORSIOGRAPH POS^N C. DIA. 1.115" MAGNIFICATION $\frac{6}{7}$

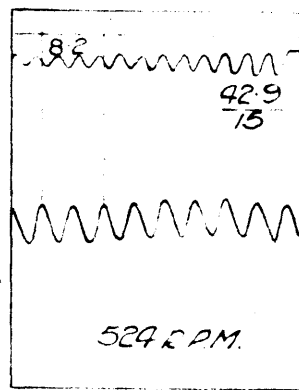
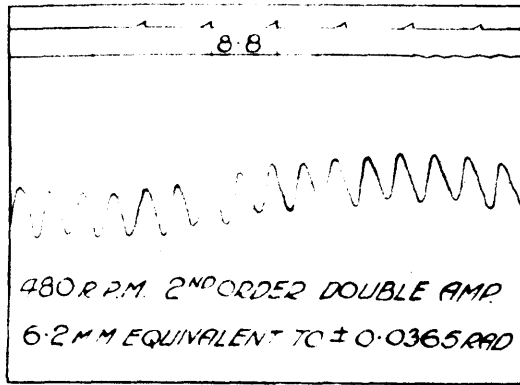
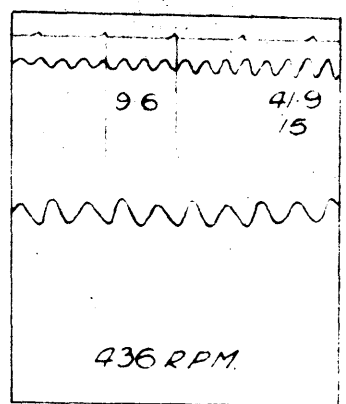
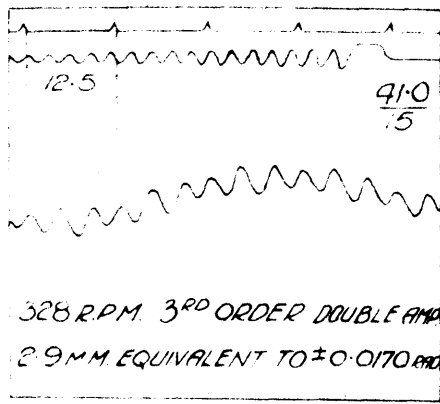
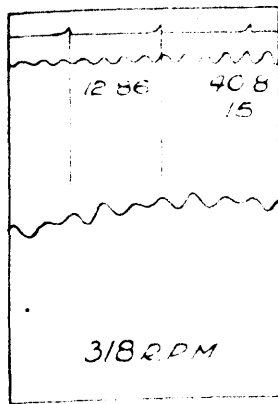


FIG. 44 SERIES III GRAVITY OIL FEED TO MAIN BEARING.

MASS SYSTEM M.3. 1P. WITH RINGS.

TORSIOGRAPH POS^N C. DIA. 1.115" MAGNIFICATION $\frac{6}{7}$

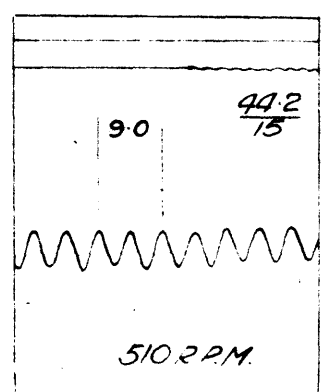
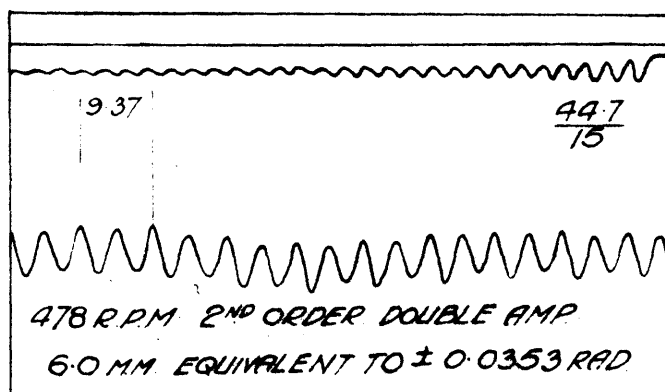
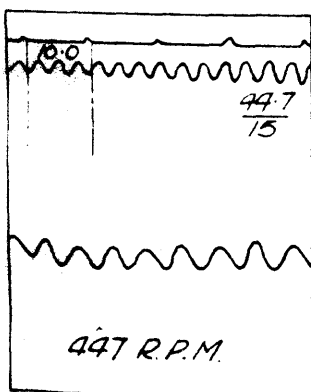
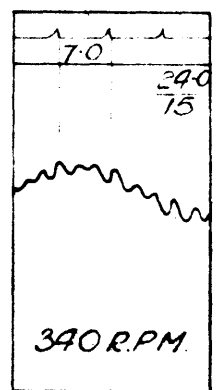
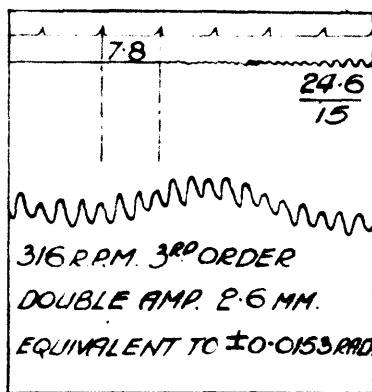
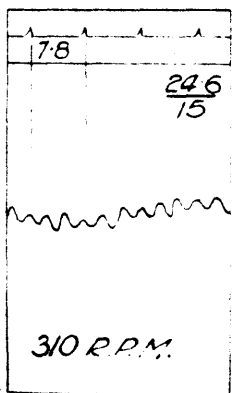


FIG. 45 SERIES III GRAVITY OIL FEED TO MAIN BEARING.

MASS SYSTEM M.3. 1P. WITHOUT RINGS.

TORSIOGRAPH POS^N C. DIA. 1.115" MAGNIFICATION $\frac{6}{7}$

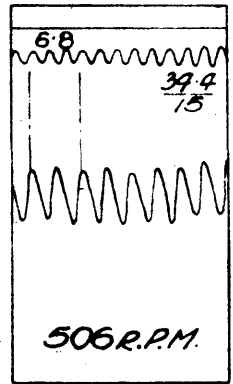
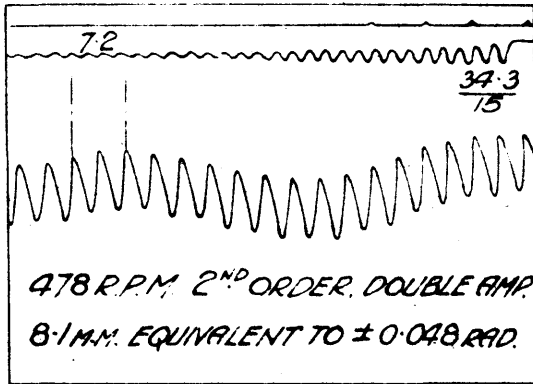
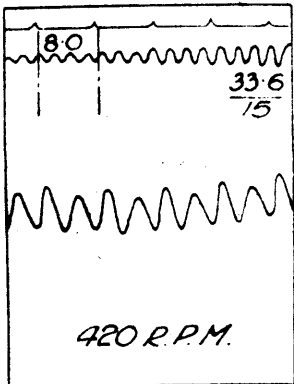
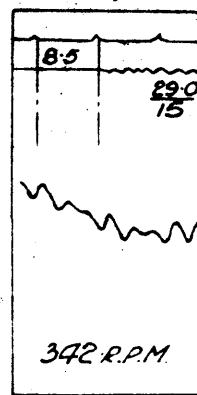
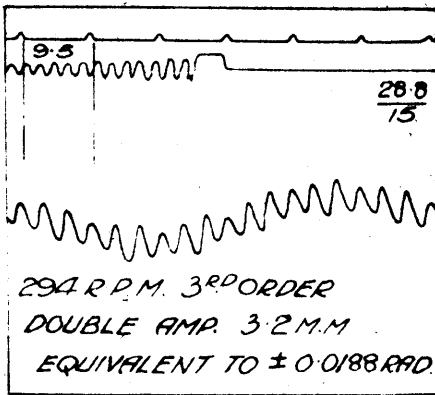
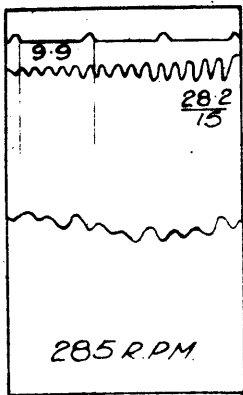


FIG. 46. SERIES III. GRAVITY OIL FEED TO MAIN BEARING.
MASS SYSTEM M3. 2p. WITH RINGS.
TORSIOGRAPH POS^N C. DIA. 1.115" MAGNIFICATION $\frac{6}{1}$

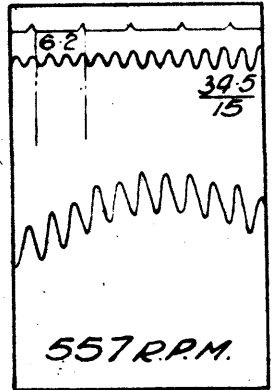
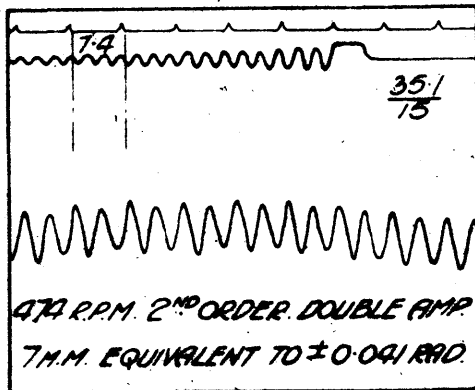
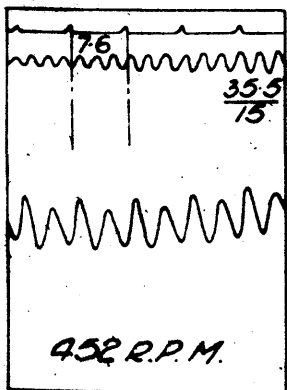
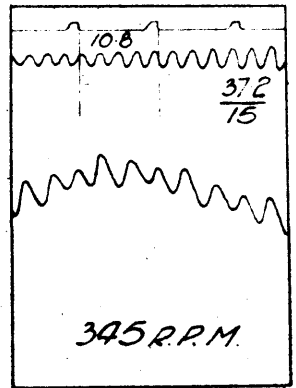
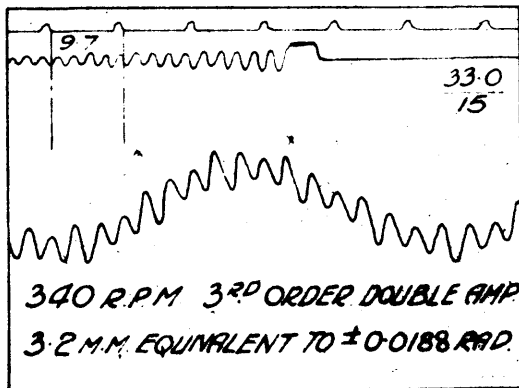
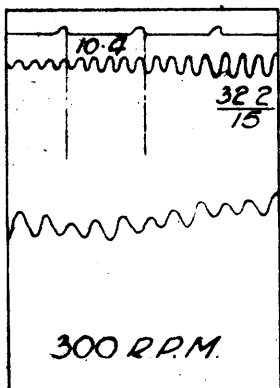


FIG. 47. SERIES III. GRAVITY OIL FEED TO MAIN BEARING.
MASS SYSTEM M3. 2p. WITHOUT RINGS.
TORSIOGRAPH POS^N C. DIA. 1.115" MAGNIFICATION $\frac{6}{1}$

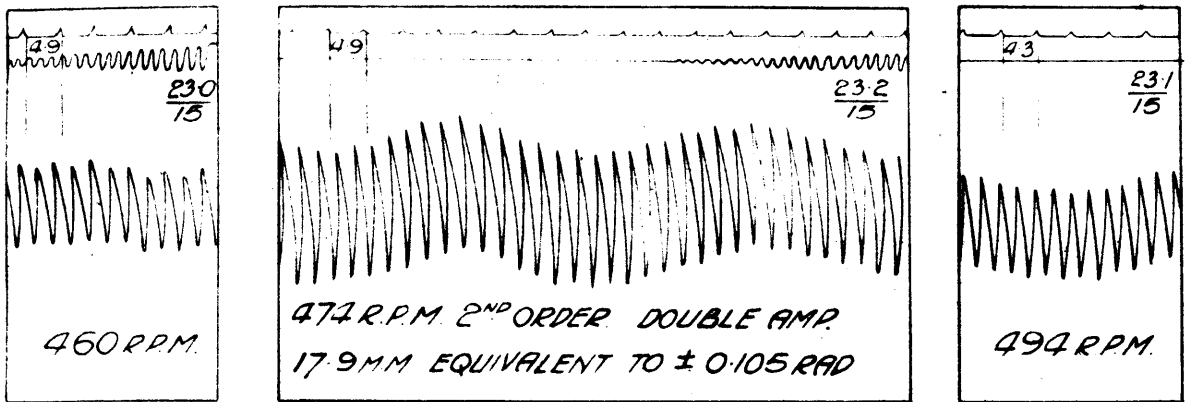
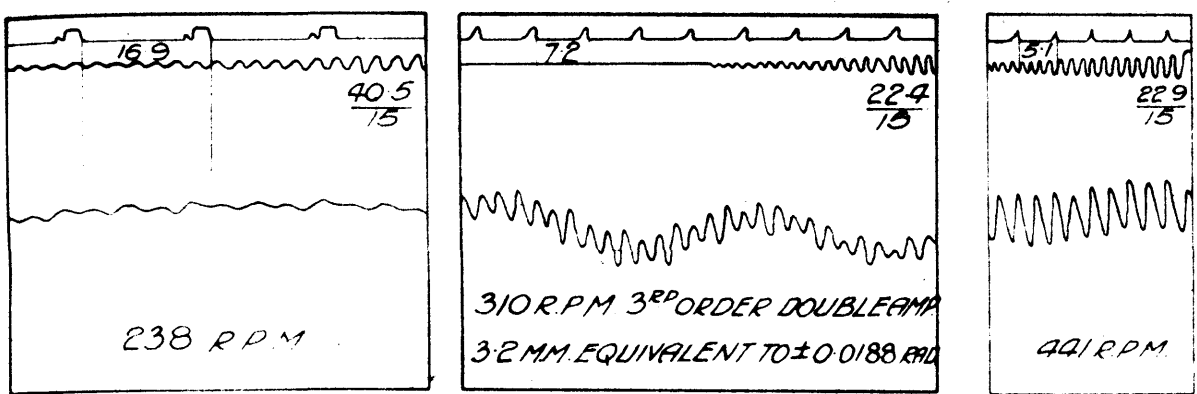


FIG. 48 SERIES III GRAVITY OIL FEED TO MAIN BEARING.
MASS SYSTEM M3 3p. WITHOUT RINGS.
TORSIOGRAPH POS^N C. DIA. 1.115" MAGNIFICATION $\frac{6}{1}$

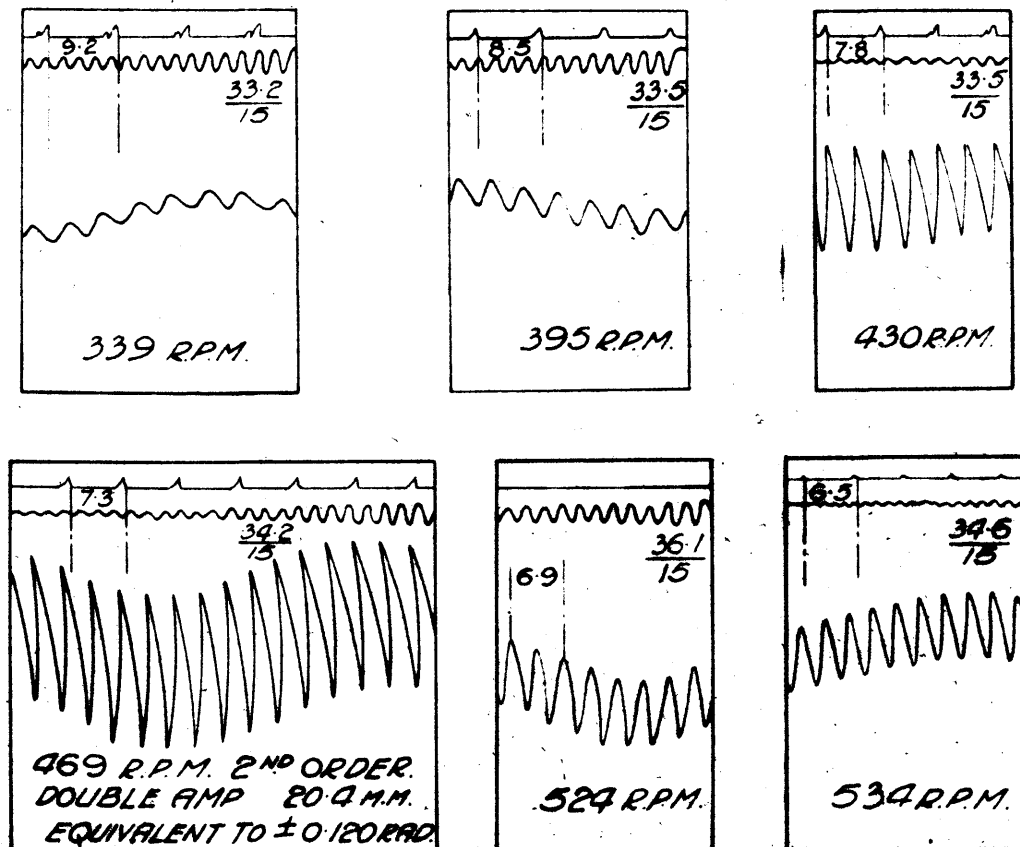
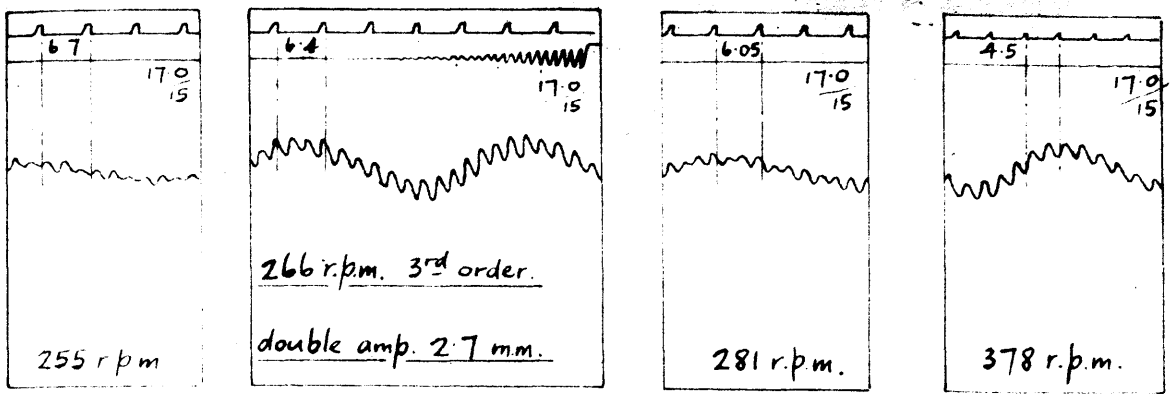


FIG. 49. SERIES III GRAVITY OIL FEED TO MAIN BEARING.
MASS SYSTEM M3 4p. WITHOUT RINGS.
TORSIOGRAPH POS^N C. DIA. 1.115" MAGNIFICATION $\frac{6}{1}$



equivalent to ± 0.0158 rad.

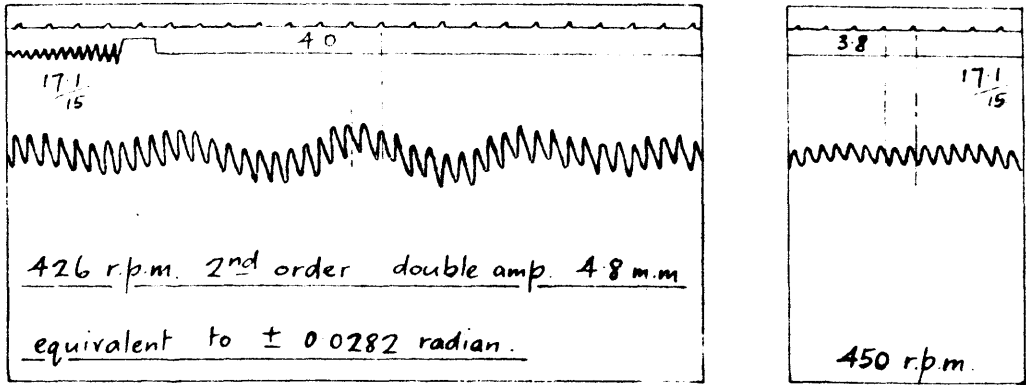
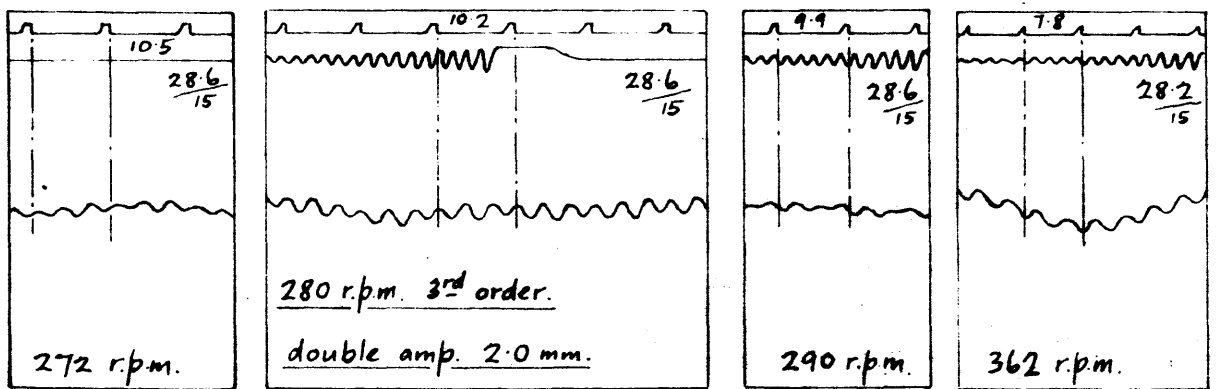


Fig. 50. Series III. Gravity oil feed to main bearing.

Mass system M4. 1p. with rings.

Torsigraph posⁿ dia. 1.115" Magnification $\frac{6}{1}$



equivalent to ± 0.0117 radian

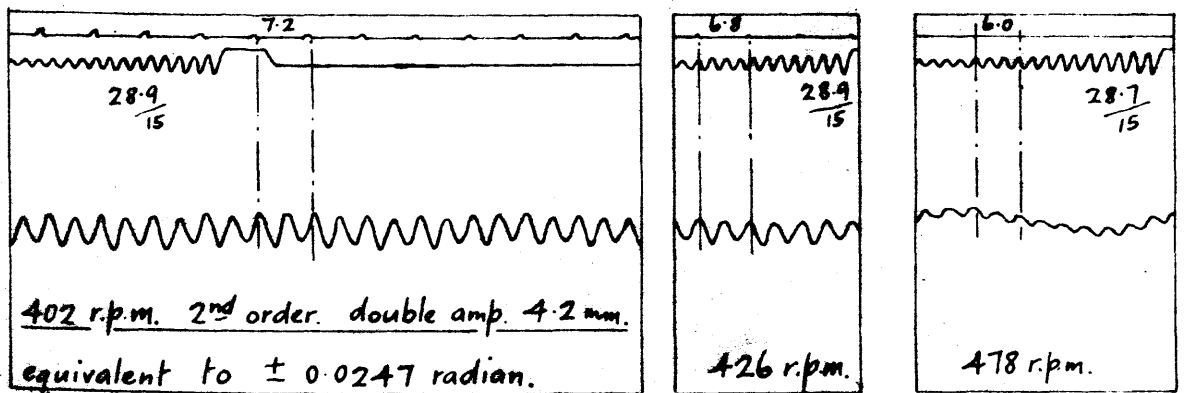
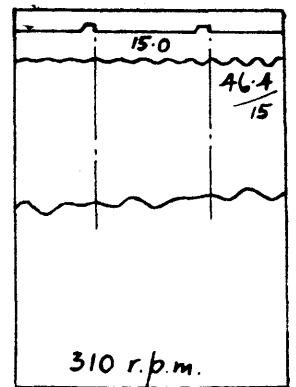
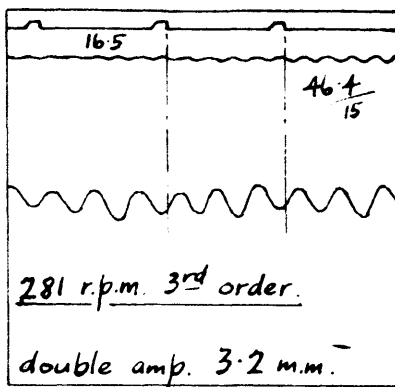
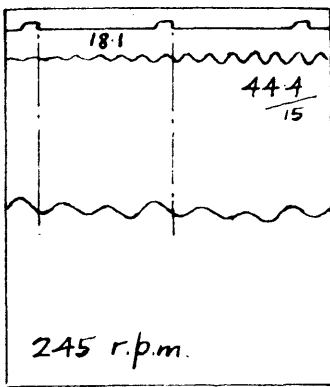


Fig. 51. Series III. Gravity oil feed to main bearing.

Mass system M4. 1p. without rings.

Torsigraph posⁿ C. dia. 1.115" Magnification $\frac{6}{1}$



equivalent to ± 0.0188 rad.

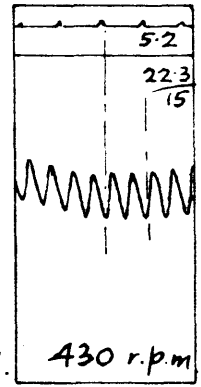
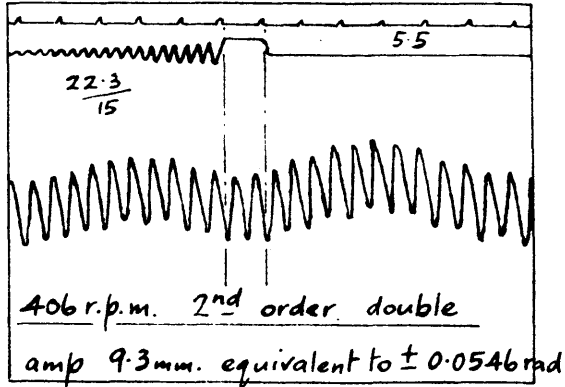
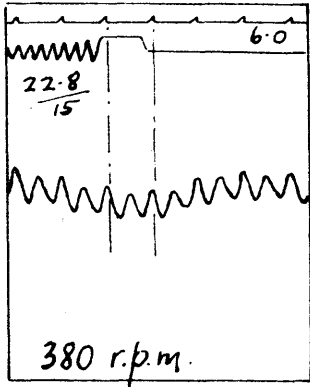


Fig. 52. Series III Gravity oil feed to main bearing.

Mass system M4.2p with rings.

Torsion graph posⁿ dia. 1.115" Magnification $\frac{6}{1}$

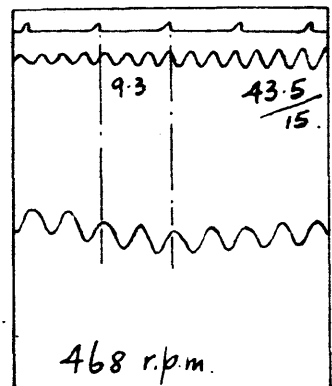
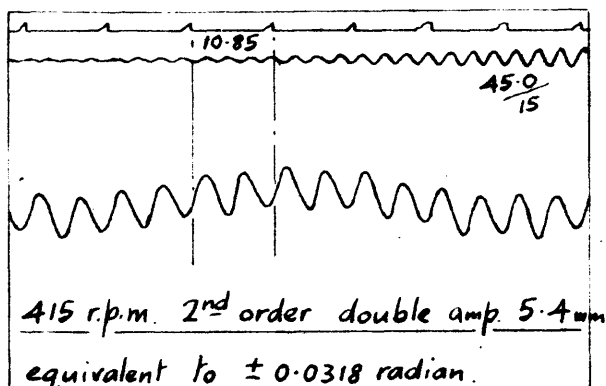
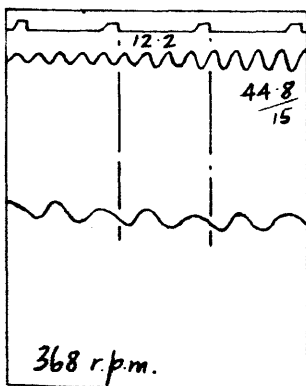
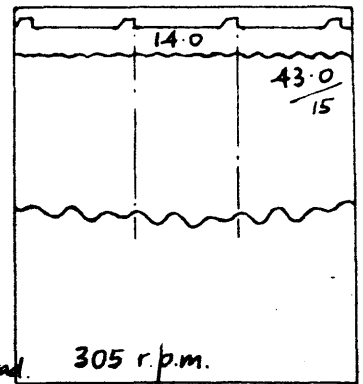
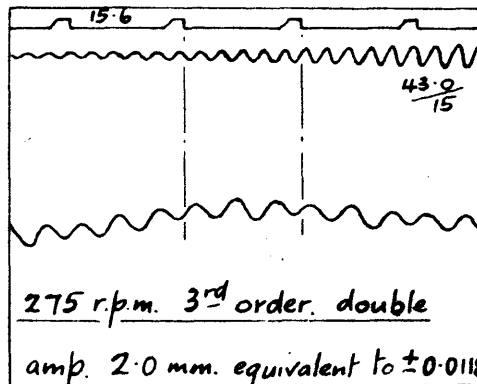
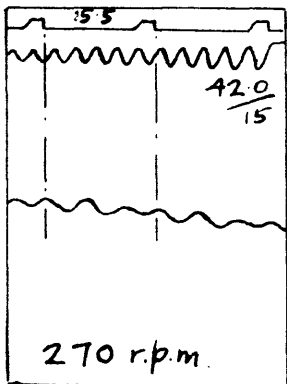


Fig. 53 Series III Gravity oil feed to main bearing.

Mass system M4.2p without rings.

Torsion graph posⁿ c dia. 1.115" Magnification $\frac{6}{1}$

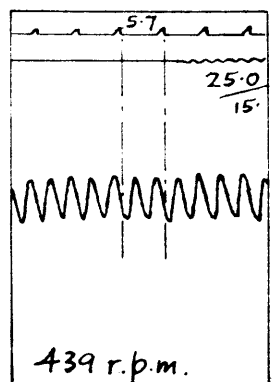
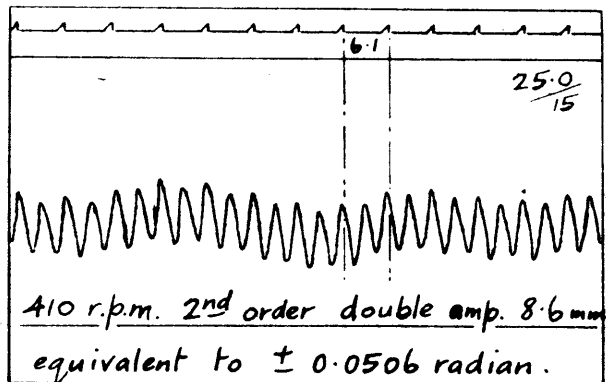
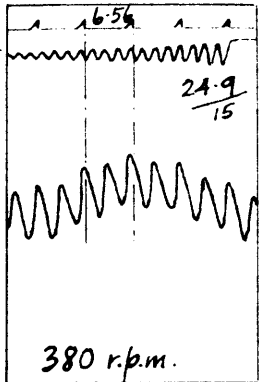
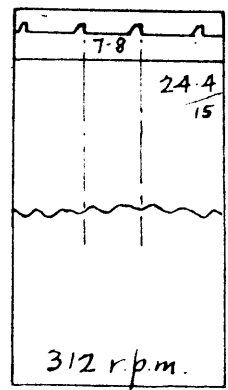
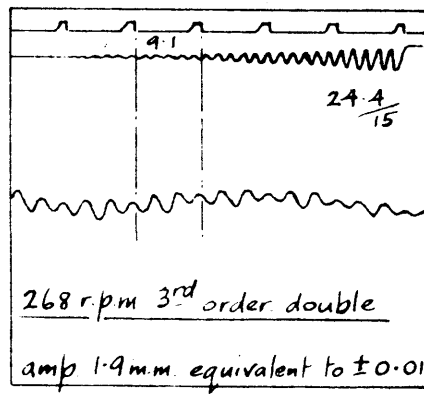
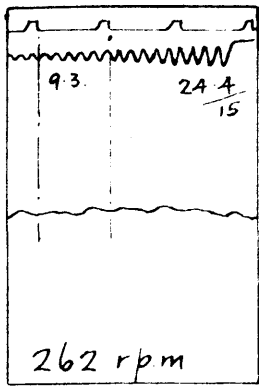


Fig. 54. Series III. Gravity oil feed to main bearing.

Mass system M4. 3p. without rings.

Torsion graph position. dia. 1.115" Magnification $\frac{6}{1}$

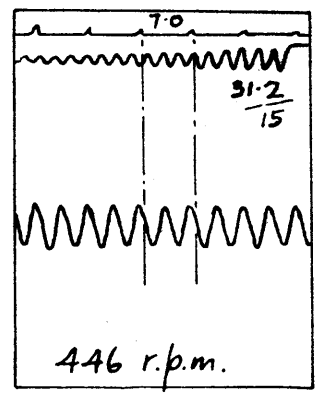
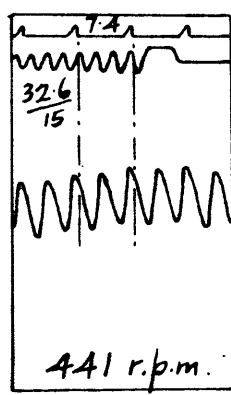
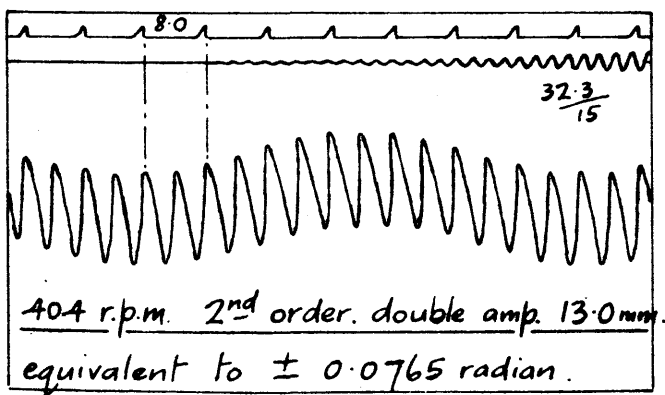
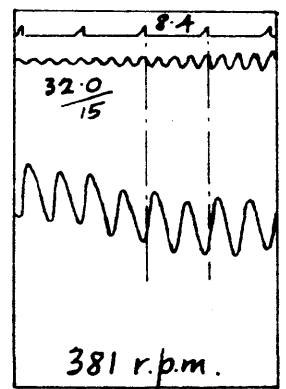
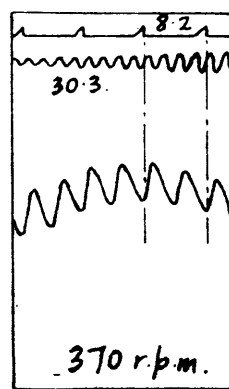
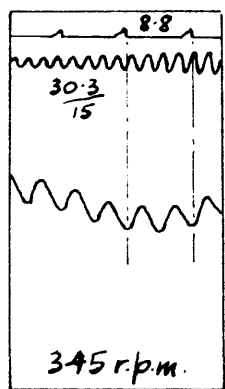
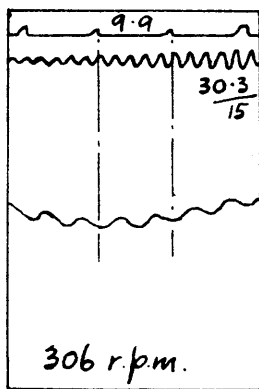


Fig. 55. Series III Gravity oil feed to main bearing.

Mass system M4. 4p. without rings.

Torsion graph position C. dia 1.115". Magnification $\frac{6}{1}$

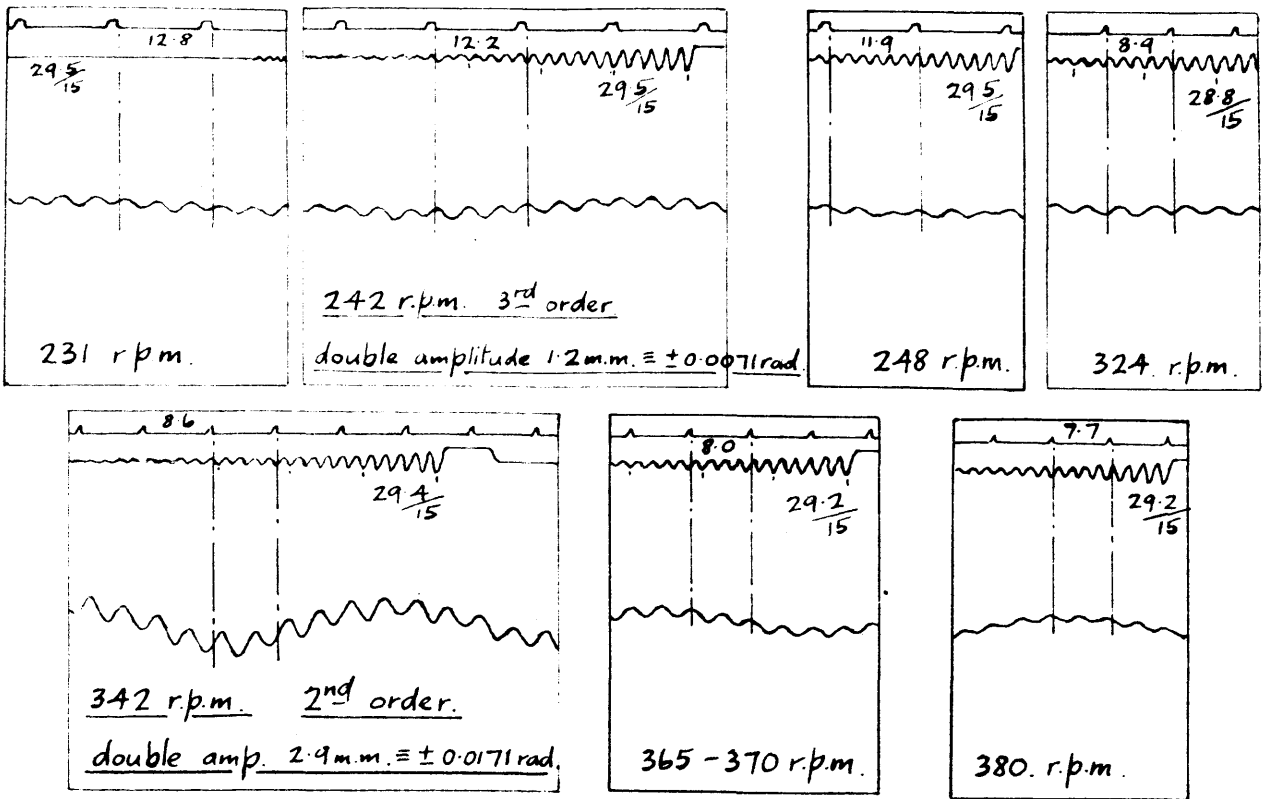


Fig. 56. Series III. Gravity oil feed to main bearing.

Mass system M.5. lb. without rings. Torsiongraph posⁿ C.

$d = 1.115$ " Magnification $\frac{6}{1}$.

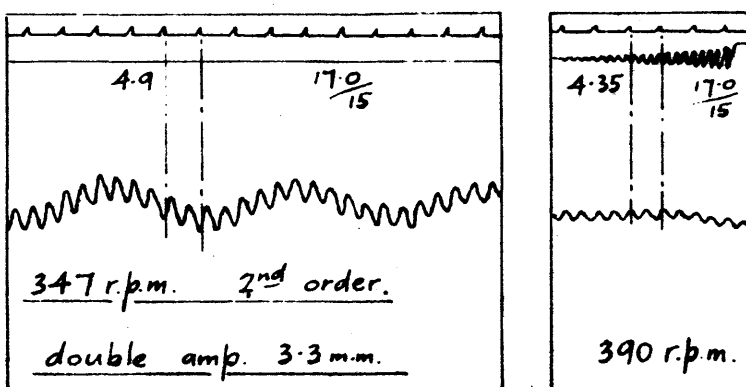
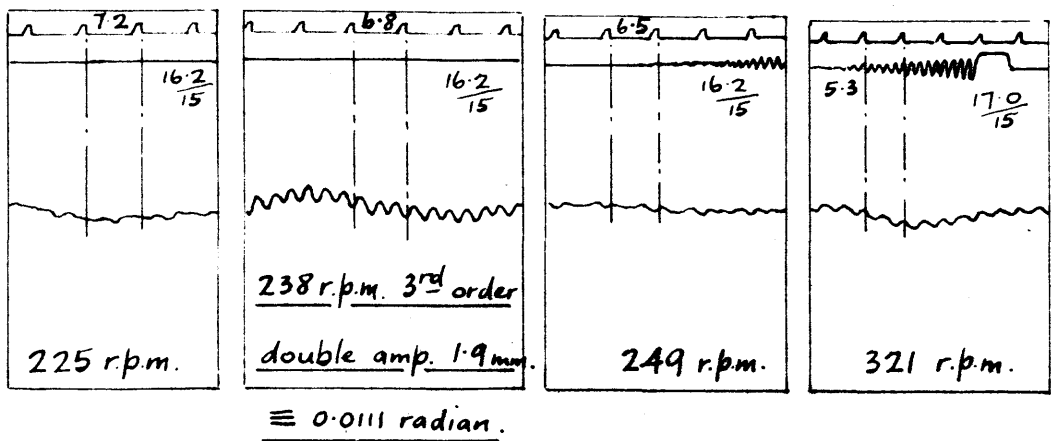


Fig. 57. Series III. Gravity oil feed to main bearing.

Mass system M.5. lb. with rings.

Torsiongraph position C. dia = 1.115" Magnification $\frac{6}{1}$.

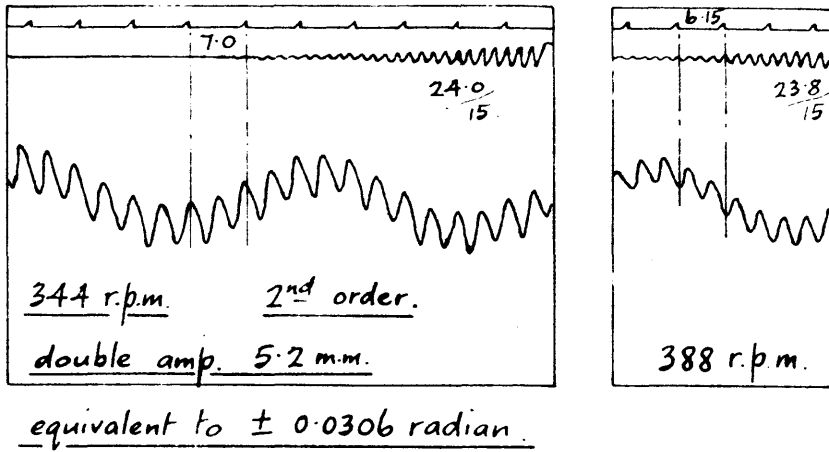
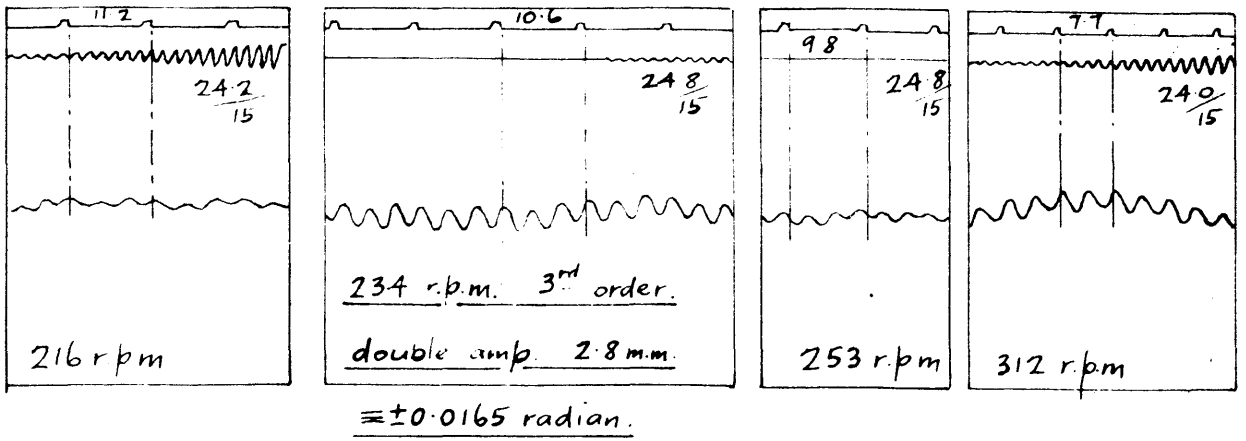


Fig. 58. Series III. Gravity oil feed to main bearing.
 Mass system M5. 2p. with rings.
 Torsiograph posⁿ C. dia. 1.115" Magnification $\frac{6}{1}$.

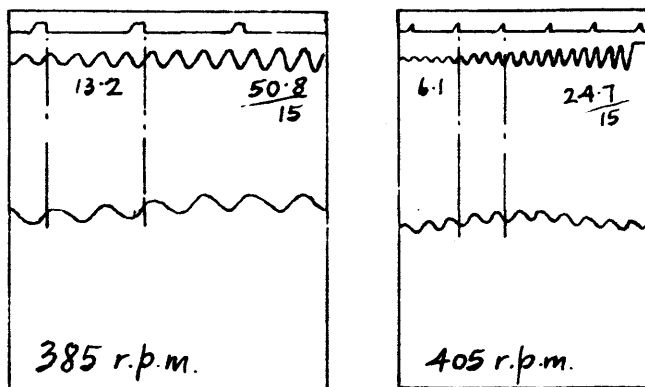
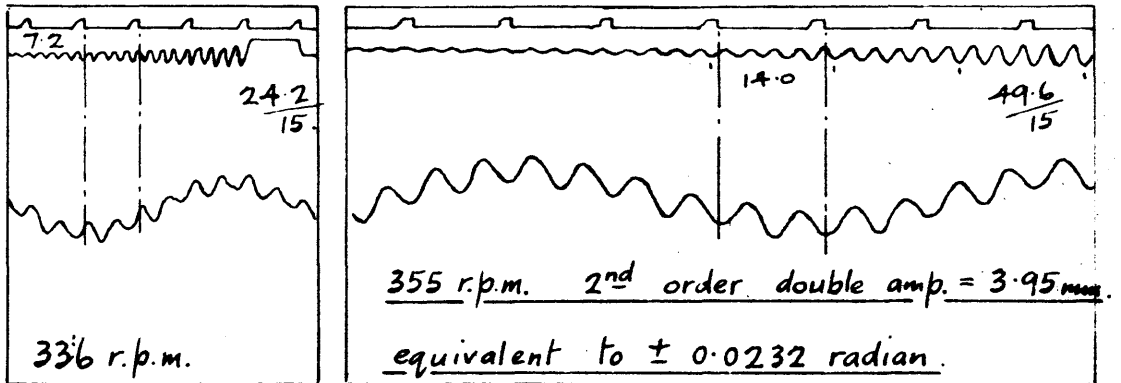


Fig. 59. Series III Gravity oil feed to main bearing.
 Mass system M.5. 2p. without rings.
 Torsiograph posⁿ C. dia. 1.115" Magnification $\frac{6}{1}$.

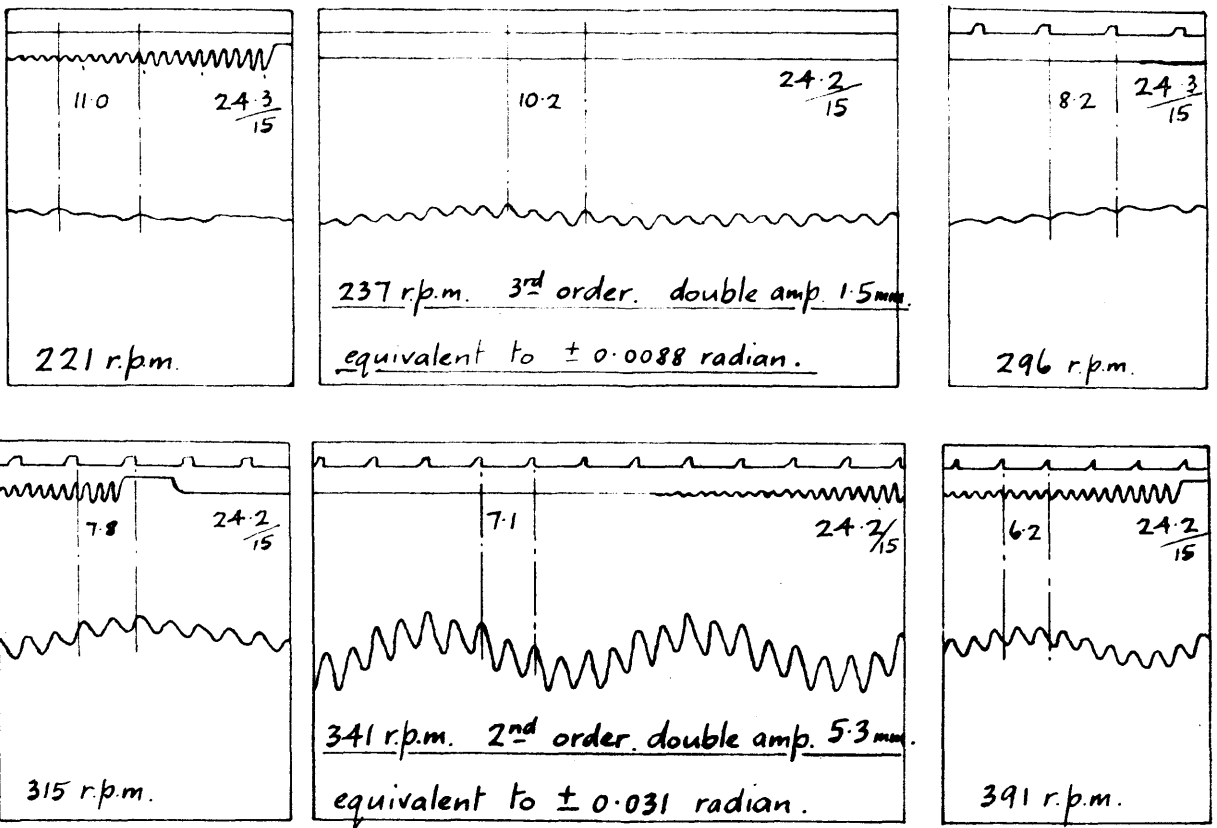


Fig. 60. Series III. Gravity oil feed to main bearing.

Mass system. M5.3p. without rings.

Torsiograph posⁿ C. dia. 1.115" Magnification. $\frac{6}{1}$

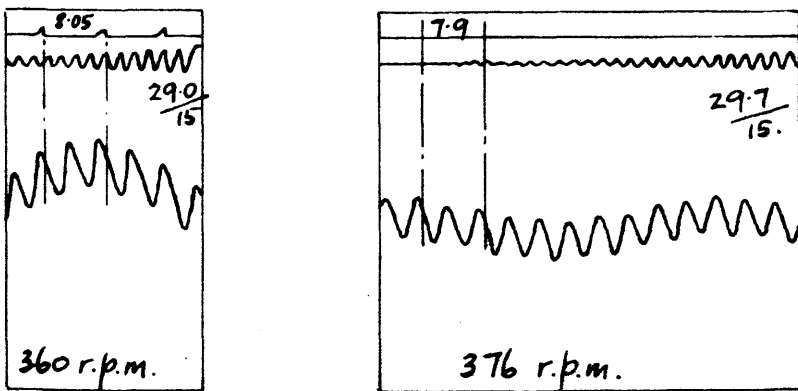
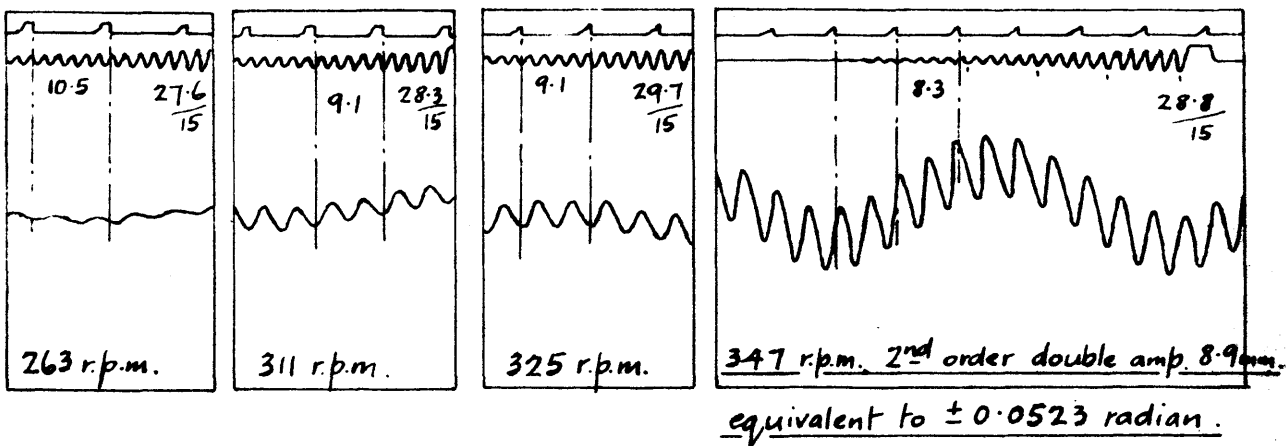


Fig. 61. Series III. Gravity oil feed to main bearing.

Mass system. M5.4p. without rings.

Torsiograph posⁿ C. dia. 1.115" Magnification $\frac{6}{1}$

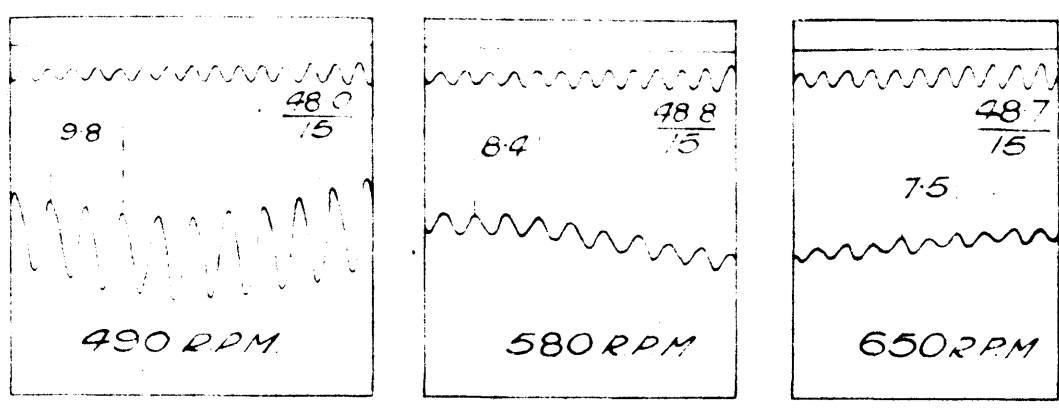
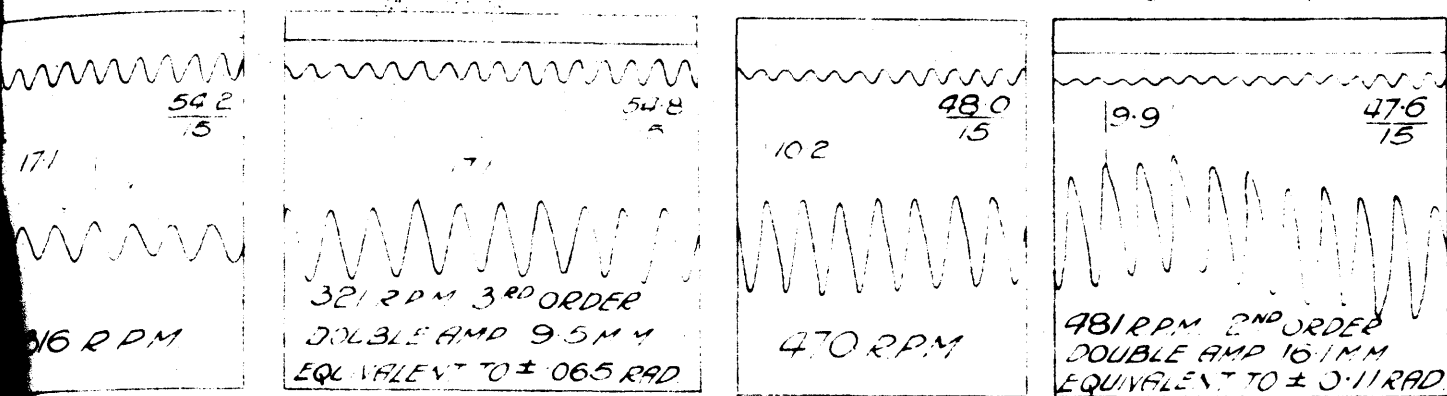


FIG. 62. SERIES I. IMPERFECT LUBRICATION

MASS SYSTEM M3. 1P WITH RINGS.

TORSIOGRAPH POSN A. DIA 1.92" MAGNIFICATION $\frac{3}{1}$

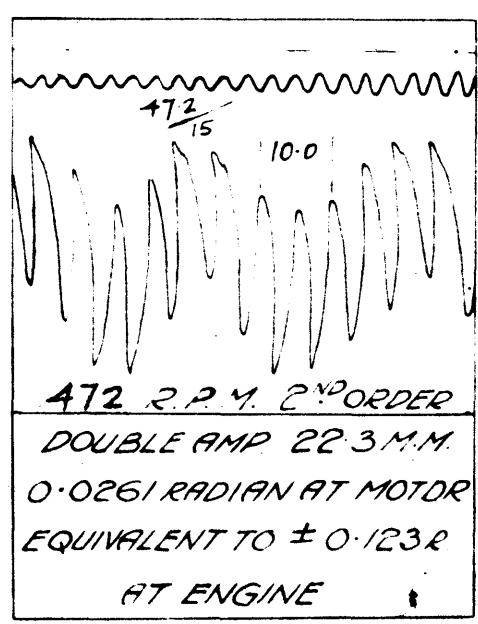


FIG. 19. SERIES I. IMPERFECT LUBRICATION

MASS SYSTEM M3 1P WITH RINGS.

TORSIOGRAPH POSN. E. DIA 11.2" MAGNIFICATION $\frac{3}{1}$

gravity feed removed giving imperfect lubrication conditions was examined and the representative records in the vicinity of resonance are given in Fig. 62.

IV. Power Tests.

Observations were taken of the power input to the motor over the speed range, the pistons being fitted with and without rings. These tests were required mainly for checking the energy dissipated by vibration at resonance. However, since the ammeter had to work on a 0 - 30 ampere range on account of the total power, it was found that definite increases in current taken, in the vicinity of resonance, could be read accurately only for the cases where excessive amplitude occurred. Hence observations at resonance are reliable for mass-system *M1.4p.* series only and these are plotted in Fig. 63.

In this figure the full line *G* to *E* represents the additional power absorbed when slowly approaching the critical from a lower speed. After sustaining and balancing at resonance an additional increase in power causes a general acceleration of the entire system until balance is found at *F*. This effect is also shown on the Torsiograph record *M1.4p.-* no rings - Fig. 37. Similarly the chain dotted line from *F* to *E* is obtained by slowly decreasing the speed until resonance is again reached. A period of deceleration follows any further decrease in power. This general behaviour is most marked with the very large amplitudes.

Analysis of the Torsiograph Records.

For similar portions of the records, representing balanced conditions, the average speed of each revolution of the shaft was calculated from the paper speed and cycle displacement. It is necessary to calculate the paper speed throughout the entire

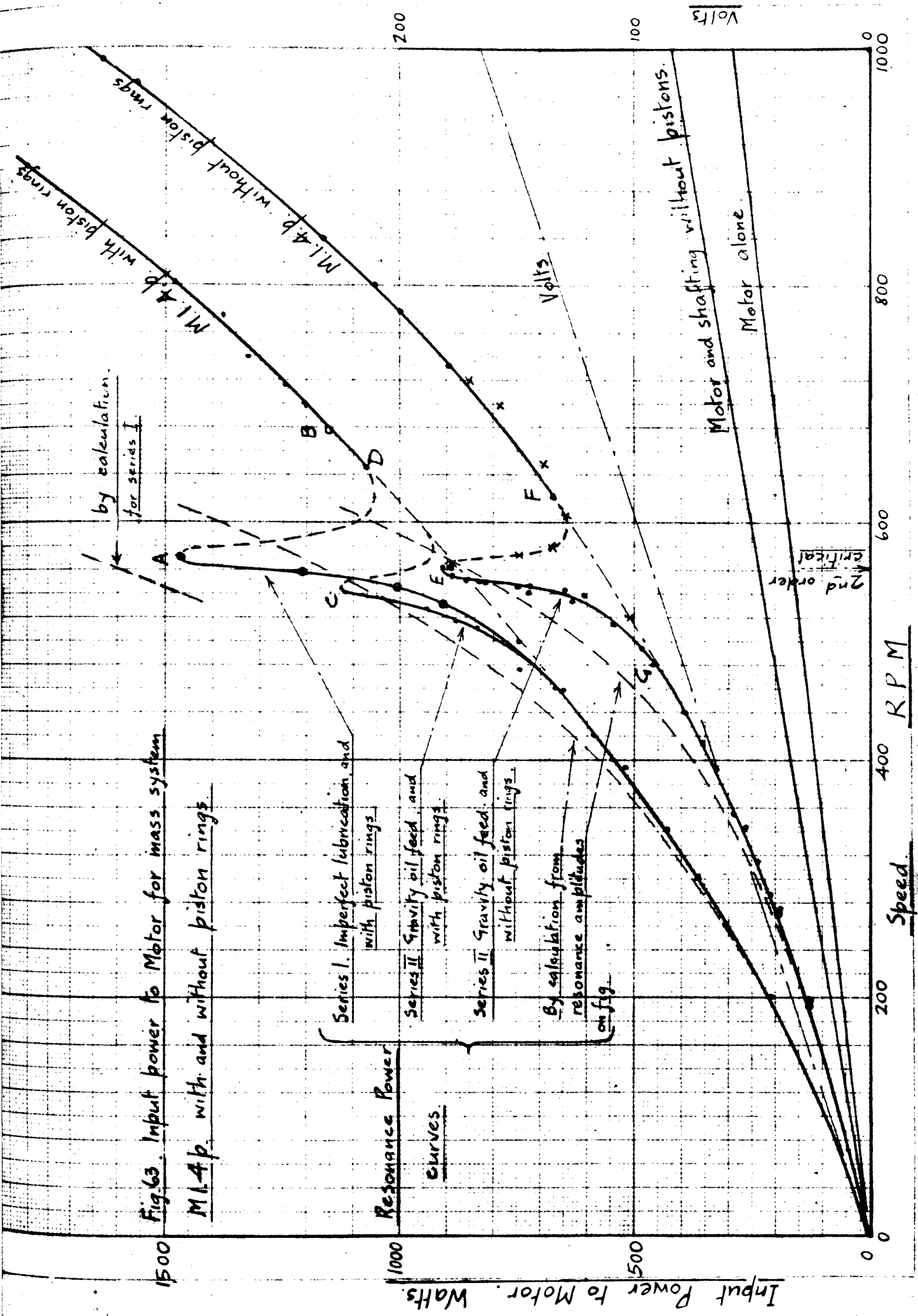


Fig. 63. Input power to Motor for mass system

M.I. 4p. with and without piston rings

Series I. Imperfect lubrication and with piston rings

Series II Gravity oil feed and with piston rings

Series II Gravity oil feed and without piston rings

By calculation from resonance amplitudes on fig.

Resonance Power curves.

Input Power to Motor. Watts

Speed

RPM

Volts

Volts

Motor and shafting without pistons.

Motor alone.

roll since variations occur due to the clockwork drive and diminution of paper roll diameter.

It is seen from the records that the shaft oscillations sometimes appear superimposed upon a low frequency wave arising from the instrument itself. There is no possibility of the shaft oscillations being amplified by this surge, since the natural frequency of the instrument used is 58.5 v.p.m. and is well below the frequencies and running speeds examined in the experiments. It is quite a simple matter to subtract the high frequency shaft oscillations from the record.

In order to determine the amplitude of any particular order of vibration, those due to all the other orders must be further subtracted from the record. Harmonic analysis of such small diagrams, traced by a pen of $3\frac{1}{32}$ in. radius, working on a pivot, can only be done with difficulty. Fortunately in the present case the 2nd and 3rd orders are the only ones of any importance, and combination of these two ratios with different phasing is a simple matter.

Taking amplitude ratios for these orders, suggested by harmonic analysis of some of the records, the vibration diagrams in the vicinity of 2nd order resonance with 3rd order forcing and vice-versa can be easily built up.

The exciting torques are $-Q_2 \sin 2\theta$ and $-Q_3 \sin 3\theta$, giving rise to motions $-y_2 \sin(2\theta - \alpha)$ and $-y_3 \sin(3\theta - \alpha)$ respectively, where α in the extreme cases is $0, \frac{\pi}{2}$ and π . In the vicinity of 2nd order resonance, the 3rd order motion is $+y_3 \sin 3\theta$ where $y_2 > y_3$, hence in passing through the 2nd order critical, the curve changes from $-y_2 \sin 2\theta + y_3 \sin 3\theta$ to $+y_2 \sin 2\theta + y_3 \sin 3\theta$. At the critical the curve is $+y_2 \cos 2\theta + y_3 \sin 3\theta$. Due to the paper moving from left to right, these equations are drawn by the torsigraph as given in Fig. 64.

2nd order

below resonance

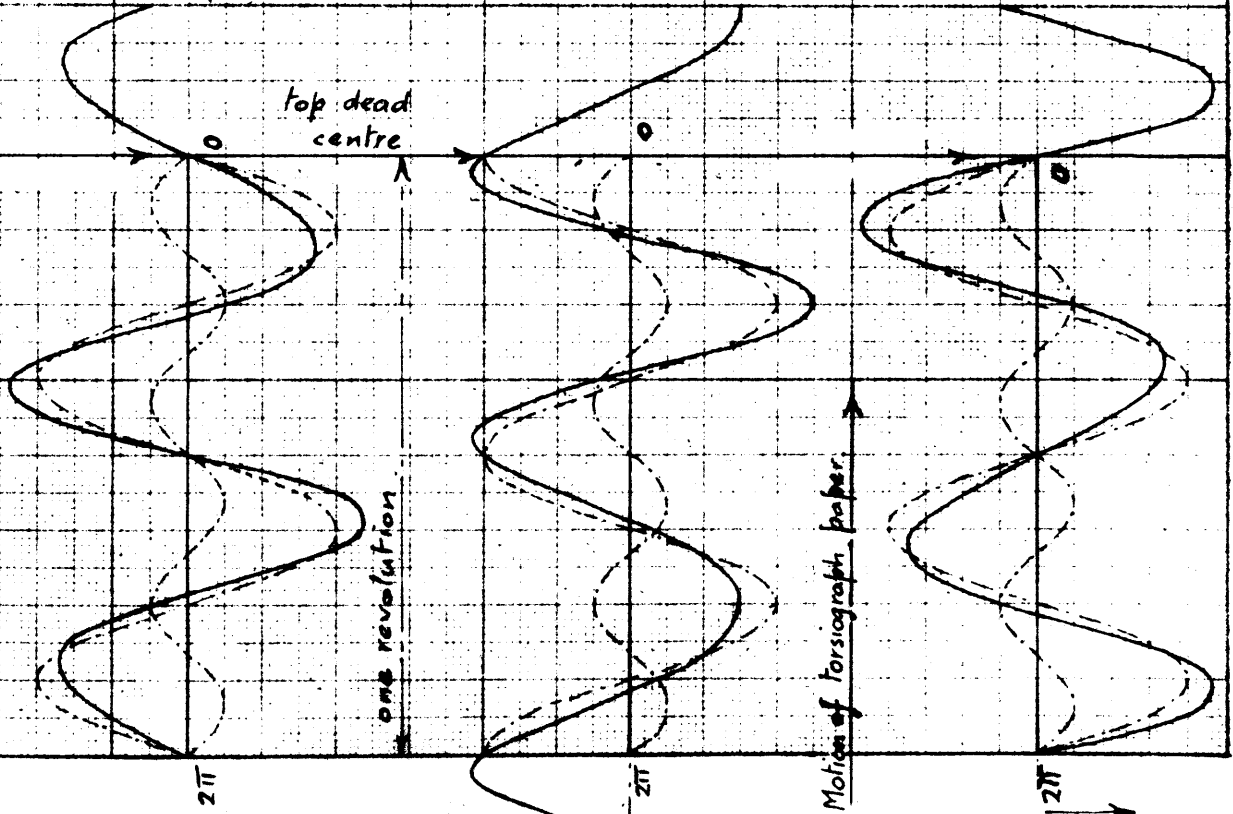
$$-y_2 \sin 2\theta + y_3 \sin 3\theta$$

resonance

$$y_2 \cos 2\theta + y_3 \sin 3\theta$$

above resonance

$$y_2 \sin 2\theta + y_3 \sin 3\theta$$



The mean of the maximum and minimum double amplitudes gives the 2nd order double amplitude.

accelⁿ

mean line

retardⁿ

top dead centre

3rd order

below resonance

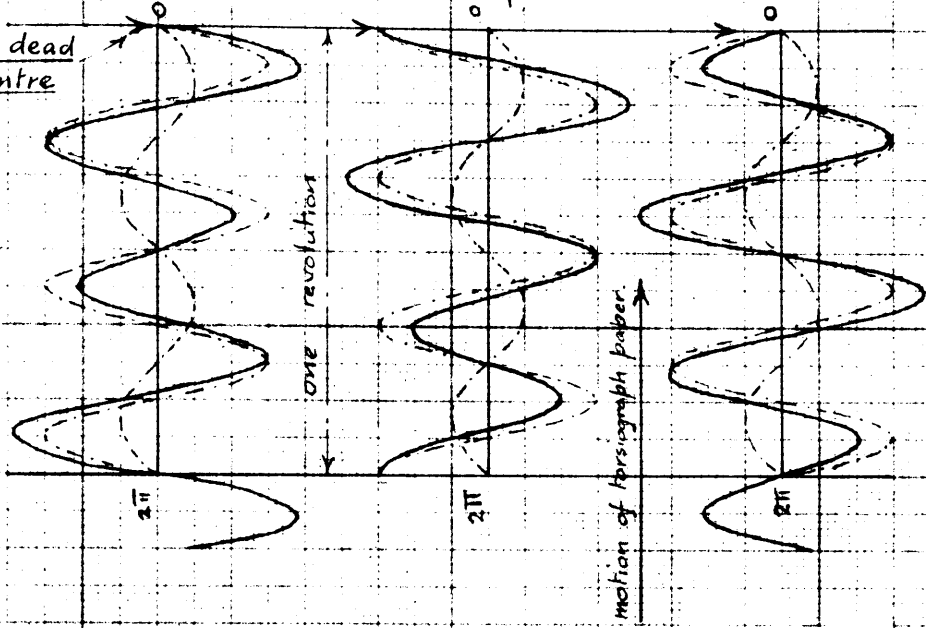
$$-y_2 \sin 2\theta - y_3 \sin 3\theta$$

resonance

$$-y_2 \sin 2\theta + y_3 \cos 3\theta$$

above resonance

$$-y_2 \sin 2\theta + y_3 \sin 3\theta$$



The mean of the maximum and minimum double amplitudes gives the 3rd order double amplitude.

Fig. 64 2nd and 3rd order vibrations in the vicinity of resonance.

as drawn by the torsigraph.

Similarly in the vicinity of the 3rd order critical, the 2nd order forced vibration is $-y_2 \sin 2\theta$ hence choosing suitable amplitude ratios $y_2 < y_3$, the changes in the record for the extreme conditions are also given in Fig. 64.

As the speed increases Fig. (f) tends to Fig.(a) with change in relative amplitude ratios.

The diagrams are quite representative of those appearing on the torsigraph records and therefore a close study of them practically explains all the records at the speeds concerned.

It will be noticed for the 2nd order that the type of diagram below resonance is the reverse of that above, and at resonance the form is very distinctive, having a flat boundary at the top. For the 3rd order, diagrams on either side of resonance are of similar form but have different phase angles, while exact resonance gives a decided form.

Close scrutiny of the torsigraph records at the lower speeds where the dead centre timing operated show that the phase angle is indicated fairly well at resonance, but it is not possible to obtain the correct value on either side of resonance particularly with slow and irregular paper speeds. No great loss of value is incurred, however, as the essential features at resonance are given clearly.

Further examination of the diagrams on Fig. 64, shows that the double amplitude at resonance for any particular order can be obtained by taking the mean of the maximum and minimum double amplitudes. This also applies above and below the critical speeds for both the 2nd and 3rd orders.

This simple procedure was adopted when measuring the amplitudes from the records. For the tests with the opposed pistons, the records are quite simple, since the vibrations are due entirely to the 2nd order torque.

Thus for each revolution of the portions of records analysed the amplitude and corresponding speed was determined, and amplitude-speed curves plotted for each test. These graphs are given in Figs. 65 to 77, for all mass arrangements, and the corresponding undamped vibration curve for the engine mass plotted in accordance with equation (29).

Description of Results.

Taking Fig. 65 giving the results from the mass-system 11.1p., it is seen that the general curve of experimental amplitudes follows the theoretical quite closely although there are slight irregularities, but these are within the limits of accuracy of speed measurement from the torsigraphs. At resonance the frequencies agree to within 3 per cent. It can be shown that with ^{the} small damping present, the difference between the frequency at which maximum amplitude occurs and the resonant frequency is about 1 per cent., so that it is not possible to detect the difference by the torsigraph.

Effect of each piston.

Each piston gives practically the same curve and maximum amplitude so that all pistons may be regarded as being similar.

Lubrication.

It is seen from Fig. 73 that the effect of main bearing lubrication is very great in the control of amplitude. The maximum amplitude attained when imperfect lubrication prevails is practically twice that when oil is supplied to the bearing. The same marked difference is seen with the 3rd order amplitudes. By comparing the 3rd order resonance records for the same mass-systems under the different lubrication conditions, the effect is also portrayed by the differences in ^{the} type of diagram. With the greater damping, the ratio of the 3rd order resonance amplitude to the 2nd order forced vibration

Fig. 65 Series No. I. Imperfect Lubrication

Amplitude-speed curves of engine for each piston

Miss-system, M.I.P. with piston rings

Piston No.	Force-mech. position
4	B
3	A
2	B
1	B

Piston No.	2 nd order	3 rd order
○	± 0.199	± 0.086
×	± 0.207	± 0.0875
+	± 0.189	± 0.080
●	± 0.202	± 0.084
⊙	± 0.182	± 0.082

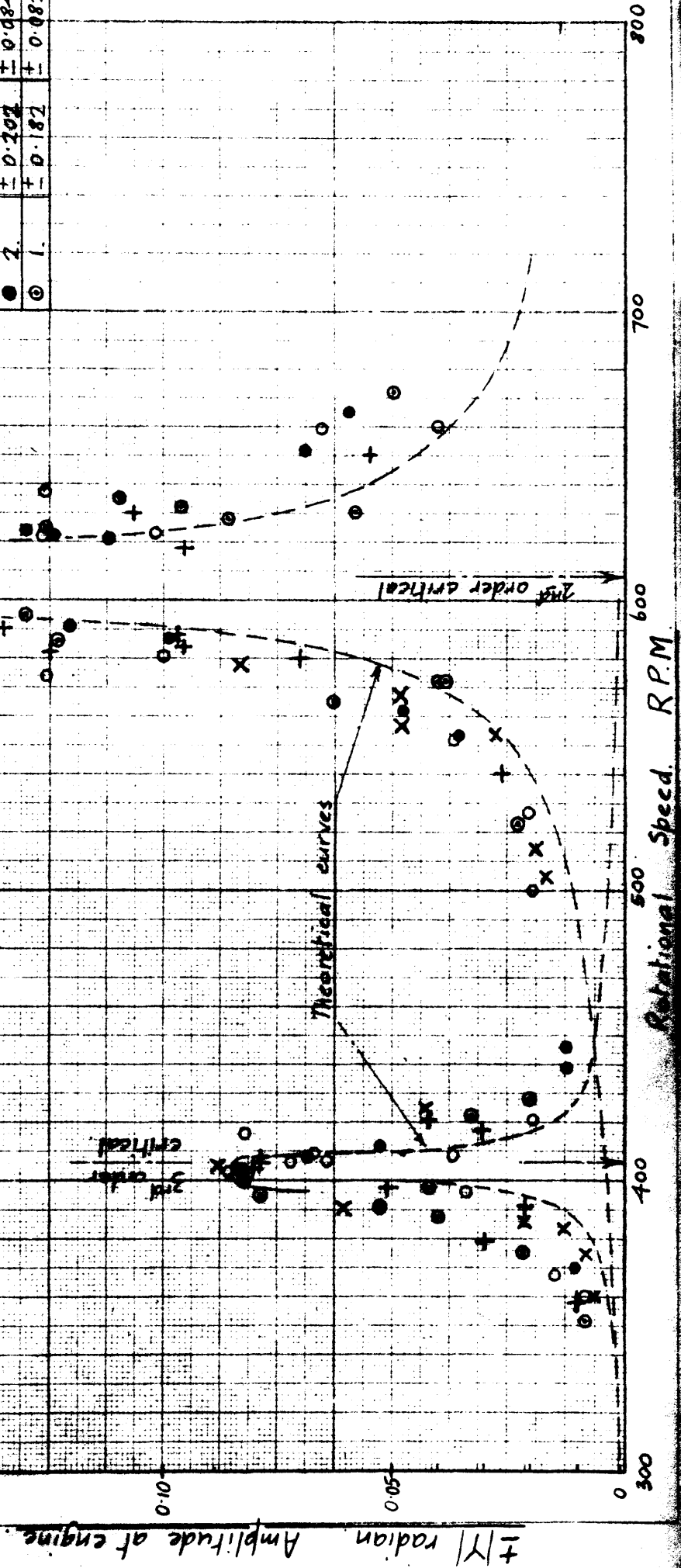


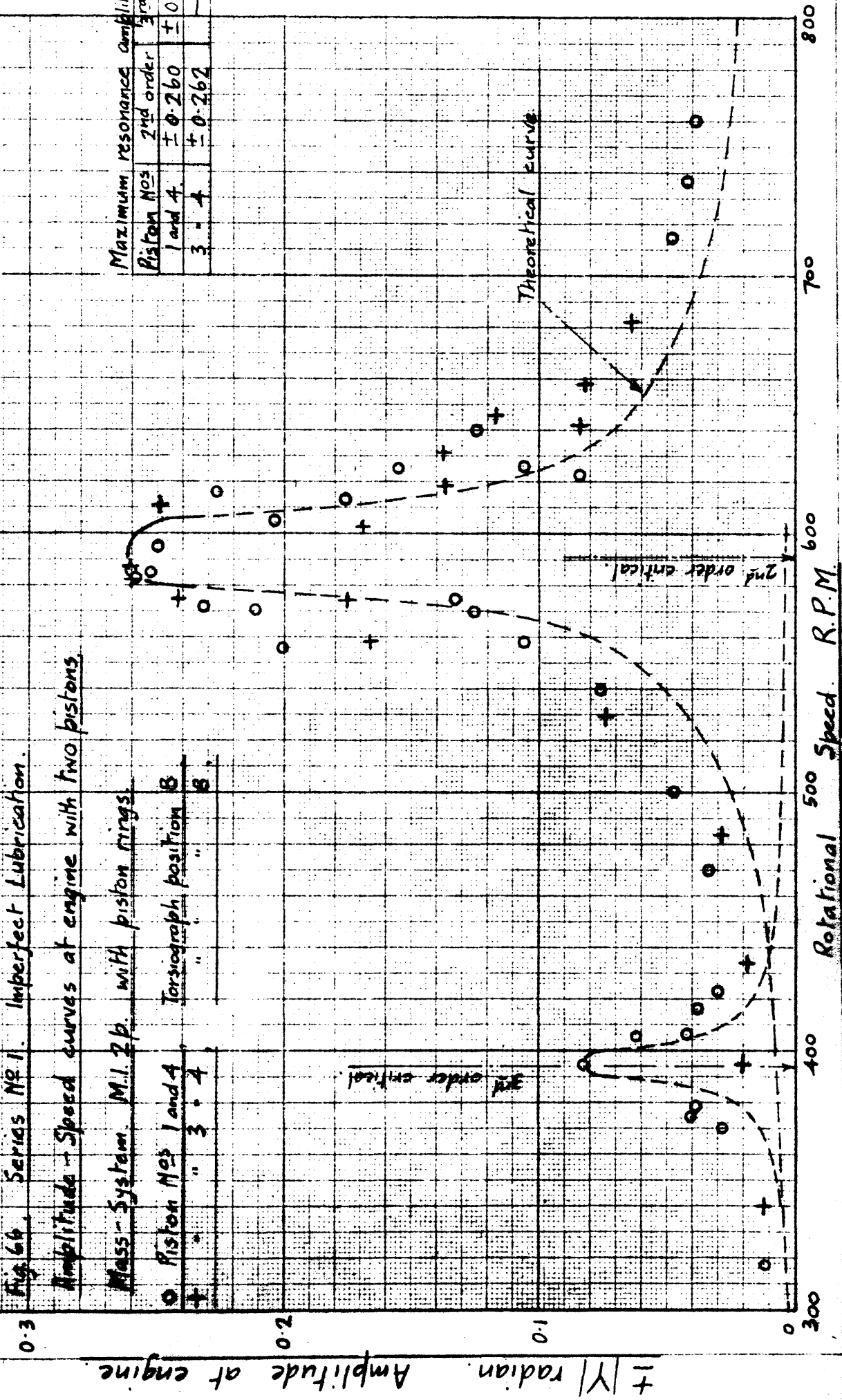
Fig. 64. Series No. 1. Imperfect Lubrication.

Amplitude-Speed curves at engine with two pistons.

Mass-System M.I. 2 p. with piston rings.

Piston Nos	Torsigraph position
1 and 4	B
3 - 4	"
3 - 4	B

Piston Nos	2nd order	3rd order
1 and 4	± 0.260	± 0.0821
3 - 4	± 0.262	



$\pm Y |$ radian. Amplitude of engine.

Rotational Speed R.P.M.

Fig. 67. Series No 1. Imperfect Lubrication

Amplitude - Speed curves at engine with three pistons

Mass - System M1.3p. with piston rings

+ Torsigraph position B. 2nd order maximum resonance amplitudes

o " " C ± 0.348 and ± 0.308 radian.

3rd order = ± 0.0546 radian.

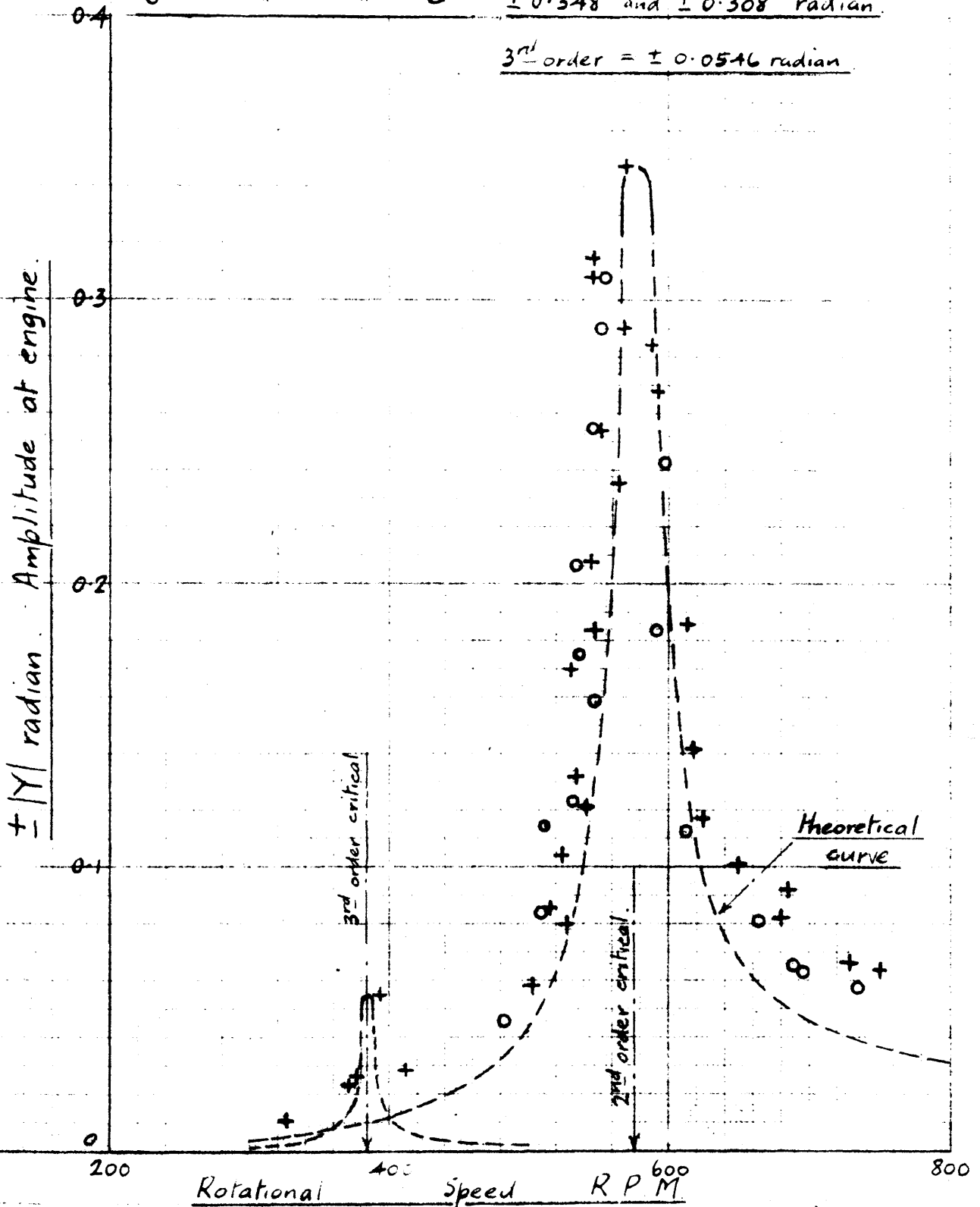


Fig 68. Series M#1 Imperfect Lubrication.

Amplitude-Speed curves at engine with four pistons.

Mass-System. M1.4p. with piston rings.

Torsiograph position C

2nd order maximum
resonance amplitude
= ± 0.402 radian.

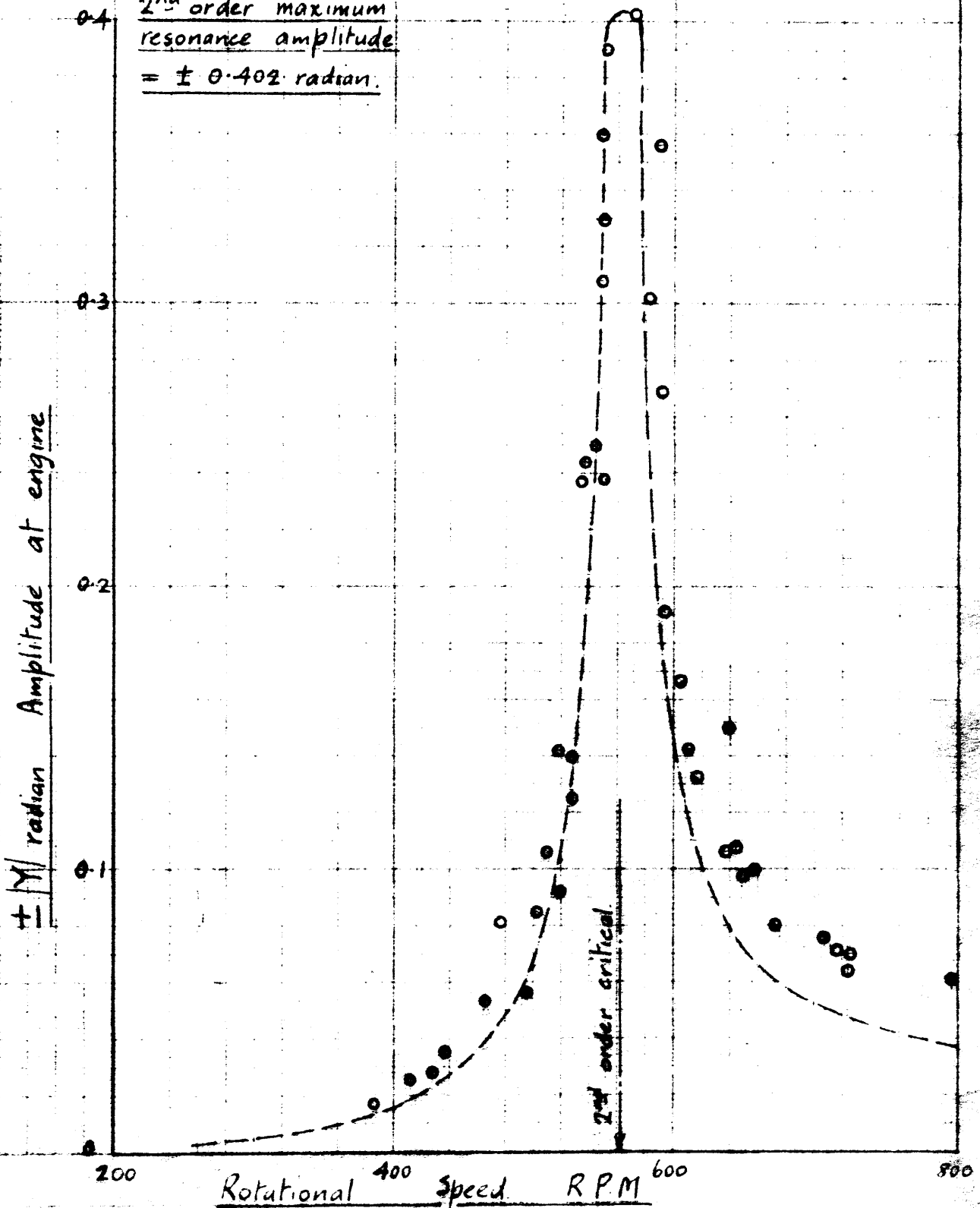


Fig 69

Series No II - Gravity oil feed to main bearing.

Amplitude - speed curves at engine with one piston

Mass - System M 1 lb (a) with piston rings +

(b) without " " 0

Torsigraph position C

$\pm Y$ |radian. Amplitude of engine

Maximum resonance amplitudes		
2 nd order		3 rd order
$a \pm 0.0865$		± 0.0294
$b \pm 0.0835$		± 0.0247

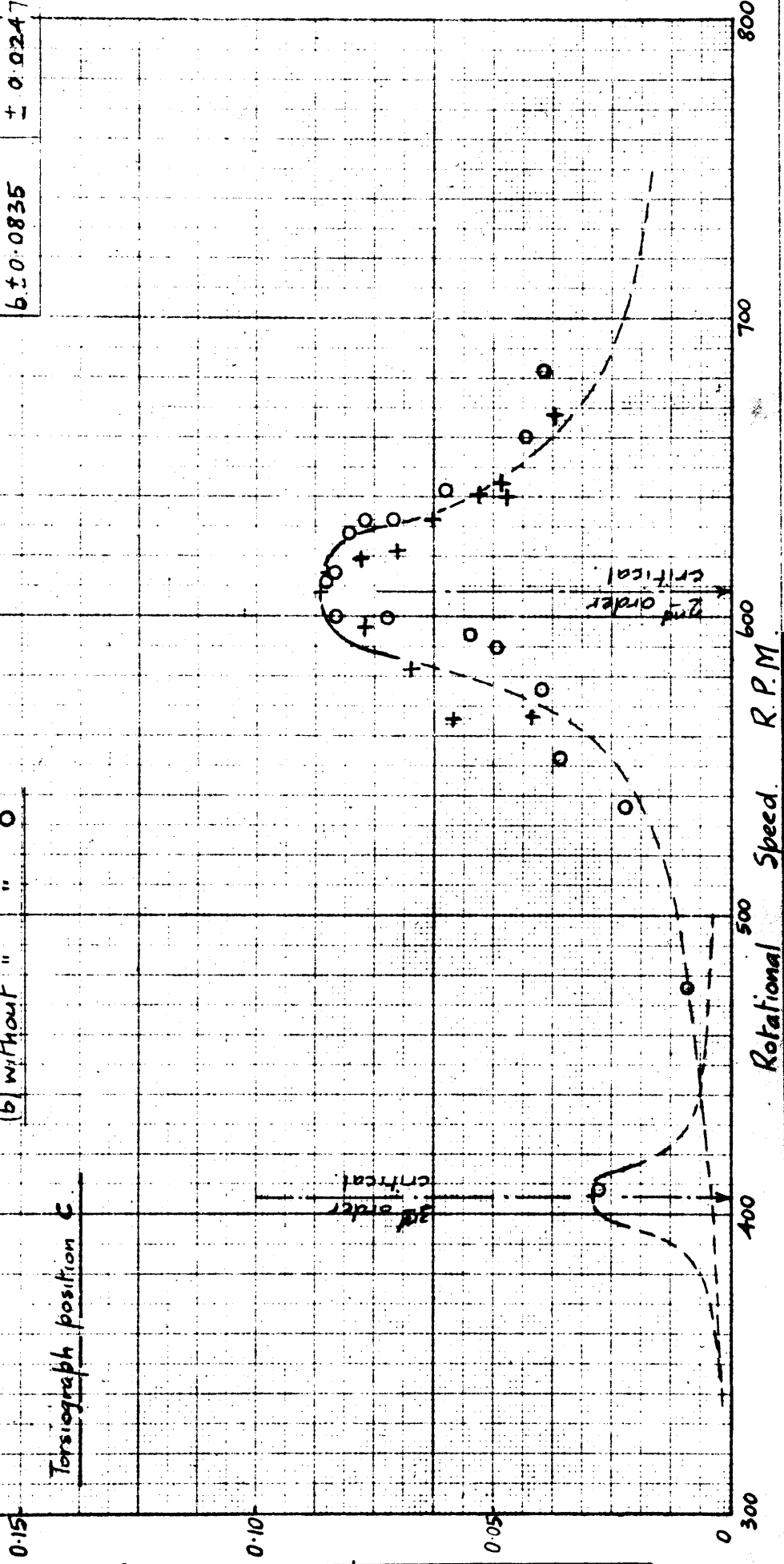


Fig. 70 Series No II Gravity oil feed to main bearing

Amplitude - speed curves at engine with two pistons

Mass - System M1 2/p (a) with piston rings +

(b) without " " 0

Torsigraph position C

Maximum resonance amplitude		
2 nd order	3 rd order	
$a \pm 0.092$	± 0.0382	
$b \pm 0.106$	± 0.0375	

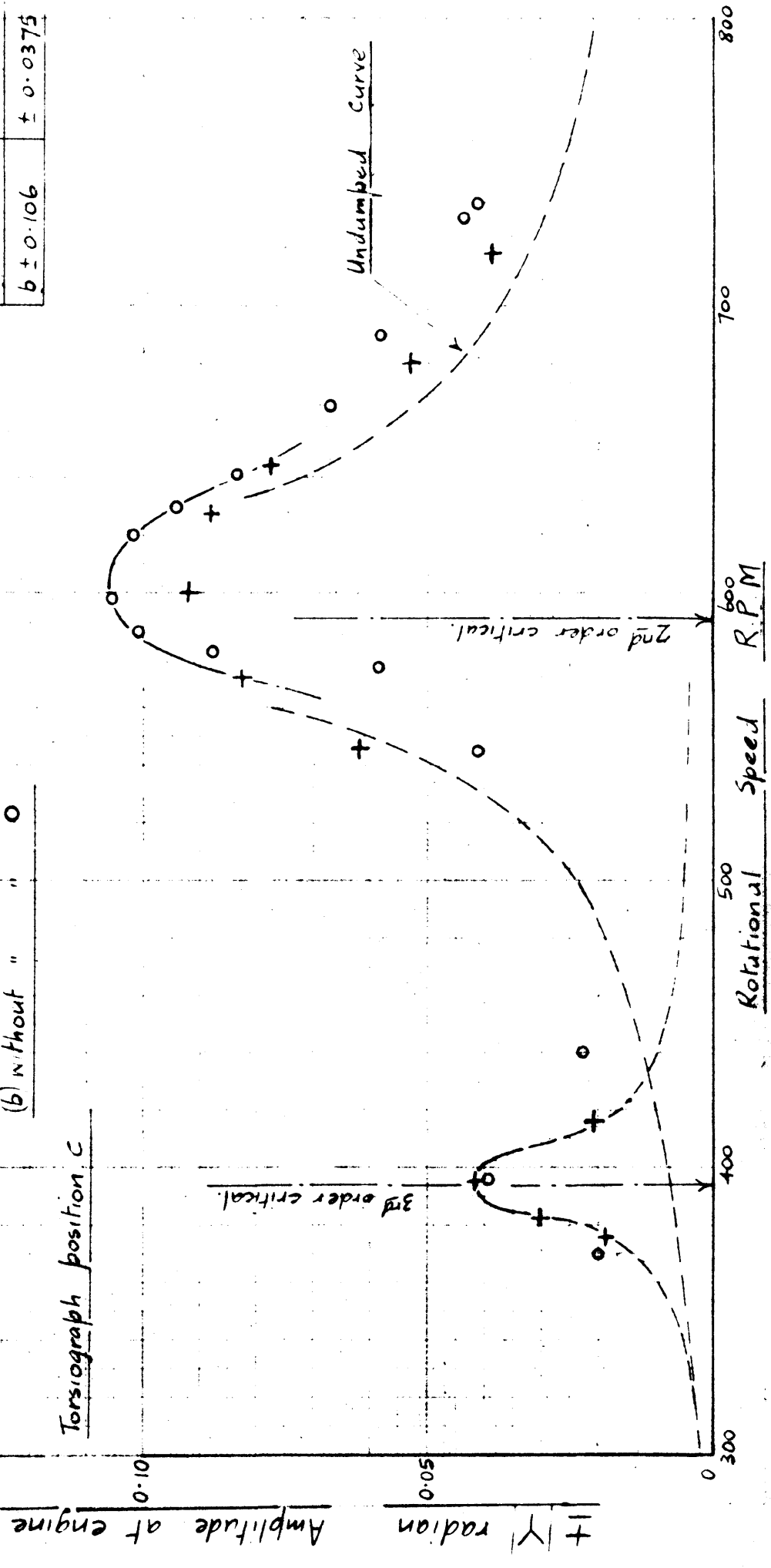


Fig T3. Collected results for mass-system M.I.

Series I and II

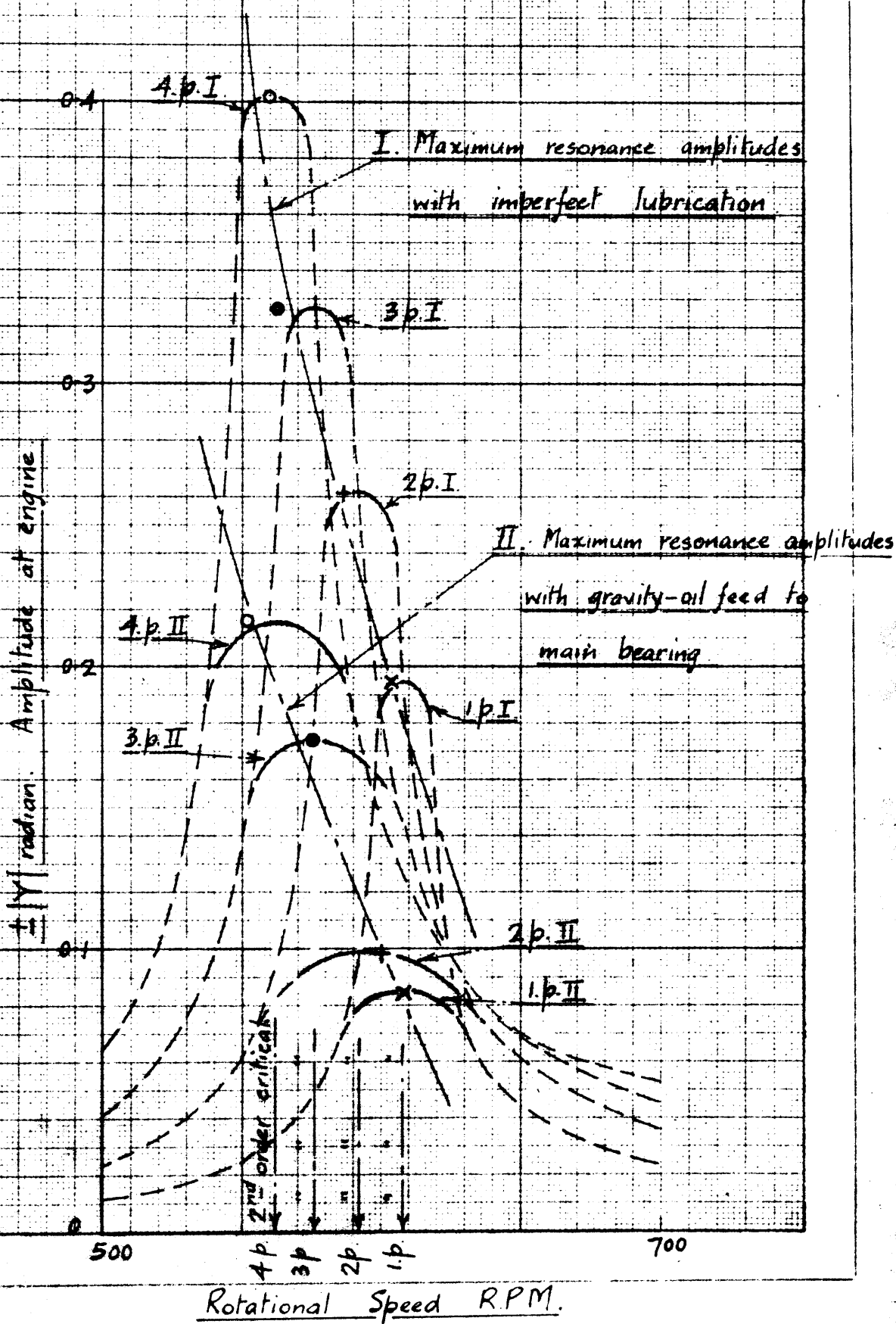


Fig. 74 Collected results for mass-system M.2

Series III

Gravity oil feed to main bearing.

Maximum resonance amplitudes 2nd order.

△	One piston	with rings	--- ± 0.0435	radian.
□	"	without "	--- ± 0.0412	"
+	Two pistons	with rings	--- ± 0.0558	"
x	"	without "	--- ± 0.0576	"
●	Three	" " "	--- ± 0.1122	"
○	Four	" " "	--- ± 0.145	"

Torsiograph position. C

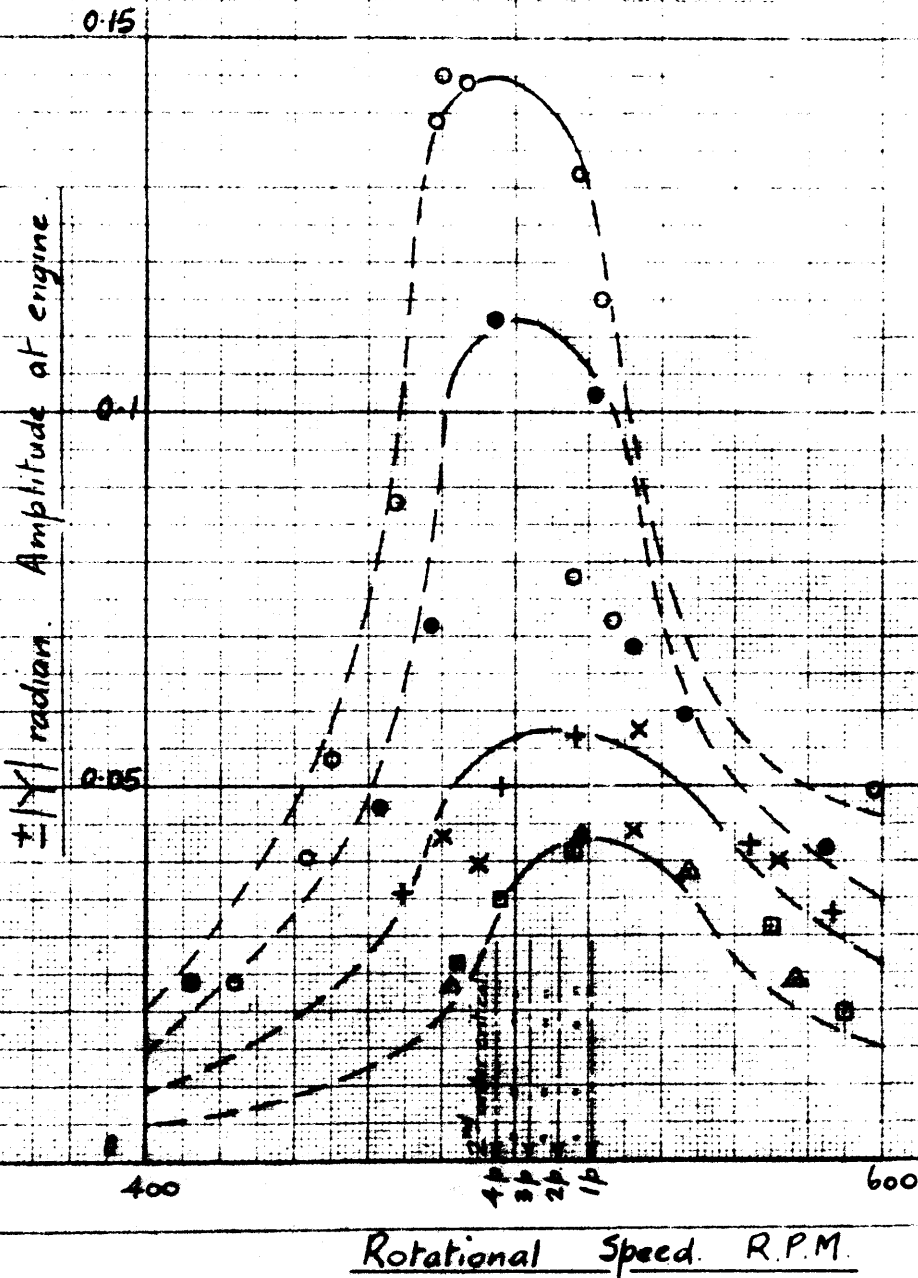


Fig. 75. Collected results for mass-system M3.

Series III. Gravity oil feed to main bearing.

	Maximum resonance amplitude. 2 nd order	Torsiograph position
△ One piston, with rings	± 0.0365 radian	
□ " " without "	± 0.0353 "	
+ Two pistons with rings	± 0.048 "	
X " " without "	± 0.041 "	
● Three " " "	± 0.105 "	
○ Four " " "	± 0.120 "	

Series I. Imperfect Lubrication

▽ One piston with rings. Maximum resonance amplitude. 2nd order. ± 0.110 radian.
Torsiograph position. C.

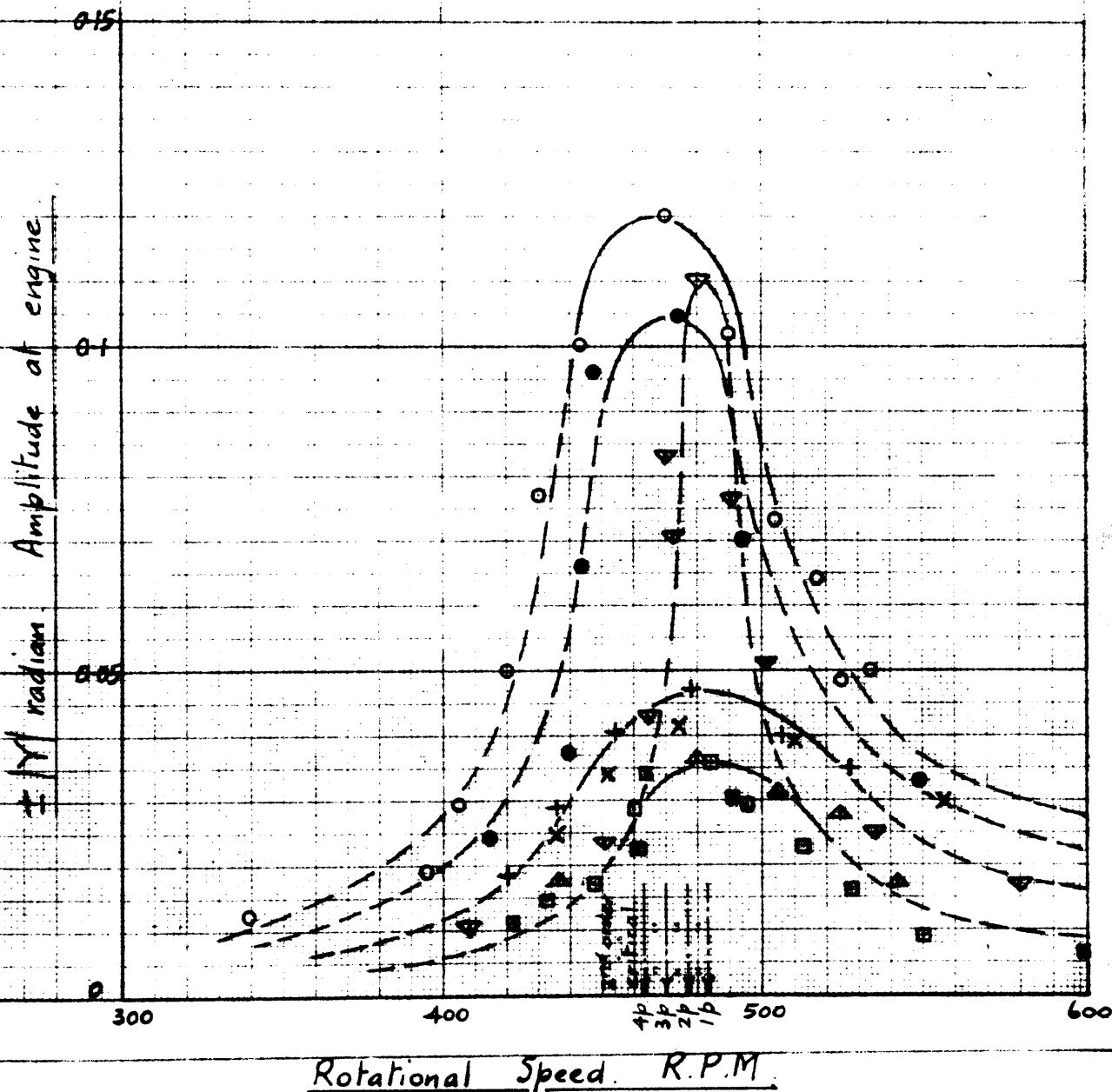


Fig 77. Collected results for mass system M5.

Series III Gravity oil feed to main bearing

	Max ^m resonance amplitude 2 nd order
△ One piston with rings	± 0.0194 radian
□ " " without "	± 0.0171 " "
+ Two pistons with rings	± 0.0306 " "
X " " without "	± 0.0232 " "
● Three " " "	± 0.0310 " "
○ Four " " "	± 0.0523 " "

Torsigraph position C

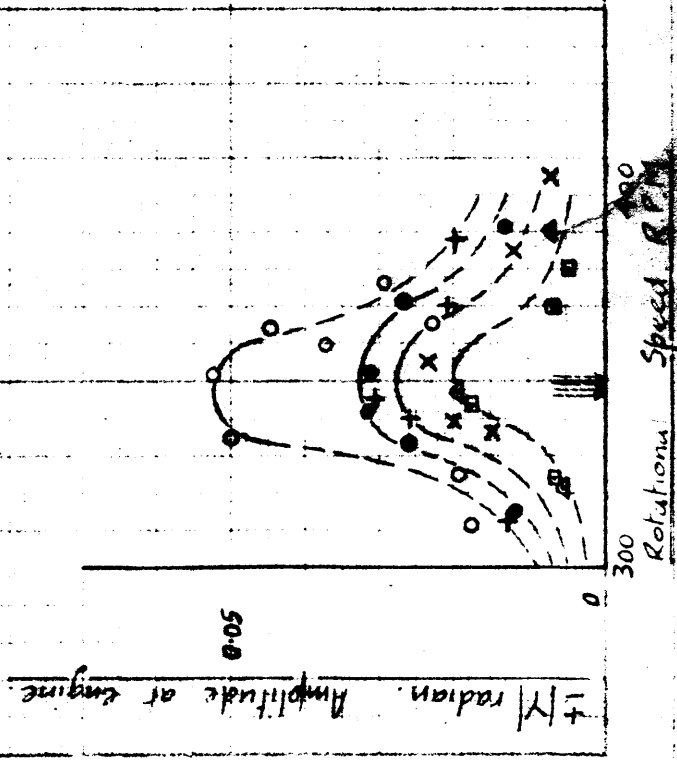
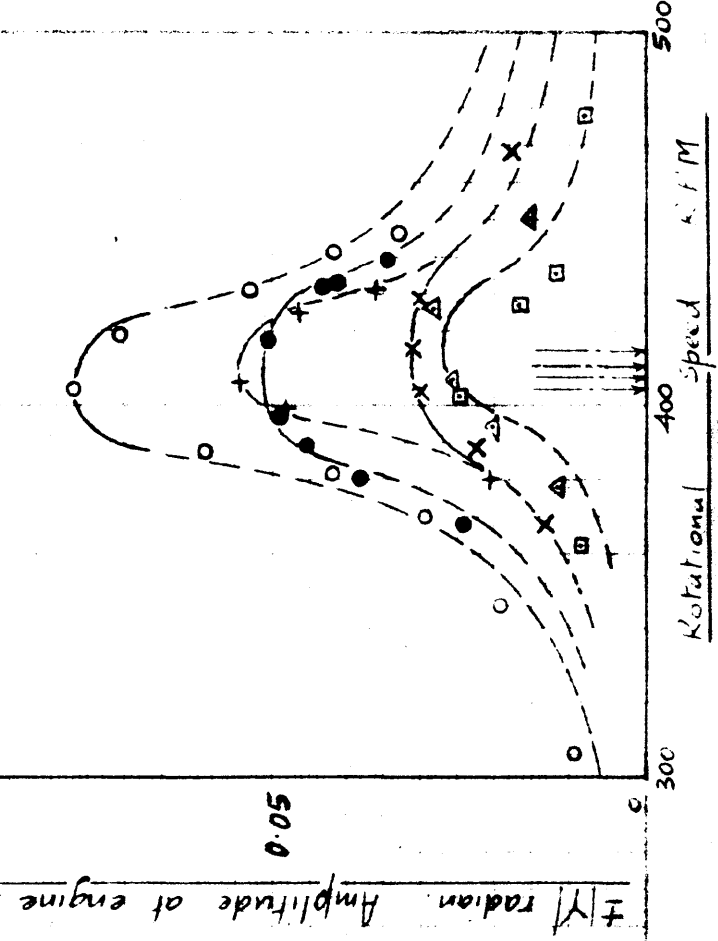


Fig 76. Collected results for mass system M4

Series III Gravity oil feed to main bearing

	Maximum resonance amplitude 2 nd order
△ One piston with rings	± 0.0282 radian
□ " " without "	± 0.0247 " "
+ Two pistons with rings	± 0.0546 " "
X " " without "	± 0.0318 " "
● Three " " "	± 0.0506 " "
○ Four " " "	± 0.0765 " "

Torsigraph position C



is much smaller than with the imperfect lubrication, thus causing a greater distortion in the resultant diagram.

Piston Rings.

It is also seen that the vibration amplitudes when the pistons were fitted with and without rings are practically similar in all respects.

The remainder of the graphs for mass-system M1., and also for M3., all show precisely similar features.

Phase Angle at Resonance.

So far as can be estimated from the torsigraph records, the phase angle at resonance, as shown by the nature of the combined diagrams and also by the dead centre timing at the lower frequencies is 90° .

Resonance Amplitudes.

The maximum resonance amplitudes for the 2nd order vibration and their corresponding critical speeds are plotted in Fig. 78 and envelope curves drawn for the series with the different number of pistons. The series II and III with gravity oil feed to the main bearing show the variation of resonance amplitude with frequency when vibration is stimulated by a periodic torque varying as the frequency squared.

A similar behaviour in amplitude variation appears to exist for the one-piston-imperfectly-lubricated series.

The relation between the various piston arrangements for the two types of lubrication is shown for mass-system M1., on Fig. 73. It is seen that the nature of each set of results is similar.

The 3rd order maximum amplitudes are also given in Fig. 79, but the values are not so clear as those of the 2nd order on account of their small magnitude. A further plot of the 3rd order is made

Fig. 78 Envelope curves of resonance amplitudes.

2nd order

M.I. Imperfect lubrication

Maximum Resonance Amplitude at Engine. $\pm Y_r$ radian.

Critical Speed R.P.M.

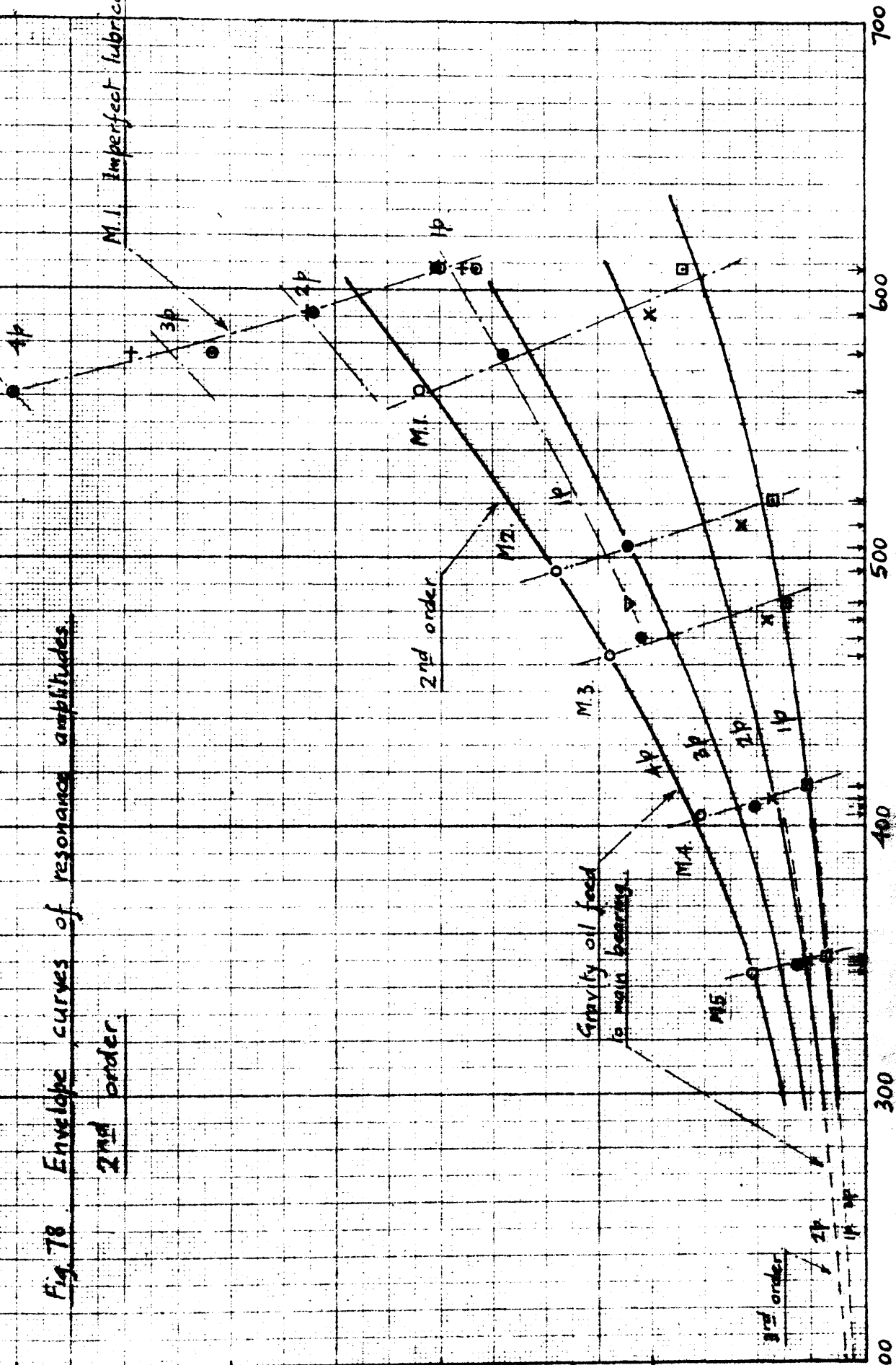
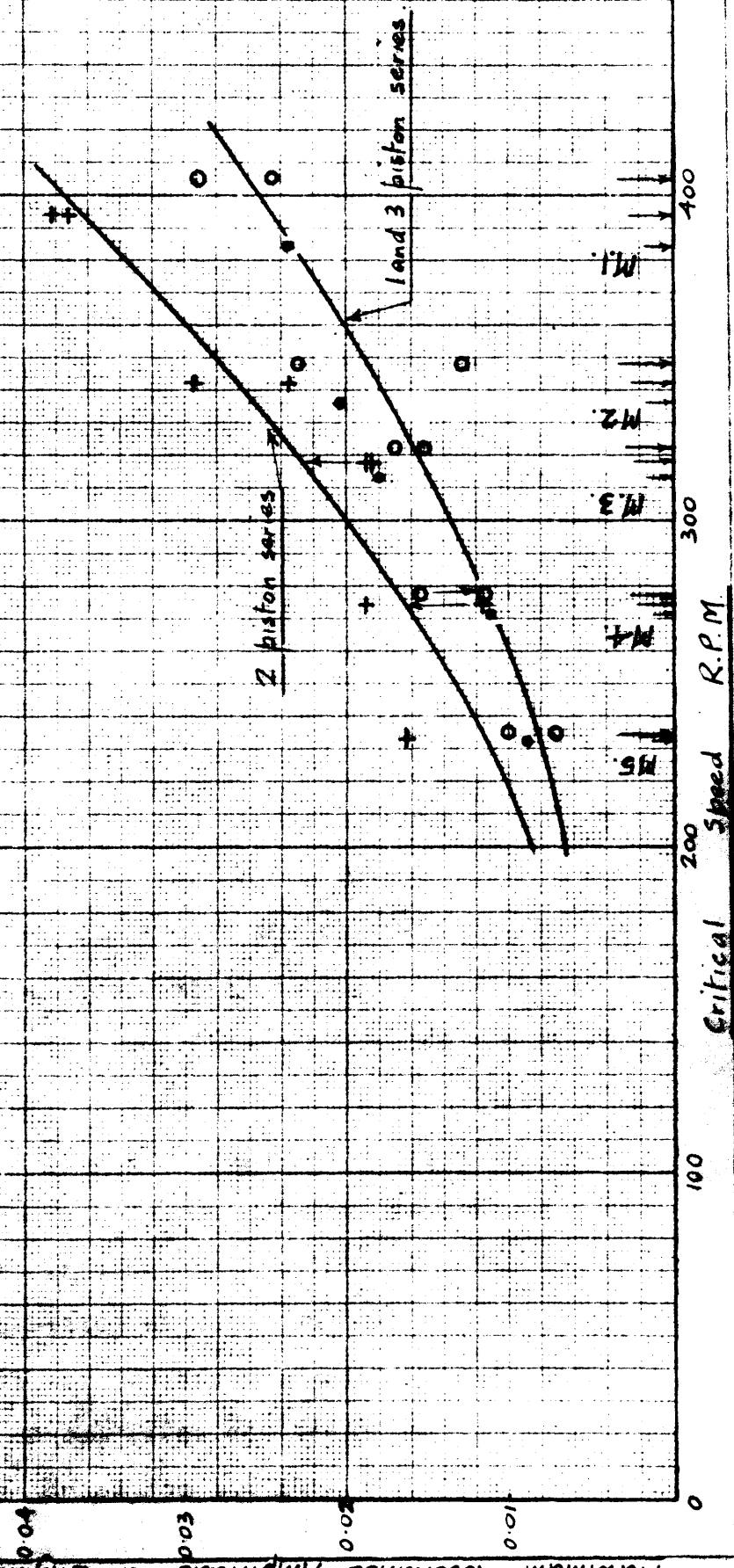


Fig. 19. Envelope curves of resonance amplitudes for 3rd order torque

Gravity oil-feed to main bearing

- 1 piston with and without rings.
- + " " " " " "
- " " " " " "

Maximum Resonance Amplitude of Engine $\pm |Y|$ radian



on Fig. 78 where their relation to the 2nd order values is seen.

Analysis of Results.

(1) Energy of Vibration.

The vibrational energy given to the dynamical system by the harmonic torques is equal to the energy dissipated by all the damping actions in the system. The energy input of a harmonic torque $Q \sin \omega t$, giving rise to a vibration $\theta \sin(\omega t - \phi)$ is $\pi Q \theta \sin \phi$ per vibration and at resonance, where ϕ is 90° , it becomes a maximum. From the analysis of the torsigraph records it was concluded that the vibration was ostensibly sinusoidal, having a 90° phase angle at the maximum amplitude. Hence the vibrational energy at resonance is taken to be $\pi Q \theta$, where θ is the maximum resonance amplitude shown on Fig. 78, and Q the amplitude of the harmonic torque given in pages 25 and 29.

This energy is dissipated in heat and appears as additional power supplied by the motor. On Fig. 63, the calculated resonance power is shown superimposed on the mean power. By comparing the experimental values of total power at resonance with the calculated, for the different conditions, shown at A, C, and E, reasonable agreement is obtained. Thus the vibrational energy is confirmed.

The derived energy values are given in Tables 5 - 7, for the 2nd and 3rd orders. The amplitudes are taken at convenient critical speeds from Fig. 78. and the corresponding mass-ratios of motor and engine from Fig. 80. It is seen that all the 3rd order quantities are very small, hence for general effects, attention may be concentrated almost solely on the larger 2nd order values.

The various sources of dissipation within the experimental plant may now be discussed with a view to examining their nature and relating their relative values to the total energy dissipated.

Table 5 . Input Energy , Electrical damping , Shaft-Hysteresis and damping due to simple shear resistance of oil film.

2nd order. One piston series. Gravity oil-feed to bearing.

$$Q = -0.0132 \omega^2 (1+3Y^2) \text{ in. lb.}$$

A				B.					
critical speed. R.P.M.	Amplitude at engine $\pm Y$ rad ⁿ	$1+3Y^2$	Torque coefft. Q in. lb.	Input. $\pi Q Y$ in. lb/vib ⁿ	Vibration power. Watts.	Max. value of k	Electrical damping $12.6 k^2 \eta Y^2 / r^2$ in. lb/vib.	mass ratio r	natural frequency η rad/sec.
600	0.075	1.0169	53.0	12.5	28.2	1.43	0.292	7.92	125.6
500	0.043	1.0056	36.3	4.94	9.3	"	0.188	5.13	104.6
400	0.024	1.0017	23.1	1.74	2.62	1.49	0.170	2.82	83.8
350	0.018	1.001	17.7	1.00	1.41	"	0.176	1.94	73.3

C.				D.					
critical speed r.p.m.	$1 + \frac{1}{r}$	Relative twist on shaft. $\bar{\theta}$ $= x + y$ radian	shear stress f_s lb/in ²	Hysteresis energy. in. lb/vib.	viscosity λ cgs units	Simple shear resistance of oil film. $0.61 \lambda \eta y^2$ in. lb/vib.	SUM $B+C+D = E$ in. lb/vib.	Energy unaccounted for.	
								A-E in. lb/vib.	Per cent.
600	1.126	0.0845	3420	1.0	2.0	0.863	2.155	10.34	82.9
500	1.195	0.0514	2080	0.32	2.1	0.248	0.756	4.18	84.7
400	1.355	0.0325	1,310	0.11	2.2	0.065	0.345	1.40	80.5
350	1.515	0.0273	1,100	0.008	2.25	0.029	0.213	0.79	79.0

2nd order. Two piston series. Gravity oil-feed to bearing.

$$Q = -0.0264 \omega^2 (1+3y^2) \text{ in. lb.}$$

A				B.				
critical speed r.p.m.	Amplitude at engine $\pm y$ rad ⁿ	$1+3y^2$	Torque coefft. Q in. lb.	Input energy. $\pi Q y$ in. lb/vib ⁿ	Vibration power Watts.	Max. value of k	Electrical damping $12.6 k^2 \eta y^2 / r^2$ in. lb/vib.	y^2
600	0.115	1.0399	108.4	39.2	88.6	1.38	0.64	0.0133
500	0.07	1.0147	73.6	16.16	30.4	"	0.466	0.0049
400	0.038	1.0043	46.5	5.56	8.4	1.34	0.343	0.00144
350	0.028	1.0024	35.6	3.12	4.12	"	0.345	0.000784

C				D.				
critical speed. r.p.m.	$1 + \frac{1}{r}$	Relative twist on shaft. $\bar{\theta}$ $= x + y$ rad	shear stress f_s lb/in ²	Hysteresis energy in. lb/vib ⁿ	Simple shear resistance of oil film $0.61 \lambda \eta y^2$ in. lb/vib.	SUM $B+C+D = E$ in. lb/vib.	Energy unaccounted for.	
							A-E in. lb/vib.	Per cent.
600	1.126	0.1298	5250	2.64	2.04	5.32	33.88	86.5
500	1.195	0.0837	3390	0.96	0.655	2.08	14.08	87.0
400	1.355	0.0515	2080	0.32	0.16	0.82	4.74	85.2
350	1.515	0.0424	1718	0.23	0.08	0.66	2.46	79.0

Table 6 Input energy continued

2nd order Three piston series Gravity oil-feed to bearing

$Q = -0.0396 \omega^2 (1+3y^2) \text{ in. lb}$ A

B.

critical speed r.p.m.	amplitude at engine $\pm y \text{ rad.}^2$	$1+3y^2$	Torque coefft. Q in lb	Input energy $\pi Q y$ in. lb/vib ^m	vibration power Watts.	max. value of k	Electrical damping $12.6k^2 y^2 / r^2$ in. lb/vib.	y^2 .
600	0.174	1.0909	170.7	93.3	210.0	1.31	1.316	0.0303
500	0.107	1.0344	113.0	38.13	71.7	"	0.982	0.01145
400	0.056	1.0094	70.0	12.27	18.5	"	0.715	0.00314
350	0.039	1.0046	53.6	6.57	8.68	"	0.64	0.00152

C.

D

critical speed. r.p.m.	$1 + \frac{1}{r}$	relative twist on shaft $x+y \text{ rad}$	shear stress f_s lb/in ²	Hysteresis energy in. lb/vib ^m	simple shear resistance of oil film $0.61 \lambda y^2$ in. lb/vib.	sum B+C+D = E in. lb/vib.	Energy unaccounted for.	
							A - E in. lb/vib.	per cent.
600	1.126	0.196	7940	6.95	4.65	12.92	80.38	86.2
500	1.195	0.128	5180	2.55	1.54	5.07	33.06	86.8
400	1.355	0.076	3080	0.80	0.353	1.87	10.40	84.9
350	1.515	0.0591	2390	0.44	0.15	1.23	5.34	81.4

2nd order Four piston series Gravity oil-feed to bearing

$Q = -0.0528 \omega^2 (1+3y^2) \text{ in. lb}$ A

B.

critical speed r.p.m.	amplitude at engine $\pm y \text{ rad.}^2$	$1+3y^2$	Torque coefft. Q in lb	Input energy $\pi Q y$ in. lb/vib.	vibration power watts.	max. value of k	Electrical damping $12.6k^2 y^2 / r^2$ in. lb/vib.	y^2
600	0.24	1.1728	244.8	184.4	416.0	1.27	2.35	0.0576
500	0.148	1.0657	155.0	72.2	135.8	"	1.77	0.0219
400	0.076	1.0173	94.0	22.44	33.9	"	1.24	0.00577
350	0.053	1.0084	71.6	11.92	15.75	"	1.11	0.00281

C

D

critical speed r.p.m.	$1 + \frac{1}{r}$	relative twist on shaft $x+y \text{ rad}$	shear stress f_s lb/in ²	Hysteresis energy in. lb/vib ^m	simple shear resistance of oil film $0.61 \lambda y^2$ in. lb/vib.	sum B+C+D = E in. lb/vib.	Energy unaccounted for	
							A - E in. lb/vib.	per cent
600	1.126	0.272	11,000	14.5	8.85	25.7	158.7	86.0
500	1.195	0.177	7170	5.53	2.94	10.24	62.0	85.8
400	1.355	0.103	4170	1.57	0.65	3.46	19.0	84.6
350	1.515	0.0804	3250	0.90	0.28	2.30	9.6	80.5

Table 7. Input energy (continued.)

Imperfect lubrication series.

2nd order. Critical speed 560 r.p.m. Mass ratio $r = 6.85$

$Q = -0.0132 \omega^2 (1 + 3y^2) \text{ in. lb}$

No of pistons p.	amplitude at engine $\pm y \text{ rad}^m$	y^2	$1 + 3y^2$	Torque coefft Q in. lb.	A		B	
					Input energy $\pi Q y$ in. lb/vib.	vibration power Watts.	max. value of k	Electrical damping $\frac{12.6 k^2 \gamma^2}{r^2}$ in. lb/vib.
1	0.16	0.0256	1.0768	48.7	24.5	51.7	1.38	1.54
2	0.232	0.0538	1.1614	105.0	76.6	162.0	1.28	2.78
3	0.310	0.0961	1.2883	175.0	170.4	360.0	1.16	4.10
4	0.402	0.1611	1.4833	269.0	339.2	717.0	1.00	5.10

C.

No of pistons p.	$1 + \frac{1}{r}$	relative twist on shaft. $x + y \text{ rad}$	shear stress f_s lb/in ²	Hysteresis energy. in. lb/vib.	sum $B + C = D$ in. lb/vib.	Energy unaccounted for	
						A - D in. lb/vib.	per cent.
1	1.146	0.1835	7450	6.1	7.64	16.86	69.0
2	"	0.266	10,800	14.0	16.78	59.82	78.0
3	"	0.356	14,400	27.5	31.6	138.8	81.5
4	"	0.461	18,620	50.2	55.3	283.9	83.7

Imperfect lubrication series.

3rd order. $Q = -0.0054 \omega^2 (1 + 6.75y^2) \text{ in. lb for 1 piston.}$

No of pistons p.	critical speed r.p.m	amplitude at engine $\pm y \text{ rad}^m$	y^2	$1 + 6.75y^2$	Torque coefft Q in. lb	Input energy $\pi Q y$ in. lb/vib
1	405	0.084	0.00705	1.0475	10.13	2.67
2	395	0.082	0.00674	1.0455	19.28	4.96
3	384	0.055	0.00302	1.0204	8.90	1.54

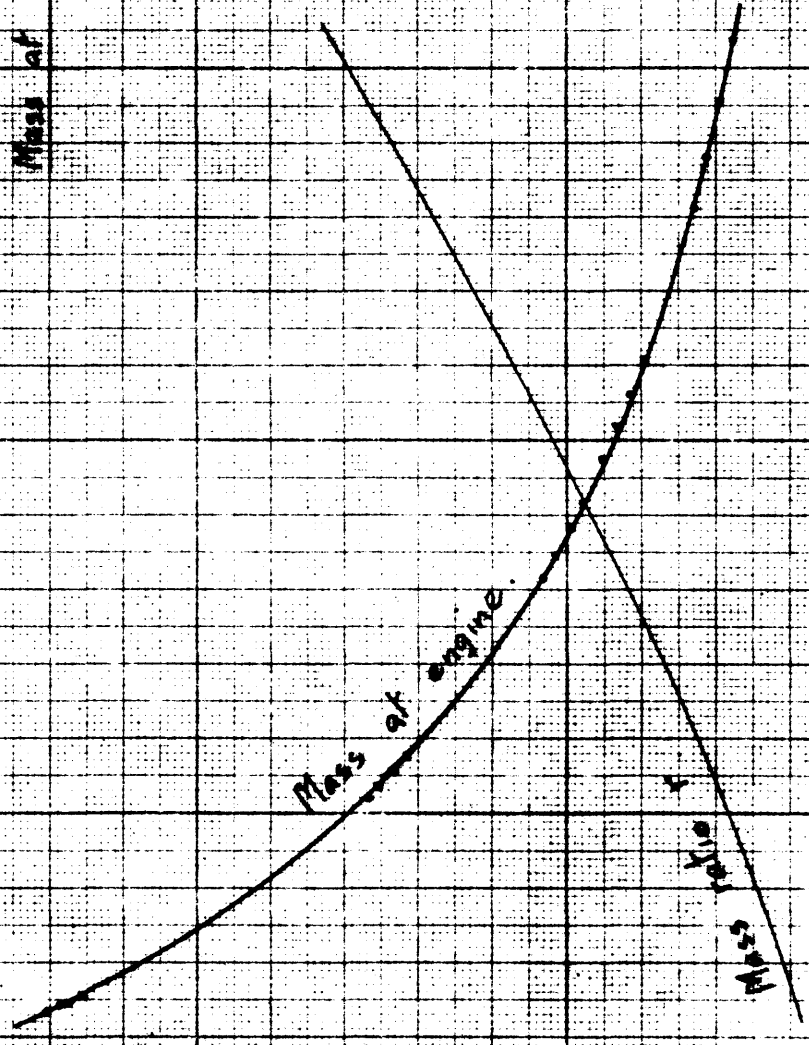
Gravity oil-feed to main bearing. 3rd order.

<u>One and three piston series</u>					<u>Two piston series.</u>			
$Q = -0.0054 \omega^2 (1 + 6.75y^2) \text{ in. lb.}$					$Q = -0.0108 \omega^2 (1 + 6.75y^2) \text{ in. lb}$			
critical speed r.p.m	amplitude at engine $\pm y \text{ rad}^m$	$1 + 6.75y^2$	torque coefft. Q in. lb.	Input energy $\pi Q y$ in. lb/vib ^m	amplitude at engine $\pm y \text{ rad}^m$	$1 + 6.75y^2$	torque coefft. Q in. lb.	Input energy $\pi Q y$ in. lb/vib ^m
400	0.0251	1.0042	9.5	0.751	0.0375	1.0095	19.1	2.25
350	0.0190	1.0024	7.28	0.434	0.0280	1.0053	14.6	1.29
300	0.0135	1.0012	5.32	0.226	0.020	1.0027	10.7	0.67
250	0.0091	1.0006	3.70	0.106	0.013	1.0012	7.4	0.30

Fig. 80. Mass of engine and corresponding

natural frequency

Mass of Motor = 4.51 lb in sec²



Mass of motor	Mass of engine - lb in sec ²
0	0
5.0	10
10.0	20

Natural Frequency, Vib per min.

Examination of Possible Sources of Dissipation.

In considering the possible source of dissipation, the system might be divided up into elements comprising the motor, shafting, piston, big-end, and crankshaft.

(a) Damping at Motor.

At the motor, electrical damping and slight frictional effects occur.

The D.C. shunt motor was coupled so that speed regulation could be obtained by variable resistances in the armature circuit. With this arrangement there is constant excitation, hence the back e.m.f. E , is strictly proportional to speed. When a decrease in speed takes place a corresponding decrease in back e.m.f., occurs, resulting in a corresponding increase of armature current I_a and consequent increase in torque and vice versa. Thus changes in speed introduce changes in torque which oppose the speed changes.

If the speed is given by $w + nw x \cos nwt$, then the damping may be determined as follows :

$$\begin{aligned} \text{Mechanical power to the shaft} &= EI_a \\ &= \frac{(V-E)E}{R_a} \quad \text{--- (30)} \end{aligned}$$

where V is the voltage applied to the terminals and R_a the resistance between the terminals.

$$\text{But } E = kw + nkwx \cos nwt.$$

Substituting in equ.(30) and reducing, the periodic torque coefficient becomes

$$Q_m = \frac{k^2 n w x}{R_a}$$

Hence the damping work per vibration = $\pi Q_m x$

$$= \frac{\pi \times 12 k^2 \eta x^2}{1.36 R_a} \quad \text{in. lb.} \quad \text{--- (31)}$$

where $\frac{\eta}{2\pi}$ is the natural frequency of the system.

The resistances of the armature and the field, taken after a run, were 2.2 ohms and 378 ohms respectively hence in the equation $E = V - IR_a$, I may be taken as the total current at resonance. From Fig. 63 $V = 1.58 \omega$, hence the corresponding gradient k for the back emf. E at resonance, is given by :-

$$k = 1.58 - \frac{2.2 \times \text{total power}}{1.58 \omega^2}$$

By estimating the total power at each critical speed, the appropriate values of k are determined and these are given in Tables 5 to 7.

A constant voltage across the armature terminals has been assumed, but the voltage absorbed by the resistances in series with the armature will also vary with the current changes, since voltage drop is the product of resistance and current. Thus a decrease in speed which causes an increase in current and torque will also cause a decreased voltage applied to the armature which will consequently tend to decrease the speed still further. This secondary action which tends to augment the initial speed change will thus tend to diminish the effect of the electrical damping torque.

It will also be noticed that x is the amplitude at the motor end of the system and will be $\frac{1}{r}$ times that at the engine, r being the mass ratio. With natural frequencies ranging from 1,200 v.p.m. to 700 v.p.m., r varies from 7.92 to 1.94. Hence the work per vibration due to electrical damping which varies as the square of the amplitude, will be quite negligible at the higher frequencies but will be slightly more effective at the lower, where the vibration at the motor end begins to assume comparative values.

Calculating the electrical damping from equ.(31) and inserting the values in tables 5 - 7 it will be seen that this damping is almost negligible throughout the tests.

Similarly the frictional effects occurring at the ring-oil bearings are considered negligible on account of the mass ratio, and also the brush friction being constant can have no effect.

It may be concluded, therefore, that there are no damping forces of any importance induced at the motor.

(b) Shaft Damping.

For the shafting, the dissipation of energy will be that due to hysteresis in the shaft material. The small plummer blocks supporting the shaft are not considered effective as damping sources.

Hysteresis in Shaft Material.

Internal friction of shaft material has been shown by Rowett⁷, Föppl¹⁴, Kimball¹⁵, and others to be independent of velocity and to be dependent only upon amplitude. Below the fatigue limit the energy dissipation due to this cause is comparatively small and is not a definite value since it changes with the condition and history of the material. As found by Lea¹⁶, it tends to decrease when the stress is below the fatigue limit and increase when above, so that there is no simple law.

An attempt was made to measure the hysteresis of the shaft used in the experimental plant by forced vibration experiments about rest. The masses at the motor end were removed and replaced by a 6 in. crank and connecting rod driven by a $\frac{1}{32}$ in., eccentric at the motor. Even with this small eccentric it was found to be necessary to keep the crankshaft coupled to the shafting, otherwise the amplitude at resonance would have led to fracture. The introduction of the constant friction damping in the apparatus completely obscured the very small hysteresis effect hence no reliance could be placed upon any hysteresis results deduced therefrom.

7. loc. cit.

14. Föppl, Die Dauerprüfung der Werkstoffe. p.p. 99.

15. Kimball. Trans. Amer. Soc. Mech. Eng. 1926.

16. Lea. Proc. Roy. Soc. Series A. Vol. 93. 1916 - 17.

Reversed static experiments were then carried out. A length of 1 in. diameter bar from the same material was arranged in a 15,000 in. lb. Avery reversed torsion machine; the ends of the bar were machined triangular to suit the grips. A gauge length of 24 in. was employed and a standard angular scale measure with vernier could be easily read to 0.02° . This corresponds to a torque of 17.1 in. lb. and a shear stress of 87.2 lb. per in². It was recognised that this was not sufficiently accurate to detect small elastic hysteresis, the experimental error being about ten times too large for this purpose, but would serve to measure large hysteresis effects should these occur within the stress range of the experiments. Reversed torsion tests were carried out accordingly with progressive torque ranges but no hysteresis was apparent for the range occurring in the vibration experiments. The torsion test was then completed in the usual manner until the reduced area at the grips gave out.

The results are plotted in Figs. 81 and 82, and give a shear stress at the limit of proportionality of 13.2 tons per in². Fig. 83 gives the results of a tensile test on the same material using a Lamb's mirror extensometer and the proportional limit is found to be 31.2 tons per in². These results are representative of the shafting material which had been cold worked during manufacture and had been given no subsequent annealing.

The maximum shear stress occurring in the vibration experiments is 8.3 tons per in² and is well within the proportional limits, hence it is impossible to detect elastic hysteresis from these simple tests. Since the effects appear to be quite small, and are really beyond the experimental error of normal extensometers, it is reasonable to assume for comparative purposes the results of published data in order to assess the probable hysteresis damping.

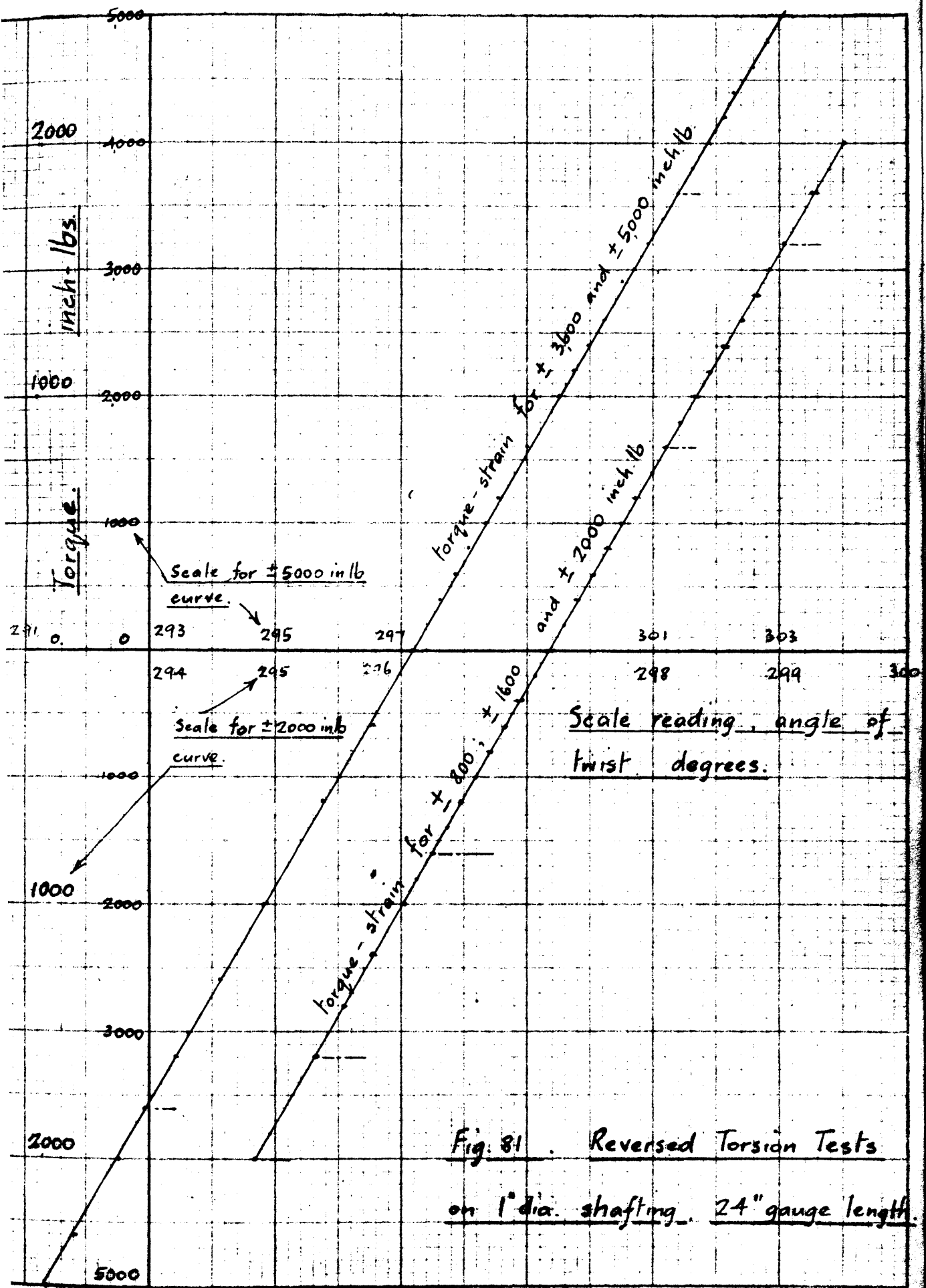


Fig. 82 Completed Torsion Test on 1" dia shafting.

2.4" gauge length.

Limit of proportionality = 13.2 Tons/in² (shear)

Modulus of Rigidity $G = 12.0 \times 10^6$ lb/in²

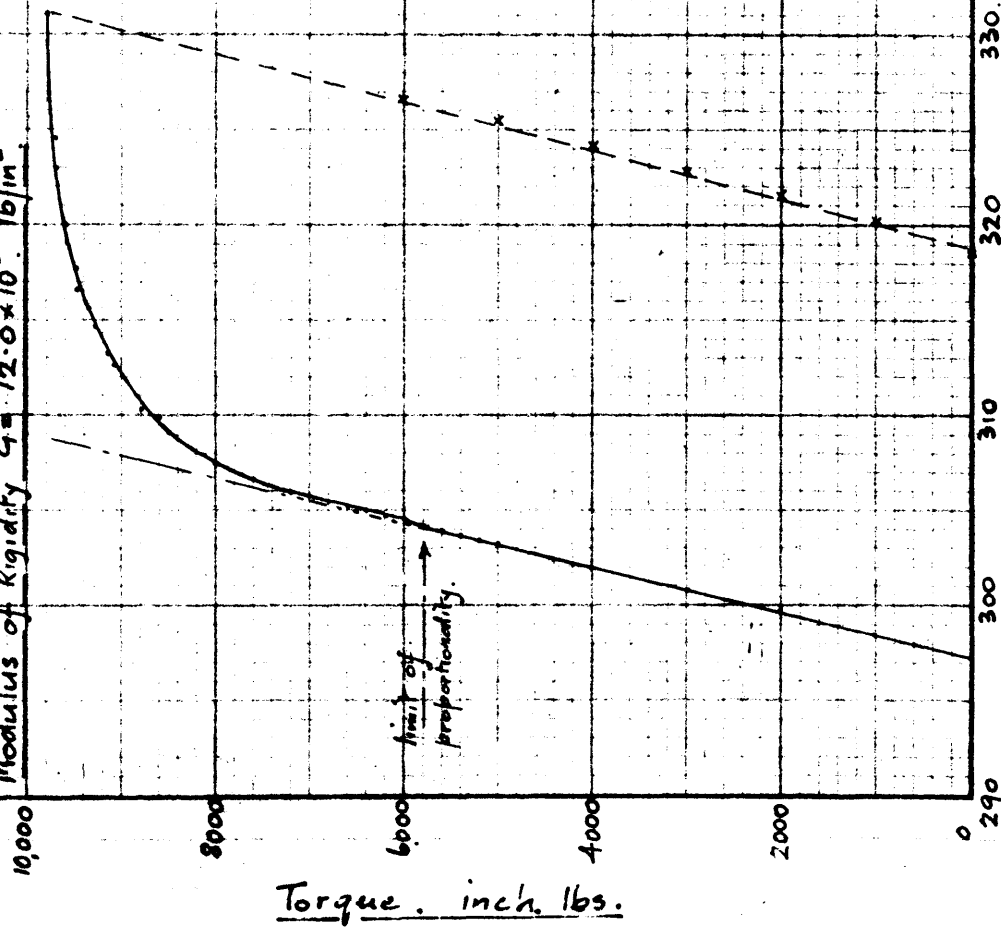


Fig. 83 Tensile test on 1" dia shafting material.

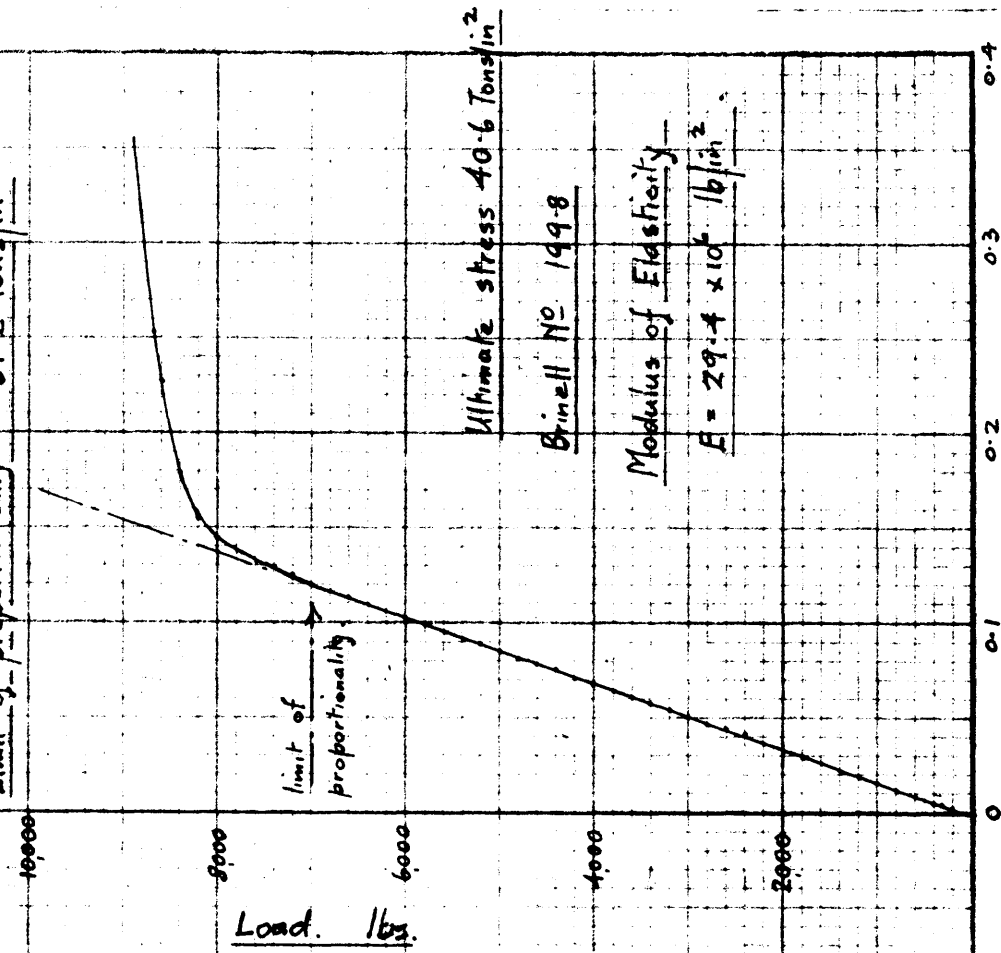
Specimen dia = 0.3571"

Gauge length = 2"

Reduction in area = 56.8%

Elongation on 2" = 13.25%

Limit of proportionality = 31.2 Tons/in²



The experimental data for a range of steels given by Rowett⁷, Föppl¹⁴, and Dorey¹⁷, are plotted in Fig. 84. This represents the available information on hysteresis that is directly applicable to damping calculations. The particulars of the steels are given on each curve. Using Rowett's values, Lewis⁴ expressed the hysteresis below the fatigue limit as :-

$$W = 1.37 \times 10^{-10} f_s^{2.3} \quad \text{lb. in. per in.}^3 \text{ per cycle.} \quad \text{--- (32)}$$

where f_s is half the shear stress range in lbs. per in.².

This expression is substituted for Rowett's values and is seen amply to cover the hysteresis properties for all the steels, below their approximate torsional fatigue limit, with the exception of the annealed C Steel-Föppl, and the normalised 29 ton mild steel forging which had been previously overstressed. Above the fatigue limit the hysteresis value increases, and Dorey shows the change occurring at a shear stress approximately between 0.55 of the torsional elastic limit and 0.20 of the ultimate tensile stress.

For the shafting in the experimental apparatus this change point will be about 7.25 to 8.1 tons per in.², shear. This value was exceeded only in one series of tests when a stress of 8.4 tons per in.², was attained. Hence, since the material was cold worked during manufacture and no subsequent annealing took place, the Lewis equation may be taken as giving a liberal estimate of the hysteresis damping in the experiments.

In the two-mass system the stress in the elastic member is uniform throughout the length, hence on integrating for the equivalent shaft 1 in. dia. x 148 in. long the total hysteresis becomes :-

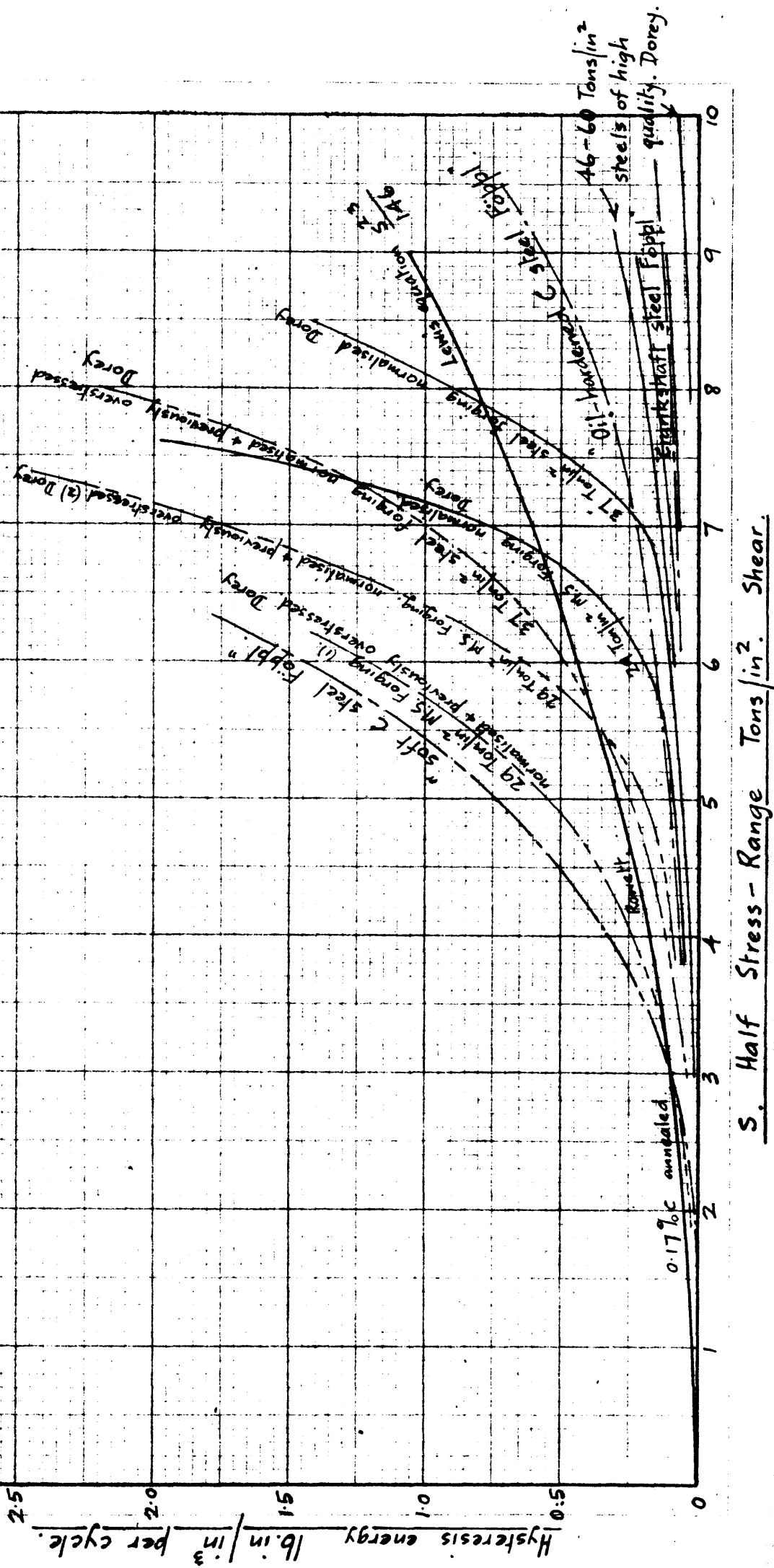
$$\begin{aligned} W &= \frac{\pi \times 1.37 \times 148}{10^{10} \times 2(2.3+2)} f_s^{2.3} \\ &= \frac{74.2}{10^{10}} f_s^{2.3} \quad \text{lb. in. per cycle.} \quad \text{--- (33)} \end{aligned}$$

7. 4. loc. cit.

14. ibid.

17. Dorey, Trans. Inst. Mech. Eng. (1932) (Advance Proof).

Fig. 84 Collected data on Hysteresis in Steels.



Using this equation, plotted in Fig. 85, the hysteresis energy is calculated for the stresses represented by the relative amplitudes and is given in tables 5 - 7.

Consider a specific case from table 6. With four pistons, the amplitude for the second order critical speed of 600 r.p.m. is 0.241 radian, giving an input energy of 184.4 lb. in. per vibration. The maximum stress in the shaft is 4.92 tons per in.², and from equ. (33) the corresponding hysteresis is 14.5 lb. in. per vibration.

From a similar examination of the tables, it must be concluded that the energy absorbed by hysteresis in the shafting material is less than 10 per cent. of the input energy for the lubricated series and less than 25 per cent. for the imperfectly lubricated series.

(c) Damping at Piston and Big-End Bearing.

At the piston and big-end, frictional influences and impacts arise. From the experiments on the pistons, the effects of pouring oil into the cylinder while running at resonance did not result in any decided change in resonance amplitudes from that which prevailed when lubrication was not continuous. Similarly, there was little or no difference in amplitude when the pistons were fitted with and without piston rings.

The type of lubrication present at the piston with or without rings is inherently of the solid to semi-fluid type; it was concluded that if a partial film did form at mid stroke the viscous resistance would be small on account of the decrease in viscosity of the oil consequent on the frictional work done upon it.

At the big-end bearing, the experiments showed that no definite change in resonance amplitude could be effected by introducing the normal splash lubrication together with syringing. It was concluded that the lubrication arrangements were incomplete and that semi-fluid friction prevailed.

Fig 85

Lewis equation for damping due to hysteresis
applied to 1" dia. shaft 148" long.

$$W = \frac{74.2 f_s^{2.3}}{10^{10}} \text{ lb.in per cycle}$$

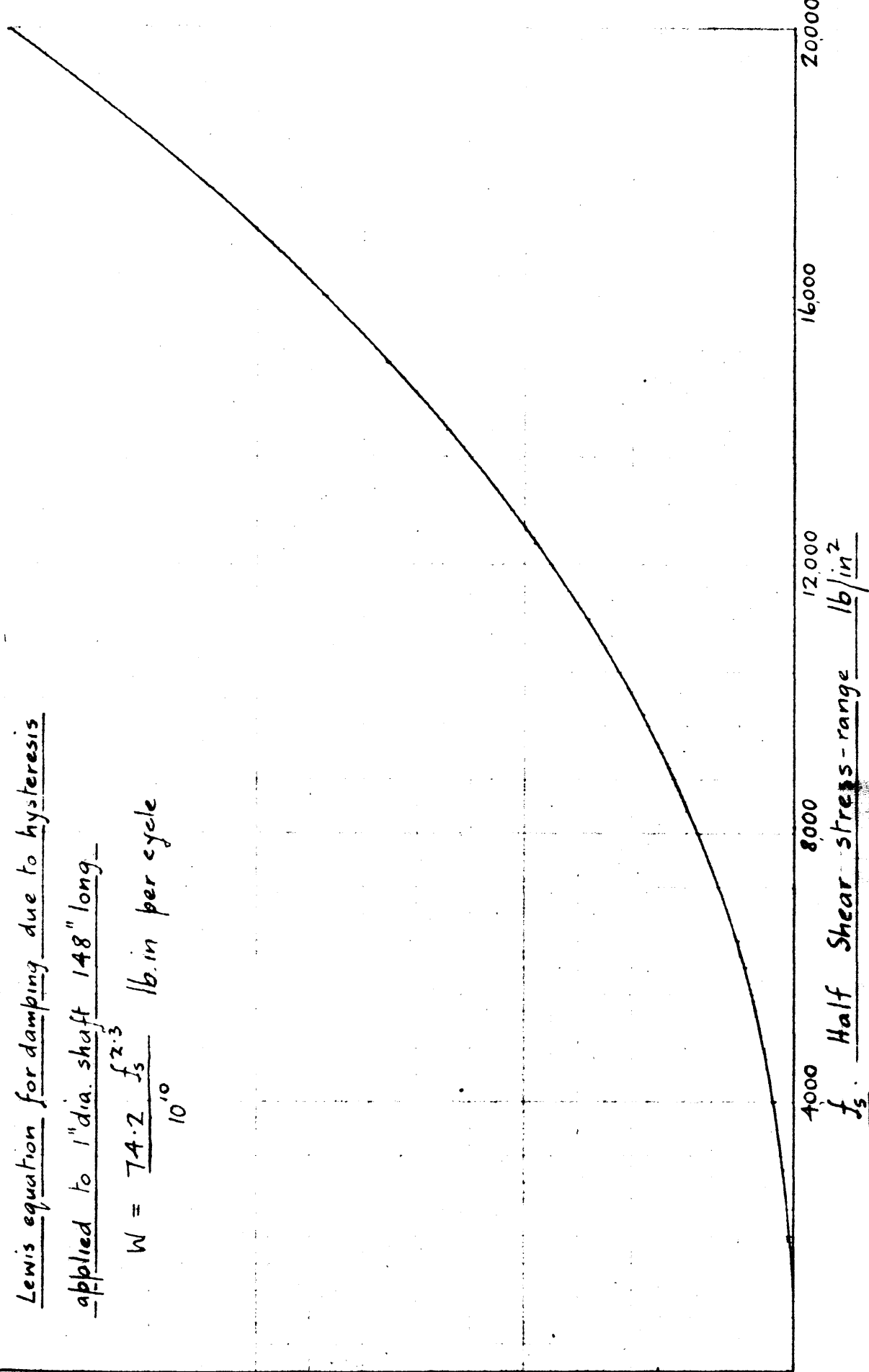
Hysteresis damping W. lb.in per cycle.

60

40

20

0



This was further tested by an analysis of the friction coefficients at the piston, gudgeon pin and crankpin, on the basis of the resultant torque due to solid friction.

The forces due to side thrust on the cylinder walls, gudgeon pin and crankpin were expressed by the usual Fourier series and reduced to frictional torques on the crankshaft. Absolute values were taken since this torque always opposes motion. Harmonic analysis of the resultant curve reduced the torque to a mean value plus a series of periodic terms.

From a series of power tests away from resonance, given on Fig. 63, the mean torque required for the piston and big-end system with and without rings was derived from the difference between the total power and that required to drive the motor and crankshaft alone.

Comparing the mean torque so obtained with that calculated, the average friction coefficient operating at the cylinder walls, gudgeon and crankpins was found to be 0.17. Also the friction torque expression due to the resistances at these surfaces was approximately :-

$$T = \omega^2 \left\{ -0.0026 - 0.0003 \cos 2\theta - 0.0006 \cos 3\theta \dots \right\} \text{ in. lb., per piston,}$$

and that due to ring friction :-

$$T = -10 + 6.72 \cos 2\theta + 1.16 \cos 3\theta \dots \text{ in. lb., per piston.}$$

Tests were carried out on the Deeley Oil Tester for the oil used and frictional coefficients for Ni.Cr. Steel on Cast Iron and Ni.Cr. Steel on White-Metal were found to be 0.189 and 0.196 respectively.

Since there is always a slight reduction in the Deeley values with speed, the results compare favourably, and show that there can only be semi-fluid friction at the piston and big-end bearing.

Effect of Semi-fluid Friction as damping.

Semi-fluid friction is composed of solid and viscous friction. The solid friction always opposes the motion and is entirely independent of the velocity.

If periodic speed variations occur in a rotating shaft and the absolute velocity is unidirectional, the solid friction can have no effect on the periodic motion other than merely controlling the mean position about which the variations are taking place. The action is thus similar to the effect of gravity on a mass suspended by a spring; during vibrations the gravity force is always in balance with the initial tensile force in the spring produced by the statical deflection.

For unidirectional motion the velocity ωr must be greater than the vibrational velocity $nwr\theta \cos nwt$, that is unidirectional motion is determined by $n\theta < 1$ both for rotation and reciprocation.

There is no record of any installation in practice in which $n\theta > 1$ although in the experimental plant the extreme case with imperfect lubrication gave a second order amplitude of ± 0.454 radian. This is just below the limiting value ± 0.50 radian for this order.

Pure solid friction will therefore have no effect in the dissipation of the superimposed vibrations.

With fluid friction, however, speed variations give rise to viscous tractions which result in corresponding energy dissipation. Hence with semi-fluid friction, the damping effect will be viscous in character.

Finally in the piston line, vibration impacts are liable to occur, quite apart from those due to rotation. If the forces induced by oscillation exceed the driving loads at any time, the clearances will be crossed twice during that vibration. This occurs in practically all engines when large oscillations take place.

The consequent damping will be due to the concurrent influences caused by the relative motion at the clearances rather than by the impact itself. This relative motion might be regarded as being similar to

slip in which case both the constant and viscous resistances operating will come into play.

However, in the experimental piston line, the driving pressures at the clearances are light and the oil films are only partial, hence no great dissipation is likely to arise from this effect.

It may be concluded therefore, that the damping influences attributed to the piston and big-end bearing are small and can only be expressed in an overall manner.

(d) Damping at the Crankshaft.

At the crankshaft, the main and roller bearings are the sources of frictional resistances. The roller bearing resistance will possibly be semi-fluid in nature but will be so small in magnitude that it can be neglected.

The experiments showed that the lubrication of the main bearing was very important in the control of amplitude. The ultimate amplitude attained at resonance when no oil was supplied to the bearing was practically twice that which occurred when gravity oil feed was fitted. This positive demonstration under these extreme conditions points to the dissipation of the oil film as the main source of damping and therefore it is necessary to examine this damping more fully.

Damping in the Main Journal Bearing.

In the case of a film lubricated bearing, the viscous drag will respond to speed fluctuations, giving rise to a corresponding viscous torque. As a first attempt the simple case of damping due to the periodic viscous torque will be considered.

The torque on the journal due to the shear force of the layer of film adjacent to the journal is given by Boswall¹⁸ as :-

18. Boswall, "The Theory of Film Lubrication" p.p. 270.

$$M_1 = \frac{\lambda u R}{m} \left\{ \frac{4\pi(a^2+2)}{(a^2-1)^{\frac{1}{2}}(2a^2+1)} \right\} \text{ --- --- --- (34)}$$

where, λ is the viscosity of the oil in c.g.s. units.

u the peripheral velocity at journal surface.

R the radius of journal.

mR the eccentricity.

nR the difference of radius.

and a is the ratio. $\frac{n}{m}$.

Assuming that the speed variations are small and do not affect the eccentricity, the film thickness will be that due to the steady running conditions.

Let the velocity of the shaft surface be :

$$\bar{u} = \eta R \theta \cos \eta t + u$$

where η is the angular velocity.

Hence substituting \bar{u} for u in equ. (34) the periodic torque coefficient becomes :-

$$T = \frac{\lambda \eta R^2 \theta}{m} \left\{ \frac{4\pi(a^2+2)}{(a^2-1)^{\frac{1}{2}}(2a^2+1)} \right\} \text{ --- --- --- (35)}$$

from which the work dissipated in the bearing of length L will be :-

$$W = \pi \theta^2 \lambda \eta R^2 L \left\{ \frac{4\pi(a^2+2)}{m(a^2-1)^{\frac{1}{2}}(2a^2+1)} \right\} \text{ per vibration. --- (36)}$$

The values of a and m are determined from the running conditions of the bearing.

Normal Running Conditions.

From Boswall¹⁸ the working position of the journal is given by :-

$$\eta = 0.00123 a \left\{ \frac{12\pi}{(a^2-1)^{\frac{1}{2}}(2a^2+1)} \right\}^{\frac{1}{2}} \left\{ \frac{\lambda_a R_E N_s}{W_{IE}} \right\}^{\frac{1}{2}} \text{ --- --- --- (37)}$$

where λ_a is the average viscosity in c.g.s. units.

R_E " " radius in inches.

N_s " speed in r.p.m.

W_{IE} " load in lbs. per inch width.

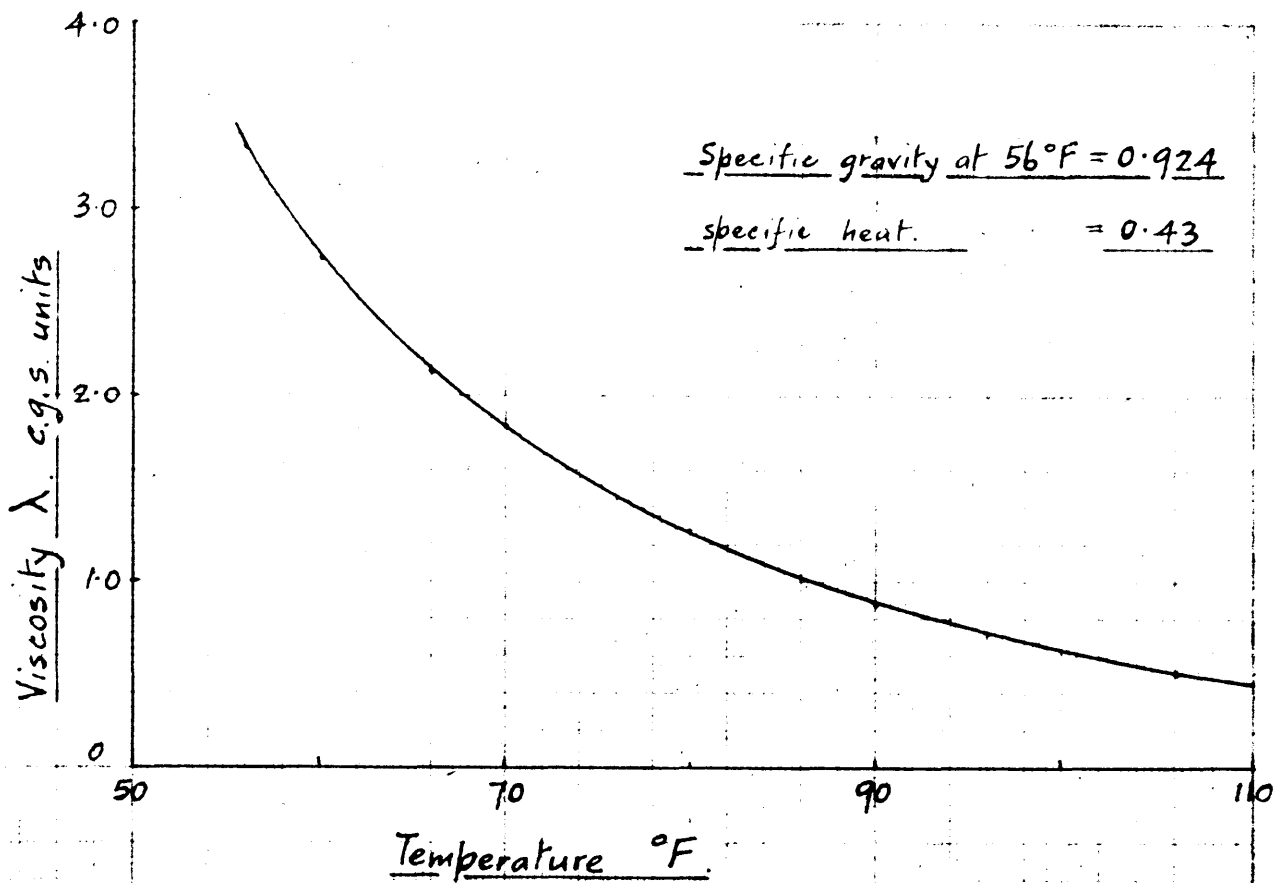
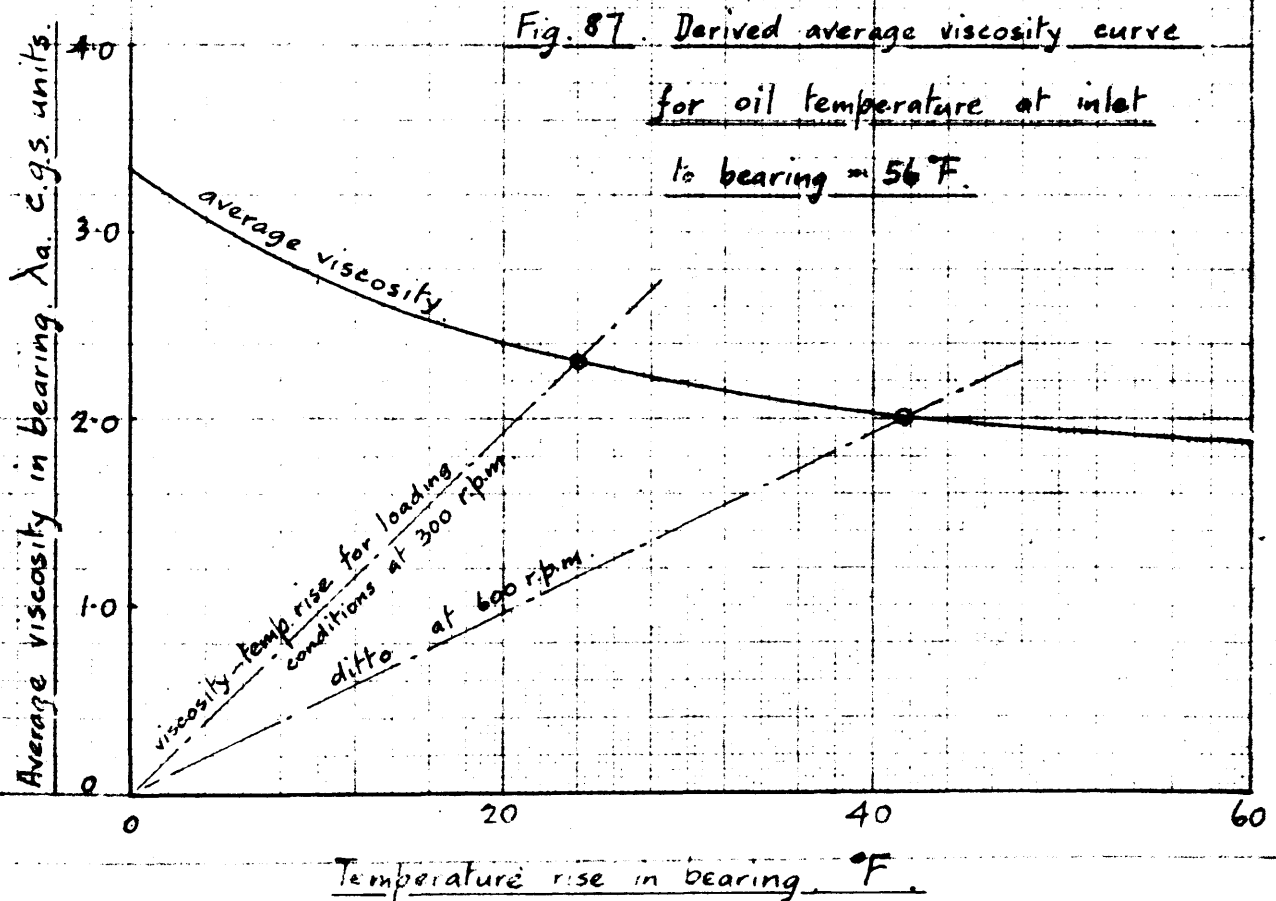


Fig. 86. Viscosity-Temperature Characteristics.



Substituting in equ. (37) the value of a becomes 444, for the condition at 600 r.p.m. Hence for the normal running conditions the journal will be practically concentric with the brass throughout the speed range.

Reverting to the work dissipated in the bearing the large values of a simplify equation (36), which on reduction becomes :-

$$W. \text{ per vibration} = 0.61 \lambda_a \eta \theta^2 \text{ in. lb., } \text{--- (39)}$$

a result which could be obtained directly by taking mean values.

From the experimental values in table 6 the amplitude for the second order critical speed of 600 r.p.m. is 0.241 radian with four pistons, giving an input energy of 184.4 in.lb. per vibration. Substituting the appropriate values in equ. (39) the energy dissipated is only 8.9 in.lb. per vibration.

This result might be considered as being the minimum applying to the concentric position only. Therefore, to take into account the effects of misalignment as interpreted by a variable a value in equ. (36), a plot of this equation for various values of a is given in Fig. 88. It is seen that there is very little change in the energy quantity for values of eccentricity that can obtain.

From these results it must be concluded that the damping in the bearing is not due to simple shear resistance caused by speed fluctuation. Such a result is not unexpected since similar viscous tractions are operating in normal running conditions and no abnormal friction ensues.

Damping due to the film appears only at resonance and must arise from the vibrational energy at the bearing, and also from the periodic deformation of the journal caused by the inertia torques of oscillation.

It is necessary, therefore, to examine these distortions.

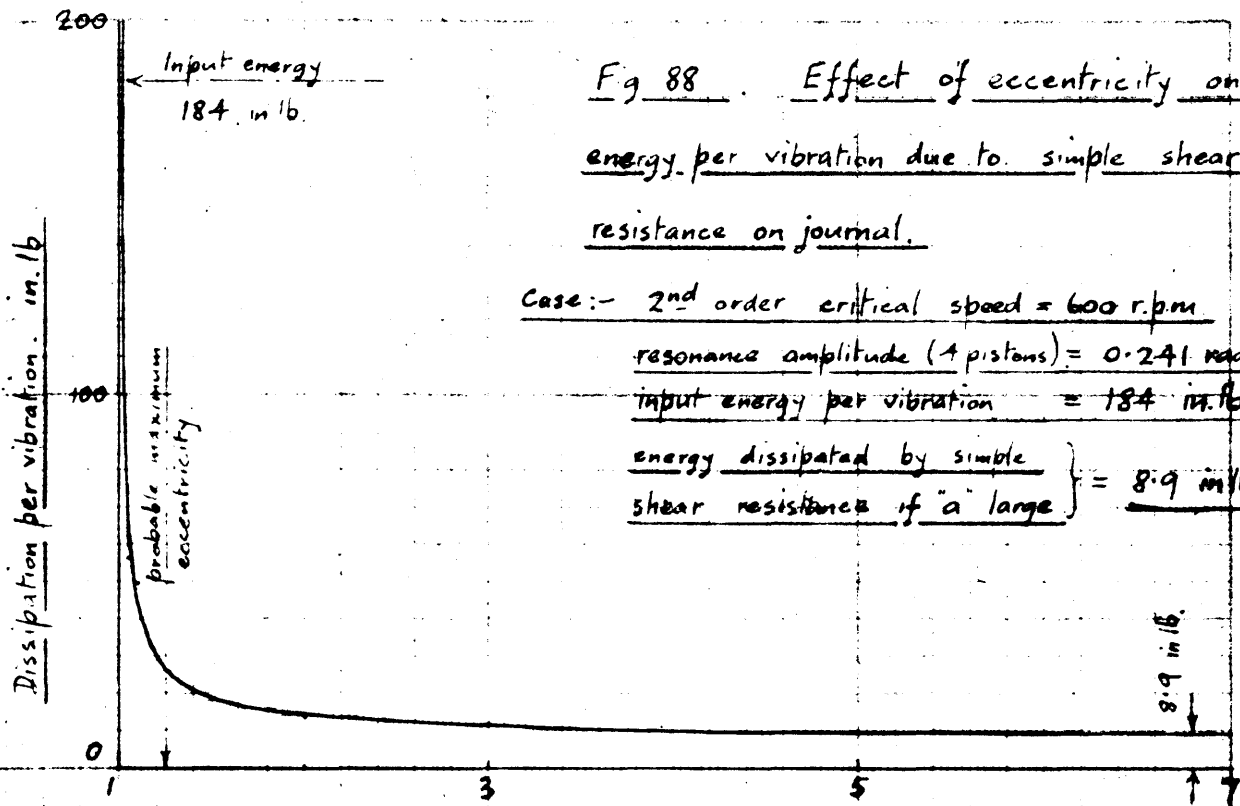


Fig 88 . Effect of eccentricity on energy per vibration due to simple shear resistance on journal.

Case:- 2nd order critical speed = 600 r.p.m
resonance amplitude (4 pistons) = 0.241 radian
input energy per vibration = 184 in/lb.
energy dissipated by simple shear resistance if "a" large } = 8.9 in/lb

$$a = \frac{rR}{mR} = \frac{\text{radius difference}}{\text{eccentricity}}$$

Elastic Deformation at Journal due to Inertia Torques of Oscillation.

The inertia torques of oscillation are a maximum at the ends of the swing and the reversed effective forces at the crankshaft act in the plane perpendicular to the plane of the throw. The roller bearing may be taken as a simple support, but the long journal bearing must be regarded as a distributed oil film support, offering resistance to displacement. For simplicity the long 1 inch diameter shafting is disregarded since it is comparatively flexible.

Considering the forces as being concentrated at the crankpin centres, the forces and couples acting on the crankshaft are shown in Fig. 89. The inertia forces acting at the crankpins are balanced by a torque M at the journal where a constraint is introduced by the oil film resistance.

With the constraint removed, the extreme deflections of the shaft axis are shown in Fig. 90. The flexular rotation at the supports is similar, but a slight relative displacement takes place on account of the torque proceeding from the journal to the cranks. The forces and couples on each component are shown in Fig. 91.

Using the shaft values given in page 21 and applying the slope deflection method to each component, the lateral displacement at the journal ab is found to be :-

$$\pm \frac{0.12 M}{10^6} \text{ inch.}$$

and the rotation at the journal becomes :-

$$\pm \frac{0.202 M}{10^6} \text{ radian.}$$

where M is the inertia torque in lb.in.

For the mass system $M1.4p$ the polar moment of inertia of the crankmasses is 0.66 lb.in.^2 and the

natural frequency 1200 v.p.m. With an amplitude of 0.24 radian the maximum inertia torque becomes 2,500 lb.in. Hence with no constraint, the lateral motion at the extreme ends of the journal is as shown on Fig. 92.

$$\begin{aligned}\text{Outside edge (a)} &= \pm 0.00138 \text{ in.} \\ \text{Inside edge (b)} &= \pm 0.00078 \text{ in.}\end{aligned}$$

The maximum travel available, due to clearance is ± 0.00125 in..

It would appear therefore that the possible deformations of the journal are quite appreciable. These motions will be constrained by the bearings and will be superimposed upon a rotation having large speed fluctuations. It is quite impossible to calculate the energy dissipated in the oil film under such complicated conditions. However, since an approximation as to the magnitude and nature of the effect is required an attempt is made to examine the possible dissipation in the oil film.

The Dissipation of Energy due to Journal Vibration.
in a flooded Bearing.

For simplicity it will be assumed that lateral motion of the journal is the main characteristic. Consider an oil flooded bearing of infinite width, in which the journal is given a periodic lateral motion. That is, the centre of the journal at the strip considered has a motion $rA \cos \omega t$ along the bearing centre line YY' Fig. 93. The oil contained in the interspace is therefore given a periodic circumferential flow.

Since the film thickness is small compared to the curvature and the effects in the two passages are similar, one passage, YOY' may be considered as two plane surfaces developed as shown on Fig. 93. In the bearing, the film thickness at A remains practically constant hence the top plane is taken as oscillating about O such that the end Y has a motion $rA \cos \omega t$.

Considering unit strip dz , perpendicular to the plane of the paper, the volume within the interspace remains constant, hence the mean velocity of the oil, \bar{u} at x may be obtained as follows:-

$$\begin{aligned} \text{volume of oil to the right of } x &= Q_R \\ &= A + \left(\frac{\ell}{4} - \frac{x^2}{\ell}\right) r A \cos \gamma t \end{aligned}$$

$$\therefore \frac{d(Q_R)}{dt} = -\left(\frac{\ell}{4} - \frac{x^2}{\ell}\right) r A \gamma \sin \gamma t \quad \text{--- (40)}$$

$$\text{but } \frac{d(Q_R)}{dt} = \bar{u} \times h_t \quad \text{--- (41)}$$

where h_t is the distance between the planes at position x and time t .

$$\text{Thus } h_t = A \left(1 + \frac{2xr}{\ell} \cos \gamma t\right) \quad \text{--- (42)}$$

Substituting in (41), the mean velocity at x becomes :-

$$\bar{u} = \frac{-\left(\frac{\ell}{4} - \frac{x^2}{\ell}\right) r \gamma \sin \gamma t}{\left(1 + \frac{2xr}{\ell} \cos \gamma t\right)} \quad \text{--- (43)}$$

Also, with infinite width the lubricant flows in one plane only, giving the pressure condition

$$\frac{\partial P}{\partial x} = \lambda \frac{\partial^2 u}{\partial y^2} \quad \text{--- (44)}$$

where λ is the viscosity of the oil.

From this equation

$$u = \frac{1}{\lambda} \frac{\partial P}{\partial x} \left(\frac{y^2}{2} - \frac{yh}{2}\right) \quad \text{--- (45)}$$

and the mean value across the section is

$$\bar{u} = -\frac{1}{\lambda} \frac{\partial P}{\partial x} \frac{h_t^2}{12} \quad \text{--- (46)}$$

Equating the mean values of \bar{u} from (43) and (46) and substituting for h_t , give :-

$$\frac{\partial P}{\partial x} = \frac{12 \lambda r \gamma \left(\frac{\ell}{4} - \frac{x^2}{\ell}\right) \sin \gamma t}{A^2 \left(1 + \frac{2xr}{\ell} \cos \gamma t\right)^3} \quad \text{--- (47)}$$

But from (45)

$$\begin{aligned} \frac{\partial u}{\partial y} &= \frac{1}{\lambda} \frac{\partial P}{\partial x} \left(y - \frac{h}{2} \right) \\ &= \frac{3r\eta \left(\frac{\ell}{2} - \frac{2x^2}{\ell} \right) (2y-h) \sin \eta t}{A^2 \left(1 + \frac{2x}{\ell} r \cos \eta t \right)^3} \end{aligned}$$

$$\therefore \left(\frac{\partial u}{\partial x} \right)^2 = \frac{9r^2\eta^2 \left(\frac{\ell}{2} - \frac{2x^2}{\ell} \right)^2 (2y-h)^2 \sin^2 \eta t}{A^4 \left(1 + \frac{2x}{\ell} r \cos \eta t \right)^6} \quad \text{--- (48)}$$

Now the rate of dissipation of energy per unit volume¹⁹ for the pressure condition given by (44) is :-

$$2\lambda \left(\frac{\partial u}{\partial x} \right)^2$$

Hence, rate of dissipation per unit area ($dy \cdot dz$) at x ,

$$\begin{aligned} &= \int_0^h 2\lambda \left(\frac{\partial u}{\partial x} \right)^2 dy \\ &= \frac{6\lambda r^2 \eta^2 \left(\frac{\ell}{2} - \frac{2x^2}{\ell} \right)^2 \sin^2 \eta t}{A \left(1 + \frac{2x}{\ell} r \cos \eta t \right)^3} \quad \text{--- (49)} \end{aligned}$$

Therefore, the total rate of dissipation F , per unit strip (dz),

$$= \frac{6\lambda r^2 \eta^2}{A} \int_{-\frac{\ell}{2}}^{+\frac{\ell}{2}} \frac{\left(\frac{\ell}{2} - \frac{2x^2}{\ell} \right)^2 \sin^2 \eta t}{\left(1 + \frac{2x}{\ell} r \cos \eta t \right)^3} dx \quad \text{--- (50)}$$

After approximate integration, (50) becomes,

$$F = \frac{2\lambda r^2 \eta^2 \ell^3}{5A}$$

or for the complete circumference,

$$F = \frac{\lambda r^2 \eta^2 \pi^3 d^3}{10A}$$

where d is the journal diameter.

Hence, work per vibration per unit strip is :-

$$19.5 \frac{d^3}{A} \lambda \eta r^2 \quad \text{--- (51)}$$

Assuming a mean viscosity of 2.0 c.g.s. units, the work dissipated per unit strip is :-

$$W = \frac{19.5 \times 5.36 \times 2.0 \times 2.08 \times 12 \times \eta r^2}{1728 \times 10^3 \times 0.00125}$$
$$= 2.42 \eta r^2 \text{ lb. in. per inch. per vibration.}$$

From the nature of the journal deflections as shown in Fig. 92 the oil film at the outer portion of the bearing a to x , will suffer the greatest distortion. Taking the energy as being dissipated in this half of the bearing only, the oil film dissipation will be $4.84 \eta r^2$ lb. in. per vibration.

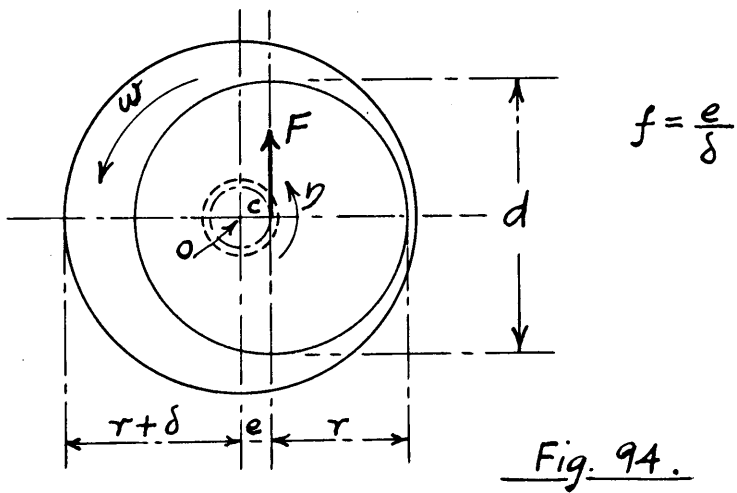
Applying this equation to the four piston case where the natural frequency is 1200 v.p.m. and the input energy 184 lb.in. per vibration, the value of r becomes 0.55 if the total input is assumed to be absorbed in this manner. The corresponding mean amplitude of journal eccentricity is 0.00069 inch.

Thus considering only half the bearing as being applicable to equation (51), the amplitude of journal eccentricity is of the right order of magnitude, thereby confirming the results demonstrated by the experiments with and without gravity oil supply.

It is interesting to compare the somewhat similar lubrication effects caused by the whirling of a journal in its bearing. In this case the simplest aspect of the problem is that of a journal rotating round its own centre with an additional rotation of the eccentricity about the bearing centre. The forces induced on the journal by such actions have been examined by Robertson²⁰ in a paper which has just been published.

20. Robertson, Philosophical Magazine, Jan. 1933, p.p. 113.

Fig. 94 represents the problem.



O is the centre of the bearing, C that of the journal and OC the eccentricity e . The radial clearance of the bearing is δ and the radius of the journal r . The rotations of the journal round C is ω and that of the eccentricity round O is η . The component force on the journal, normal to the eccentricity reduces to :-

$$F_n = \left[\frac{12\pi\lambda L r^3}{\delta^2} \right] \left[\omega - 2\eta \right] \left[\frac{f}{(2+f^2)(1-f^2)^{\frac{1}{2}}} \right]$$

and the component along the eccentricity is :-

$$F_e = - \left[\frac{12\pi\lambda L r^3}{\delta^2} \right] \left[(1-f^2)^{-\frac{3}{2}} \frac{df}{dt} \right]$$

Now in order to compare these effects with those suggested by the approximate analysis it is only necessary to determine the work done during a whirl.

Considering the superimposed effects, the force in operation during a whirl of constant eccentricity is :-

$$\bar{F}_n = \left[\frac{24\pi\lambda L r^3}{\delta^2} \right] \left[\frac{\eta f}{(2+f^2)(1-f^2)^{\frac{1}{2}}} \right]$$

from which the work done is :-

$$W \text{ per whirl} = 2\pi e \bar{F}_n = \frac{59.2 \lambda L d^3 \eta}{\delta} \frac{f^2}{(2+f^2)(1-f^2)^{\frac{1}{2}}} \quad \text{--- (52)}$$

The work done is therefore a function of $\frac{f^2}{(2+f^2)(1-f^2)^{\frac{1}{2}}}$, which is practically proportional to f^2 for values of f less than $\frac{1}{2}$, after which it gradually increases and then tends to infinity when f approaches unity. This is a typical lubrication expression indicating rapid increase in resistance as the journal tends to come in contact with the bearing.

However, for the values of f less than $\frac{1}{2}$ the expression $(2+f^2)(1-f^2)^{\frac{1}{2}}$ has a practically constant value of 2, hence the work per whirl reduces to:-

$$W \text{ per whirl} = \frac{29.6 \lambda L d^3 \eta f^2}{\delta} \quad \text{--- (53)}$$

With the exception of a 50 per cent. difference in coefficient, this expression is exactly similar in form to equation (51) obtained by considering the dissipation due to viscosity for the approximate journal motion.

Now both these expressions (51) and (53) indicate an apparent limiting capacity of bearing damping when f is unity, but at this severe condition it is certain that the resistance of the oil film would increase rapidly. It would seem therefore that the correct form of bearing damping should include the typical bearing expression. $(2+f^2)(1-f^2)^{\frac{1}{2}}$.

However, in the present experiments, examination of the energy quantities in relation to the simple expression $4.84 \eta r^2$, shows that the maximum value of f for the lubricated series is 0.55. Even for the imperfectly lubricated series, where the maximum amplitude was so severe that the limiting condition for unidirectional motion was almost exceeded, the energy quantity would only

be sufficient to make $f = 0.75$. Therefore the simple expression should be quite capable of representing the bearing damping in the experiments.

Again with extremely small energy quantities of about 1.0 lb.in. per vibration such as occur with the 3rd order vibrations, the corresponding eccentricities are less than 10^{-4} inch. As this is relatively small and hardly appreciable, it is probable that the damping effects at the bearing will not be proportionately developed, and so the method of analysis presented above would give an overstatement of the damping. It is considered inadvisable to extend the analysis to this case so far as it has been investigated since the amplitudes and energy quantities are extremely small and indefinite. A change of the system to increase the 3rd order energy quantities would really be necessary to examine the matter further.

However, it may be taken that the simple line of analysis is competent to explain fully the damping influences in the relatively large and definite amplitude vibrations of the 2nd order. This damping expression implies a straightforward velocity damping and therefore suggests a further examination of the results on an overall velocity damping basis.

Overall Velocity Damping.

The most rational way of dealing with velocity damping is by means of a non-dimensional factor. This factor is derived from the equation of motion for the single mass-elastic system. The standard equation is :-

$$M\ddot{y} + R\dot{y} + Fy = Q \sin \omega t \quad (54)$$

where $M\ddot{y}$ is the inertia torque due to the mass, M in engineers' units. lb.in.sec².

$R\dot{y}$ is the damping torque, R being the damping factor, lb.in. per radian per sec.,

F_y is the elastic torque,

$Q \sin \omega t$ is the applied harmonic torque.

Also $\frac{\omega}{2\pi} = \frac{1}{2\pi} \sqrt{\frac{F}{M}}$ = the natural frequency of the system.

At resonance the non-dimensional factor becomes $\frac{M_D}{R}$ and gives the ratio of the actual twist to that which would occur if the external torque were applied statically. This factor has no dimensions and is adopted by B.C. Carter⁵ for single crank engines, and is the most general way of dealing with this system.

The calculations showing the reduction to this factor for the present arrangement are given in table 8. The effect of each group of pistons is shown on Fig. 95 by plotting the factor on a base of number of pistons.

From inspection it is seen that with gravity oil-feed to the main bearing the values show very good agreement for each piston series thus confirming the validity of the non-dimensional factor. If a mean line be drawn through the points a slight positive gradient is obtained suggesting damping in the piston lines, but this is very small on account of the imperfect lubrication existing in each line.

For the series with imperfect lubrication at the main bearing the gradient is larger and is possibly due to further damping caused by the very severe amplitudes developed. Taking mean values for each group of pistons, the average ratio of damping for the lubricated condition to that for imperfect lubrication is approximately 2 to 1.

Table 8

Non-Dimensional Factor $\frac{R}{M\eta}$

2nd order.

Gravity oil-feed to main bearing.
(continued from table)

critical speed r.p.m.	$M\eta$ lb.in.sec	Input energy in.lb/vib	← One piston series →			← Two piston series →			
			$\pi\eta y^2$	$\frac{R}{\pi\eta y^2}$ in.lb.sec	$\frac{R}{M\eta}$	Input energy in.lb/vib	$\pi\eta y^2$	$\frac{R}{\pi\eta y^2}$ in.lb.sec	$\frac{R}{M\eta}$
600	71.7	12.5	2.22	5.64	0.0787	39.2	5.25	7.47	0.1035
500	92.2	4.94	0.608	8.13	0.0882	16.16	1.61	10.04	0.1089
400	134.0	1.74	0.151	11.50	0.0860	5.56	0.378	14.71	0.1098
350	170.8	1.00	0.0745	13.42	0.0787	3.12	0.180	17.33	0.1016

critical speed r.p.m.	$M\eta$ lb.insec.	Input energy in.lb/vib.	← Three piston series →			← Four piston series →			
			$\pi\eta y^2$	$\frac{R}{\pi\eta y^2}$ in.lb.sec	$\frac{R}{M\eta}$	Input energy in.lb/vib	$\pi\eta y^2$	$\frac{R}{\pi\eta y^2}$ in.lb.sec	$\frac{R}{M\eta}$
600	71.7	93.3	11.96	7.80	0.1086	184.4	22.65	8.15	0.1136
500	92.2	38.13	3.77	10.11	0.1098	72.2	7.20	10.01	0.1086
400	134.0	12.27	0.824	14.90	0.1110	22.4	1.513	14.82	0.1108
350	170.8	6.57	0.350	18.80	0.110	11.92	0.647	18.50	0.1083

Imperfect lubrication series.

2nd order

critical speed. 560 r.p.m.

$M\eta = 77.4$ lb.in.sec.

No. of pistons p	Input energy in.lb/vib	$\pi\eta y^2$	$\frac{R}{\pi\eta y^2}$ in.lb.sec	$\frac{R}{M\eta}$
1	24.5	9.42	2.6	0.0336
2	76.6	19.80	3.87	0.050
3	170.4	35.40	4.82	0.0623
4	339.2	59.4	5.71	0.0738

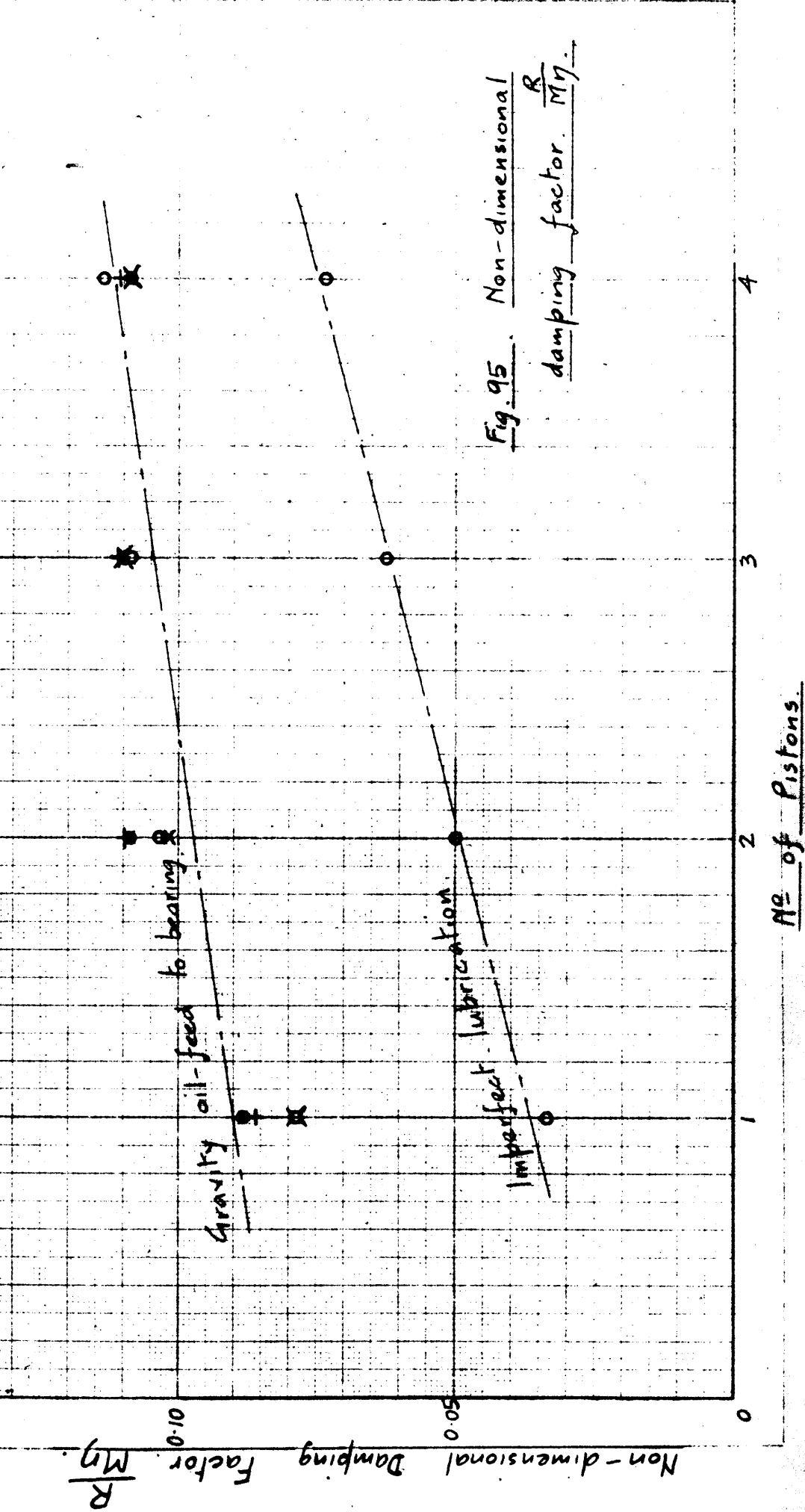


Fig. 95. Non-dimensional damping factor $\frac{R}{Mg}$.

PART III.

APPLICATION OF THE NON-DIMENSIONAL FACTOR TO RESULTS
OBTAINED FROM FURTHER EXPERIMENTS CARRIED OUT ON MULTI-
CRANK ENGINES.

In view of the constancy of the non-dimensional factor in the experimental apparatus, it was thought that it might give a proper basis for analysis of a number of multi-crank engines on which torsional oscillation investigations had been carried out.

The first attempt at a solution of the problem was the determination of an equivalent amplification factor for multi-mass systems. By assuming the free vibration form at resonance, and applying strain energy methods, this factor was reduced to give the ratio:— actual torque at the node \div torque at the node for equivalent static twist to the free vibration form. A number of engines were reduced on this basis, but the results were not quite suitable for direct application, in view of the length of calculation necessary on such an empirical basis.

However, since the main bearings and big-ends of these engines are all lubricated, the distribution of damping and inertia quantities throughout the engine can be averaged. Hence the essential features of reduction are retained if the average damping factor per cylinder be reduced to the non-dimensional form $\frac{M D}{R}$ where M and R are the inertia and the damping quantities per cylinder respectively.

Where the crankshaft is stiff relatively to the flexible portion of the system, the two methods merge into the simple single mass form.

Method of Analysis.

For calculating R , only the conditions at resonance need be considered and the energy method developed by Wydler³ and Lewis⁴ is adopted. At resonance

3. Wydler, loc. cit.

4. Lewis, loc. cit.

the vibrational energy supplied by the stimulating impulses is absorbed entirely by the damping forces. Considering the single crank system as represented by equation (54), the work done at the cylinder by the periodic torque during one vibration at resonance is :-

$$W = \pi Q y \quad \text{--- --- --- --- ---} \quad (55)$$

while the work absorbed by the damping at the same point is :-

$$D = \pi R b y^2 \quad \text{--- --- --- --- ---} \quad (56)$$

Extending to a multi-crank engine and considering a particular order, the total work done at resonance by the corresponding harmonic torques at all the cylinders during a vibration will be :-

$$W = \pi \sum_1^m Q_r y_r \quad \text{--- --- --- --- ---} \quad (57)$$

$\sum_1^m Q_r y_r$ is the vector summation of the energy quantities at each cylinder, due account being taken of the phase relation between the harmonic torques at the various cylinders. The free vibration form is assumed at resonance and with internal combustion engines, the torque coefficients are equal in magnitude throughout. The vector summation may then be regarded as applying to the relative amplitudes taken from the elastic curve at each cylinder, but acting in the phase of the harmonic torque under consideration.

Let α be ^{the} measured amplitude at the forward end of the engine, where the corresponding relative ordinate of the elastic curve is unity, then if y_1, y_2, y_3, \dots etc., are the corresponding ordinates at each cylinder, the total work becomes :-

$$W = \pi Q \alpha \sum_1^m y_r \quad \text{--- --- --- ---} \quad (58)$$

Similarly the work absorbed by the damping forces, considered concentrated at each cylinder, is approximately :-

$$D = \pi R \eta \alpha^2 \sum_1^m y_r^2 \quad \text{--- --- --- --- ---} \quad (59)$$

and from equations (58) and (59) the overall damping factor per cylinder is :-

$$R = \frac{Q \sum_1^m y_r}{\eta \alpha \sum_1^m y_r^2} \quad \text{--- --- --- --- ---} \quad (60)$$

Taking the average mass per cylinder, the non-dimensional factor becomes :-

$$\frac{M \eta}{R} = \frac{M \eta^2 \alpha \sum_1^m y_r^2}{Q \sum_1^m y_r} \quad \text{--- --- --- --- ---} \quad (61)$$

Expressed in this manner the factor may be interpreted as the ratio of the induced inertia torque at the cylinder masses to the applied torque, $\eta^2 \alpha$ being the acceleration.

This interpretation is quite in accordance with the conception of oil film dissipation due to inertia reaction at the big-end and engine bearings.

Derivation of Factor for all Classes of Engines.

The results of torsigraphic investigations which had been made on a few engine systems by Professor Mellanby and the author, together with those obtained from various technical journals, were analysed on this basis. Since engine damping only was required, allowance was made for propeller damping where this occurred.

The necessary details of each dynamical system, together with the information required for the calculations, are given and the final results appear in tabular form.

On examining the results it will be seen that there is a wide variation in the non-dimensional factor, corresponding to the form of the elastic curve at the

engine. Now, in the derivation of the damping factor it has been assumed that the damping actions, such as occur at the big-end bearings, are directly dependent on the amplitude at the cylinders. However, the damping at the main bearings of multi-crank engines is not directly expressed by the amplitude at the cylinders, but is rather a function of the reactions due to web distortion on the crankshaft. Now for similar crankshafts, the form of the elastic curve at the engine may be taken as a simple measure of the journal displacements and can be expressed by $\frac{\sum_1^m \theta_r}{m}$, where m , is the number of cylinders and θ_r the relative amplitudes at cylinder r . This factor also indicates the position of the node relative to the engine. Plotting $\frac{M_D}{R}$ on a base of $\frac{\sum_1^m \theta_r}{m}$, as shown on Fig. 109, a better classification is obtained.

The value $\frac{\sum_1^m \theta_r}{m}$ has the possible limits 1 to 0, corresponding to the case where the node is well outside the engine, and to the case where it occurs exactly at the engine centre line respectively. In the ~~former~~ first case the engine vibrates as one mass while in the latter, one half of the engine vibrates in opposition to the other. This range is practically covered by the list of engine systems given, and it will be noticed that the first and second modes of vibration for engine system in Fig. 96b, practically give the extreme values of $\frac{\sum \theta}{m}$. Particular attention may therefore be given to this engine since the non-dimensional factor obtained for each mode will indicate the possible values at the limits of the vibration form factor.

Engine No. A.^a

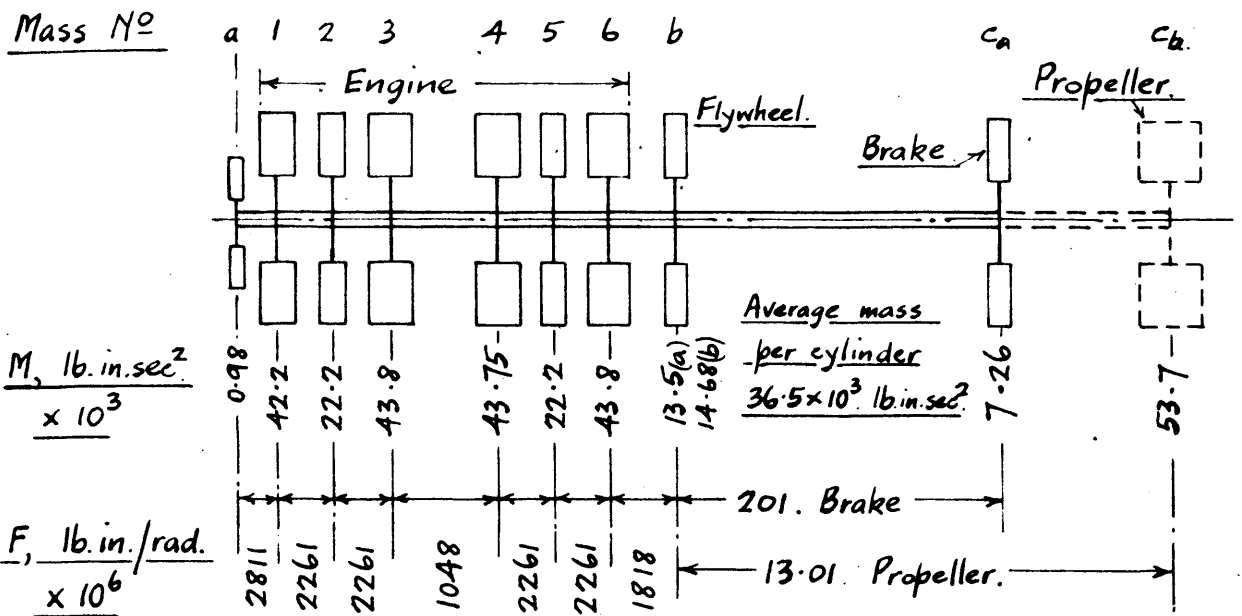
Two dynamical systems are available as shown in Figs. 96a and 96b, where it will be seen that the one-node form on the test bed Fig. 96a is practically similar to the two node form at sea Fig. 96b. A $7\frac{1}{2}$ order resonance condition was observed in both cases where

a. 6th Report, Mar. Oil-Eng. Trials Comm., Trans. Inst. Mech. Eng. 1931, vol. 121, page 268.

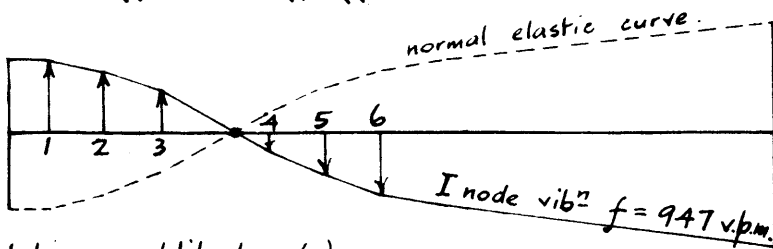
Fig. 96.

Engine No A. 6 cylinder, 4 stroke single acting supercharged oil engine. (Messrs Scott's Shipbuilding & Eng^g Co)

Equivalent dynamical system of (a) Engine - Flywheel - Brake, and (b) Engine - Flywheel - Propeller.

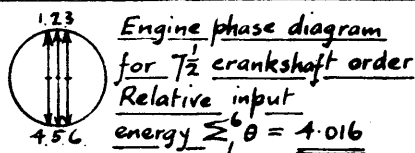
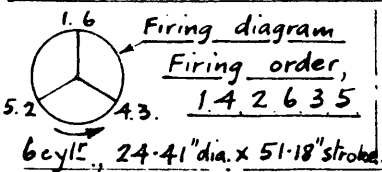


Torsional vibration form. (a)



Relative amplitudes (a)

Mass No	a	1	2	3	4	5	6	b.	c.
I node	1.0000	0.9966	0.8092	0.5430	-0.2534	-0.5744	-0.8396	-0.9702	-1.5010

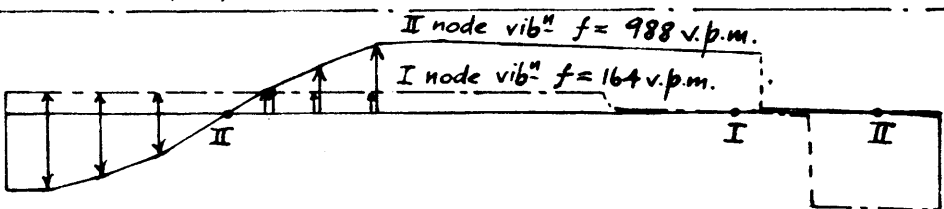


Relative damping work $\sum_1^6 \theta^2 = 3.040$

Elastic curve form at engine factor $(\frac{\sum \theta^2}{\sum \theta}) = 0.1136$

Measured: (Brake system) $7\frac{1}{2}$ order, I node critical at 123 r.p.m. Amplitude at mass No a = $\pm 0.33^\circ$ (Brake running free). Harmonic torque coefft. (from cards) at M.E.P = 20.4 lb/in^2 is $2.1 \text{ in lb/in}^2/\text{in radius}$. $\therefore R \text{ per line} = 58300 \text{ lb.in.sec}$. Hence $M/R = 62.0$

Torsional vibration forms. (b)



Mass No	a	1	2	3	4	5	6	b.	c.
I node.	1.0000	0.9999	0.9943	0.9858	0.9553	0.9357	0.9134	0.8792	-4.1858.
II node	1.0000	0.9963	0.7931	0.5063	-0.3395	-0.6608	-0.9129	-0.9910	+0.0229

Measured: 3rd order I node critical at 56 r.p.m. Amplitude at mass No a = $\pm 1.98^\circ$
 $7\frac{1}{2}$ " " 2 " " " 132 " " " " " " = $\pm 0.284^\circ$

3rd order I node: Phase diag gives $\sum_1^6 \theta = 5.784$; $\sum_1^6 \theta^2 = 5.586$; Elastic form factor $(\frac{\sum \theta^2}{\sum \theta}) = 0.9637$

3rd order torque coefft. at 56 r.p.m including inertia = $211,840 \text{ in.lb./cylinder}$. Propeller damping $P = 92100 \text{ in.lb.sec}$. \therefore Engine damping, $R \text{ per line} = 73000 \text{ in.lb.sec}$. Hence $M/R = 8.8$.

$7\frac{1}{2}$ order 2 node: Phase diag gives $\sum_1^6 \theta = 4.209$; $\sum_1^6 \theta^2 = 3.262$; Elastic form factor $(\frac{\sum \theta^2}{\sum \theta}) = 0.064$

Harmonic torque coefft. = $2.85 \text{ lb.in. per in}^2 \text{ per in radius}$. (from cards at M.E.P = 118 lb/in^2).

$\therefore R \text{ per line} = 85700 \text{ lb.in.sec}$. Hence $M/R = 44.1$

the elastic form factor was approaching zero, and a 3rd order critical was obtained for the value of the factor approximately unity,

During the torsigraphic investigation of the system in Fig. 96a, the circulating water was shut off from the brake, which was thus running free and the engine was driving against its own frictional resistance. The damping at the brake is therefore negligible.

In Fig. 96b for the two-node form, the engine was working under power and a node occurred practically at the propeller, hence the damping at the propeller is also negligible. The results from the two arrangements may therefore be taken as a fairly reliable indication of the damping at the engine for low values of the elastic form factor.

Estimation of Damping.

It is necessary to determine the value of the harmonic torques and these depend to a certain extent upon the mean power torque. The $7\frac{1}{2}$ harmonic order arises in the engine and is due entirely to the gas pressures. Indicator cards were available for the speed range and a harmonic analysis of the corresponding torque curves was made only for the orders required.

At the $7\frac{1}{2}$ order criticals the average mean effective pressures for the two cases were found to be 20.4 and 118 lb. per in² for Figs. 96a and b respectively. Hence, from a plot of harmonic coefficient on a base of m.e.p., the corresponding values at these two conditions were found to be 2.10 and 2.85 lb. per in² per inch radius respectively.

From the firing order given in Fig. 96a, and the appropriate engine phase diagram, the vector summations of the relative amplitudes at the engine are as given in Figs. 96a and b. The engine had six cylinders, 24.41 in. diameter, 51.18 in. stroke,

therefore for Fig. 96a, $7\frac{1}{2}$ order one-node critical, the harmonic torque per cylinder becomes :-

$$Q = 2.1 \times 468 \times \frac{51.18}{2} = 25,200 \text{ lb.in.}$$

Hence, from equation (60), the overall damping factor is :-

$$\begin{aligned} R \text{ per line} &= \frac{25,200 \times 4.016 \times 57.4}{99.2 \times 3.04 \times 0.33} \\ &= 58,400 \text{ in. lb. sec.} \end{aligned}$$

and consequently from equation (61) the non-dimensional factor is found to be :-

$$\frac{M_D}{R} = \frac{36.5 \times 10^3 \times 99.2}{58,400} = 62.0$$

The elastic form factor at the engine is 0.114.

Similarly, from the data given in Fig. 96b, the value of $\frac{M_D}{R}$ for the $7\frac{1}{2}$ order two-node critical is found to be 44.1 for the elastic form factor 0.064.

Considering the 3rd order one-node critical at 56 r.p.m., Fig. 96b, the disturbing torques again arise only at the engine, but in this case they are due both to the gas and the inertia forces.

From the trial results the m.e.p. at the condition required was about 38-40 lb. per in². Again, from the cards, the 3rd order harmonic torque due to the gas pressure was found to be $22.7 \sin(30 - 4^\circ.40')$ lb. per in² per in. radius. Hence $Q_1 = 272,000$ in.lb. per cylinder.

The unbalanced 3rd order inertia torque for the engine is :-

$$-6 \frac{W}{g} \omega^2 r^2 c \sin 3\omega t.$$

where W is the reciprocating parts = 5,350 lb. per line, $\frac{\omega}{2\pi}$ is the rotational speed, r is the crank radius, and c is the torque coefficient = 0.1922 for $\frac{l}{r} = 4.0$, where l is the length of the connecting rod.

Substituting the values, the inertia torque becomes :-

$$Q_2 = - 60,160 \text{ in.lb. per cylinder.}$$

From the engine phase diagram, the gas pressure torques of all the cylinders are in phase, hence the net harmonic torque per cylinder is approximately :-

$$Q_1 + Q_2 = 211,840 \text{ in. lb.}$$

The input work per vibration is by equation (58) and further data from Fig. 96b

$$\begin{aligned} W &= \pi \times 211,840 \times \frac{1.98}{57.4} \times 5.784 \\ &= 132,800 \text{ in.lb.} \quad \text{--- (62)} \end{aligned}$$

In this case, however, the amplitude of oscillation is large at the propeller and consequently the vibrational energy dissipated there must be allowed for.

By Lewis⁴ and Porter⁵, the propeller damping is approximately given by :-

$$p = \frac{34.4 T}{N} \quad \text{--- (63)}$$

for normal propellers and slips, where T is the propeller torque in.lb., N is the revolutions per min., and p is the damping factor lb.in.sec.

From page 262 of the Trials Report^a, the torque at propeller shaft by torsionⁿmeter was 19,750 ft.lbs. at 70.5 r.p.m. Hence the propeller torque at 56 r.p.m. is approximately $19,750 \times 12 \times \left(\frac{56}{70.5}\right)^2 = 150,000 \text{ in.lb.}$

From equation (63) the corresponding propeller damping is :-

$$p = 92,100 \text{ in.lb.sec.}$$

The amplitude at the propeller is obtained from Fig. 96b as $\pm 8.29^\circ$. Therefore, by equation (56) the energy absorbed by the propeller damping is :-

$$D_p = 106,000 \text{ in.lb. per vibration.} \quad \text{--- (64)}$$

Hence, from equations (62) and (64) the energy absorbed by the engine is :-

$$D_E = 26,800 \text{ in.lb. per vibration.} \quad \text{--- (65)}$$

4. loc. cit.

5. Porter, loc. cit.

a. loc. cit.

and from equations (50) and (51) the value of R per line is 73,000 in.lb.sec., giving $\frac{M\eta}{R} = 8.8$ for an elastic form factor of 0.964.

Comparing equations (64) and (65) it will be seen that, due to the large amplitude at the propeller, about 80 per cent. of the total vibrational energy is absorbed at that source. Hence a 10 per cent. error in calculating the propeller damping would result in practically 100 per cent. change in the engine factor. However, even allowing for such a change, it is seen that the engine factor is greatly different from that obtained with the node occurring within the engine.

Again, it might be thought that the difference in the engine factor may be due to such effects as hysteresis in the shafting material. The maximum shear stresses at the nodes for the resonance conditions in all three cases do not exceed 3 tons per in². Referring to the collected data on hysteresis given in Fig. 84 page 48, it is seen that the Lewis equation $\frac{S^{2.3}}{146}$ lb.in. per in³, where S is in ton per in², amply covers all the steels up to 3 tons per in². Now this equation expresses Rowett's values for mild steel in the annealed condition, hence it will give a liberal estimate of the hysteresis energy for the two systems.

Applying the equation to the actual dimensions and stresses at each point, the total hysteresis energy for the one-node case, Fig. 96b where the maximum stresses occur in the tunnel shafting, is less than 33 per cent. of the energy attributed to engine damping, equation (65).

Similarly, for the two-node case, Fig. 96b, where the maximum stresses occur within the crankshaft, the energy due to hysteresis is only about 28 per cent. of that ascribed to the engine. It may be concluded, therefore, that the difference in engine factor is not due to hysteresis.

Engine No. E.

Further mass systems of a similar form in which the node occurs within the engine are given in Fig. 97. Practically similar results are obtained, and these are plotted in Fig. 109. Exact resonance for the one-node at sea was not obtainable, since the running speed was too low for critical values of any importance.

Amplification Factor at Values of $\frac{\sum \theta}{m} = 1$.

(a) Direct Values. Values of $\frac{\sum \theta}{m} = 1$ can only occur directly in radial engines or in systems having comparatively rigid crankshafts oscillating against a very heavy mass. B. C. Carter²¹ states that the amplification factor for radial engines is about 5 - 10, and gives a specific case from test as 8.3. The experimental apparatus of the present work may also be classified in this category. The pistons were open to the atmosphere, but very little change in the damping would be expected in the normal engine. From Fig. 95 the average value of $\frac{M_D}{R}$ is approximately 10.

(b) Indirect Values. Further values for elastic form factors approximately unity can be obtained indirectly as in the one-node critical for Engine No. A, by subtracting the damping due to the propeller.

Engine No. C.

Fig. 98 gives the necessary data obtained from a four cylinder triple expansion steam engine driving a three-bladed propeller. A 3rd order one-node critical was observed at 141 r.p.m. This was found to be stimulated mainly by the engine, since unequal crank spacing was adopted for balancing purposes, and also because the power distribution was not uniform throughout the cylinders.

From the indicator cards taken during the trials, the 3rd order torque coefficient, including

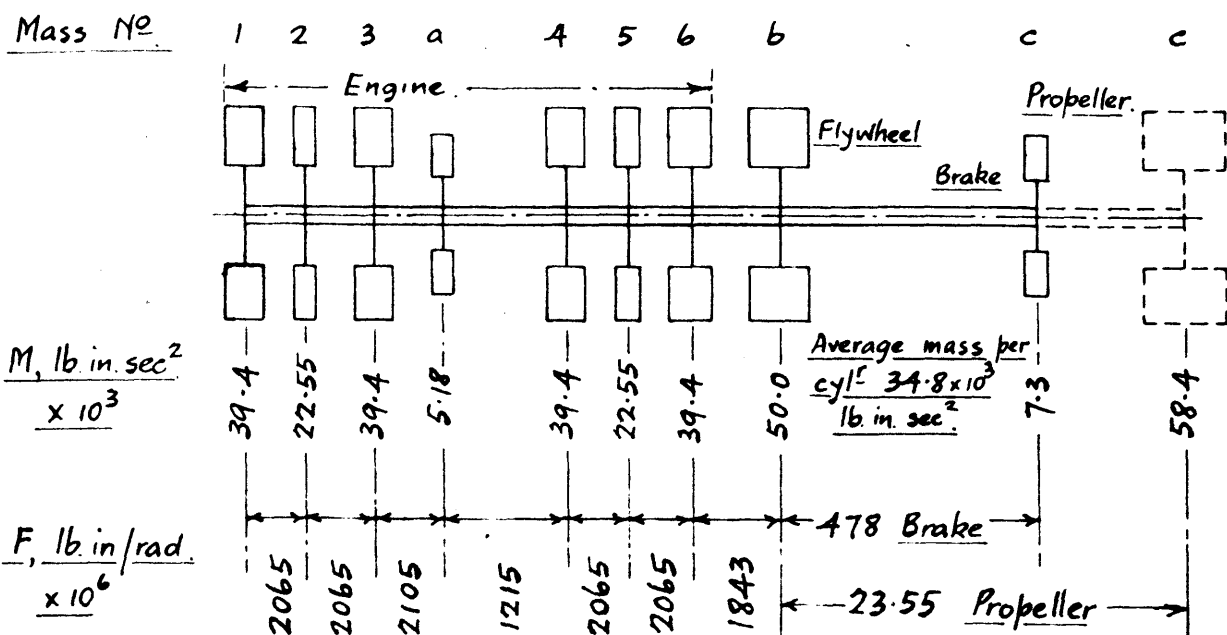
21. Carter, The Journal of the Roy. Aero. Soc. 1927. p. 278.

Fig 97.

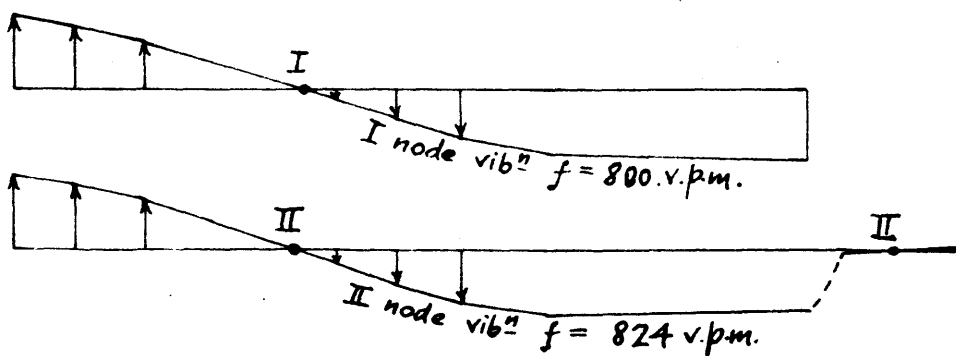
Engine No B. 6 cylinder, 2-stroke, single acting oil engine.

(Messrs. Scott's Shipbuilding & Eng^y Coy.)

Equivalent dynamical system.



Torsional
Vibration
Forms.



Relative Amplitudes.

Mass No	1	2	3	a	4	5	6	b	c
I node (Brake)	1.0000	0.8662	0.6662	—	-0.1183	-0.3968	-0.6446	-0.8256	-0.9183
II node (Prop ^r)	1.0000	0.8579	0.6459	0.3490	-0.1770	-0.4620	-0.709	-0.873	+0.050

Measured: Brake system (brake running free) } 9th order 1 node critical at 90 r.p.m.
 Amplitude at Mass No 1 = 0.729°
 Propeller system: 9th order 2 node critical at 93 r.p.m.
 Amplitude at Mass No 1 = 0.515°

Firing order. 1 6 2 4 3 5 6 cyl^s, 27" dia x 45" stroke.

Brake system, 9th order 1 node: Engine phase diagram $\sum_1^6 \theta = 3.692$; $\sum_1^6 \theta^2 = 2.785$

Elastic form factor $\frac{(\sum_1^6 \theta)}{6} = 0.229$; Harmonic torque coefft. = 3.20 lb/in^2 per in radius (from cards at M.E.P. $12.5 - 20 \text{ lb/in}^2$).

$\therefore R$ per line = $51200 \text{ lb.in. sec.}$ Hence $M^2/R = 57.0$.

Propeller system, 9th order 2 node: Engine phase diagram $\sum_1^6 \theta = 3.857$;

relative damping work $\sum_1^6 \theta^2 = 2.905$; elastic form factor $\frac{(\sum_1^6 \theta)}{6} = 0.193$.

Harmonic torque coefft. = 3.50 lb/in^2 per in radius (from cards at m.e.p 50 lb/in^2).

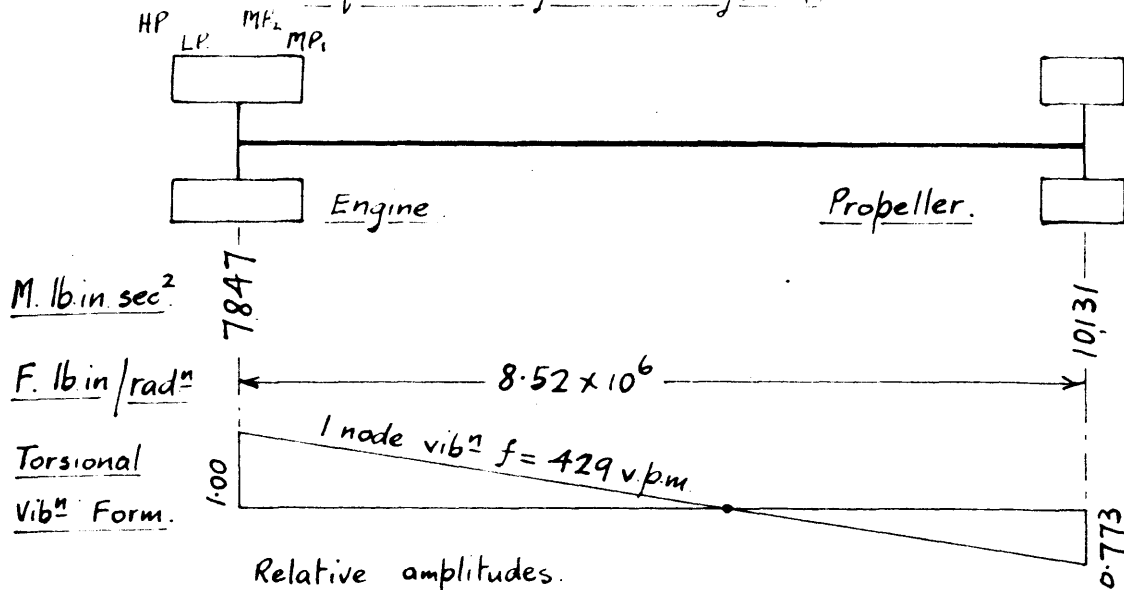
$\therefore R$ per line = $77300 \text{ lb.in. sec.}$ Hence $M^2/R = 38.9$.

Fig. 98.

Engine No C. 4 cylinder triple-expansion steam engine.

(Messrs D. Rowan & Coy.)

Equivalent dynamical system.



M. lb.in.sec²

F. lb.in/rad²

Torsional
Vibⁿ Form.

Relative amplitudes.

Mass No	H.P.	LP.	M.P ₂	M.P ₁	Prop ^r .
1. node.	1.000	0.9904	0.9332	0.8909	-0.7331
	Mean 1.000				-0.773

Measured: 3rd order 1 node critical at 141-143 r.p.m. Amplitude at equivalent engine mass = ± 0.724°

Corresponding amplitude at propeller = ± 0.56°

141 r.p.m. 3rd order torque coefft. including inertia effects = 62,000 in lb. at engine

Input energy = 2460 in. lb per vibⁿ Propeller torque = 383,000 in. lb.

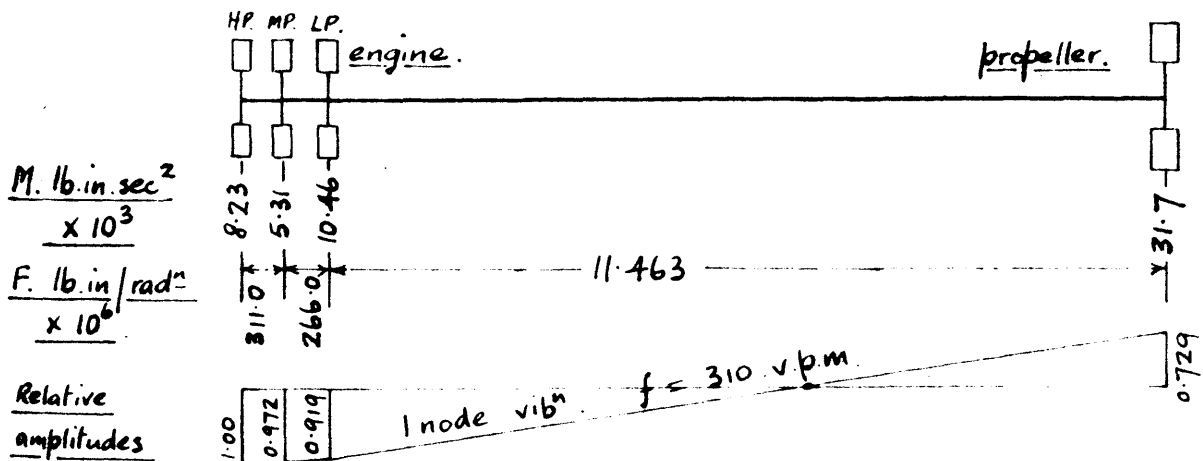
∴ Propeller damping P = 93,500 in. lb. sec. Energy absorbed by propeller = 1260 in. lb. per vibⁿ

Energy attributed to engine = 1200 in. lb. (by difference) ∴ Engine damping R = 53,500 in. lb. sec. Hence $\frac{M\eta}{R} = 6.6$. Elastic form factor $\frac{(\sum \theta)}{4} = 0.954$

Fig. 99. Engine No D. 3 cylinder triple-expansion steam engine.

(Messrs. Scott's Shipbuilding & Eng^y Coy.)

Equivalent dynamical system.



M. lb.in.sec²
x 10³

F. lb.in/rad²
x 10⁶

Relative
amplitudes

Measured: 3rd order 1 node critical at 45 r.p.m.. Amplitude at engine mass = ± 1.725° and amplitude at propeller ± 1.27°

95 r.p.m.: 3rd order torque coefft including inertia = 194,200 in lb at engine. Input energy = 18,400 in. lb per vibⁿ

Propeller torque = 875,000 in lb. ∴ propeller damping P = 317,000 in. lb. sec.. Energy absorbed by propeller = 14,600 in lb per vibⁿ

Energy attributed to engine = 3800 in. lb. (by difference) ∴ Engine damping R = 44,600 in lb. sec.

Hence $\frac{M\eta}{R} = 16.0$. Elastic form factor = 0.972

inertia effects, was found to be 13.5 per cent. of the mean indicated torque at 141 r.p.m., giving a value 62,000 in. lb. From the data given in Fig. 98 the input vibrational energy is 2,460 in.lb. per vibration. The trial results also give a propeller torque of about 383,000 in.lb. at 141 r.p.m., from which the propeller damping factor becomes :- 93,500 in.lb.sec. With an amplitude at the propeller of $\pm 0.56^\circ$ the energy absorption becomes :- 1,260 in.lb. per vibration. By difference, therefore. the energy attributed to engine damping is :- 1,200 in.lb. per vibration giving

$$R = 53,500 \text{ in.lb.sec.}$$

Whence $\frac{M_D}{R} = 5.6$ for an elastic form factor of 0.954.

Engine No. D.

Fig. 99 gives the results from a three-cylinder triple expansion steam engine, driving a four-bladed propeller. A 3rd order one-node critical was observed at 95 r.p.m. From an analysis of the indicator cards the 3rd order torque coefficients were determined and these were combined with the corresponding inertia torque. The damping attributed to the engine was estimated as shown, giving a non-dimensional factor of 16.0.

In both engines C and D, the maximum vibration stress at the node was less than 1.5 tons per in² so that the hysteresis effect is hardly appreciable.

Engine Nos. E and F.

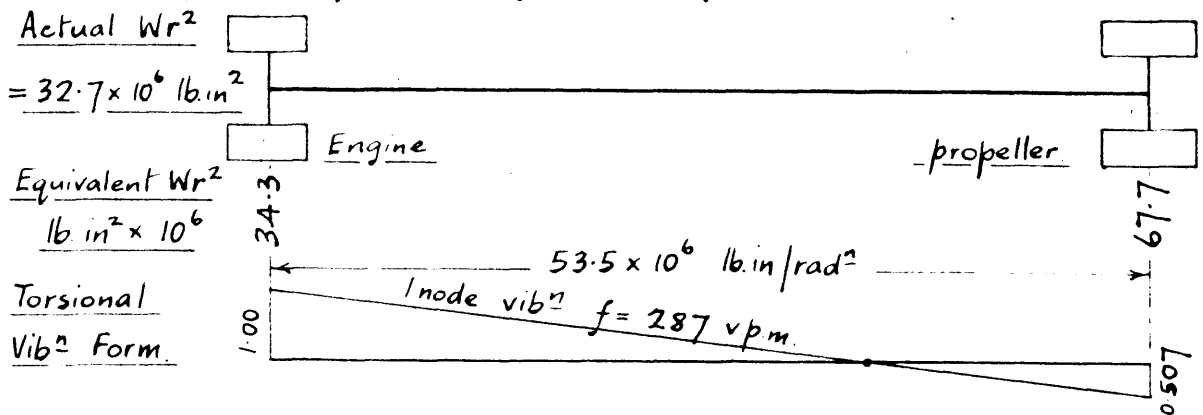
Further examples of the form factor approximately unity are deduced from the data given by F. P. Porter, Trans. A.S.M.E., A.P.M., 51-22, 1929. Both engines are of the 4-cylinder triple expansion type, driving a 3-bladed propeller. The mass systems and other necessary information are given for each case in Figs. 100 and 101. The torque coefficients for the engine given in Fig. 100 were given in detail, and as the engine in Fig. 101 was exactly similar, the torque

Fig. 100. Engine No E. 4-cylinder triple-expansion steam engine.

"Oklahoma" (F.P. Porter, Trans. A.S.M.E., A.P.M. 51-22 1929.)

Full power rating, 10,850 i.h.p. at 82 r.p.m.

Equivalent dynamical system



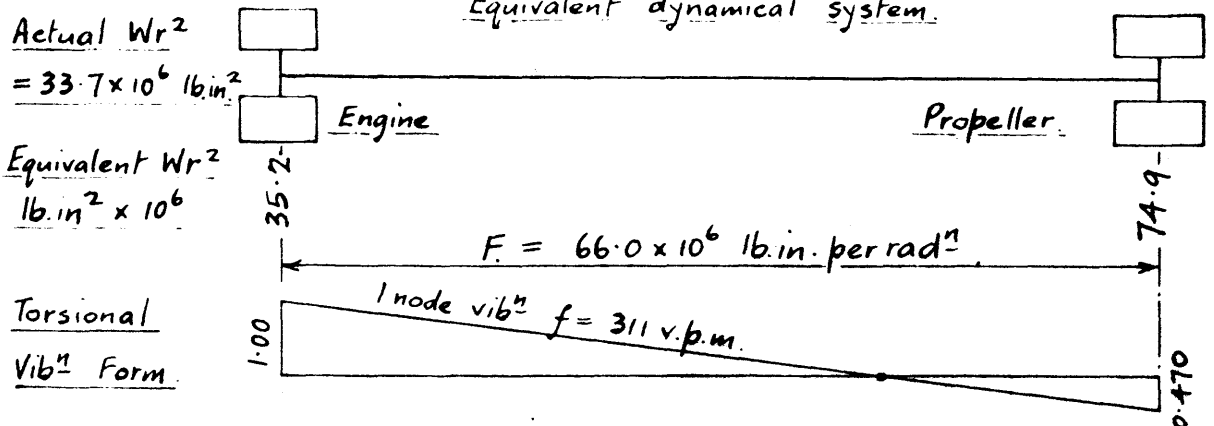
Measured: 4th order 1node critical at 72 r.p.m. Amplitude at propeller = $\pm 1.25^\circ$; corresponding amplitude at engine = $\pm 2.48^\circ$

72 r.p.m.: 4th order torque coefft. resultant = 400,000 in.lb. at engine (given). Input energy = 54,300 in.lb. per vibⁿ. Propeller torque = 1,340,000 in.lb. Propeller damping $p = 642,000 \text{ in.lb. sec.}$ Energy absorbed by propeller = 28,800 in.lb./vibⁿ. Energy attributed to engine = 25,500 in.lb./vibⁿ (by difference). Engine damping $R = 144,000 \text{ in.lb. sec.}$ Hence $M^2/R = 17.7$. Elastic form factor = 1.

Fig. 101. Engine No F. 4 cylinder triple-expansion steam engine. "Texas."

(F.P. Porter, Trans. A.S.M.E., A.P.M. 51-22 (1929). Full power rating 14,250 i.h.p. at 82 r.p.m.

Equivalent dynamical system.



Measured: 3rd order 1node critical at 102 r.p.m. Amplitude at engine $\pm 1.46^\circ$ and $\pm 1.3^\circ$, mean $\pm 1.38^\circ$; Amplitude at propeller $\pm 0.65^\circ$

4th order 1node critical at 78 r.p.m. Amplitude at engine $\pm 2.40^\circ$ Amplitude at propeller $\pm 1.10^\circ$.

Ratio Resultant torque coefft. for "Texas" = 1.312
 Resultant torque coefft. for "Oklahoma"

3rd order at 102 r.p.m. Resultant 3rd order torque coefft = 446,000 in.lb. at engine. Input energy = 33,700 in.lb. per vibration. Propeller torque = 3,990,000 in.lb. Propeller damping $p = 1,320,000 \text{ in.lb. sec.}$ Propeller absorption = 17,300 in.lb. per vibⁿ. Energy attributed to engine = 16,400 in.lb. per vibⁿ. Engine damping $R = 277,000 \text{ in.lb. sec.}$ Hence $M^2/R = 10.25$. Elastic form factor = 1.

4th order at 78 r.p.m. Resultant 4th order torque coefft. = 605,000 in.lb. at engine. Input energy = 79,500 in.lb. per vibration. Propeller torque = 2,160,000 in.lb. Propeller damping $p = 952,000 \text{ in.lb. sec.}$ Energy absorbed by propeller = 35,800 in.lb. per vibⁿ. Energy attributed to engine = 43,700 in.lb. per vibⁿ. Engine damping $R = 244,000 \text{ in.lb. sec.}$ Hence $M^2/R = 11.65$. Elastic form factor = 1.

coefficients are taken in the horse power ratio.

In Fig. 100 a 4th order one-node critical was observed at 72 r.p.m. and on reduction the value of $\frac{M_D}{R}$ becomes 17.7.

Similarly from engine F, where both a 3rd and 4th order one-node were observed $\frac{M_D}{R}$ is shown to be 10.25 and 11.65 for a form factor of unity.

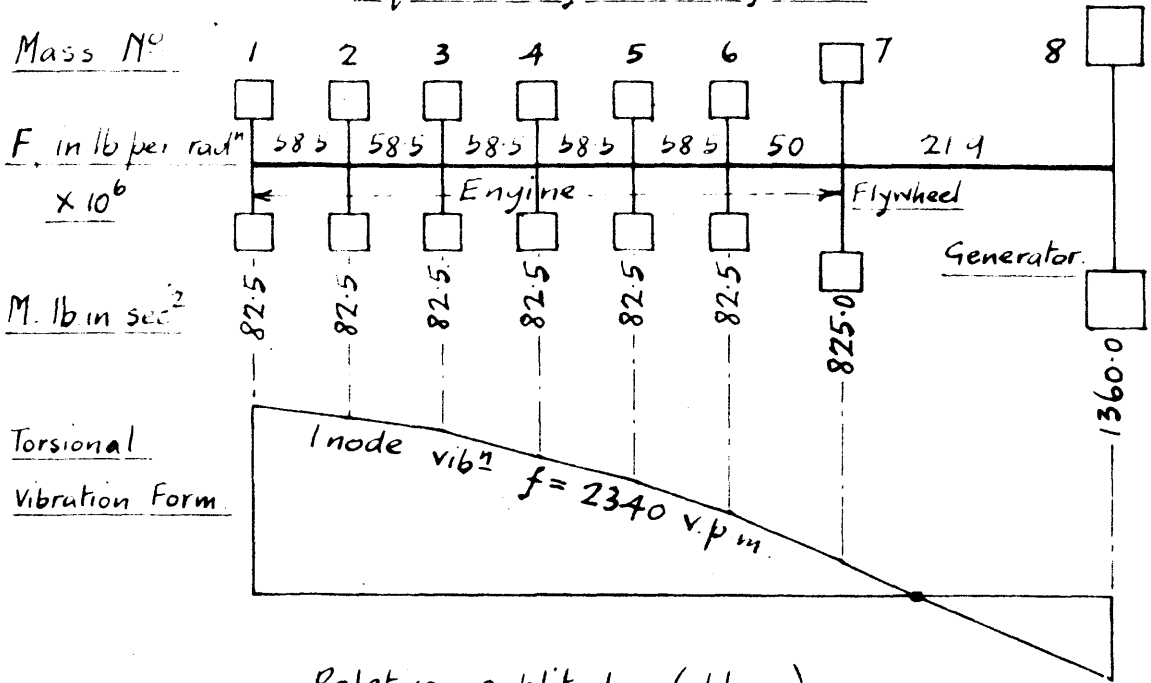
Examining the factors deduced by difference from marine propeller systems, it would appear that for elastic form factors of unity, these indirect values approximate to those obtained directly as in (a).

Values of $\frac{\sum \theta}{m}$ between 0 and 1 . For values of $\frac{\sum \theta}{m}$ corresponding to intermediate form factors, results are taken from published data and reduced accordingly. Details are given in Figs. 102 - 104 of oil engine generator sets. In each case the masses at the comparatively flexible crankshafts oscillate against the heavy flywheel and generator. A further result is given in "Drehschwingungen in Kolbenmaschinenanlagen" by H Wydler, of a 10-cylinder oil engine, but as a friction clutch was fitted between the engine and generator, there appears to be some possibility of the clutch having slipped. Taking the values as measured, however, the nondimensional factor becomes 9.6 for a form factor $\frac{\sum_{i=1}^{10} \theta}{10} = 0.673$, which is seen to be low and is in accordance with possible clutch slip.

In Figs. 105 and 106 similar details are given of straight-in-line air craft drives, in which cases, the engine oscillates against a very heavy airscrew. The measured amplitudes given in Fig. 105 show the difficulties in recording oscillations at such high rotational speeds and frequencies. In ^{the} "Reports and Memoranda"²² dealing with the 8-cylinder engine the elastic curve for the original shaft was not shown,

Fig 102 Engine No G. 6 cylinder 4 stroke single-acting oil-engine.
(Wydler, "Drehschwingungen in Kolbenmaschinenanlagen.")

Equivalent dynamical system.



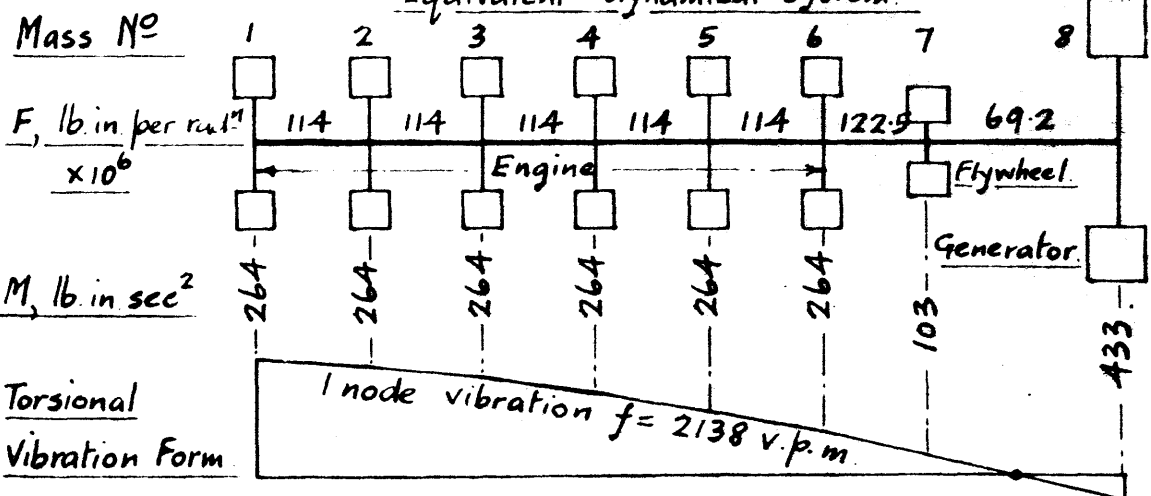
Relative amplitudes. (approx)

Mass No	1	2	3	4	5	6	7	8
1 node.	1.000	0.959	0.88	0.765	0.616	0.447	0.257	-0.482

Measured: 6th order, 1 node critical at 390 r.p.m. Amplitude at mass No 1 = $\pm 1.13^\circ$. 6th order 1 node gives: $\sum \theta = 4.66$; $\sum \theta^2 = 3.86$ and elastic form factor = 0.776. 6 cyl^s, 35 cm. dia x 35 cm. reduced stroke. Harmonic torque coefft. 5.16 lb/in² per in. radius (given) $\therefore R$ per line = 1325 in. lb. sec, Hence $M/R = 15.3$

Fig 103 Engine No H. 6 cylinder 4 stroke single-acting oil-engine.
(Wydler, "Drehschwingungen in Kolbenmaschinenanlagen")

Equivalent dynamical system.



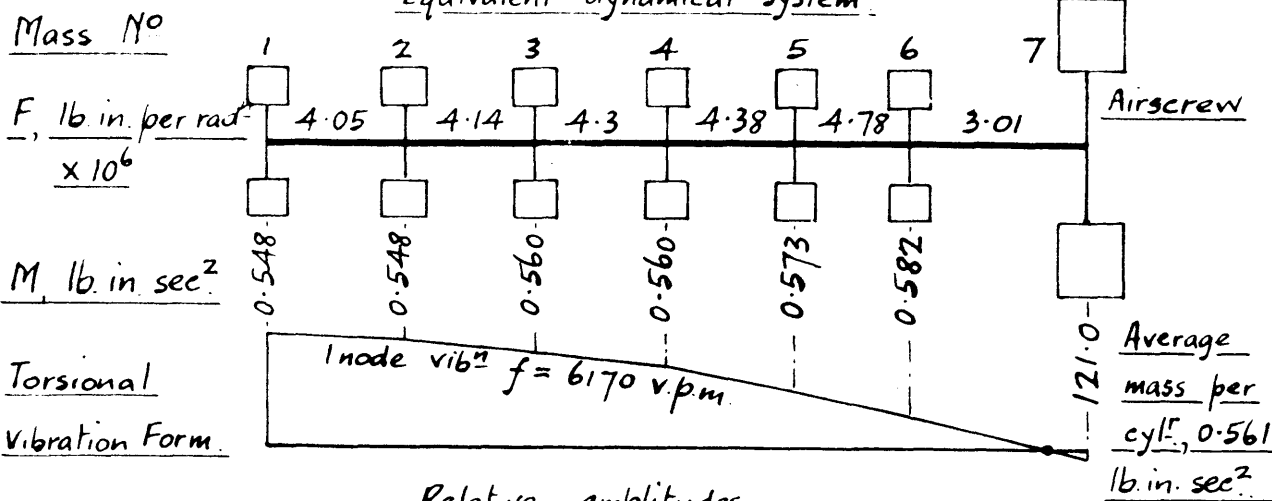
Relative amplitudes.

Mass No	1	2	3	4	5	6	7	8
1. node	1.000	0.947	0.848	0.712	0.543	0.350	-	-0.203

Measured: 6th order 1 node critical at 358 r.p.m. Amplitude at mass No 1 = $\pm 1.19^\circ$. 6th order 1 node gives: $\sum \theta = 4.32$; $\sum \theta^2 = 3.43$; elastic form factor 0.72. 6 cyl^s, 45 cm. dia x 42 cm. stroke (reduced) Harmonic torque coefft., 5.28 lb/in² per in. radius (given) $\therefore R$ per line = 2910 lb. in. sec. Hence $M/R = 20.3$

Fig 104 Engine No J. 6-cylinder 4 stroke single-acting petrol engine BMW IV (A. Stieglitz; "DrehSchwingungen in Reihenmotoren" Luftfahrtforschung, No 5 July 24. 1929.)

Equivalent dynamical system.



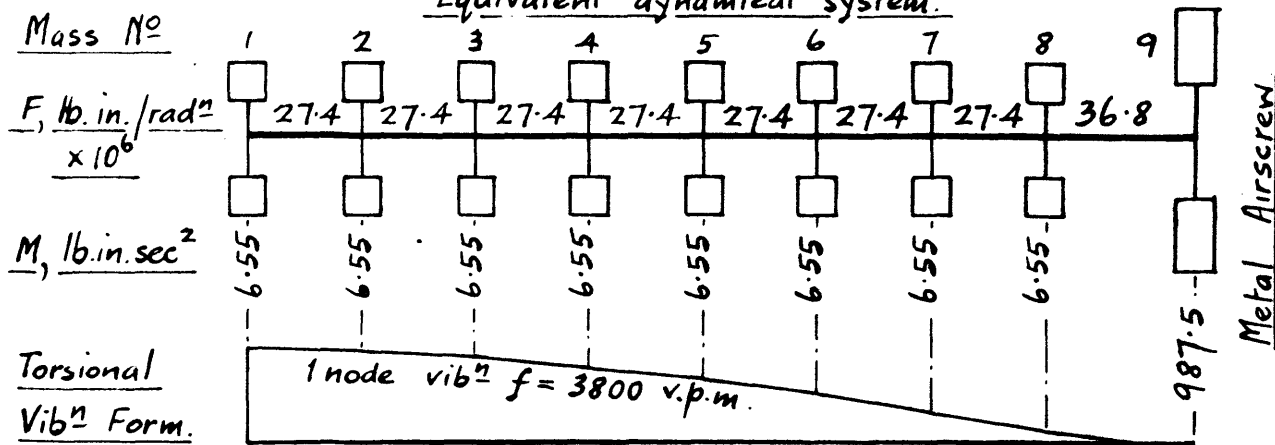
Relative amplitudes

Mass No	1	2	3	4	5	6	7
1 node	1.000	0.943	0.836	0.687	0.505	0.312	-0.020

Measured: 6th order 1 node critical at about 1000 r.p.m. Amplitude at mass No 1 by Geiger Torsiograph = $\pm 0.7^\circ$ and later by new device = $\pm 1.5^\circ$. 6th order 1 node gives: $\sum_1^6 \theta = 4.29$; $\sum_1^6 \theta^2 = 3.42$; elastic form factor = 0.71. 6 cyl^r, 5.36 in. dia. x 7.5 in. stroke. Harmonic torque coefft. = 1.92 lb/in² per in. radius (given). R per line = 26.6 and 12.4 in. lb. sec., for 0.7° and 1.5° respectively. Hence $M/R = 13.6 - 28.5$

Fig 105 Engine No K. 8 cylinder 4 stroke single-acting oil engine. (Tornado Airship Engine. R & M. No 1303. E. 39. Carter & Muir).

Equivalent dynamical system.

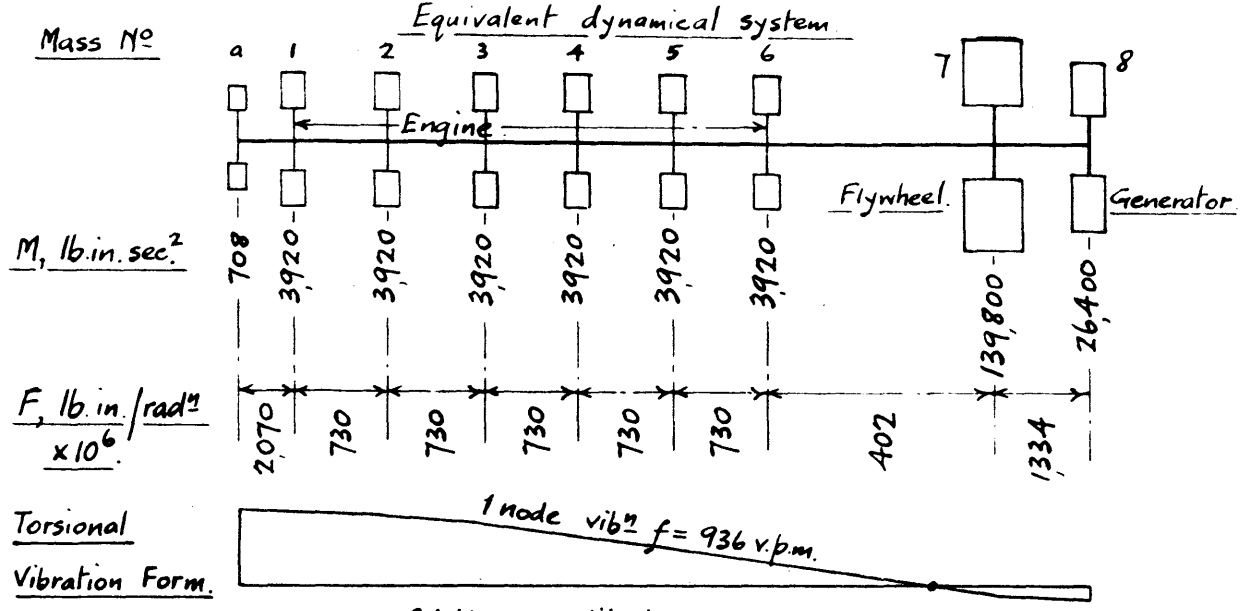


Relative amplitudes.

Mass No	1	2	3	4	5	6	7	8	9
1 node	1.0000	0.9622	0.8880	0.7804	0.6432	0.4816	0.3020	0.1110	-0.0343

Measured: 4th order 1 node critical at 950 r.p.m. Amplitude at mass No 1 = $\pm 7.92^\circ$. 4th order 1 node gives: $\sum_1^8 \theta = 5.1684$; $\sum_1^8 \theta^2 = 4.075$; elastic form factor = 0.646. 8 cyl^r, 8 1/4 in. dia x 12 in. stroke. Firing order 1.5.7.8.4.3.2.6. Harmonic torque coefft. = 15.45 lb/in² per in. radius at M.E.P. 121 lb/in². (Lewis). $\therefore R \text{ per line} = 114 \text{ in. lb. sec.}$ Hence $M/R = 22.9$

Fig. 106 Engine No L. 6 cyl^s, 4 stroke single-acting oil-engine. U.S. Army Dredger, "Dan C. Kingman" Class [Fox: "Torsional Vibrations in Diesel Engines", Journal Am. Soc. Naval Eng. Aug. 1926 & Porter: Trans. Am. Soc. Mech. Eng. A.P.M. 50. 8. (1927-28)]

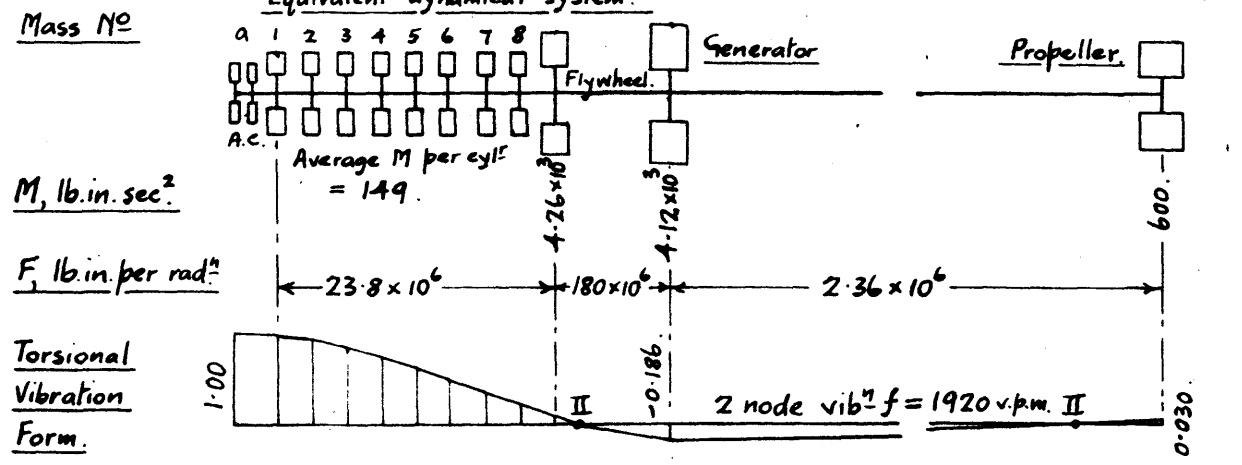


Relative amplitudes.

Mass No	a	1	2	3	4	5	6	7	8
1 node.	1.000	0.9969	0.9383	0.8333	0.6871	0.5068	0.3008	-0.1002	-0.1235

Measured: 6th order 1 node critical at 156 r.p.m. Amplitude at mass No a = ± 1.8°
 9th " " " " 104 " " " " " = ± 0.53°
 6th & 9th orders, 1 node: Phase diagram $\sum \theta = 4.263$; $\sum \theta^2 = 3.388$; elastic form factor 0.711. 6 cyl^s, 22 in. dia. X 32 in. stroke.
 6th order: Harmonic torque coefft. = 4.74 lb/in² per in radius (Lewis) at M.E.P. = 83.5 lb/in². R per line = 11,800 in. lb. sec. Hence $M^2/R = 33.9$.
 9th order: Harmonic torque coefft. = 1.52 lb/in² per in radius (Lewis) at M.E.P. = 42.0 lb/in². R per line = 12,800 in. lb. sec. Hence $M^2/R = 30.0$.

Fig. 107 Engine No M. 8 cyl^s 4 stroke single-acting oil-engine. U.S. Submarine S. 29. 13 1/2 in. dia X 15 in. stroke. 600 b.h.p. at 380 r.p.m. [Porter: Trans. Am. Soc. Mech. Eng. A.P.M. 50. 8. 1928.]



Relative amplitudes.

Mass No	1	2	3	4	5	6	7	8
II node.	0.957	0.912	0.833	0.745	0.627	0.500	0.363	0.203

Firing order, 1.5.7.3.8.4.2.6.

Measured: 5 1/2 order 2 node critical at 350 r.p.m. Amplitude at mass a. = ± 1.002°
 8th " " " " 241 " " " " " = ± 0.99°
 5 1/2 order 2 node: Engine phase diag, $\sum \theta = 1.285$; $\sum \theta^2 = 3.815$; elastic form factor $(\sum \theta^2)^{1/2} / 8 = 0.643$
 Harmonic torque coefft. = 6.35 lb/in² per in radius at M.E.P. = 92 lb/in² (Lewis) ∴ R per line = 655 in. lb. sec. Hence $M^2/R = 45.6$.
 8th order 2 node: Engine phase diag, $\sum \theta = 5.14$; $\sum \theta^2 = 3.815$; elastic form factor = 0.643.
 Harmonic torque coefft. = 2.0 lb/in² per in radius at M.E.P. = 59 lb/in² (Lewis) ∴ R per line = 831 in. lb. sec. Hence $M^2/R = 36.0$.

Fig. 108. Collected Results.

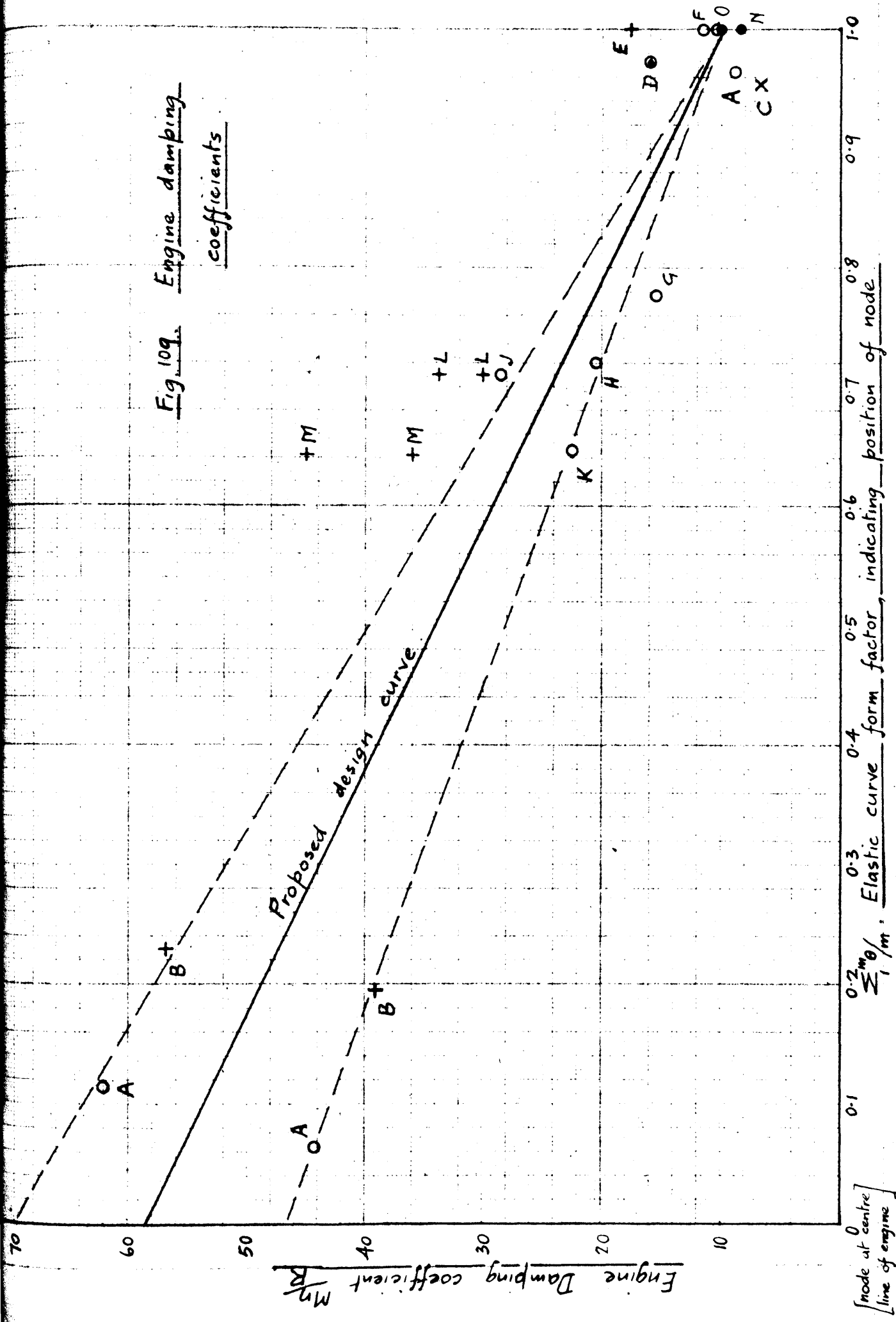
Engine.	Fig. No.	Frequency v.p.m.	Node	Order.	Amplitude at 1st mass $\pm d$ deg.	M.E.P. lb/in ²	Torque coeff. lb/in ² per in. radius	Engine damping.		$\frac{M\ddot{z}}{R}$	Elastic form factor at engine. $\Sigma \theta/m$.
								Direct or Indirect.	R per line in. lb. sec.		
A. 6-cyl 4 stroke single-acting oil-engine.	96a.	947	1	7½	0.33	20.4	2.1	direct	58,300	62.0	0.1136
	96b.	988	2	7½	0.284	118.	2.85	"	85,700	44.1	0.064
	"	164	1	3	1.98	38	22.7	indirect	73,000	8.8	0.964
B. 6-cyl 2 stroke single-acting oil-engine.	97.	800	1	9	0.729	12-20	3.20	direct	51,200	57.0	0.229
	"	824	2	9	0.515	50	3.50	"	77,300	38.9	0.193
C. 4-cyl triple exp ^m steam engine.	98.	429	1	3	0.724	—	—	indirect	53,500	6.6	0.954
D. 3-"	"	310	1	3	1.725	—	—	indirect	44,600	16.0	0.972
E. 4-"	"	287	1	4	2.48	—	—	indirect	14,000	17.7	1
F. 4-"	"	311	1	3	1.38	—	—	indirect	277,000	10.25	1
	"	"	1	4	2.40	—	—	"	244,000	11.65	1
G. 6-cyl 4 stroke single-acting oil-engine.	102	2340	1	6	1.13	—	5.16	direct	1,325	15.3	0.776
H. 6-"	"	2138	1	6	1.19	—	5.28	direct	2,910	20.3	0.72
J. 6-cyl 4 stroke single-acting petrol engine.	104	6170	1	6	1.5	—	1.92	direct	12.4	28.5	0.71
K. 8-cyl 4 stroke single-act ⁿ oil-engine.	105	3800	1	4	7.92	121	15.45	direct.	114.0	22.9	0.646
L. 6-"	"	936	1	6	1.80	83.5	4.74	direct	11,800	33.9	0.711
	"	"	1	9	0.53	42.0	1.52	"	12,800	30.0	0.711
M. 8-"	"	1920	2	5½	1.002	92.0	6.35	direct	655	45.6	0.643
	"	"	2	8	0.99	59.0	2.0	"	831	36.0	0.643
N. 9-cyl radial engine. (B. C. Carter.)										8.3	1
O. Present experimental apparatus.										10.0	1

Referred to above.

(B. C. Carter.)

Present experimental apparatus.

Fig 109. Engine damping coefficients



$\sum \frac{m_0}{l}$. Elastic curve form factor, indicating position of node

[node at centre]
[line of engine]

but details of the crank were given, so that the dynamical system could be deduced. The mass system given in Fig. 106 therefore is only approximate, but is quite representative of the actual form, since the difference in the elastic curve for the initial and final systems is very slight.

Finally, the dynamical system and details for submarine drives as given by Porter⁵ are shown in Fig. 107. As before the comparatively flexible engine shaft oscillates against the heavy generator, nodes occurring practically at the flywheel and propeller.

The final results for all the engines are given in Fig. 108 and a plot of $\frac{M\eta}{R}$ on a base of elastic form factor is shown in Fig. 109.

Examining this curve, it is seen that with the exception of the submarine engine system the points conform to the mean line to within 30 per cent. Such a large percentage difference may appear abnormal, but it must be remembered that each point is the result of numerous calculations in which some of the factors employed cannot be estimated very accurately.

The chief factors affecting the result are the vibration form and frequency, the measurement of amplitude, the harmonic torque, and the simple conception of damping factor.

Since vibration frequency can now be estimated to within 3 - 5 per cent., and since form and frequency are interconnected, no great error can arise from the estimated values.

The measurement of the torsional oscillations for the moderate rotational speeds and frequencies dealt with can also be relied upon, while the harmonic analysis of the small torsigraphic records obtained can also be made with fair accuracy.

The harmonic torque coefficients which are taken from indicator cards are the most likely source of error. From an examination of a large number of

harmonic analyses, H. Constant,²³ shows that the harmonics below the 2nd crankshaft order of four-stroke cycle engines determine the general shape of the torque curves, apart from inertia effects, and depend mainly upon the mean torque of the cylinder. They can, therefore, be estimated to within 5 per cent. on an average. However, in engine torsional oscillations it is the higher harmonics that must be considered.

The higher harmonics arise from the apparent irregularities in the torque curves. In rough analysis, therefore, these are liable to be smoothed out. They are also affected by engine design and running conditions, and therefore the error involved in the estimation of their average magnitude, even for a single cylinder torque curve, may be quite large.

Generally the value obtained from the single cylinder torque curve is taken as applying throughout in a multi-cylinder engine. but this ideal condition is not realized. H. Constant gives the values of the harmonics from the individual cards of a 9-cylinder radial engine under normal tuning, and shows clearly that there is a large percentage difference in magnitude between the higher orders for the different cylinders. Taking the plotted values given by him, there is a 30 per cent. difference in the 3rd order and a 50 per cent. in the $5\frac{1}{2}$ order.

Carrying the examination further, H. Constant compared the resultant harmonics for the engine based on individual card analysis, with the resultant obtained in the usual way by taking an exactly similar card throughout. From the final graph it is found that there is a difference of about 20 per cent. in the main $4\frac{1}{2}$ order for that engine.

It is possible, therefore, that such results will apply to the heavy oil engines given here. For the oil engines subjected to experiment, harmonic analysis

23. Constant, Journal of the Roy. Aero. Soc., March. 1932.

was carried out only on the indicator cards which gave m.e.p. values practically equal to the average for the test. This, however, is no guarantee that the higher orders obtained will represent the mean effect throughout the cylinders, but it is the most rational course to adopt.

Again, with regard to the damping at the main bearings of ~~the~~ multi-crank engines, the journal displacements due to crank web distortion will not be similar for engines with a different number of cranks. Therefore the simple expression for the elastic curve form at the engine, will not be sufficient in itself to account for such cases.

It would appear therefore, that the errors in calculation which accumulate in multicylinder engines by these various factors are sufficient to explain the divergence from the mean line given in Fig. 109. In view of the uncertain values of torque coefficients and other factors involved in multicylinder engines, all methods of calculating amplitudes will be approximate. Hence, under these conditions, any attempt at further refinement of overall values would be misplaced. The results apparently suffer on account of simplification, but gain by their straightforward application. The curve given in Fig. 109 is, therefore, put forward as a guide in design.

In conclusion, the author expresses his indebtedness to Professor A. L. Mellanby, D.Sc., for the interest taken in this subject and the generous provision of facilities. Thanks are also due to Professor W. Kerr, Ph.D., for the advice given in the development of the paper.

BIBLIOGRAPHY.

General.

1. Holzer, "Die Berechnung der Drehschwingungen", Springer, 1921.
 3. Wydler, "Drehschwingungen in Kolbenmaschinenanlagen", Springer, 1922.
 4. Lewis, "Torsional Vibration in the Diesel Engine" Trans. Soc. Naval Arch. and Marine Eng. New York, Nov. 1925.
 21. Carter, "Dynamic Forces in Aircraft Engines", The Journal of the Roy. Aero Soc., Jan. 1927.
 6. " "Torsional vibration in Engines" Aero. Research Comm. R. & M. No. 1053, E. 22.
 5. Porter, Trans. Amer. Soc. Mech. Eng., A.P.M. 51.22 - 1929.
 8. Hartog and Ormondroyd, "Trans. Amer. Soc. Mech. Eng., A.P.M. 52. 13 - 1930. (Discussion p. 152.)
- Steiglitz, "Drehschwingungen in Reihenmotoren" Luftfahrtforschung. No. 5. July 24, 1929.
12. Timoshenko, "Vibration problems in Engineering" Constable, 1928.
- Geiger, "Mechanische Schwingungen", Springer, 1927.

Inertia Torques and Equations of Motion.

10. Cormac, "A Treatise on Engine Balance using Exponentials" Chapman and Hall.
 9. Kerr, "The Balance of Internal Combustion Engines" Trans. Inst. Eng. & Ship. Scotland, 1927 - 28.
- Kobayashi, "An Analytical study of crank effort in reciprocating engines", Memoirs Ryojun College of Eng. Vol. IV. NO. 3. 1931.
13. Goldsburgh, "Torsional vibrations in Reciprocating Engine Shafts", Proc. Roy. Soc. Vol. CXIII. Series A, 1926 - 27.
- Also, " " " " " Vol. CIX. Series A, 1925.
- Muir and Terry, "A Harmonic Analysis of Torque Curves", Aero. Research Comm. No. 1305. E. 41.
23. Constant, "Aircraft Vibration", Journal Roy. Aero. Soc. Vol. XXXVI. March, 1932.

Crankshafts.

11. Timoshenko, "Torsion of crankshafts", Trans. Amer. Soc. Mech. Eng. 1922.
 2. Carter, "An Empirical Formula for crankshaft Stiffness in Torsion", Engineering, July, 13th 1928.
- Constant, "On the stiffness of crankshafts", Aero. Research Comm, R. & M. No. 1201. E.29.
- Marine-Oil-Engines Trials - 6th Report. Trans Inst. Mech. Eng. 1931. Vol. 121 (Crankshaft stiffness, p.287.)

Hysteresis in Steels.

7. Rowett, Proc. Roy. Soc. Series A, Vol. 89. 1914.
4. Lewis. loc cit.
15. Kimball, Trans. Amer. Soc. Mech. Eng. 1926.
16. Lea, Proc. Roy. Soc. Series A. Vol. 93. 1916 - 17.
14. Föppl, "Die Dauerprüfung der Werkstoffe" Springer.
17. Dorey, Trans. Inst. Mech. Eng. 1932, (Advance Proof).

Lubrication and Frictional Effects.

18. Boswall, "The Theory of Film Lubrication", Longmans.
 19. Lamb, "Hydrodynamics", Camb. Univ. Press.
 20. Robertson, "Whirling of a Journal in a Sleeve Bearing", Phil. Mag. Vol. 14. No.96, Jan. 1933.
- "The Mechanical Properties of Fluids", Blackie.
- Stanton, "The Friction of Pistons and Piston Rings",
Aero. Research Comm., No. 931. E.12.
